ISSN 0021-9673

VOL. 478 NO. 2 SEPTEMBER 15, 1989

THIS ISSUE COMPLETES VOL. 478

JOURNAL OF CHROMATOGRAPHY

INTERNATIONAL JOURNAL ON CHROMATOGRAPHY, ELECTROPHORESIS AND RELATED METHODS

ELSEVIER

JOURNAL OF CHROMATOGRAPHY

Scope. The *Journal of Chromatography* publishes papers on all aspects of chromatography, electrophoresis and related methods. Contributions consist mainly of research papers dealing with chromatographic theory, instrumental development and their applications. The section *Biomedical Applications*, which is under separate editorship, deals with the following aspects: developments in and applications of chromatographic and electrophoretic techniques related to clinical diagnosis or alterations during medical treatment; screening and profiling of body fluids or tissues with special reference to metabolic disorders; results from basic medical research with direct consequences in clinical practice; drug level monitoring and pharmacokinetic studies; clinical toxicology; analytical studies in occupational medicine.

Submission of Papers. Papers in English, French and German may be submitted, in three copies. Manuscripts should be submitted to: The Editor of *Journal of Chromatography*, P.O. Box 681, 1000 AR Amsterdam, The Netherlands, or to: The Editor of *Journal of Chromatography, Biomedical Applications*, P.O. Box 681, 1000 AR Amsterdam, The Netherlands. Review articles are invited or proposed by letter to the Editors. An outline of the proposed review should first be forwarded to the Editors for preliminary discussion prior to preparation. Submission of an article is understood to imply that the article is original and unpublished and is not being considered for publication elsewhere. For copyright regulations, see below.

Subscription Orders. Subscription orders should be sent to: Elsevier Science Publishers B.V., P.O. Box 211, 1000 AE Amsterdam, The Netherlands, Tel. 5803 911, Telex 18582 ESPA NL. The *Journal of Chromatography* and the *Biomedical Applications* section can be subscribed to separately.

Publication. The *Journal of Chromatography* (incl. *Biomedical Applications*) has 37 volumes in 1989. The subscription prices for 1989 are:

J. Chromatogr. + *Biomed. Appl.* (Vols. 461–497):
Dfl. 6475.00 plus Dfl. 999.00 (p.p.h.) (total *ca.* US$ 3429.00)

J. Chromatogr. only (Vols. 461–486):
Dfl. 5200.00 plus Dfl. 702.00 (p.p.h.) (total *ca.* US$ 2708.00)

Biomed. Appl. only (Vols. 487–497):
Dfl. 2200.00 plus Dfl. 297.00 (p.p.h.) (total *ca.* US$ 1146.00).

Our p.p.h. (postage, package and handling) charge includes surface delivery of all issues, except to subscribers in Argentina, Australia, Brasil, Canada, China, Hong Kong, India, Israel, Malaysia, Mexico, New Zealand, Pakistan, Singapore, South Africa, South Korea, Taiwan, Thailand and the U.S.A. who receive all issues by air delivery (S.A.L. — Surface Air Lifted) at no extra cost. For Japan, air delivery requires 50% additional charge; for all other countries airmail and S.A.L. charges are available upon request. Back volumes of the *Journal of Chromatography* (Vols. 1–460)are available at Dfl. 195.00 (plus postage). Claims for missing issues will be honoured, free of charge, within three months after publication of the issue. Customers in the U.S.A. and Canada wishing information on this and other Elsevier journals, please contact Journal Information Center, Elsevier Science Publishing Co. Inc., 655 Avenue of the Americas, New York, NY 10010. Tel. (212) 633-3750.

Abstracts/Contents Lists published in Analytical Abstracts, ASCA, Biochemical Abstracts, Biological Abstracts, Chemical Abstracts, Chemical Titles, Chromatography Abstracts, Clinical Chemistry Lookout, Current Contents/Physical, Chemical & Earth Sciences, Current Contents/Life Sciences, Deep-Sea Research/Part B: Oceanographic Literature Review, Excerpta Medica, Index Medicus, Mass Spectrometry Bulletin, PASCAL-CNRS, Pharmaceutical Abstracts, Referativnyi Zhurnal, Science Citation Index and Trends in Biotechnology.

See inside back cover for Publication Schedule, Information for Authors and information on Advertisements.

0021-9673/89/$03.50

Printed in The Netherlands

CONTENTS

(Abstracts/Contents Lists published in Analytical Abstracts, ASCA, Biochemical Abstracts, Biological Abstracts, Chemical Abstracts, Chemical Titles, Chromatography Abstracts, Current Contents/Physical, Chemical & Earth Sciences, Current Contents/Life Sciences, Deep-Sea Research/Part B: Oceanographic Literature Review, Excerpta Medica, Index Medicus, Mass Spectrometry Bulletin, PASCAL-CNRS, Referativnyi Zhurnal and Science Citation Index)

In articles with more than one author, the name of the author to whom correspondence should be addressed is indicated in the article heading by a 6-pointed asterisk (*)

Journal of Chromatography, 478 (1989) 287–309
Elsevier Science Publishers B.V., Amsterdam — Printed in The Netherlands

CHROM. 21 641

UNAVOIDABLE FLOW-RATE ERRORS IN HIGH-PERFORMANCE LIQUID CHROMATOGRAPHY

JOE P. FOLEY*, JEFFREY A. CROW, BETH ANN THOMAS and MARLON ZAMORA
Department of Chemistry, Louisiana State University, Baton Rouge, LA 70803-1804 (U.S.A.)
(First received February 21st, 1989; revised manuscript received May 25th, 1989)

SUMMARY

Two different types (low-pressure mixing and high-pressure mixing) of high-performance liquid chromatographic (HPLC) solvent delivery systems were evaluated for their flow-rate accuracy using three common hydro-organic mobile phases: methanol–water, acetonitrile–water and tetrahydrofuran–water. Both systems delivered flow-rates 2–12% lower than the desired (set) values, depending on the mobile phase composition. Further investigations revealed that these errors in flow-rate were due in part to non-ideal mobile phase behavior (non-zero volumes of mixing, non-zero compressibilities, pressure dependent viscosities, and deviations from Darcy's law) and non-ideal stationary phase behavior (column expansivity and packing compression). An approach to correct for the systematic errors in flow-rate is described for binary solvent mixtures. The approach utilizes correction factors based on non-ideal mobile and stationary phase behavior and has been experimentally confirmed for the mobile phases and columns we examined. Although approximate in nature, our approach reduces the systematic errors in flow-rate about ten-fold, and provides a means for estimating the instrumental contribution to flow-rate error as well. This leaves only an instrumental bias which can be measured and then factored out for all further experiments with that instrument. The resulting improvements in flow-rate accuracy provided by our approach will be extremely useful to researchers who need very accurate retention data for physicochemical measurements as well as to HPLC manufacturers and users for quality control and troubleshooting of these solvent delivery systems.

INTRODUCTION

Although not commonly appreciated, deviations in the flow-rate from the programmed value are an everyday occurrence in high-performance liquid chromatography (HPLC). Despite claims from numerous HPLC manufacturers who insist that their systems are virtually error free, flow-rate errors can often exceed 5% and may sometimes be a significant source of error in analytical or physicochemical measurements[1–5].

The sources of flow-rate errors in HPLC can be broadly classified into four

0021-9673/89/$03.50

categories: (1) non-ideal mobile phase behavior, (2) non-ideal stationary phase (packing and column hardware), (3) instrumental imperfections (mechanical limitations of the solvent delivery systems), and (4) operator error. The first category, non-ideal mobile phase behavior, can be described almost entirely in terms of four physical phenomena: (i) the change in volume which occurs when two of more solvents are blended, (ii) the compressibility of any pure solvent or mixtures of solvents, (iii) the pressure dependence of viscosity of any pure solvent or mixtures of solvents, and (iv) deviations in Darcy's law. The second category, "non-ideal stationary phase properties", refers to the very slight compression of the packing and the expansion of the column wall due to the high pressures; this results in a slightly greater than predicted column permeability. The last two categories, instrumental imperfections and operator error, cannot be defined as precisely but certainly include leaks, dissolved gases in the mobile phase, faulty check valves, insufficient pulse dampening, and flow restrictions such as plugged frits.

Whereas flow-rate errors due to category 4 can be identified and eliminated if sufficient attention to detail is given, it is difficult to distinguish experimentally between errors due to categories 1, 2 and 3. Furthermore, although all the underlying phenomena of category 1 are reasonably well understood[6–10], a unified treatment of their effects on flow-rate in HPLC has yet to be presented. Although some non-ideal mobile phase and stationary phase effects on flow-rate were examined previously[6], the study was limited by design to theoretical calculations for pure solvents, which are seldom used as mobile phases in HPLC.

The purpose of the present work was the following: (1) to experimentally determine the flow-rate accuracy of modern HPLC systems; (2) to identify and describe quantitatively all the sources of error for the flow-rates and, if possible, to deconvolute the instrumental, mobile phase and stationary phase contributions; and (3) to develop a practical method for eliminating or at least minimizing flow-rate errors and the resultant systematic biases in flow-rate dependent parameters.

Due to both potentially larger flow-rate errors and the greater interest in reversed-phase (RP) liquid chromatography, we decided to investigate typical RP-HPLC solvent systems exclusively in this study, although the theory we present here is applicable to all liquid mobile phases. In future articles we plan to discuss the significance of these flow-rate errors on analytical and physicochemical measurements, including the effect of these flow-rate errors on the measurement of retention time and volume, and the possibility of extending the theory and our practical solution to normal-phase liquid chromatography and supercritical fluid chromatography.

THEORY

The theory for the mobile phase and stationary phase phenomena that give rise to flow-rate errors is described below.

Volume of mixing

When miscible solvents are mixed, the observed volume after mixing (V_{total}) is not always equal to the sum of the individual volumes (ΣV_i) due to attractive (or repulsive) interactions between the different solvent molecules. In general, ΔV_{mix} is negative ($V_{\text{total}} < \Sigma V_i$, attractive interactions) and this results in a negative deviation

in the flow-rate ($F_{observed} < F_{expected}$) according to eqn. 1 if the solvents are not pre-mixed.

$$F_{observed} = \frac{V_{total}}{\Sigma V_i} F_{expected} \tag{1}$$

For an ideal solution, $V_{total} = \Sigma V_i$, and thus we may write

$$\frac{F}{F_{ideal}} = \frac{V_{total}}{\Sigma V_i} \tag{2}$$

Because the magnitude of ΔV_{mix} is larger for reversed-phase solvents than for normal-phase chromatography, V_{total} will be smaller and the errors in flow-rate expressed by eqn. 2 will be larger for RP-HPLC. The more negative ΔV_{mix} values in RP-HPLC are attributed to the greater solvent–solvent interactions, *e.g.*, hydrogen bonding.

Katz *et al.*[10] measured the volumes of mixing for the three common RP-HPLC "binary" solvent systems (methanol–water, acetonitrile–water, and tetrahydrofuran–water) over the entire composition range and developed a theory which enables V_{total} to be predicted (with ΣV_i understood to be unity). They showed that these so-called binary solvent systems of methanol–water, acetonitrile–water, and tetrahydrofuran–water are really a more complex ternary system consisting of free organic solvent, M, free water, W, and associated organic solvent–water, MW. The equation for the calculation of V_{total} in eqn. 2 is

$$V_{total} = \Sigma f_i = f_m + f_w + f_{mw} \tag{3}$$

where Σf_i is the sum of the volume fractions of (free) organic solvent, f_m; (free) water, f_w; and associated organic–water, f_{mw}. The individual volume fractions in turn are calculated via eqns. 4–6

$$f_m = [M]V_m \tag{4}$$

$$f_w = [W]V_w \tag{5}$$

$$f_{mw} = [MW]V_{mw} \tag{6}$$

where the square brackets denote molar concentration and V denotes molar volume. The molar concentrations are calculated using eqns. 7–9

$$[W] = \frac{-\left(K + \frac{\varphi_{org}}{V_m} + \frac{\varphi_{org}}{V_w} - \frac{1}{V_w}\right) + \sqrt{\left(K + \frac{\varphi_{org}}{V_m} + \frac{\varphi_{org}}{V_w} - \frac{1}{V_w}\right)^2 + 4K\left(\frac{1}{V_w} - \frac{\varphi_{org}}{V_w}\right)}}{2} \tag{7}$$

$$[\mathrm{MW}] = \frac{1 - \varphi_{\mathrm{org}}}{V_{\mathrm{w}}} - [\mathrm{W}] \tag{8}$$

$$[\mathrm{M}] = \frac{\varphi_{\mathrm{org}}}{V_{\mathrm{m}}} - [\mathrm{MW}] \tag{9}$$

where K is the association constant of the organic solvent and water and φ_{org} is the apparent volume fraction of the organic solvent $= V_{\mathrm{org}}/(V_{\mathrm{org}} + V_{\mathrm{water}})$.

It should be noted here that the volume of mixing phenomenon is essentially independent of pressure, in contrast to solvent compressibility, the pressure coefficient of viscosity and other factors discussed below. Thus for a given temperature, only one calculation is required for each mobile phase composition.

Compressibility, pressure dependence of viscosity, deviations from Darcy's law, and column expansivity/packing compression

A couple of approaches in estimating these effects on the retention time and retention volume in liquid chromatography have already been described by Martin *et al.*[6]. By design their studies were limited to theoretical calculations for *pure solvents*. Moreover, the better approach they described required the use of an equation of state known as the Tait equation[11]. Unfortunately, an extensive literature search revealed that the parameters needed for the Tait equation are only available for certain pure solvents (including water and methanol, but not acetonitrile and tetrahydrofuran)[6] and are generally unavailable for mixtures of solvents. Because our study is concerned with typical HPLC mobile phases which are nearly always mixtures, we were thus precluded from using the Tait equation of state. The method we have developed is admittedly somewhat less rigorous than the Tait equation approach, but is much simpler (calculations can be done on a spreadsheet without numerical integration) and can be applied consistently to both pure solvents and binary mixtures. In addition, our study includes experimental data which shows that our approach is equally accurate (see below).

The starting point for our approach is Darcy's law (eqn. 10),

$$u = -\frac{B^0}{\varepsilon\eta}\frac{\mathrm{d}P}{\mathrm{d}z} \tag{10}$$

which relates the local linear velocity u of an unretained solute to the specific permeability B^0 and external porosity ε of the column, the viscosity η of the mobile phase and the local pressure gradient $\mathrm{d}P/\mathrm{d}z$. The negative sign in eqn. 10 indicates the linear velocity (and hence flow-rate) will be toward the region of lower pressure.

In calculating the effects of the various phenomena on the flow-rate, we shall assume that they are independent of one another. Although this is not always strictly true, our assumption results in negligible error because the effects of each of the phenomena are small. Later in this paper we shall demonstrate the accuracy of this approach for two mobile phase phenomena, compressibility and the pressure dependence of viscosity, which could be expected to exhibit a high degree of synergism. Since the assumption holds for this combination, it should hold for any other combination as well.

Since we are starting with Darcy's law, the results obtained for the various phenomena will be expressed in terms of linear velocities (u). These results will be equally applicable to flow-rate due to the relationship $F = uA_c$, where A_c is the cross-sectional area of the column (a constant for all intents and purposes). Thus the final equation obtained for a given phenomenon will frequently be expressed in terms of flow-rate in addition to linear velocity.

Mobile phase compressibility. Compressibility defines how the volume of a sample of matter decreases with increasing pressure. Obviously a gas is much more compressible than a liquid, but liquids may also be compressed. The net effect of mobile phase compressibility is an increase in flow-rate relative to an ideal solvent that is incompressible. This can be shown as follows, beginning with the mathematical definition of compressibility, β (readers only interested in the result should skip to eqn. 16).

$$\beta = -\frac{1}{V}\left(\frac{\partial V}{\partial P}\right)_T \tag{11}$$

(where T = temperature). Since $\partial V/\partial P$ is negative, β will always be positive. In previous treatments, the exact variation of solvent compressibility with pressure has been debated. Although it is generally agreed that the compressibility of a liquid does vary somewhat over a sufficiently wide range of pressure, the assumption of a constant compressibility ($d\beta/dP = 0$) is reasonable and leads to negligible error for pressures commonly encountered in HPLC ($\leqslant 5000$ p.s.i.)[6]. With that assumption, integration of eqn. 11 yields

$$V = V_o e^{-\beta(P - P_o)} \tag{12}$$

where the V and V_o are equimolar volume elements of the mobile phase at pressures P and P_o, where P_o is the outlet pressure and P is the pressure at some point before the outlet ($P > P_o$). Assuming the HPLC column is homogeneous and that its average cross-section A_c is independent of pressure (see ref. 6), a similar equation relates the local linear velocity u to the linear velocity at the column outlet u_o (eqn. 12a).

$$u = u_o e^{-\beta(P - P_o)} \tag{12a}$$

Substitution of eqn. 12a into eqn. 10 (Darcy's Law) yields

$$u_o e^{-\beta(P - P_o)} = -\frac{B^0}{\varepsilon \eta_c}\frac{dP}{dz} \tag{13}$$

where the subscript "c" for the viscosity means we have assumed it is a constant independent of pressure. Rearrangement and integration of eqn. 13 yields

$$u_o = \frac{B^0}{\varepsilon \eta_c L}\left(\frac{e^{\beta \Delta P} - 1}{\beta}\right) \tag{14}$$

where L = column length and $\Delta P = P_i$ (inlet pressure) $- P_o$ (outlet pressure). Since $\beta = 0$ for an ideal, incompressible liquid, we have

$$u_o(\text{ideal}) = \lim_{\beta \to 0}(u_o) = \frac{B^0}{\varepsilon \eta_c L} \lim_{\beta \to 0}\left(\frac{e^{\beta \Delta P} - 1}{\beta}\right) \tag{15}$$

Using L'Hospital's rule, we obtain

$$u_o(\text{ideal}) = \frac{B^0}{\varepsilon \eta_c L} \lim_{\beta \to 0}\left(\frac{\Delta P e^{\beta \Delta P}}{1}\right) = \frac{B^0 \Delta P}{\varepsilon \eta_c L} \tag{15a}$$

The relative deviation in linear velocity and hence, in flow-rate, is

$$\frac{F_o}{F_o(\text{ideal})} \approx \frac{u_o}{u_o(\text{ideal})} = \frac{1}{\beta \Delta P}(e^{\beta \Delta P} - 1) \tag{16}$$

which, by using $e^x = 1 + x + \frac{x^2}{2} + \frac{x^3}{3!} + \ldots$, can be transformed to

$$\frac{F_o}{F_o(\text{ideal})} \approx \frac{u_o}{u_o(\text{ideal})} = \left(1 + \frac{\beta \Delta P}{2} + \frac{(\beta \Delta P)^2}{6} + \frac{(\beta \Delta P)^3}{24} + \ldots\right) \tag{16a}$$

Since β and ΔP are always positive, the error in flow-rate due to mobile phase compressibility will always be positive.

Although isothermal compressibilities are known from a variety of pure solvents, they are generally unavailable for the binary mixtures in this study. Therefore it was assumed as before[9] that the compressibility of a binary mixture can be calculated from the compressibilities of the pure solvents, *i.e.*,

$$\beta_{\text{mixture}} = (1 - \varphi_{\text{org}})\beta_{\text{water}} + \varphi_{\text{org}}\beta_{\text{org}} \tag{17}$$

where φ_{org} represents the volume fraction of the organic strong solvent.

Pressure dependence of mobile phase viscosity. The effect of viscosity on flow-rate (via Darcy's law) and the variations of viscosity with mobile phase composition in HPLC are well known. What is sometimes overlooked by chromatographers is the pressure dependence of mobile phase viscosity. Because of the pressure dependence, a higher inlet pressure is required to reach the same flow-rate than that required by a mobile phase whose viscosity is independent of pressure. The net effect of the pressure dependence of viscosity is a decrease in flow-rate, as we shall now show (readers only interested in the result should skip to eqn. 23).

The pressure dependence of viscosity can be expressed as

$$\eta = \eta_o \exp(\alpha P) \tag{18}$$

where η is the viscosity at pressure P, η_o is the viscosity at standard pressure, and α is the pressure coefficient for the solvent. Substitution of eqn. 18 into eqn. 10 yields

$$u = -\frac{B^0}{\varepsilon\eta_o \exp(\alpha P)} \frac{dP}{dz} \tag{19}$$

which upon integration gives

$$u = \frac{B^0}{\varepsilon\eta_o L} \frac{[\exp(-\alpha P_o) - \exp(-\alpha P_i)]}{\alpha} \tag{20}$$

Since $\alpha = 0$ when the mobile phase viscosity is independent of pressure, we have

$$u(\text{ideal}) = \frac{B^0}{\varepsilon\eta_o L} \lim_{\alpha \to 0} \left\{ \frac{[\exp(-\alpha P_o) - \exp(-\alpha P_i)]}{\alpha} \right\} \tag{21}$$

Using L'Hospital's rule, we obtain

$$u(\text{ideal}) = \frac{B^0}{\varepsilon\eta_o L} \lim_{\alpha \to 0} \left[\frac{\alpha(P_i - P_o)}{\alpha} \right] = \frac{B^0 \Delta P}{\varepsilon\eta_o L} \tag{22}$$

The relative deviation in linear velocity (and flow-rate) is then

$$\frac{F}{F_{\text{ideal}}} \approx \frac{u}{u_{\text{ideal}}} = \frac{\exp(-\alpha P_i) - \exp(-\alpha P_o)}{\alpha \Delta P} \tag{23}$$

As before with compressibility the pressure coefficients of viscosity are generally available for pure solvents but not for mixtures. Thus in the absence of any other information we shall assume that the pressure coefficient of viscosity for a binary mixture can be calculated from the pressure coefficients of viscosity of the pure solvents, *i.e.*,

$$\alpha_{\text{mixture}} = (1 - \varphi_{\text{org}})\alpha_{\text{water}} + \varphi_{\text{org}}\alpha_{\text{org}} \tag{24}$$

The apparent validity of this assumption will be discussed later. Note that we are *not* assuming that the viscosity of a mixture varies linearly with pressure (it does not), but only that the *pressure coefficient of viscosity* varies in this manner. The *viscosities* of all mobile phases used in this study were obtained from experimental data (see eqns. 35–37 and related text).

Deviations from Darcy's law. Another potential source of flow-rate error in HPLC is the failure of Darcy's law at the relatively high reduced velocities (compared to gas chromatography) that are generally used. Martin *et al.*[6] also examined this phenomenon and showed that

$$\frac{F}{F_{\text{ideal}}} \approx \frac{u'}{u'_{\text{ideal}}} = \frac{1}{1 + \dfrac{1.75\rho d_p u'}{150\eta(1 - \varepsilon_e)}} \tag{25}$$

where u' is the superficial velocity, ρ and η are the density and viscosity of the mobile phase, ε_e is the interparticle porosity and d_p is the particle diameter. The superficial velocity u' is the linear velocity of the mobile phase within the column if the column packing was removed. It is given by the product of the linear velocity u and ε_e, where ε_e is the external porosity [$u' = (\varepsilon_e)u$]. Since $\varepsilon_e \approx 0.4$, u' will be *ca.* 40% of u.

Whereas errors due to volume of mixing effects are primarily dependent on the nature of the solvents being mixed and errors due to compressibility and viscosity effects are primarily dependent on the pressure drop (at a given temperature), the errors due to deviations from Darcy's law are directly dependent on several variables (ρ, η, d_p and u') which can have a wide range of values. The values we used for these parameters in our calculation of this effect were chosen so as to be typical for *analytical* (*cf.* preparative) HPLC separations at room temperature (*ca.* 25°C) and reversed-phase mobile phases. Our calculations revealed that for $u \leqslant 0.5$ cm/s ($u' \leqslant 0.2$ cm/s), $\varepsilon_e = 0.4 \pm 0.05$, d_p (particle diameter) $\leqslant 10$ μm, a temperature of 25°C, and all possible values of ρ and η for methanol–water, acetonitrile–water and tetrahydrofuran–water mobile phases, the error is always less than 0.12% and is therefore negligible compared to the other effects which are on the order of 1–6%. In the present study we used columns with $d_p \approx 5$ μm (other conditions as before), and the error was less than 0.06%. It should be noted, however, that there may be some separations for which deviations from Darcy's law are not negligible. These include (1) preparative-scale separations that utilize stationary phase particles with diameters in excess of 25 μm; and (2) high-temperature separations (>45°C) in which the kinematic viscosity (η/ρ) is very low.

Errors due to compression of the stationary phase and expansion of the column. Although the compressibility of a solid is less than that of a liquid, and although the elasticity of a solid (as defined by Young's modulus) is generally considered to be small, the effects of stationary phase compressibility and column expansivity are not always negligible. Their combined effect on linear velocity (and hence, flow-rate) was shown by Martin *et al.*[6] to be

$$\frac{F}{F_{ideal}} \approx \frac{u}{u_{ideal}} = 1 + \left[\frac{3\lambda_c}{\varepsilon_e} + \left(\frac{3}{\varepsilon_e} - \frac{5}{3}\right)\frac{\beta}{2}\right]\Delta P \tag{26}$$

where ε_e is the external porosity, β is the compressibility and λ_c is calculated from

$$\lambda_c = \frac{2}{Y_c\left[1 - \left(\frac{r_{int}}{r_{ext}}\right)^2\right]} \tag{27}$$

Y_c is Young's modulus of the column metal, and r_{int} and r_{ext} refers to the internal and external radius of the column, respectively. As shown in eqns. 26 and 27, the effect of column expansivity on flow-rate increases as the ratio of internal to external radius increases. Since the thickness of most stainless-steel analytical HPLC columns is *ca.* 1 mm, the ratio will vary from 0.3 to 0.7 for the typical inner diameter of 1 to 4.6 mm. Thus the column expansivity effect will generally be greater for the larger diameter columns.

Assuming a 4.6 mm I.D. column made of stainless steel ($Y_c \approx 2 \cdot 10^6$ atm) and

a stationary phase of silica or derivatized silica ($\beta = 2.72 \cdot 10^{-6}$ atm^{-1}), the column expansivity effect ranges from 0.1 to 0.9% over the pressure range 735–5000 p.s.i. (50–340 atm). Thus in precise work with conventional columns this effect may sometimes need to be accounted for.

Total error in flow-rate due to combined effect of all phenomena

Assuming that all of the various non-ideal phenomena which affect the flow-rate are small, they can be treated independently of one another and the overall effect on the flow-rate can be calculated as

$$F_{obs} = \left(\frac{F}{F_{ideal}}\right)_{total} F_{nominal} \tag{28}$$

where

$$\left(\frac{F}{F_{ideal}}\right)_{total} = \left(\frac{F}{F_{ideal}}\right)_{\Delta V_{mix}} \left(\frac{F}{F_{ideal}}\right)_{\beta} \left(\frac{F}{F_{ideal}}\right)_{\alpha} \left(\frac{F}{F_{ideal}}\right)_{Darcy} \left(\frac{F}{F_{ideal}}\right)_{column} \tag{29}$$

In eqn. 29, the relative deviations in flow-rate due to (i) volume of mixing, (ii) mobile phase compressibility, (iii) pressure dependence of viscosity, (iv) deviations in Darcy's law, and (v) column expansivity/packing compression are given by eqns. 2, 16, 23, 25 and 26. The data required to calculate these individual effects are given in Table I.

With the exception of the volume of mixing, all the phenomena discussed are interrelated via Darcy's law (eqn. 10), and the accuracy of the independent treatment of these effects may thus be questioned. However, we shall now show by comparing the results of two phenomena treated independently with the results obtained by considering the phenomena together (simultaneously) that the *independent treatment results in negligible error*. The two phenomena we have chosen are (1) the mobile phase compressibility and (2) the pressure dependence of mobile phase viscosity.

TABLE I

VOLUME OF MIXING, COMPRESSIBILITY AND VISCOSITY DATA FOR SOME RP-HPLC SOLVENTS

Solvent	*Volume of mixing*[a]			*Compressibility*[b] $\beta \cdot 10^6$/atm	*Viscosity*[c] $a \cdot 10^5$/atm
	K	V_m	V_{mw}		
Methanol	0.0045	40.68	55.46	127[6]	47.6[6]
Acetonitrile	0.206	52.25	53.26	74[15]	48.5(est.)
Tetrahydrofuran	0.0468	81.11	88.80	70[16]	53.0[17]
Water	–	18.00	–	46.3[6]	5.0[6]

[a] See eqns. 1–9 and related text. Data obtained from ref. 10.

[b] See eqns. 16 and 17. Numbers in brackets indicate references from which data were obtained. The viscosities may be obtained via eqns. 35–37.

[c] Pressure coefficient of viscosity. Refer to eqn. 18 and related equations. Numbers in brackets indicate references from which data were obtained.

Simultaneous treatment of compressibility and pressure-dependent viscosity effects on flow-rate. These effects can be treated simultaneously by substitution of eqns. 12a and 19 into eqn. 10. The resulting equation

$$u_o = \frac{B^0 e^{\beta(P-P_o)}}{\varepsilon\eta_o e^{\alpha P}} \frac{dP}{dz} \tag{30}$$

can be integrated to yield

$$u_o = \frac{B^0}{\varepsilon\eta_o L} \frac{e^{-\beta P_o}}{\beta - \alpha}[e^{(\beta-\alpha)P_o} - e^{(\beta-\alpha)P_i}] \tag{31}$$

Since $\alpha, \beta = 0$ for an incompressible liquid whose viscosity is independent of pressure, we have

$$u_o(\text{ideal}) = \frac{B^0}{\varepsilon\eta_o L} \lim_{\alpha,\beta\to 0} \left[\frac{e^{-\beta P_o}(e^{(\beta-\alpha)P_o} - e^{(\beta-\alpha)P_i})}{\beta - \alpha}\right] \tag{32}$$

The first term of the numerator (within brackets) goes to unity. Using L'Hospital's rule for the remaining expression, we obtain

$$u_o(\text{ideal}) = \frac{B^0}{\varepsilon\eta_o L} \lim_{\alpha,\beta\to 0} \left[\frac{e^{(\beta-\alpha)P_o} - e^{(\beta-\alpha)P_i}}{1}\right] = \frac{B^0}{\varepsilon\eta_o L}(P_o - P_i) \tag{33}$$

The relative deviation in linear velocity (and flow-rate) is then

$$\frac{F}{F_{\text{ideal}}} \approx \frac{u_o}{u_{o_{\text{ideal}}}} = \frac{e^{-\beta P_o}\{e^{(\beta-\alpha)P_o} - e^{(\beta-\alpha)P_i}\}}{(\beta - \alpha)(P_o - P_i)} \tag{34}$$

Results for eqn. 34 are shown in Table II along with results obtained previously by Martin *et al.*[6] as well as the results obtained when we treated the compressibility and pressure-dependent viscosity effects separately (eqns. 16 and 23) and then simply combined (multiplied) them.

As shown in Table II, the results of our simultaneous treatment of mobile phase compressibility and the pressure-dependence of viscosity (eqn. 34) are in good agreement with those of Martin *et al.*. More importantly, virtually the same results are obtained with the independent approach (multiplication of eqns. 16 and 23), indicating that a negligible error results from the independent treatment of (1) mobile phase compressibility and (2) the pressure dependence of viscosity effects. *Given the accuracy of the independent approach for these two highly interrelated phenomena, any errors resulting from the independent treatment of the remaining phenomena will undoubtedly be even smaller ($<0.05\%$), and thus completely negligible.* Note that for simplicity we used eqn. 34 instead of eqns. 16 and 23 in all subsequent calculations of $\left(\frac{F}{F_{\text{ideal}}}\right)_{\text{total}}$.

TABLE II

COMPARISON OF CALCULATED FLOW-RATE DEVIATIONS BASED ON THE EFFECTS OF MOBILE PHASE COMPRESSIBILITY AND THE PRESSURE DEPENDENCE OF MOBILE PHASE VISCOSITY[a]

	Water	*Methanol*	*Blend*[b]
$\frac{F(\beta)}{F_{ideal}}$ (eqn. 16)	1.0046	1.0124	1.0085
$\frac{F(\alpha)}{F_{ideal}}$ (eqn. 23)	0.9947	0.9553	0.9745
$\frac{F(\beta)}{F_{ideal}} \cdot \frac{F(\alpha)}{F_{ideal}}$	0.9993	0.9672	0.9828
$\frac{F(\beta,\alpha)}{F_{ideal}}$ (eqn. 34)	0.9991	0.9669	0.9826
$\frac{F(\beta,\alpha)}{F_{ideal}}$ (ref. 6)	0.9991	0.9660	–

[a] Pressure drop = 200 bar (≈2900 p.s.i.). Other conditions and parameters as in ref. 6 to permit comparison. Slightly different conditions and values of parameters were used in subsequent figures and tables.

[b] Water–methanol (50:50, v/v). Compressibilities and pressure coefficients of viscosity calculated using eqns. 17 and 24.

EXPERIMENTAL

HPLC systems

Flow-rates were measured on two types of chromatographic systems. System A was a high-pressure mixing ternary HPLC system with three identical single-piston high-pressure reciprocating pumps. Each pump head was of 5-ml capacity with a flow-rate range of 0.005–5 ml/min and a stroke volume of 40 μl. Flow through the pump cylinder was controlled by two ball check valves which allow flow in only one direction. System B was a low-pressure mixing quaternary HPLC system which employs a set of four solenoid valves to proportion the individual mobile phase components before they enter the single-piston high-pressure pump. The pump head was of 10-ml capacity with a flow-rate range of 0.01–10 ml/min and a stroke volume of 100 μl. Flow through the pump head was controlled by three check valves. Pump settings on both chromatographs were optimized for minimum pulsation, flow-rate accuracy, solvent compressibility, and/or minimum vapor lock as recommended by the manufacturer for reversed-phased systems.

Reversed-phase C_8 or C_{18} columns (Rainin, Woburn, MA, U.S.A.) with dimensions 150 mm × 4.6 mm I.D. and a particle diameter of 5 μm were used to provide the pressure drops typically encountered. At a flow-rate of 2 ml/min, the pressure ranged from 770 to 4520 p.s.i.

Mobile phase preparation

Mobile phase components acetonitrile (ACN), methanol (MeOH) and tetrahydrofuran (THF) were HPLC grade. Water used was either HPLC grade or triply distilled and doubly deionized. All mobile phase components were filtered through 0.22-μm or 0.45-μm Nylon-66 filters and degassed before use. Mobile phase components were degassed individually either by sparging with helium or by heating in an ultrasonic bath under a partial vacuum.

Flow-rate measurement

Flow-rates of methanol–water, acetonitrile–water and tetrahydrofuran–water mixtures were measured at 25% organic intervals from 0–100% organic. Flow-rates were measured both volumetrically (volume/time) and gravimetrically (mass/time $\div$ density). The volume of a previously calibrated 10-ml graduated cylinder was read to the nearest 0.05 ml and time was measured to the nearest second. Weighings were performed to the nearest 0.1 mg on an analytical balance (Mettler, Hightstown, NJ, U.S.A.) and were made immediately following collection to minimize any errors due to evaporation. Densities of the pure solvents and mixtures were obtained from ref. 12. In general the agreement between volumetric and gravimetric flow-rates was very good ($\Delta < 0.2\%$), and experimental results are shown only in terms of the measured volumetric flow-rates.

RESULTS AND DISCUSSION

As explained in the Experimental section, we have elected to illustrate the errors in flow-rate (theoretically predicted and experimentally measured) on a (nominally) constant flow-rate basis.

Predicted flow-rate errors

As noted earlier, the data required to calculate the individual effects of (i) volume of mixing, (ii) mobile phase compressibility, (iii) pressure dependence of viscosity, (iv) deviations in Darcy's law, and (v) column expansive/packing compression on flow rate for the binary mobile phases of methanol–water, acetonitrile–water or tetrahydrofuran–water are given in Table I. These effects were then calculated using eqns. 2, 16, 23, 25, and 26, and except for negligible deviations in Darcy's law (see discussion in Theory) are illustrated in Fig. 1.

As shown in Fig. 1a, errors in flow-rate due to volume of mixing effects usually exceed -1.5% in RP-HPLC, and in the case of methanol–water mixtures can be as negative as -3.5% at a methanol content of 60–65%. That methanol–water mixtures give the largest flow-rate errors is not surprising, since the attractive forces required for negative volumes of mixing are largest with methanol mixtures because of greater hydrogen bonding. Flow-rate errors are smallest for acetonitrile–water mixtures, for which the error never exceeds -2.0%.

Whereas errors in flow-rate due to volume of mixing effects are independent of the pressure drop ΔP across a column, the errors due to the remaining effects depend greatly on the value of ΔP. Since for a given flow-rate ΔP varies with viscosity according to eqn. 10 and since viscosity varies with mobile phase composition, we assumed for convenience a value of 2000 p.s.i. for ΔP for the 100% aqueous phase (no

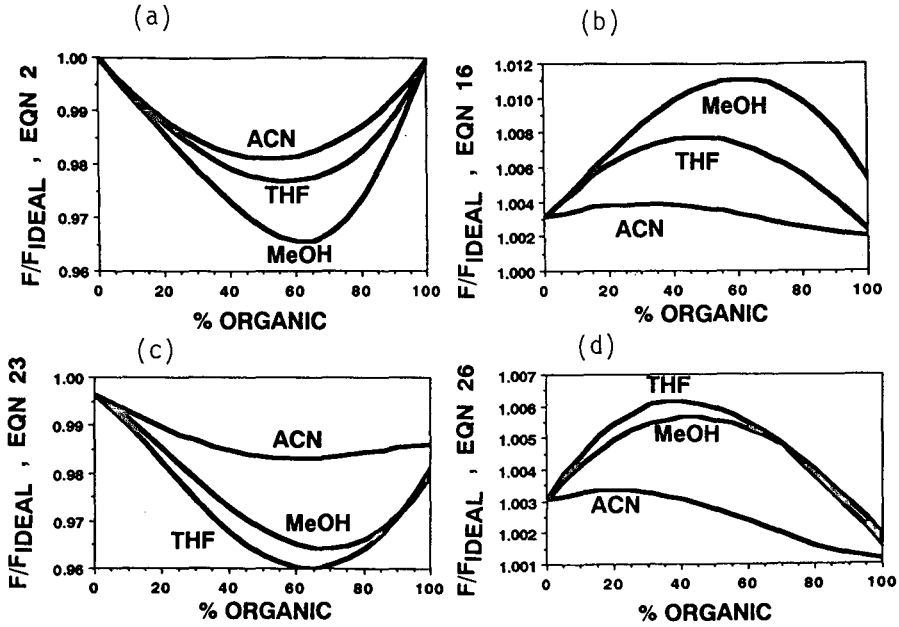

Fig. 1. Effect of (a) volume of mixing (organic solvent+ water); (b) mobile phase compressibility; (c) pressure dependence of mobile phase viscosity; and (d) column expansivity/packing compression on flow-rate for three common reversed-phase solvent systems. See eqns. 2, 16, 23 and 26. Comparisons are based on equal nominal flow-rates for all mobile phases and a pressure drop of 2000 p.s.i. for pure water. Pressures at other mobile phase compositions were calculated from viscosity data; see eqns. 35–37 and related text.

organic solvent). All other ΔP values for organic-water mixtures (or pure organic solvents) were calculated according to $\Delta P_{\text{org–water}} = \Delta P_{\text{water}} (\eta_{\text{org-water}}/\eta_{\text{water}})$. The viscosities (centipoise, cP) for the mixed mobile phases were calculated from the polynomial expressions below, which were obtained from curve fits of experimentally measured data[13,14].

$$\eta_{\text{MeOH–water}} = 0.875 + 0.03644\,(\%\text{MeOH}) - 4.762 \cdot 10^{-4}\,(\%\text{MeOH})^2 + \\ + 7.809 \cdot 10^{-7}\,(\%\text{MeOH})^3 \qquad (35)$$

$$\eta_{\text{ACN–water}} = 0.907 + 0.01016\,(\%\text{ACN}) - 3.218 \cdot 10^{-4}\,(\%\text{ACN})^2 + \\ + 1.665 \cdot 10^{-6}\,(\%\text{ACN})^3 \qquad (36)$$

$$\eta_{\text{THF–water}} = 0.846 + 0.04821\,(\%\text{THF}) - 7.548 \cdot 10^{-4}\,(\%\text{THF})^2 + \\ + 2.313 \cdot 10^{-6}\,(\%\text{THF})^3 \qquad (37)$$

The effect of mobile phase compressibility on flow-rate is illustrated in Fig. 1b. Because the errors resulting from this effect are positive, they compensate somewhat

for the errors due to the volume of mixing effect (Fig. 1a) which are negative. This compensation is incomplete, however, since these errors are typically 2.5 times smaller (usually $< 1\%$). As observed with the volume of mixing effect, the largest errors due to mobile phase compressibility were observed with the methanol–water mobile phases and the smallest with acetonitrile–water. Note that although water is the least compressible solvent (see Table I), the relative error in flow-rate due to compressibility is somewhat larger with pure water than with acetonitrile or tetrahydrofuran, and is comparable to methanol. This apparent anomaly is explained by the greater viscosity of water, which for a given flow-rate requires a higher pressure drop (ΔP). The larger ΔP gives rise to a larger flow-rate error in eqn. 16.

The effect of the pressure dependence of viscosity on flow rate is illustrated in Fig. 1c. Once again, the smallest errors are observed for the acetonitrile–water mobile phases (-0.4 to -1.5%), but in contrast to what is seen previously, however, the largest errors are observed with tetrahydrofuran–water instead of methanol–water, although the difference is slight (-4% *vs.* -3.5%). The difference in the flow-rate errors for these mixed mobile phases are *not* due to differences in the pressure coefficients of viscosity for the organic solvents (they are all about the same, see Table I), but to differences in the pressures required for the same flow-rate because of the different viscosities of the mixed mobile phases (*cf.* eqns. 35–37). The different ΔP values give rise to different flow-rate errors in eqn. 23.

The effect of column expansion/packing compression on flow-rate is illustrated in Fig. 1d. As expected, the errors are considerably larger for the tetrahydrofuran–water and methanol–water mixtures than for the acetonitrile–water mixtures, since this effect depends strictly on the pressure drop which is considerably smaller for the latter. Note however, that this effect is the smallest of the four illustrated (*cf.* Fig. 1a–c), with the largest error barely exceeding 0.6% for a mobile phase of 35% tetrahydrofuran (at 3800 p.s.i.).

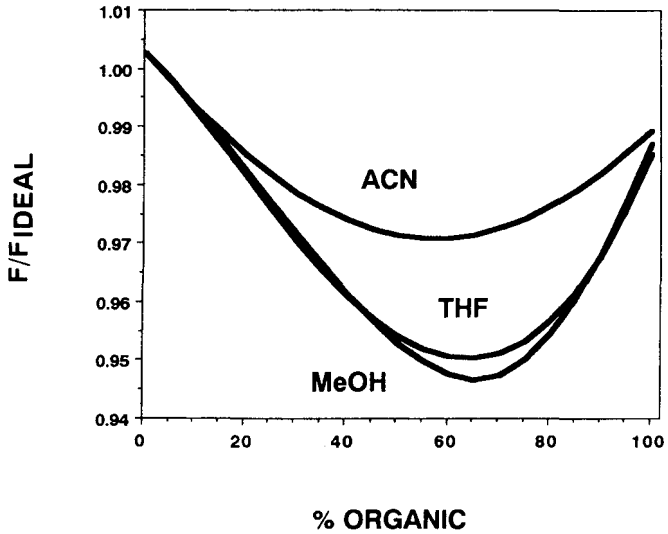

Fig. 2. Total predicted error in flow-rate due to the combined effects of the phenomena in Fig. 1. See also eqn. 29. Conditions as in Fig. 1.

The total error in flow-rate resulting from the combined effects of all phenomena as calculated via eqn. 29 is illustrated in Fig. 2. The lowest errors were obtained for pure water (+0.3%), followed by the pure organic solvents ($\approx$ −1.5%), and then the hydro-organic mixtures (−2 to −5.5%). These results were generally expected, since water is the least compressible of all the solvents employed in this study, and its viscosity is also the least dependent on the pressure. Also, for pure solvents there is no volume of mixing effect.

Given the large compressibilities and pressure coefficients of viscosity of the pure organic solvents relative to those of water and the hydro–organic mixtures, it may first seem surprising that the corresponding errors in flow-rate are not larger for the pure organic solvents than what are shown in Fig. 2. This apparent discrepancy is explained by the much lower viscosities of these pure solvents, and the compensatory effect that the resulting smaller pressure drops has on the various flow-rate effects.

Among the hydro-organic mobile phases, the total errors in flow-rate predicted for the tetrahydrofuran–water and methanol–water phases are nearly twice as large as those predicted for the acetonitrile–water mixtures. This is due primarily to two factors. First, the volume of mixing effect is much larger. Second, the "viscosity hump" observed for the tetrahydrofuran–water or methanol–water mixtures is much larger than for the acetonitrile–water mixture. As noted before, the higher viscosities translate into higher pressure drops, which in turn result in larger flow-rate errors, as seen from eqns. 16, 23 and 26.

Experimentally observed flow-rates

Fig. 3 and 4 show the experimentally measured flow-rates (open symbols) along with the corrected values (closed symbols) for a low-pressure and a high-pressure mixing HPLC system. In general, the uncorrected flow-rates in Figs. 3 and

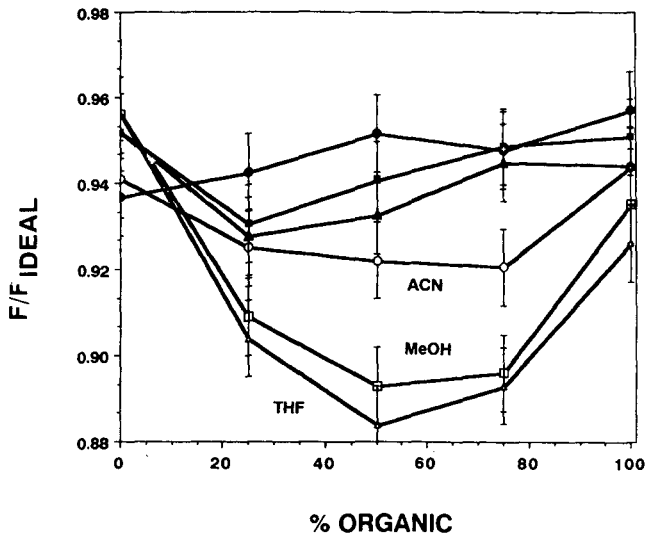

Fig. 3. Comparison of uncorrected (open symbols) and corrected (closed symbols) flow-rates for a low-pressure mixing HPLC system. Error bars represent one standard deviation. Organic solvents: methanol (■, □), acetonitrile (●, ○), and tetrahydrofuran (▲, △).

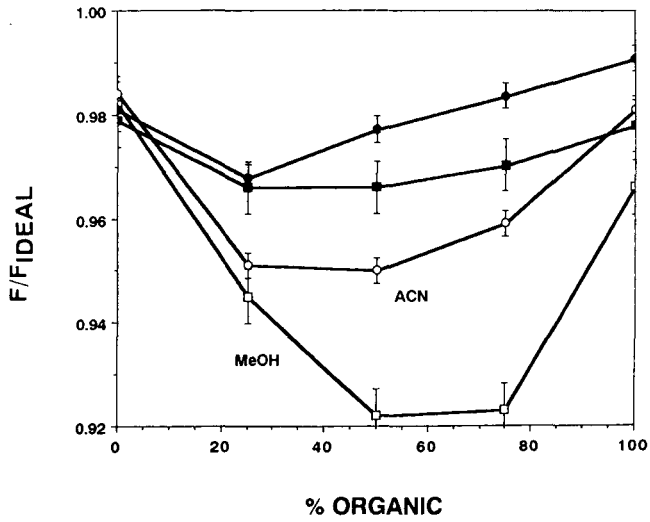

Fig. 4. Comparison of uncorrected (open symbols) and corrected (closed symbols) flow-rates for a high-pressure mixing HPLC system. Symbols as in Fig. 3.

4 correspond very closely to those predicted in Fig. 2, although they are all 2–4% more negative than predicted. Although our uncorrected experimental results in Fig. 3 for tetrahydrofuran–water and methanol–water appear to be reversed from Fig. 2 (larger error for tetrahydrofuran–water instead of slightly smaller), a closer inspection reveals that the differences are within experimental error.

The near-constancy of the corrected flow-rates (within experimental error) shown in Fig. 3 and 4 illustrates the success of our correction factor approach. As shown, the variations in flow-rate have been reduced from 8 to 2% or less, and the systematic negative deviations observed with the hydro-organic mixtures have virtually been eliminated. Unfortunately, the corrected flow-rates are still biased toward low values, indicating that either our theoretical corrections are incomplete or, more likely, that instrumental contributions to errors in flow-rate cannot be assumed to be negligible. Because we obtained different biases with the low-pressure and high-pressure HPLC systems, we are confident that the observed biases are due primarily to instrumental effects.

To date we have been unsuccessful in identifying any specific instrumental contributions to the biases observed in the flow-rates. It is difficult to model instrumental contributions due to the wide variety of pump designs employed in commercial HPLC instrumentation. Two non-instrumental effects which can be disregarded immediately, however, are (1) mobile phase evaporation and (2) inaccurate volumetric glassware. These effects can be discounted simply because they do not explain the results we observed for the corrected flow-rates. If mobile phase evaporation had been a problem, we would have expected to see a skewing of the flow-rate errors in the direction of higher organic solvent content, since all the organic solvents studied evaporate much more quickly than water. However, no such skewing is evident in the data in Fig. 3 and 4. Likewise, if inaccurate volumetric glassware had

been the problem, our gravimetric and volumetric flow-rate measurements would not have been consistent within experimental error (see Experimental section).

As shown in Figs. 3 and 4, the high-pressure mixing HPLC pumping system provided a somewhat higher flow-rate accuracy for all three binary mobile phases over the entire solvent composition range. However, one should not infer from these results that all high-pressure mixing HPLC pumping systems will always be more accurate than all low pressure mixing systems. Our results are based on the comparison of only one model/brand of each type of HPLC solvent delivery system and can only be considered tentative at best. The main point to be appreciated is that both types of HPLC systems may contribute significantly to the total error in flow rate.

Correcting for errors in flow-rate

Since the phenomena described above cannot be eliminated entirely for any combination of known mobile and stationary phases, the best that we can hope to do is to correct for these errors based on what we have predicted theoretically. Thus we propose the use of correction factors based on the theory summarized by eqn. 29. Depending on whether they are being used on a post-run or a pre-run basis, the correction factor is given by the left hand side of eqn. 29 or its reciprocal, respectively. In the *post-run* mode, the correction factor would be used to calculate the *actual-flow-rate* from the current (nominal) setting of the HPLC system, as shown in eqn. 38.

$$F_{\text{actual}} = \left(\frac{F}{F_{\text{ideal}}}\right)_{\text{total}} F_{\text{setting}} \tag{38}$$

In the *pre-run* mode, the correction factor would be used to calculate a *flow-rate setting* for the HPLC so that an accurate desired flow rate is obtained, as shown in eqn. 39. This pre-run correction factor

$$F_{\text{setting}} = \left(\frac{F_{\text{ideal}}}{F}\right)_{\text{total}} F_{\text{desired}} \tag{39}$$

approach amounts to the use of flow-rate programming to compensate for predictable flow-rate errors.

For ease of use, the correction factors can be organized into tables according to experimental conditions (pressure drops, mobile phase composition, stationary phase parameters). If done for a sufficient number of pressure drops and mobile phase compositions, correction factors for pressure/composition combinations not provided in the tables could be obtained by linear interpolation. Since for a given set of conditions the pre-run and post-run correction factors are just reciprocals of each other, only one type needs to be reported. In the tables that follow, we report *pre-run* correction factors for the convenience of those who wish to conduct constant flow-rate experiments in the future.

Since column expansivity/packing compression is independent of mobile phase composition for a given pressure drop, it is convenient to separate the correction factors arising from the stationary phase phenomenon from those resulting from the

mobile phase. This separation permits column-related corrections factors to be tabulated in a concise manner for more than one ratio of inner to outer column radius. This is highly desirable since this ratio varies considerably among the plethora of commercially available HPLC columns.

Shown in Table III are the pre-run column expansion/packing compression correction factors for silica-based, stainless-steel RP-HPLC columns. A ratio of internal to external column radius ranging from 0.3 to 0.9 was assumed, corresponding roughly to 1–5 mm I.D. and a column wall thickness of about 1 mm. As shown in Table III, for a constant column wall thickness, the error in flow-rate increases exponentially with the column radius.

TABLE III

FLOW-RATE CORRECTION FACTORS (PRE-RUN) FOR COLUMN EXPANSION/PACKING COMPRESSION[a]

r_{int}/r_{ext}	*Pressure (p.s.i.)*						
	100	*500*	*1000*	*2000*	*3000*	*4000*	*5000*
0.30	0.9999	0.9994	0.9989	0.9988	0.9967	0.9956	0.9945
0.50	0.9999	0.9994	0.9988	0.9986	0.9963	0.9951	0.9939
0.70	0.9998	0.9992	0.9985	0.9969	0.9954	0.9938	0.9923
0.80	0.9998	0.9990	0.9980	0.9961	0.9941	0.9922	0.9902
0.85	0.9998	0.9988	0.9976	0.9952	0.9929	0.9905	0.9882
0.90	0.9997	0.9984	0.9968	0.9936	0.9903	0.9873	0.9842

[a] Conditions: stainless-steel HPLC column (Young's modulus $\approx 2 \cdot 10^6$ atm) with silica based packing ($\varepsilon_e \approx 0.4$, $\beta = 2.72 \cdot 10^{-6}$ atm^{-1}. Refer to eqns. 26 and 27 in text.

Shown in Tables IV–VI are the pre-run mobile phase correction factors for methanol–water, acetonitrile–water and tetrahydrofuran–water. Each correction factor listed is the product of the individual correction factors for the (i) volume of mixing, (ii) mobile phase compressibility, and (iii) pressure-dependence of viscosity, taken from the reciprocals of eqns. 2 and 34. As mentioned earlier, errors resulting from deviations in Darcy's law are generally negligible ($<0.06\%$ in our study); for this reason they were not incorporated into our correction factors.

Other discussion

Post-run vs. pre-run correction of flow-rate errors. Whereas good accuracy can be obtained by using either pre- or post-run correction factors, a near constant flow-rate can only be achieved if flow-rate errors are corrected on a pre-run basis. For best results, we recommend the following procedure. First, measure the pressure drop under the desired conditions of mobile phase and nominal (uncorrected) flow-rate. Next, calculate a correction factor based on this observed pressure drop and adjust the flow-rate setting accordingly. If the adjustment of the flow-rate setting results in a change in pressure drop of more than 10–20%, it may be necessary to recalculate the correction factor using the new observed pressure drop and adjust the flow-rate again.

TABLE IV

FLOW-RATE CORRECTION FACTORS (PRE-RUN) FOR METHANOL–WATER[a]

Methanol (%)	*Pressure (p.s.i.)*						
	0	*500*	*1000*	*2000*	*3000*	*4000*	*5000*
0	1.000	1.000	1.000	1.000	1.000	1.001	1.001
10	1.007	1.008	1.009	1.010	1.011	1.013	1.014
20	1.014	1.016	1.017	1.020	1.022	1.025	1.027
25	1.018	1.020	1.021	1.024	1.027	1.031	1.034
30	1.021	1.023	1.025	1.029	1.033	1.036	1.040
40	1.028	1.030	1.033	1.038	1.043	1.048	1.053
50	1.033	1.036	1.039	1.045	1.052	1.058	1.064
60	1.035	1.039	1.043	1.051	1.058	1.066	1.073
70	1.034	1.039	1.043	1.052	1.060	1.069	1.078
75	1.031	1.036	1.041	1.050	1.059	1.069	1.078
80	1.026	1.032	1.037	1.047	1.057	1.067	1.077
90	1.014	1.020	1.026	1.037	1.048	1.059	1.070
100	1.000	1.006	1.012	1.024	1.037	1.049	1.061

[a] See eqns. 29 and 39. Temperature assumed to be 25°C, although these correction factors are believed to be valid over the range 20–45°C.

Possible limitations of the correction factor approach. At this time we would like to discuss several questions which may come to mind about potential shortcomings about our approach. As the reader will see, many of these "problems" are either misconceptions about our approach or are easily solved or circumvented.

(1) Are the data needed to calculate the correction factors available or known precisely? As mentioned in this report, the data necessary for our approach are

TABLE V

FLOW-RATE CORRECTION FACTORS (PRE-RUN) FOR ACETONITRILE–WATER[a]

Acetonitrile (%)	*Pressure (p.s.i.)*						
	0	*500*	*1000*	*2000*	*3000*	*4000*	*5000*
0	1.000	1.000	1000	1.000	1.000	1.001	1.001
10	1.006	1.007	1.008	1.009	1.011	1.013	1.014
20	1.012	1.013	1.015	1.018	1.020	1.023	1.026
25	1.014	1.016	1.017	1.021	1.025	1.028	1.032
30	1.015	1.018	1.020	1.024	1.029	1.033	1.038
40	1.018	1.021	1.024	1.030	1.036	1.041	1.047
50	1.019	1.023	1.026	1.034	1.041	1.048	1.056
60	1.019	1.023	1.027	1.036	1.045	1.054	1.062
70	1.016	1.022	1.027	1.037	1.047	1.057	1.068
75	1.015	1.020	1.026	1.037	1.047	1.058	1.069
80	1.013	1.019	1.024	1.036	1.047	1.059	1.071
90	1.007	1.014	1.020	1.033	1.046	1.059	1.072
100	1.000	1.007	1.015	1.029	1.043	1.057	1.072

[a] Conditions as in Table IV.

TABLE VI

FLOW-RATE CORRECTION FACTORS (PRE-RUN) FOR THF–WATER[a]

THF (%)	*Pressure (p.s.i.)*						
	0	*500*	*1000*	*2000*	*3000*	*4000*	*5000*
0	1.000	1.000	1.000	1.000	1.000	1.001	1.001
10	1.007	1.008	1.008	1.010	1.012	1.013	1.015
20	1.012	1.014	1.016	1.019	1.022	1.026	1.029
25	1.015	1.017	1.019	1.023	1.027	1.031	1.036
30	1.017	1.020	1.022	1.027	1.032	1.037	1.042
40	1.021	1.024	1.028	1.034	1.041	1.047	1.054
50	1.023	1.027	1.031	1.040	1.048	1.056	1.064
60	1.023	1.029	1.033	1.043	1.053	1.063	1.173
70	1.022	1.028	1.033	1.045	1.056	1.068	1.079
75	1.020	1.026	1.032	1.044	1.057	1.069	1.081
80	1.017	1.024	1.031	1.044	1.057	1.070	1.083
90	1.010	1.018	1.025	1.040	1.054	1.069	1.084
100	1.000	1.008	1.016	1.032	1.048	1.064	1.081

[a] Conditions as in Table IV.

generally available in the literature for pure solvents, although not necessarily for mixed solvent systems. Accurate estimates of the pertinent properties of mixed mobile phases can obtained via equations similar to eqns. 17, 24, and 35–37; alternatively, most of the data are easily measured. Although few reports prior to our study, if any, have confirmed the assumption represented by eqn. 24, our results discussed earlier (the near-constancy of the corrected flow-rates in Figs. 3 and 4) do support this assumption. For the volume of mixing phenomenon, although a well established theory or experimental data are not always available for every possible binary mobile phase, the phenomenon is easily measured as demonstrated by Katz *et al.*[10]. In the case of normal-phase solvents, the volume of mixing may be small enough to be neglected.

(2) Due to the temperature dependence of the physical properties of the phenomena which affect the flow-rate, will the approach require the generation of a set of correction factors at every different temperature of interest? Over the most widely used range of temperatures in HPLC (20–45°C), the change in the pertinent physical properties (β, α, ρ) of the mobile and stationary phase is actually only slight (generally $\leqslant 15\%$). Thus even for extremely accurate work, the correction factors presented in Tables III–VI (for $T = 25$°C) are likely to suffice over the entire 20–45°C range. Note that although mobile phase viscosity is strongly temperature dependent, it does not directly impact any phenomenon except for deviations in Darcy's law, which as discussed earlier is negligible over this temperature interval.

For temperatures exceeding 45°C, errors in flow-rate due to the various pressure-dependent phenomena should be considerably smaller because of the lower mobile phase viscosities and corresponding smaller pressure drops. These errors may or may not be negligible relative to the errors due to non-zero volumes of mixing and deviations from Darcy's law, depending on the specific experimental conditions. As noted earlier, deviations from Darcy's law may no longer be negligible but are easily

estimated from the kinematic viscosities and eqn. 25 and are likely to be reasonably constant for a given mobile phase; volumes of mixing are easily measured.

(3) Can the approach be used with gradient elution? Although we have not yet examined errors in flow-rate during gradient elution, it is likely that our pre-run correction factor approach can be used successfully with gradient elution to provide a more constant flow-rate. We envision its application as follows. First, a trial of the desired gradient is run to permit the measurement of the pressure drop across the HPLC column at several intervals (different compositions of mobile phase) during the gradient. Based on the measured pressure drops and the corresponding average mobile phase (mobile phase at the midpoint of the column for a linear gradient), a series of pre-run correction factors is then calculated and incorporated into the flow-rate settings at each of the intervals. An example of this approach is shown in Table VII.

TABLE VII

EXAMPLE OF USE OF PRE-RUN CORRECTION FACTORS TO ACHIEVE A CONSTANT FLOW-RATE OF 1.50 ml/min DURING REVERSED-PHASE GRADIENT ELUTION WITH METHANOL–WATER

Time (min)[a]	*Methanol (%)*[b]	*Pre-run correction factors*			
		ΔP (p.s.i.)[c]	*Table III*	*Table IV*	*Flow-rate setting*[d]
0	20	3245	0.9936	1.023	1.560
2	30	3570	0.9930	1.035	1.577
4	40	3705	0.9928	1.047	1.595
6	50	3670	0.9928	1.054	1.606
8	60	3465	0.9932	1.062	1.619
10	70	3110	0.9939	1.061	1.618
12	80	2610	0.9949	1.053	1.608
14	90	1980	0.9961	1.037	1.585
16	100	1620	0.9968	1.019	1.559

[a] Retention time for an unretained solute assumed to be 1 min.

[b] Arbitrary, but typical gradient of 5%/min.

[c] In this example, ΔP was calculated as discussed in the Experimental section, assuming a value of 2000 p.s.i. at 0% methanol. In practice, ΔP would be measured at each solvent composition as discussed in the Results and Discussion section.

[d] Product of the pre-run correction factors from Table III, Table IV, and an instrumental correction factor arbitrarily assumed to be 1.023 in this example. Correction factors from Tables III and IV obtained by interpolation.

An operationally simpler approximation to this procedure for correction which may be sufficiently accurate for gradient elution flow-rates is (1) to estimate the changes in pressure drops of the mobile phase gradient from known changes in viscosity (for temperatures $\approx$25°C, eqns. 35–37 can be used) and (2) to assume that the average mobile phase experienced by the column at any time is equivalent to the mobile phase composition at the gradient mixer at that same instant. The latter assumption is reasonable provided the gradient delay volume is small and/or the gradient is shallow.

(4) Can the approach be used with ternary mobile phases? Although in principle the approach we have developed for binary mobile phases could be adapted to ternary solvent systems, it would admittedly be somewhat less practical, since it would require a matrix of mobile phase correction factor tables (10 or so) organized according to the pressure drop and the percentage of the second and third solvents instead of just one mobile phase correction factor table like those of Tables IV–VI.

(5) Is the instrumental contribution to flow-rate error accounted for explicitly by our approach? It is difficult if not impossible to develop a general model for instrumental contributions to flow-rate errors because of the wide variety of pump designs employed in commercial HPLC instrumentation. Presumably, however, the instrumental contribution is the error remaining in the corrected flow-rates, since as shown in Figs. 3 and 4 this error is essentially constant and more or less independent of the organic solvent. Thus although our approach does not allow the instrumental contribution to be predicted from theory, it does provide a means for measuring it experimentally.

(6) Will similar errors in flow-rate be observed using HPLC equipment other than that of the present study? Probably. The mobile and stationary phase contributions to flow-rate error are by definition HPLC-independent, and since they account for roughly half of the total error in flow-rate, we would expect at least moderately similar results regardless of the equipment used. A more definitive answer requires knowledge of the instrumental contributions of *all* HPLC systems, which as noted above in (5) is impossible to predict and is clearly beyond the scope of the present study. We recognize that more HPLC systems need to be examined, and we encourage others to report results for their HPLC systems using our approach (we are also planning additional studies). It is conceivable that, for some systems not examined in the present study, the instrumental contribution will not be constant but will depend on the mobile phase composition.

If the instrumental contribution turns out to be similar for all HPLC systems, then of course errors in flow-rate for all HPLC systems will be very similar. If not, flow-rate errors may vary somewhat from instrument to instrument, depending on the relative contributions from the solvent delivery system and the mobile and stationary phases. Certainly a desirable goal for HPLC manufacturers would be the design of new solvent delivery systems or modification of existing ones so that, if used properly, they contribute negligibly to errors in flow-rate.

CONCLUSION

The theory of Katz *et al.*[10] and Martin *et al.*[6] was adapted to explain the majority of the errors in flow-rate commonly observed (but typically unreported) in RP-HPLC for the three most popular binary mobile phases: methanol–water, acetonitrile–water and tetrahydrofuran–water. Although all three hydro–organic mobile phases give rise to significant errors in flow-rate, the acetonitrile–water mobile phases typically result in distinctly lower errors (2–3%) than the other binary mobile phases (3–5%) and are generally to be preferred if flow-rate accuracy is somewhat important but, for whatever reason, the corrections described here cannot be applied. Instrumental contributions to flow-rate errors cannot be predicted from theory but can be measured experimentally. Our method can, in principle, be applied to any binary mobile phase

(including normal-phase solvent systems) to reduce flow-rate errors during isocratic and gradient elution either before (pre-run) or after (post-run) the experiments are performed. Use of our approach will decrease flow-rate errors by ten-fold or more, particularly if the instrumental contribution are small or are measured as we have suggested and then factored out. If flow-rate settings are adjusted prior to experiments using pre-run correction factors (eqn. 39) interpolated from those we reported in Tables III–VI and any error resulting from instrumental contributions is also factored out, a virtually constant and error-free flow-rate ($\pm 0.5\%$) will be obtained. The resulting improvements in flow-rate will be useful to two groups of people: (1) HPLC manufacturers and users for quality control and troubleshooting of these solvent delivery systems, and (2) researchers who need very accurate retention data for physicochemical measurements.

ACKNOWLEDGEMENTS

J.P.F. and J.A.C. gratefully acknowledge helpful discussions with Carl Knopf and Randall Hall. J.P.F. gratefully acknowledges partial support of this work from the LSU Council on Research. J.A.C. is recipient of an LSU Alumni Fellowship.

REFERENCES

1 L. R. Snyder and J. J. Kirkland, *Introduction to Modern Liquid Chromatography*, Wiley, New York, 1979.
2 S. Prabhu and J. L. Anderson, *Anal. Chem.*, 59(1) (1987) 157–163.
3 S. G. Weber, *J. Electroanal. Chem. Interfacial Electrochem.*, 145 (1983) 1–7.
4 J. H. M. Van den Berg, C. B. M. Didden and R. S. Deelder, *Chromatographia*, 17(1) (1983) 4–8.
5 S. R. Bakalyar and R. A. Henry, *J. Chromatogr.*, 126 (1976) 327–45.
6 M. Martin, G. Blu and G. Guiochon, *J. Chromatogr. Sci.*, 11 (1973) 641–654.
7 M. Martin, G. Blu, C. Eon and G. Guiochon, *J. Chromatogr.*, 112 (1975) 399–414.
8 P. Achener, S. Abbott and R. Stevenson, *J. Chromatogr.*, 130 (1977) 29–40.
9 M. Martin and G. Guiochon, *J. Chromatogr.*, 151 (1978) 267–289.
10 E. Katz, K. Ogan and R. P. Scott, *J. Chromatogr.*, 352 (1986) 67–90.
11 P. G. Tait, *Scientific Papers, Vol. 2*, London, University Press, 1898.
12 J. Timmermans, *Physico-Chemical Constants of Binary Systems in Concentrated Solutions*, Interscience, New York, 1960.
13 H. Colin, J. C. Diez-Masa, G. Guiochon, T. Czajkowska and I. Miedziak, *J. Chromatogr.*, 167 (1978) 41–65.
14 W. Hayduk, H. Laudie and O. H. Smith, *J. Chem. Eng. Data*, 18(4) (1973) 373–376.
15 V. W. Schaffs, *Z. Phys. Chem.*, 194 (1944) 28–38.
16 M. Nakagawa, Y. Miyamoto and T. Moriyoshi, *J. Chem. Thermodyn.*, 15(1) (1983) 15–21.
17 E. Von Kuss, *Z. Ang. Phys.*, 7 (1955) 372–376.

Journal of Chromatography, 478 (1989) 311–324
Elsevier Science Publishers B.V., Amsterdam — Printed in The Netherlands

CHROM. 21 625

EFFECTS OF TEMPERATURE AND DENSITY ON RETENTION IN CAPILLARY SUPERCRITICAL-FLUID CHROMATOGRAPHY

T. A. BERGER
Hewlett-Packard, PO Box 900, Route 41 and Starr Rd., Avondale, PA 19311 (U.S.A.)
(First received September 30th, 1988; revised manuscript received May 16th, 1989)

SUMMARY

Retention of fluoranthene using carbon dioxide and a methyl silicone capillary column was measured at multiple, constant densities while changing temperature. Log k' *vs.* $1/T$ plots (at constant density) yielded straight lines with different slopes. Each slope gave a value for the total enthalpy of interaction between solute, mobile, and stationary phase, at each density. Gas chromatographic measurements using the same column and low pressure carbon dioxide gave a value for the interaction of the solute and the stationary phase. The difference between the total enthalpy and the solute–stationary phase enthalpy gave an approximate value for the solute–mobile phase enthalpy of interaction. Solubility problems emerged as temperature was decreased while density was held constant.

INTRODUCTION

Supercritical-fluid chromatography (SFC) is a bridge between gas chromatography (GC) and liquid chromatography (LC). In GC, solute volatility and solute–stationary phase interactions determine retention. Increasing temperature tends to increase volatility and decrease retention. In LC, solute volatility is unimportant. Instead, the mobile phase acts as a solvent and the competition between solute–stationary phase interactions and solute–mobile phase interactions determines retention. In SFC both volatility and solvation of the solute by the mobile phase are important.

In SFC, a number of authors have observed maxima in solute partition coefficients, k', *vs.* temperature (while keeping pressure constant) on both packed and capillary columns[1–7]. Leyendecker *et al.*[7] explained this behavior as the counteraction of two effects. At temperatures above the maxima, solute volatility dominates over solvation effects. At temperatures below the maxima, decreasing temperature produces increasing density and, consequently, increasing solvation of the solute by the mobile phase. Solvation dominates over volatility in this temperature region.

The change from volatility dominated retention phenomena to solvation dominated retention phenomena could be construed as a change from one type of pure performance to the other. Maxima in constant pressure plots of k' or log k' *vs.*

0021-9673/89/$03.50

temperature are frequently referred to as indicating a change in retention mechanism[6,8]. However, Klesper's explanation of these maxima, as the counteraction of two effects, suggests that two mechanisms are always operating and it is the sum of the two that is observed. This subtle difference in interpretation is often overlooked.

Giddings' concept of threshold density[9] has also been widely misunderstood. He clearly states that threshold density is only a convenient means of comparing the relative solubility of solutes and is dependent on the type and sensitivity of the detector used. The concentration of solute in the mobile phase can increase from virtually nil at atmospheric pressures to measurable levels in some manner related to density. However, if the detector used is not very sensitive this steady increase in concentration is not observed. Plots of detector output *vs.* density would yield a horizontal line (equal to detector background noise) until some "threshold density" is reached. Above this density, both detector signal and solute concentration increase in proportion to the mobile phase density. Unfortunately, the shape of such curves has been widely interpreted as indicating the sudden onset of solvation effects at this characteristic "threshold" density of each solute. Instead, differences between threshold densities merely indicate the relative solvation power of the mobile phase for various solutes.

From the literature, one is often left with the erroneous impression that the complex retention behavior typical in SFC is caused by some unusual or unique aspect of supercritical gases in comparison to subcritical gases or liquids. It is often assumed that solvation of solutes by gases only occurs above the critical temperature of the gas. As early as 1972, Doran[10] demonstrated that organic vapors like pentane, used as a chromatographic carrier gas, produced nearly identical chromatograms when used above or below the critical temperature of the gas. In another study paralleling that of Doran, Lauer *et al.*[11] used carbon dioxide as both a liquid and a supercritical gas to elute a number of solutes from packed columns. Again, no sudden changes in retention behavior were observed upon crossing the critical temperature of the mobile phase. The experimental results of both Doran and Lauer *et al.* indicate that dense gases and liquified gases tend to solvate solutes both above and below the critical point. There is no sudden onset of solvation when the critical point of the mobile phase is exceeded.

If there is no sudden onset of solvation above or even near the critical temperature, the next question must be at what density does solvation commence? Carbon dioxide has been used as a carrier gas in GC at pressures from near ambient to 50 atm (refs. 12–14). Retention of many solutes on several types of packed columns was shown to decrease with increasing pressure. While decreasing retention with increasing pressure is a general phenomenon with all carrier gases, retention decreased much faster when carbon dioxide was used compared to retention when nitrogen was used as the carrier gas. One possible explanation of this behavior is that carbon dioxide gas is a solvent for the solute. In addition, it is a better solvent than nitrogen, and its solvent strength increases with increasing pressure. Supporting this conclusion is a rather extensive, but often overlooked, body of literature describing solvation by gases as both chromatographic mobile phases and as regular solvents. Besides carbon dioxide[12–15], these gases include: steam[16–21]; organic dopants in steam, such as formic acid[22–24], and vapors of organic compounds[25–29]. Although much of this literature attributes retention shifts caused by these gases to the dynamic modification of the stationary phase[30–32] by the gases, adsorption or dissolution of the non-inert carrier[33,34] on or into the stationary phase does not appear to be substantial enough to

completely explain observed changes in solute retention. Some gases, used as the GC mobile phase, appear to exhibit solvation effects (solute–mobile phase interactions similar to those in LC) even at low densities, in addition to the normal solute–stationary phase effects typical in GC.

The purpose of this work is to verify the relationship between GC and SFC and attempt to measure both the enthalpy of interaction between the mobile phase and the solute and the enthalpy of interaction between the stationary phase and the solute as a function of density. It is also intended to demonstrate that chromatographic results obtained at constant density but different temperatures and pressures can be very different.

THEORETICAL

A number of papers have appeared which attempt to describe the thermodynamics of the retention process operating in capillary SFC. Yonker *et al.*[35] attempted to relate changes in the solvent heat capacity (constant pressure, C_p) *vs.* temperature to changes in solute retention (at constant pressure) *vs.* temperature. Unfortunately, the solutes chosen (as in most studies[1–5,7,35] showing maxima in constant pressure plots of k' *vs.* T) are quite volatile near the critical temperature of the solvents used. Since capillary SFC is only useful when solvation effects are significant, examples using solutes and temperatures where volatility provides the dominant separation phenomenon do not provide a realistic test of the theory. It was of some interest, therefore, to determine what effect the use of higher boiling solutes might have on the temperature of the maximum in plots of k' *vs.* temperature.

Chester and Innis[36] attempted to relate SFC retention to GC retention. They noted that, in GC, the slope of van't Hoff plots of ln k' *vs.* $1/T$ equals the enthalpy of interaction between the solute and the stationary phase, ΔH_{s-sp}, divided by the universal gas constant, R. Similar plots of ln k' *vs.* $1/T$ (at constant pressure) in SFC yield a straight line at high temperatures, the slope of which they assumed also yielded a value for $\Delta H_{s-sp}/R$. Small deviations from straight line performance were assumed to indicate stationary phase "swelling". At low temperatures, the curves of ln k' *vs.* $1/T$ roll over and change the sign of their slope. This corresponds to a change from volatility controlled to solvation controlled retention. The difference between the extrapolated straight line performance from high temperature and the specific values of retention at each low temperature was attributed to equal the enthalpy of interaction between the solute and mobile phase, ΔH_{s-mp}. This description can be summarized as

$$\ln k' = \frac{-\Delta H_{s-sp}}{RT} - \ln \beta + \frac{(\Delta H_{s-mp})_d}{RT}$$

where the subscript d indicates density dependence.

Chester and Innis proceeded to plot log k' *vs.* density at a small number of constant temperatures and stated that the slope of such curves yields values for ΔH_{s-mp}. However, the plots are only linear over a narrow range of densities and only a small number of temperatures covering only a narrow range of temperatures was used. No GC results for ΔH_{s-sp} were presented. While it is felt that this approach is

essentially correct, the narrow range of temperatures and densities employed, the low molecular weight of the solutes studied, and the lack of a comparison to GC results on the same column make it difficult to determine the accuracy of the theory or to provide quantitative measures of ΔH_{s-sp} or ΔH_{s-mp}.

Chester and Innis included a term to account for changes in the column phase ratio, β, caused by stationary phase "swelling". The choice of the term "swelling" is very common[3,5] and implies a strictly mechanical change in the stationary phase volume. It might be preferable to use a less descriptive name, such as stationary phase–mobile phase interactions, since either a mechanical change in the stationary phase volume and/or a change in the "polarity" of the phase could be caused by the dissolution of the mobile phase in the stationary phase[30–32].

Lauer *et al.*[11] interpreted the slope of ln k' *vs.* $1/T$ plots as being equal to the enthalpy of the overall interaction between the solute, stationary phase, and mobile phase. Yonker and Smith[8] extended this description by including the entropy of transfer in their equations. They then observed the retention of a number of lower boiling solutes over the widest range of densities studied to date. However, they do not attempt to relate SFC retention to GC retention and they use terminology for the enthalpy of transfer which produces a different value for a standard state (their ΔH_T°) at each density.

It was felt that part of the theories of both Chester and Innis[36] and Yonker and Smith[8] could be combined to produce a somewhat more complete model of retention, relating GC and SFC results and providing a fairly easy means of testing its validity.

The conventional approach to describing the thermodynamics of chromatographic retention begins with relating Gibbs free energy, ΔG°, to the solute distribution coefficient, K_D = concentration in stationary phase/concentration in the mobile phase:

$$\Delta G^\circ = -RT \ln K_D = \Delta H^\circ - T\Delta S^\circ$$

Since the distribution coefficient is also the product of the partition ratio, k', and the phase ratio, β

$$K_D = k'\beta$$

retention can be related to enthalpy:

$$\ln k' = \frac{-\Delta H^\circ}{RT} + \frac{\Delta S^\circ}{R} - \ln \beta$$

Since β is nominally a constant, plots of ln k' *vs.* $1/T$ should have a slope of ΔH°. However, retention can be described as the sum of two competing phenomena. The interaction of the solute with the stationary phase is routinely measured in GC using Van't Hoff plots. If it is assumed that the stationary phase does not change much with the introduction of a supercritical carrier gas, solute–stationary phase (s–sp) interactions should be the same in GC or SFC. It is also well known that in capillary SFC, the natural logarithm of the partition ratio (ln k') decreases linearly with increasing density.

Because of this linear dependency, any density can serve as a standard state to which the results at other densities can be referred. Meyer[37] developed the concept of molar concentrations in each phase as the proper standard state at which to define free energy. Adjustment of physical parameters to achieve molar concentrations in each phase seems unwieldy and difficult to confirm. Instead, the distribution coefficient at density = 1 g/cm^3 could be used as a standard state, although this "convenience" further requires the naming of some temperature as a standard. Using the convention of a density of 1 g/cm^3 as the standard state, the measured enthalpy from the slope of ln k' *vs.* $1/T$ plots (at constant density) can then be related to standard enthalpies of interaction between the solute and the stationary phase and the solute and mobile phase, since

$$\Delta H_{meas} = \Delta H^{\circ}_{s-sp} - \text{density} \cdot (\Delta H^{\circ}_{s-mp})$$

where ΔH°_{s-sp} is obtained from ln k' *vs.* $1/T$ plots in GC and ΔH_{meas} is obtained from similar plots obtained in SFC at various fixed densities.

The difference between ΔH_{meas} and ΔH°_{s-sp} provides a measure of ΔH°_{s-mp} since a plot of ΔH_{meas} *vs.* density will have a slope of ΔH°_{s-mp} and an intercept of ΔH°_{s-sp}. Deviations from straight line behavior between ΔH_{meas} and $1/T$ indicate the magnitude of changes in β and in stationary phase–mobile phase interactions with density.

Stationary phase–mobile phase interactions appear to be small compared with solute–mobile phase interactions. If stationary phase–mobile phase interactions are small: $\Delta H_{s-mp} + \Delta H_{sp-mp} \approx \Delta H_{s-mp}$.

EXPERIMENTAL

Instrumentation and chemicals

A Suprex Model 200A supercritical-fluid chromatograph pump module was used to pump carbon dioxide. In a few cases a Varian Model 4100 syringe pump, modified to provide constant pressure, was used instead of the Suprex unit. For pressures above 60 atm, the mobile phase was SFC grade carbon dioxide supplied in aluminum cylinders with dip tubes purchased from Scott Specialty Gases. For pressures below 60 atm, small aluminum cylinders of the same grade CO_2 with a dip tube were used but the cylinders were inverted to draw gas from the headspace above the liquid CO_2 in the tank. For pressures below 60 atm, pressure was controlled by a high pressure, two-stage, forward pressure regulator. A Hewlett-Packard Model 5890 gas chromatograph with two standard flame ionization detectors was used as the chromatographic oven. One flame ionization detector was used as the system detector and its output was monitored using a recording integrator. A Valco Model 2WI4W.06 micro injection valve was mounted on top of the gas chromatograph. A 0.8 mm outside diameter stainless steel tube was connected between the valve outlet and a "tee" located inside the GC oven. The chromatographic column was inserted through the tee and the stainless steel tube until it butted against the valve body, and was then withdrawn a fraction of a millimeter.

Empty 25 and 50 μm I.D. tubing, used for retention gaps and transfer lines, was purchased from Polymicro Devices. Linear restrictors of 5 and 10 μm I.D. were made from tubing purchased from Scientific Glass Engineering. Integral restrictors and

columns were purchased from J&W Scientific. Columns were 10 m × 50 μm I.D., with a methyl silicone stationary phase. Polycyclic aromatic hydrocarbons were purchased in a kit from Chemical Services, and were generally better than 99% pure. Long-chain fatty acids were purchased in a kit from Supelco. Most samples were prepared using carbon disulfide as the solvent to minimize detector response. All solvents were reagent grade or better.

A restrictor, serving as a split vent for split injections, was installed in the side arm of the "tee" and consisted of either a piece of 5, 10 or 25 μm I.D. tubing (linear restrictor) or an "integral" (steep taper) restrictor. Integral restrictors were preferred, but we required a large range of split restrictor flow-rates to cover the range of pressures and densities investigated. Integral restrictors were not readily available with the full range of flow-rate *vs.* pressure required. Integral (steep taper) restrictors, used as the split vent to control split ratio, were mounted in the base of the second flame ionization detector. This detector was only used as a heated zone to control the temperature of, and mass flow-rate through, the split vent independent of the oven temperature. Restrictors used at the end of the column were also integral or linear types with the former preferred, since the latter tends to cause spiking in the detector output (unless excessive temperatures are used or the solutes are very volatile).

Procedure

It was assumed that partition ratios, k', did not change significantly with mobile phase linear velocity, over the range of linear velocities employed. Since changes in efficiency were not of primary interest in this work, the reduced velocity of the mobile phase through the column was permitted to change slightly with pressure and density to minimize the number of restrictors required. Column linear velocity, estimated by solvent peak transit times, was controlled to between 2 and 5 cm/s (approximately 10 times optimum) for high density work (above ≈ 0.25 g/cm^3), and was allowed to rise somewhat as density dropped or temperature rose (more GC-like conditions with higher optimum linear velocity, μ_{opt}). Chromatograms were collected at constant pressure and temperature. Partition ratios were estimated from: the solvent (t_0) and the solute (t_R) retention times reported by the integrator, and the standard equation: $k' = (t_R - t_0)/t_0$. All experimental measurements were taken in triplicate and averaged. The data was more precise than the circles in the figures indicate.

Solutes were dissolved in carbon disulfide to allow retention data at very low values of k' to be collected. Since carbon disulfide hardly responds in the detector, the signal from the solute can be observed in the tail of large excesses of solvent. The solute, therefore, may elute during a time when significant amounts of solvent are still emerging from the column (even though the detector output may not make this obvious). This raises some uncertainty as to whether the solute, emerging with the carbondisulfide solvent, experiences a modifier effect, which could distort the data. Solvatochromic shift measurements indicated that carbon disulfide is only moderately stronger[38], as a solvent, than carbon dioxide. Binary mixtures of similar solvents tend to have solvent strengths between the two pure solvents.

The gas chromatograph was a new unit taken from the production line and the oven temperature was checked with a platinum resistance standard. Accuracy was better than 1°C and precision better than 0.01°C.

The density of carbon dioxide at different temperatures and pressures was

calculated using the equation of state of Bender[39] and Reynolds[40], which was checked against values from the Gas Encyclopedia[41].

RESULTS AND DISCUSSION

Location of maxima in k' vs. T plots at constant pressure

The theory of Yonker *et al.*[35] was tested by selecting solutes which could not be eluted in GC at temperatures near the critical temperature of the mobile phase. The retention behaviour of polycyclic aromatic hydrocarbons was measured at constant pressure and varying temperature and the results are shown in Fig. 1. Among the facts that are immediately obvious from the figure, is the location of the maxima around 115–130°C even at pressures well below 200 atm. The theory of Yonker *et al.*[35] suggested that the maxima ought to occur between 40 and 80°C, at the same temperatures as the maxima in carbon dioxide heat capacity, c_p, *vs.* temperature curves. Since the maxima in solute retention occur at temperatures up to 50°C higher than maxima in heat capacity, it appears that, while the theory may describe the general shape observed, it is certainly not very accurate. Long chain fatty acids (C_{20}–C_{24}) were also studied and gave similar results.

Constant density lines in k' vs. T plots at constant pressure

A more detailed set of *k' vs.* temperature measurements was collected, using fluoranthene as the solute over a range of fixed pressures from 90 to 140 atm and the results are presented in Fig. 2a. Again, maxima occur at temperatures above 100°C and the temperatures at which the maxima occurs increase with increased pressure. Since pressure is only a control variable, it is more informative to examine the retention phenomena in Fig. 2a as a function of density. Constant density lines can be drawn through the data represented in Fig. 2a as shown in Fig. 2b, where the light dashed lines represent constant pressure and the heavier lines approximate constant density conditions. The numbers next to the heavy lines indicate density values in g/cm^3. Note that, at densities above 0.20 g/cm^3, the constant density lines show a major change in slope, *i.e.*, maxima between 60 and 80°C. This is the same temperature region where the heat capacity of carbon dioxide, C_p, exhibits maxima. However, in Fig. 2a, the temperature of the maxima decreases with increasing pressure, whereas the maxima in

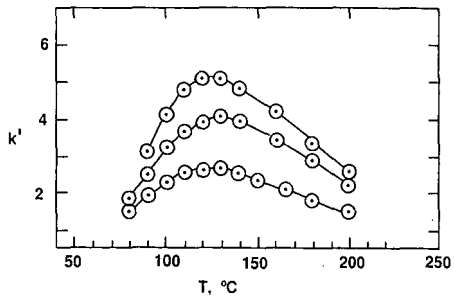

Fig. 1. Retention of selected polycyclic aromatic hydrocarbons *vs.* temperature at listed fixed pressures. Column: 10 m × 50 μm I.D., methyl silicone. Mobile phase: carbon dioxide. Upper curve: perylene at 155 atm, middle curve: benzo[e]pyrene at 160 atm. Lower curve: chrysene at 155 atm.

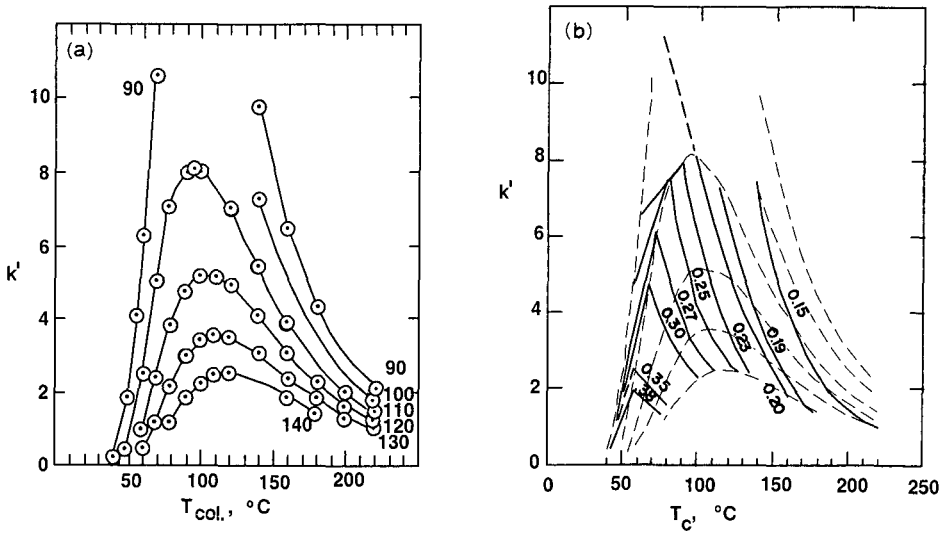

Fig. 2. (a) Retention of fluoranthene *vs.* temperature. Numbers next to curves indicate fixed pressures in atm. Same column and fluid as in Fig. 1. (b) Same data as in (a) but heavy lines indicate constant density. Numbers above heavy lines indicate density in g/cm^3.

heat capacity increase with increasing pressure. Lauer *et al.*[11] and Chester and Innis[36] found no change in slope of plots of ln k' *vs.* $1/T$ collected at constant density. However, the conditions required to cross the maxima in Fig. 2b are difficult to access experimentally. Chester and Innis used capillary columns and temperatures and pressures to the right of the density maxima in Fig. 2b. Lauer *et al.*[11] used packed columns and reported difficulty in obtaining chromatograms with a fluid density below 0.7 g/cm^3 due to severe tailing. The linear portion of their constant density plots covers the range of 22–55°C and, therefore, the pressure/temperature region to the left of the density maxima Fig. 2b. The constant density lines in Fig. 2b are only approximate. The solute studied was different from those in either of the previous studies[11,35]. Therefore, no attempt was made to directly compare the previous and present results.

Change in enthalpy vs. density from slopes of ln k' vs. 1/T at constant density

The retention of fluoranthene was restudied under carefully controlled constant density conditions and the results plotted as ln k' *vs.* $1/T$, at each of a number of constant densities. Plots of ln k' *vs.* $1/T$ at eight different densities were plotted and are shown in Fig. 3. Gas chromatograms at four different temperatures were also collected and the results were also plotted as ln k' *vs.* $1/T$ in Fig. 3. The GC results provide a quantitative measurement of the solute–stationary phase interaction, assuming the slope of the curve is $-\Delta H_{s-sp}/R$. In contrast to the confusing nature of Fig. 2a and b, Fig. 3, yields straight lines with no change in slope over the temperature range from 60 to 280°C, the pressure range from a few atmospheres to 400 atm, or for densities from 0.005 to 0.45 g/cm^3.

If the enthalpy values from the GC chromatograms are assumed to represent the

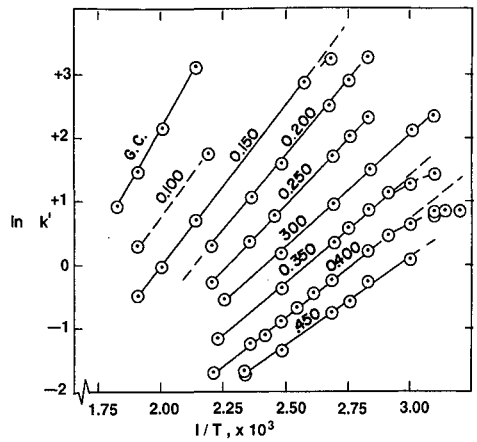

Fig. 3. Retention of fluoranthene *vs.* temperature at different constant densities. Numbers above curves are densities in g/cm^3. Note GC data on top left. Same column and fluid as in Fig. 1.

energy of interaction between the solute and the stationary phase, independent of mobile phase effects, then the difference between this value and the energy values at other densities must represent mobile phase effects. These mobile phase effects measure density-dependent interactions between the mobile phase and the solute and interactions between the two phases. The data seem to fit the relationships

$$\ln k'_{SFC} = \ln k'_{GC} + \rho(\Delta H^{\circ}_{s-mp}/RT + \Delta H^{\circ}_{mp-sp}/RT)$$

or

$$\ln k'_{SFC} = -\Delta H^{\circ}_{s-sp}/RT + \rho(\Delta H^{\circ}_{s-mp} + \Delta H^{\circ}_{mp-sp})/RT$$

where ρ is density.

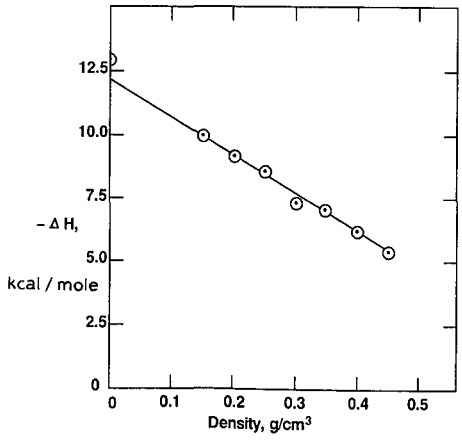

Fig. 4. Enthalpy of interaction between fluoranthene, carbon dioxide and methyl silicone stationary phase from slopes of lines in Fig. 3.

TABLE I

VALUES FOR ΔH_{s-mp} OBTAINED AT DIFFERENT DENSITIES

ΔH_{s-sp} = 12.98 kcal/mol.

Density *(g/cm³)*	ΔH_{tot} *(kcal/mol)*	ΔH_{s-mp} *(kcal/mol)*
≈0.005	12.98	–
0.15	10.00	19.9
0.20	9.30	18.4
0.25	8.65	17.3
0.30	7.42	18.5
0.35	7.13	16.7
0.40	6.22	16.9
0.45	5.65	16.29

The slopes of the lines in Fig. 3 yield calculated values of energy which are plotted *vs.* density in Fig. 4. The energy values obtained from the eight curves in Fig. 3 form a nearly straight line in Fig. 4 with a zero density intercept very nearly equal to the ΔH°_{s-sp} value obtained from the GC data (also presented in Fig. 3). The difference between the zero density intercept of the SFC data and the GC data is probably due to stationary phase–mobile phase interactions which are not directly proportional to density. If the energy values, obtained from the slopes of the curves at each density, are each subtracted from the GC value, and the results are divided by the appropriate density, a value for ΔH°_{s-mp} should be obtained (assuming ΔH°_{mp-sp} is small). Values for ΔH°_{s-mp} obtained in this way are presented in Table I and average approximately 16.5 kcal/mol at high densities.

Comparisons of solvent strength from solvatochromic shift measurements and chromatographic retention

The energy of interaction between solvatochromic dyes and supercritical mobile phases can be measured, independent of stationary phase effects. Such dyes show a shift in the wavelength of their absorption spectra proportional to the solvent

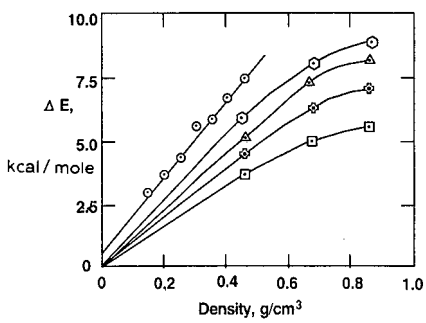

Fig. 5. Comparison of published solvatochromic dye measurements to present measurement of apparent energy of mobile phase–solute interaction. See text for details. ○, Fluoranthene; □, 4-nitrophenol; +, 4-nitroanisole; △, N,N-diethyl-4-nitroaniline; ⬡, 4-nitroaniline.

strength of the solvent in which they are dissolved. The results of such measurements can be compared to the enthalpy values obtained chromatographically. Many of the dyes used by Kamlet *et al.*[42] (to develop their π^* scale of solvent polarity) are soluble in carbon dioxide. Sigman *et al.*[43] measured the absorbance maxima of ten of these dyes in both supercritical carbon dioxide at various densities and in the CO_2 vapor phase, *i.e.*, no solvent. Energy values were calculated using Sigman *et al.*'s published wavelengths of the absorption maxima by dividing the constant, 28 592, by the wavelength of maximum absorption (in nanometers) to yield an energy in kcal/mol (ref. 44). The difference in energy between the vapor phase measurements and the SFC measurements at each density were calculated and are presented in Fig. 5.

The enthalpy values at each density, presented in Fig. 4, were subtracted from the enthalpy value obtained from the GC chromatograms. The resulting differences in enthalpy were also plotted *vs.* density in Fig. 5. Although the solutes are different, both the dyes and the chromatographic retention measurements indicate approximately the same level of mobile phase–solute interactions.

Plots of ln k' vs. density

The energies of interaction, calculated from solvatochromic shifts, tend to roll-off in Fig. 5 at high densities. In the limited range of densities studied in Fig. 5, the chromatographic results appear to produce a straight line with no appreciable roll-off. The unified chromatography theory of Martire and Boehm[45] predicts a roll-off (see Fig. 1, ref. 45) but at higher densities than covered in the experiments summarized by Fig. 3–5. They also predict minima in ln k' *vs.* density plots and crossing of such curves obtained at different temperatures. This contradicts the linear relationship between ln k' and density reported by Chester and Innes[35], but the data from the latter group was only collected over a narrow density range. Yonker and Smith[46] reported that plots of ln k' *vs.* density for a number of solutes separated on capillaries were non-linear but did not exhibit minima.

The data in Fig. 3 could be replotted as ln k' *vs.* density but does not cover a wide enough density range to fully test the model. Additional data were collected to increase the range of densities studied. With the assumption that carbon disulfide did not significantly distort retention through a modifier effect, partition ratios, k', of fluoranthene were measured at densities up to 0.74 g/cm^3; the results are shown in Fig. 6. No minima were observed and the curves collected at different temperatures did not cross, over the density range studied. However, very small values of k' were obtained at high densities. In an attempt to study higher densities with more reasonable values of k', long chain fatty acids with greater retention than fluoranthene were also evaluated. Plots of ln k' *vs.* density were similar to those in Fig. 6 but offset to slightly higher retention for any given temperature and density. No minima were observed in ln k' *vs.* density for tetracosanoic acid at densities up to 0.905 g/cm^3 but ln k' decreased to less than -3.

In a similar study on other solutes, Yonker and Smith[46] also report ln k' values as low as -3. Such small values for retention suggest a potential problem with all such measurements. Dobbs *et al.*[47] report that even small amounts of non-polar modifiers added to carbon dioxide, grossly increase the solubility of many solutes compared to their solubility in pure carbon dioxide. They specifically report that the solubility of phenanthrene doubles when the mole percent of octane in carbon dioxide doubles

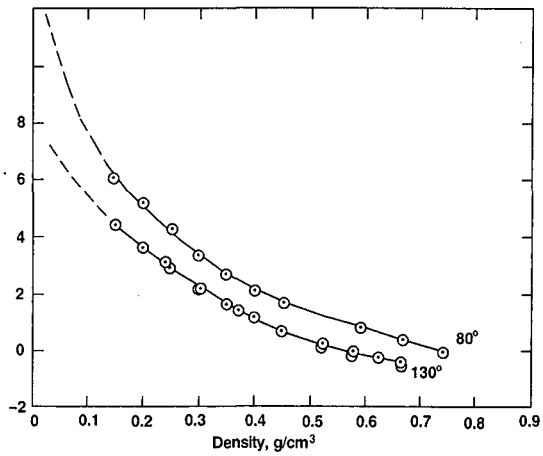

Fig. 6. Retention of fluoranthene plotted against density at higher densities than available from Fig. 3. No minima or crossing observed in range of densities studied. Carbon dioxide mobile phase, methyl silicone 10 m × 50 μm column. Numbers next to curves are temperatures.

from 3.5 to 7%. While that is not the specific system studied here it is similar. Carbon disulfide is much more "polar" than octane and is likely to have a larger modifier effect on polar solutes like the acids. With very small values of k', the solutes must experience a significant modifier effects during a substantial fraction of their residence time in the column. This suggests that the unified chromatography theory of Martire and Boehm[45] may not yet have been properly tested and may not be testable using the approach taken.

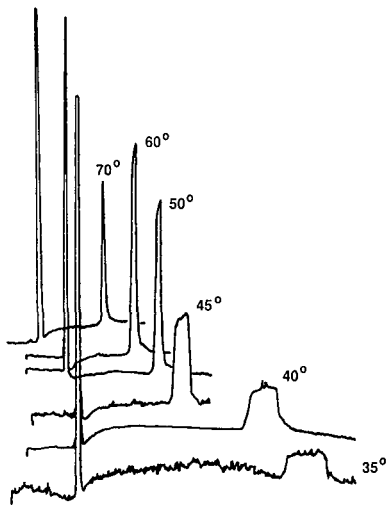

Fig. 7. Chromatograms of fluoranthene collected at a constant density of 0.400 g/cm³ but different temperatures. Numbers next to curves indicate temperature. Same column and mobile phase as previous figures.

Other results

In Fig. 3, some constant density lines became non-linear below 60°C. The constant density line for a density of 0.40 g/cm^3 in Fig. 3 is a good example. Superficially, the roll-off in ln k' below a temperature of 60°C appears to agree with the change in slope of the approximate constant density lines in Fig. 2b. However, the chromatograms presented in Fig. 7, are representative of those used to obtain the last five data points on the right end of the 0.4 g/cm^3 curve in Fig. 3. Since all the chromatograms were collected at the same density, the dramatic decrease in amplitude should logically be due to a decrease in volatility caused by the rather modest decrease in temperature of 35°C. Therefore, the solvation energy produced by substantial densities is not necessarily adequate to offset decreases in volatility caused by small decreases in temperature.

CONCLUSIONS

Solvation of solutes by some carrier gases begins at very low densities, corresponding to pressures and densities encountered in normal GC. This solvation increases steadily and linearly with increasing gas density. There are no unusual properties or capabilities of supercritical gases that suddenly or dramatically appear near or above the critical temperature.

Retention in capillary SFC can be thermodynamically and practically related to retention in GC. The energy of interaction between solutes and stationary phases can be obtained from GC retention data. SFC retention data allows calculation of the solute–mobile phase interactions, provided the GC data is available. Measured values of solute–mobile phase enthalpies were much larger than solute–stationary phase enthalpies, suggesting that carbon dioxide is a very good solvent for the solutes examined and that solvation effects should greatly enhance solute mobility. For fluoranthene in carbon dioxide, and a methyl silicone column, ΔH_{s-mp} is 16–17 kcal/mol; whereas, ΔH_{s-sp} is more like 13 kcal/mol. This difference in energy suggests that the range of solutes that can be eluted by SFC ought to be much larger than the range of GC.

Pressure and temperature are not equivalent means of changing column density. The former primarily changes solvation and tends to slightly increase partial pressure of the solute in the carrier. The latter changes both the partial pressure (or volatility) of the solute and solvation of the solute by the carrier. The technique of inverse temperature programming to increase column density while decreasing column linear velocity is gaining widespread acceptance. While this technique has some very desirable attributes, the above analysis suggests that inverse temperature programming will produce substantially different results than pressure programming producing the same density *vs.* time profile.

REFERENCES

1 S. T. Sie and G. W. A. Rijnders, *Sep. Sci.*, 2 (1967) 729–753.
2 S. T. Sie and G. W. A. Rijnders, *Sep. Sci.*, 2 (1967) 755.
3 M. Novotny, W. Bertsch and A. Zlatkis, *J. Chromatogr.*, 61 (1971) 17.
4 F. P. Schmitz, D. Leyendecker and E. Klesper, *Ber. Bunsenges. Phys. Chem.*, 88 (1984) 912.
5 B. P. Semonian and L. B. Rogers, *J. Chromatogr. Sci.*, 16 (1978) 49–60.

6 T. Takeuchi, K. Ohta and D. Ishii, *Chromatographia*, 25 (1988) 125–128.
7 D. Leyendecker, F. P. Schmitz and E. Klesper, *J. Chromatogr.*, 315 (1984) 19–30.
8 C. R. Yonker and R. D. Smith, *J. Chromatogr.*, 351 (1986) 211–218.
9 J. C. Giddings, *Science (Washington, D.C.)*, 162 (1968) 67–73.
10 T. Doran, *Gas Chromatography 1972*, Applied Science Publ., Barking, 1973, pp. 133–143.
11 H. H. Lauer, D. McManigill and R. D. Bored, *Anal. Chem.*, 55 (1983) 1370–1375.
12 D. H. Desty, *Adv. Chromatogr. (N.Y.)*, 1 (1965) 211–213.
13 S. Wicar and J. Novak, *J. Chromatogr.*, 95 (1974) 13–26.
14 A. Karmen, I. McCaffrey and R. L. Bowman, *Nature (London)*, 193 (1962) 575.
15 J. M. Prausnitz and P. R. Benson, *AIChE J.*, 5 (1959) 161.
16 A. Nonaka, *Adv. Chromatogr. (N.Y.)*, 12 (1975) 223–260.
17 S. A. Volkov, Yu. A. Sultanovich and K. I. Sakodynskii, *J. Chromatogr.*, 202 (1980) 21–28.
18 S. A. Volkov, Yu. A. Sultanovich and K. I. Sakodynskii, *J. Chromatogr.*, 202 (1980) 29–35.
19 A. Nonaka, *Anal. Chem.*, 44 (1972) 271–277.
20 M. A. Baydarovtseva, B. A. Rudenko, V. F. Kucherov and M. I. Kuleshova, *J. Chromatogr.*, 104 (1975) 271–275.
21 M. A. Baydarovtseva, B. A. Rudenko, V. F. Kucherov and M. I. Kuleshova, *J. Chromatogr.*, 104 (1975) 277–281.
22 A. Nonaka, *Anal. Chem.*, 45 (1973) 483–487.
23 B. Pileire, Ph. Beaune, M. H. Laudat and P. Cartier, *J. Chromatogr.*, 182 (1980) 269–276.
24 A. H. Woo and R. C. Lindsay, *J. Chromatogr. Sci.*, 18 (1980) 273–274.
25 T. Tsuda, N. Toforo and D. Ishii, *J. Chromatogr.*, 46 (1970) 241–246.
26 K. L. Wagman and T. G. Smith, *J. Chromatogr. Sci.*, 9 (1971) 241–244.
27 T. Tsuda and D. Ishii, *J. Chromatogr.*, 87 (1973) 554–558.
28 T. Tsuda, H. Yanagihara and D. Ishii, *J. Chromatogr.*, 101 (1974) 95–102.
29 T. Tsuda, T. Ichiba, H. Muramatsu and D. Ishii, *J. Chromatogr.*, 130 (1977) 87–96.
30 K. W. M. Siu and W. A. Aue, *J. Chromatogr.*, 189 (1980) 255–258.
31 J. F. Parcher and T. N. Westlake, *J. Chromatogr. Sci.*, 14 (1976) 343–348.
32 J. F. Parcher and P. J. Lin, *Anal. Chem.*, 53 (1981) 1889–1894.
33 J. F. Parcher and M. I. Selim, *Anal. Chem.*, 51 (1979) 2154–2156.
34 J. R. Strubinger and J. F. Parcher, *Anal. Chem.*, 61 (1989) 951–955.
35 C. R. Yonker, B. W. Wright, R. C. Petersen and R. D. Smith, *J. Phys. Chem.*, 89 (1985) 5526–5530.
36 T. L. Chester and D. P. Innis, *J. High Resolut. Chromatogr. Chromatogr. Commun.*, 8 (1985) 561–566.
37 E. F. Meyer, *J. Chem. Educ.*, 50 (1973) 191.
38 J. F. Deye, T. A. Berger and A. G. Anderson, *Anal. Chem.*, submitted for publication.
39 E. Bender, *Proc. 5th symposium on Thermophysical Properties*, Am. Soc. Testing and Materials, New York, 1970, p. 227.
40 W. C. Reynolds, *Thermodynamic Data in SI*, Department of Mechanical Engineering, Stanford University, Stanford, CA, 1979.
41 N. Marshal, *Gas Encyclopedia*, English ed., Elsevier, Amsterdam, 1976.
42 M. J. Kamlet, J. L. Abboud and R. W. Taft, *J. Am. Chem. Soc.*, 99 (1977) 6027–6038.
43 M. E. Sigman, S. M. Lindley and J. E. Leffler, *J. Am. Chem. Soc.*, 107 (1985) 1471–1472.
44 E. M. Kosower, *J. Am. Chem. Soc.*, 80 (1958) 3253–3260.
45 D. E. Martire and R. E. Boehm, *J. Phys. Chem.*, 91 (1987) 2433–2446.
46 C. R. Yonker and R. D. Smith, *J. Phys. Chem.*, 92 (1988) 1664–1667.
47 J. M. Dobbs, J. M. Wong and K. P. Johnston, *J. Chem. Eng. Data*, 31 (1986) 303–308.

Journal of Chromatography, 478 (1989) 325–338
Elsevier Science Publishers B.V., Amsterdam — Printed in The Netherlands

CHROM. 21 643

REPELLER EFFECTS IN DISCHARGE IONIZATION IN LIQUID AND SUPERCRITICAL-FLUID CHROMATOGRAPHY–MASS SPECTROMETRY USING A THERMOSPRAY INTERFACE

II. CHANGES IN SOME ANALYTE SPECTRA

W. M. A. NIESSEN*, R. A. M. VAN DER HOEVEN, M. A. G. DE KRAA, C. E. M. HEEREMANS, U. R. TJADEN and J. VAN DER GREEF

Division of Analytical Chemistry, Center for Bio-Pharmaceutical Sciences, P.O. Box 9502, 2300 RA Leiden (The Netherlands)

(First received March 15th, 1989; revised manuscript received May 25th, 1989)

SUMMARY

By changing the potential of the repeller electrode in a thermospray ion source operated under discharge-on conditions in liquid chromatography–mass spectrometry and supercritical-fluid chromatography–mass spectrometry the appearance of the mass spectra can be changed. Either abundant protonated molecules or considerable fragmentation can be obtained. The repeller-induced fragmentation can result in useful fragmentation. The selection of the most appropriate repeller potential is a delicate task because the effects appear to be compound-dependent. Compounds which are fragmented easily will generally not give useful spectra at very high repeller potentials. The results indicate that different mechanisms, *i.e.*, chemical ionization with different reagent gas compositions and collisionally induced dissociation, play important roles in fragmentation.

INTRODUCTION

Supercritical-fluid chromatography–mass spectrometry (SFC–MS) is an important technique. The field of application of SFC overlaps to some extent that of liquid chromatography (LC) and with that of gas chromatography (GC). Since SFC–MS is easier to accomplish than LC–MS, a shift from LC–MS to SFC–MS is expected, especially when with SFC–MS similar information can be obtained. The information content of SFC–MS largely depends on the type of ionization techniques that can be used.

SFC–MS has been investigated for several years, and an excellent review on the developments within this field has been written by Smith *et al.*[1]. Interfacing between SFC and MS is based on either supersonic molecular beam systems[2,3], direct fluid introduction through a diaphragm[4] or another type of restriction[5], modified thermospray interfaces[6,7] and moving belt interfaces[8].

0021-9673/89/$03.50

As usual with the moving belt, electron impact (EI) and chemical ionization (CI) are possible[8], while in the direct introduction type of interfaces, filament-assisted ionization is performed in either the EI or the CI mode. With pure carbon dioxide charge exchange (CE) CI takes place, while a reagent gas can be added to obtain proton transfer CI. Ionization by means of a discharge instead of a filament in either a conventional CI source[9] or a thermospray source[7] has also been demonstrated. Recently, it was shown that in SFC–MS, similar to LC–MS, in the discharge-on mode the potential at the repeller electrode can be used to induce fragmentation[10,11]. In LC–MS studies the repeller electrode in the discharge-on mode has been claimed to induce fragmentation, which has been explained in terms of collisionally induced dissociations (CIDs)[12,13]. From our systematic studies on the repeller effects in the discharge-on mode in both LC–MS and SFC–MS it appears that CID of analyte ions is not the only process. In the first part of this series[14] the effect of the repeller voltage on the reagent gas spectrum in the discharge-on mode with LC–MS and SFC–MS was discussed. In this second part the insights obtained are applied in the explanation of repeller-induced spectral changes in analyte mass spectra. Most emphasis is given to the SFC–MS results, although for some compounds a comparison is made with LC–MS data as well. The analytical potential of the repeller effects in both qualitative and quantitative analysis is discussed.

EXPERIMENTAL

(Tandem) MS was performed on a Finnigan MAT TSQ-70 instrument (Finnigan, San José, CA, U.S.A.), equipped with a Finnigan MAT thermospray interface. The discharge electrode was operated at potentials between 800 and 1200 V. MS–MS experiments were performed with air as a collision gas at a pressure of 0.05–0.15 Pa in the collision cell. The collision energy was optimized for each application.

The packed column SFC–MS experiments were performed on a laboratory-build SFC instrument consisting of slightly modified commercially available modules. The system has been described in detail elsewhere[15]. The mobile phase was carbon dioxide modified with 2–15% of methanol at a flow-rate of 2 ml/min. The laboratory-packed column (150 mm × 4.6 mm I.D.) was packed with either Nucleosil C_{18} (5 μm; Macherey-Nagel, Düren, F.R.G.), or Rosil aminopropyl (7 μm; Alltech, Deerfield, IL, U.S.A.). The vaporizer capillary was used as the pressure restrictor by pinching the last part of the tube until stable back pressure of typically between 30 and 35 MPa was achieved. The block temperature was kept at 150°C and the vaporizer temperature was 50°C unless stated otherwise. The analytes were dissolved in methanol.

The LC–MS experiments were performed in the flow injection (FIA) mode with 20–80% of methanol in water at a flow-rate of 1.2 ml/min. The solvent was delivered with two Model 2150 LC pumps (LKB, Bromma, Sweden) controlled by an LKB Model 2152 LC controller. A block temperature of 200°C and a vaporizer temperature of 90–110°C were used. The samples were dissolved in the solvent used in that particular experiment.

RESULTS AND DISCUSSION

Polycyclic aromatic hydrocarbons

The first group of compounds for which the repeller effects in the discharge-on mode with SFC–MS were studied systematically, were some polycyclic aromatic hydrocarbons (PAHs). In Fig. 1 mass chromatograms are given for two successive injections at two different repeller potentials (20 and 120 V) of a standard mixture of anthracene (molecular weight, MW 128), phenanthrene (MW 178) and pyrene (MW 202). A mobile phase of 7% methanol in carbon dioxide was used. Signals from the molecular ions of the PAHs are given in the upper trace of Fig. 1 and signals from the protonated molecules in the lower trace. (The chromatograms at the right and at the left are normalized at the highest peak in the two; therefore no isotope peaks are detected in the lower trace.) With a repeller potential of 20 V, peaks from the protonated molecules of the PAHs are observed (Fig. 1A), while these peaks are not detected with a repeller potential of 120 V. At a repeller potential of 120 V, peaks from the molecular ions of the PAHs are observed (Fig. 1B), which are absent at a repeller potential of 20 V.

Mass spectra of phenanthrene, obtained at low and high repeller potentials, are given in Fig. 2. At a repeller potential of 20 V a protonated molecule is observed at m/z = 179 without any fragmentation, while at a repeller potential of 120 V a molecular ion is observed at m/z = 178, with considerable fragmentation. The type of fragmentation observed is well known from the EI spectra of phenanthrene.

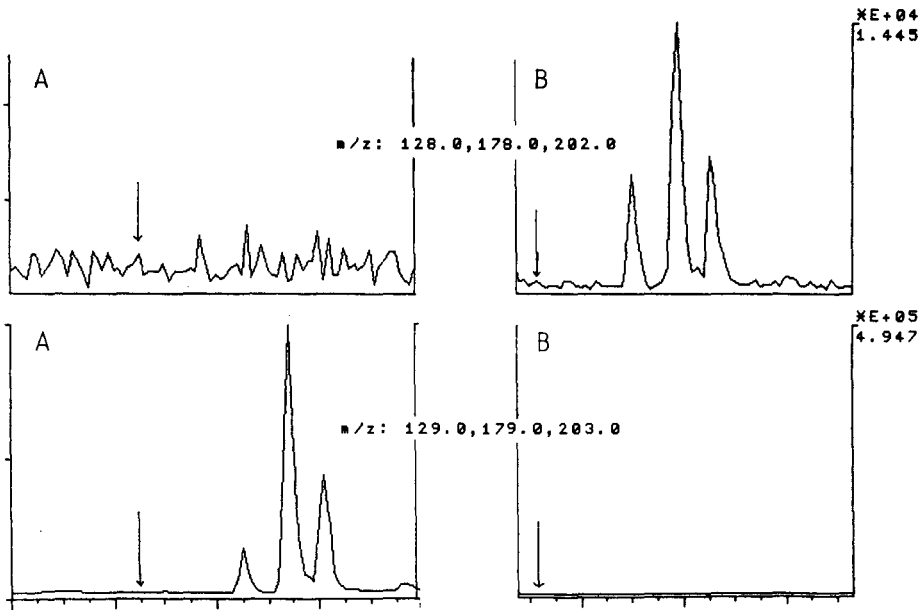

Fig. 1. Reconstructed mass chromatograms of a mixture of naphthalene (MW 128), phenanthrene (MW 178) and pyrene (MW 202) with a repeller potential of (A) 20 V and (B) 120 V. Conditions: SFC–MS with 7% of methanol in carbon dioxide and a C_{18} column. Other conditions: see text.

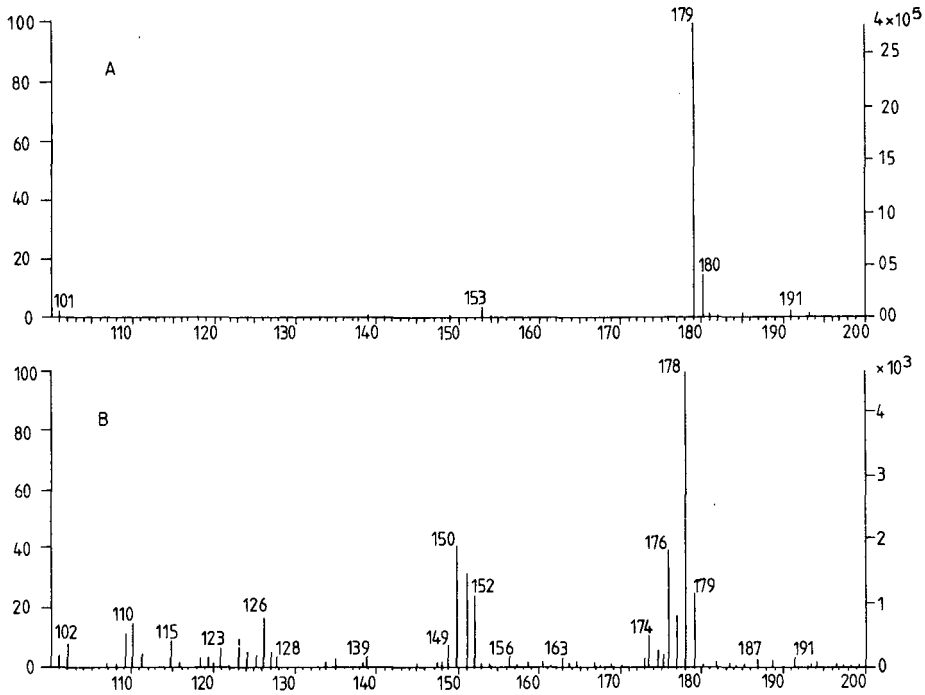

Fig. 2. Mass spectra of phenanthrene at a repeller potential of (A) 20 V and (B) 120 V. Conditions: see Fig. 1.

These results show that the change in the reagent gas spectrum, induced by the change of the repeller potential[14], influence the analyte mass spectra as well. Proton transfer CI effects are observed at low repeller potentials, while charge exchange CI effects are observed at high repeller potentials. Protonation takes place by the protonated methanol (clusters), and perhaps to some extent by the protonated carbon dioxide, while the carbon dioxide molecular ion presumably is responsible for the charge exchange effects observed. This is in agreement with the changes in the reagent gas spectra reported previously[14].

The influence of the repeller potential on naphthalene spectra has been studied at 2, 7 and 10% of methanol in carbon dioxide. Similar effects of the repeller potential on the appearance of the mass spectra were found. However, the degree of fragmentation at a particular repeller potential is related to the methanol content of the mobile phase. At a particular repeller potential, more fragmentation of naphthalene is observed with 2% of methanol than with 10% of methanol. In general, higher repeller potentials are needed to induce fragmentation in a mobile phase with an high methanol content in carbon dioxide. As indicated in the first part of this series[14] the reagent gas conditions at high repeller potentials become more dominated by methanol-related species when the methanol content in the mobile phase is increased. As a result of the decreasing intensity of the carbon dioxide molecular ion at higher percentages of methanol, the contribution of the CE effects at high repeller potentials is expected to diminish. This is indeed observed. It must be pointed out that the PAHs

are quite exceptional in that they, unlike more polar compounds, can be successfully analyzed in a wide range of methanol contents. With more polar compounds the percentage of methanol in the mobile phase cannot be chosen freely.

With 2% of methanol at very high repeller potentials considerably more fragmentation is observed in the mass spectra of the PAHs than in the corresponding spectra at 70 eV EI. Marked in this respect is the fact that the ion $[M - 2]^{+\cdot}$ is considerably more abundant in the spectra of phenanthrene and pyrene obtained under CE conditions than under EI conditions. Apparently, the appearance energy of that fragment ion can be reached readily in the more energetic CE process. As a result of these differences between CE and EI spectra, a computer library search of the CE spectra of the PAHs in the NBS EI library was not very successful.

One aspect, which is also important in judging the analytical usefulness of the repeller effects, is the sensitivity. At present, a considerable loss in intensity is observed, when comparing spectra at low and high repeller potentials. In the chromatogram in Fig. 1, for instance, the intensity of the phenanthrene peak at high repeller potential is 30 times lower than that at low repeller potential. This can be attributed only partially to the fragmentation induced. Up to a ten-fold loss in the reconstructed total ion current (RIC) has been observed for the PAHs. However, it is important to note that, by increasing the repeller potential, the intensity of the background above $m/z = 100$ and consequently the noise level is greatly reduced, which may result in similar or even better detection limits. This aspect is currently under investigation.

Diuron

The repeller effects on the mass spectra of the chlorinated herbicide diuron, N-(3,4-dichlorophenyl)-N′,N′-dimethylurea (MW 232), have been investigated with both SFC–MS and LC–MS. SFC–MS spectra obtained with 2% of methanol in carbon dioxide at low, intermediate and high repeller potentials are given in Fig. 3. Fig. 4 shows the structure of diuron and tentative structures of some related compounds discussed below. At low repeller potential, proton transfer CI is observed, resulting in a peak from the protonated molecule at $m/z = 233$ (Fig. 3A), while at high repeller potential a peak from the molecular ion at $m/z = 232$ is observed, together with several fragment ions giving structural information (Fig. 3C). A thirty-fold decrease in RIC is observed when increasing the repeller potential from 20 to 180 V. The diuron spectrum obtained at high repeller potential closely resembles the EI spectrum of diuron; a computer library search in the NBS library was successful in this case (purity 600, fit 850).

In order to test whether an EI-like spectrum can be obtained as a result of CID effects, the protonated molecule of diuron was collisionally dissociated in a low energy MS–MS experiment with the triple quadrupole instrument. The only fragment observed is at $m/z = 72$, corresponding to $[(CH_3)_2N{=}C{=}O]^+$; it is found in the EI spectrum as well. Other EI fragments are not observed. From these results it appears that the diuron mass spectrum obtained at high repeller potential can be explained more easily by CE effects with the reagent gas ions present in the source than with CID effects. However, it must be pointed out that the fragment at $m/z = 72$ apparently has a low appearance energy. It is for instance also abundantly present in the diuron spectrum obtained at a repeller potential of 60 V (Fig. 3B), where protonated methanol is the most abundant reagent gas ion. Apparently, the protonated methanol

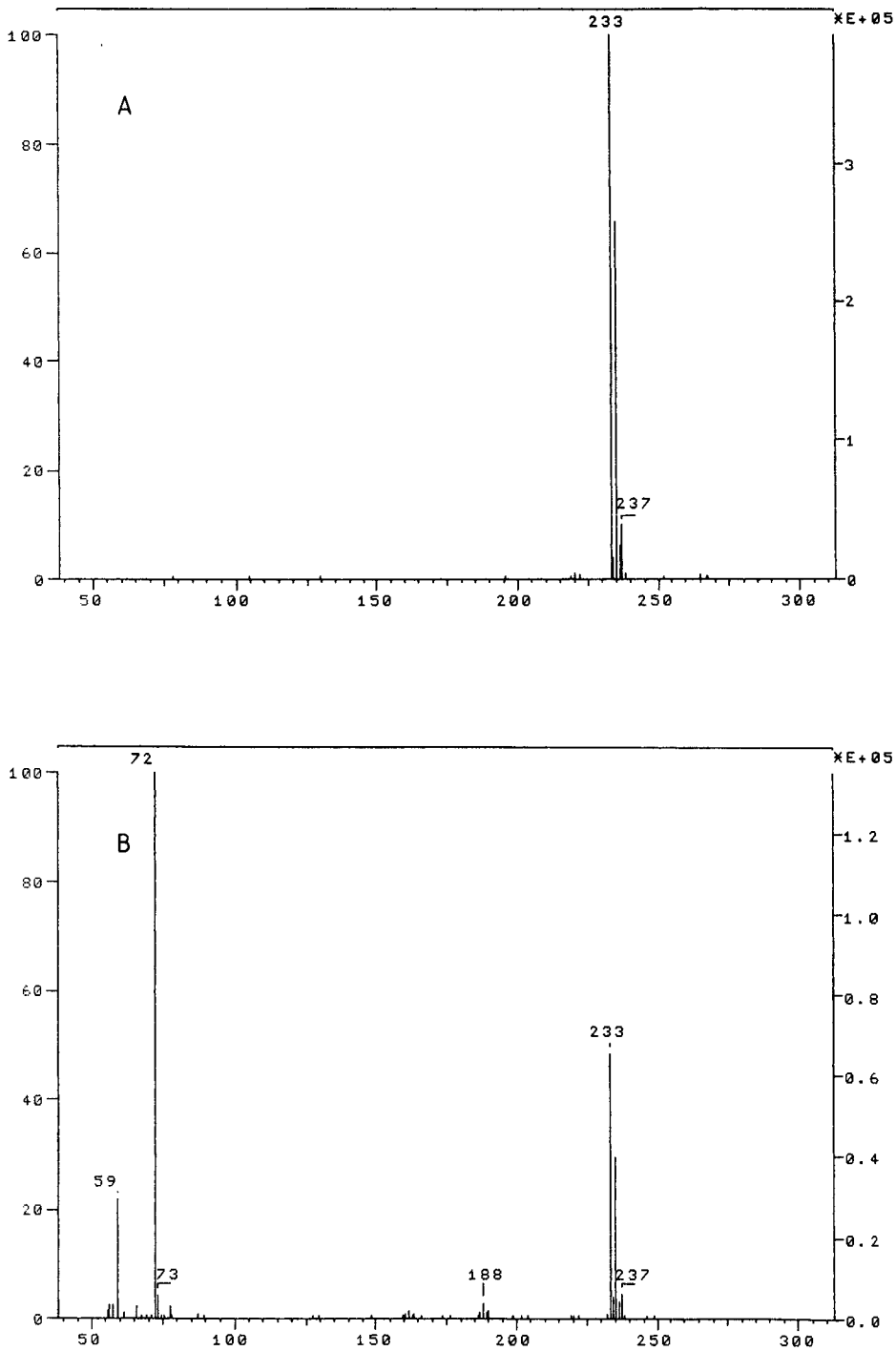

Fig. 3.

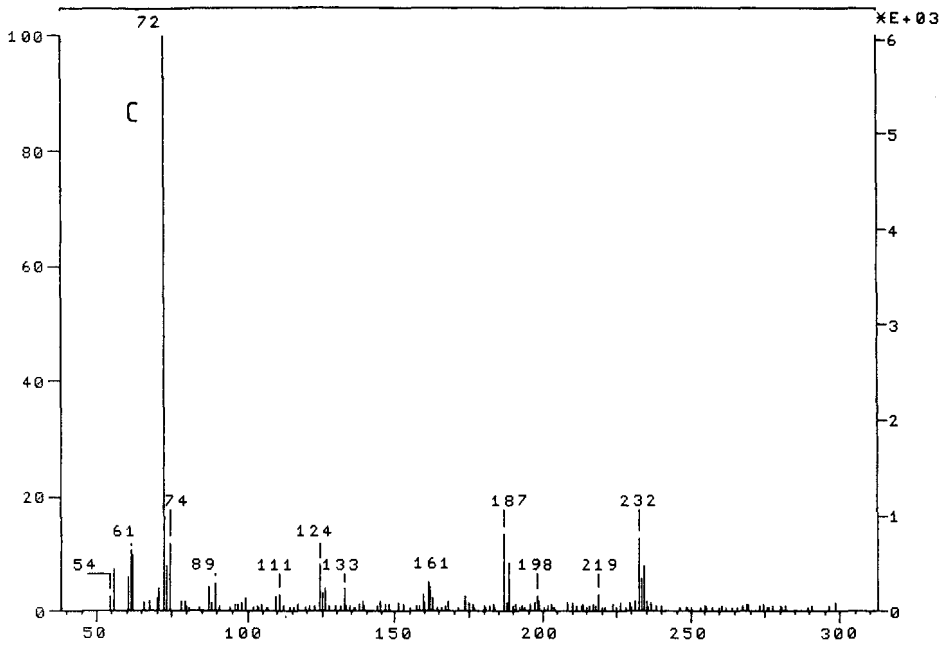

Fig. 3. Mass spectra of diuron at (A) low (20 V), (B) intermediate (60 V) and (C) high (180 V) repeller potentials. Conditions: SFC–MS with 2% of methanol in carbon dioxide and an aminopropyl column. Other conditions: see text.

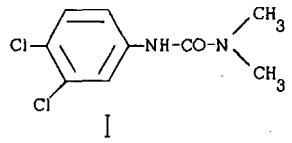

I

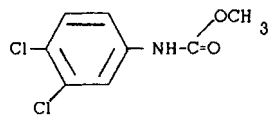

II

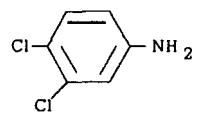

III

Fig. 4. Structure of diuron and tentative structures of some related compounds in SFC–MS and LC–MS. Explanation: see text.

clusters, the most abundant reagent gas ions at a repeller potential of 20 eV have slightly higher proton affinities than that of protonated methanol itself, resulting in a softer ionization with the clusters.

Diuron is a thermally labile compound. Therefore, the influence of the vaporizer temperature on the mass spectrum at low repeller voltage in SFC–MS has been investigated. It appears that the vaporizer temperature setting is very critical. At 60°C, instead of the usual 50°C, a peak at m/z = 220 is the most abundant; the isotope peaks present at m/z = 222 and 224 indicate the dichloro character of this thermal decomposition product. Daughter MS–MS spectra of m/z = 220 and 222 show a peak at m/z = 59 and peaks due to losses of 32 (probably methanol) and 60 mass units (probably methanol and CO). A tentative structure, II, for this compound is given in Fig. 4. At a vaporizer temperature of 100°C practically the only peak observed is at m/z = 162 with isotope peaks at m/z = 164 and 166, which is due to protonated dichloroaniline (structure III in Fig. 4), a well known thermal decomposition product of diuron and its analogues[16].

Diuron has also been investigated in LC–MS under discharge-on conditions. In a mobile phase of 80% methanol in water at a vaporizer temperature of 90°C and a repeller potential of 20 V a strong peak of the protonated molecule is observed at m/z = 233 (Fig. 5A), as well as less intense adduct peaks at m/z = 265, due to $(M + CH_3OH + H]^+$, and at m/z = 278 which will be explained below. Both ions show a dichloro character. The low-intensity peaks at m/z = 199 with monochloro character and at m/z = 165 without chloro addition indicate that the substitution of chlorine atoms by hydrogen, which has been observed under other CI conditions[17,18], takes place here as well. This effect is not observed in the SFC–MS experiments.

At the low mass end of the LC–MS spectrum peaks are detected at m/z = 74, 78 and 106. In the daughter MS–MS spectra of m/z = 74 and 106 the losses of one, and one and two methanol molecules, respectively, are observed, resulting in a fragment at m/z = 42, which might be protonated acetonitrile, but that is difficult to explain. From the daughter MS–MS spectrum of m/z = 78 it can be concluded that this peak is due to the methanol adduct of protonated dimethylamine (DMA). The peak of the dichloro compound at m/z = 278 is probably due to the DMA adduct of diuron itself, which explains the strong fragment at m/z = 46 in the daughter spectrum of m/z = 278. The presence of substantial amounts of DMA in the ion source is rather surprising, although it is formed via structure II in Fig. 4 and has been detected as one of the thermal decomposition product of diuron and its analogues as well[16]. In the reaction gas it is a compound with an higher proton affinity than that of diuron and the other reagent gas constituents.

At higher repeller potentials the intensity of the protonated molecule decreases, while a strong peak at m/z = 72 and some other minor fragments appear. The informative fragmentation, found at high repeller potential in SFC–MS, is not present in the LC–MS spectra. The RIC due to diuron first decreases with increasing repeller potential, but when the peak at m/z = 72 becomes the base peak the RIC starts to increase up to the original level. As it is less specific, the peak at m/z = 72 is of course less attractive for quantitation purposes than the protonated molecule cluster at m/z = 233–237.

In a mobile phase of 20% methanol in water at a vaporizer temperature of 110°C and a repeller potential of 20 V, the peak due to the protonated dichloroaniline

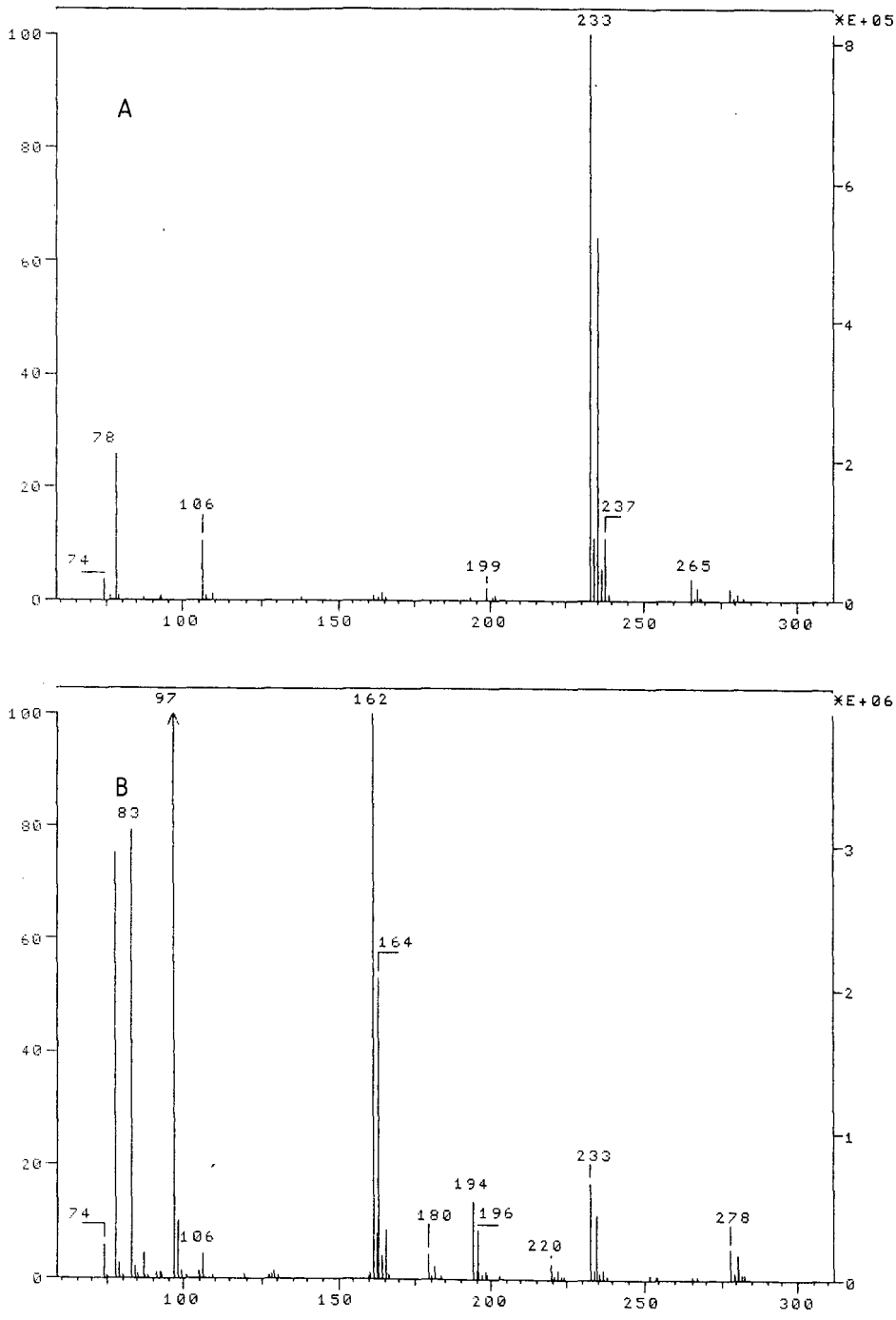

Fig. 5. Mass spectra of diuron at a repeller potential of 20 V in LC–MS, with (A) 80% methanol in water and vaporizer temperature 90°C, and (B) 20% methanol in water and vaporizer temperature 110°C. Other conditions: see text.

at m/z = 162 is the base peak, while an intense peak at m/z = 78 which has been explained above is also observed. The protonated molecule at m/z = 233 is 10–40% of the base peak depending on the condition of the vaporizer. Other peaks are solvent clusters, *e.g.*, m/z = 83, which is $[2CH_3OH + H_2O + H]^+$, m/z = 97, which is $[3CH_3OH + H]^+$, and m/z = 129, which is $[4CH_3OH + H]^+$[14]. The peaks at m/z = 180 and 194, both showing a dichloro character, can be explained as water and methanol adducts of the protonated dichloroaniline, respectively. The DMA adduct ion at m/z = 278 is also observed.

The change in the spectrum by decreasing the methanol content of the solvent is somewhat surprising. Since in fact two parameters are changed at the same time, *i.e.*, the methanol content and the vaporizer temperature, spectra of diuron have also been obtained with a vaporizer temperature of 110°C and 80% methanol in water, and with a vaporizer temperature of 90°C and 20% methanol in water. In both cases the vaporization conditions are unfavourable: the vaporizer temperature is either too low for optimum stability or too high, resulting in a dry spray. However, essentially no spectral change is observed in those two cases; the relative abundance of the protonated diuron is somewhat higher at low vaporizer temperature with 20% methanol in water. Apparently, hydrolysis of diuron to dichloroaniline takes place in the highly aqueous environment more easily than in the other solvent.

At still higher vaporizer temperatures, thermal decomposition of diuron is observed in both solvents, starting at higher temperatures with 80% methanol in water than with 20% methanol in water. Under these conditions the peak at m/z = 220 with dichloro character, which has also been found in the SFC–MS experiments, appears in the spectrum as the second most intense cluster. The methanol adduct of this compound is also observed at m/z = 252. At still higher temperatures a peak due to a monochloro compound is observed at m/z = 127. The nature of this compound is unclear.

Phenacetin and caffeine

The repeller effects in the mass spectrum of phenacetin (see Fig. 6 for the structure) have been studied in SFC–MS with a mobile phase of 2% of methanol in carbon dioxide. The mass spectra at four different repeller potentials are given in Fig. 6. At low repeller voltage a strong protonated molecule is observed without any fragmentation. At repeller potentials where the protonated molecule of methanol has become the most abundant reagent gas ion some fragmentation is observed: loss of ethene resulting in m/z = 152, loss of 42 ($H_2CC=O$, formaldehyde) resulting in m/z = 138 and the loss of ethene and formaldehyde resulting in m/z = 110. At higher repeller potential the fragment peaks become more abundant than the protonated molecule. At still higher repeller potential the phenacetin molecular ion is observed, next to fragments at m/z = 137 and 109. These peaks are also observed in the EI spectrum of phenacetin. The sensitivity decreases dramatically at higher repeller potentials.

The repeller effects in the mass spectrum of caffeine (MW 194) have been studied with SFC–MS as well as LC–MS. In SFC–MS with 2% methanol in carbon dioxide a strong protonated caffeine molecule is observed at m/z = 195 and a methanol adduct at m/z = 227 at low repeller potential. Comparable to the SFC–MS spectra of diuron and phenacetin, some fragmentation in the caffeine spectrum is

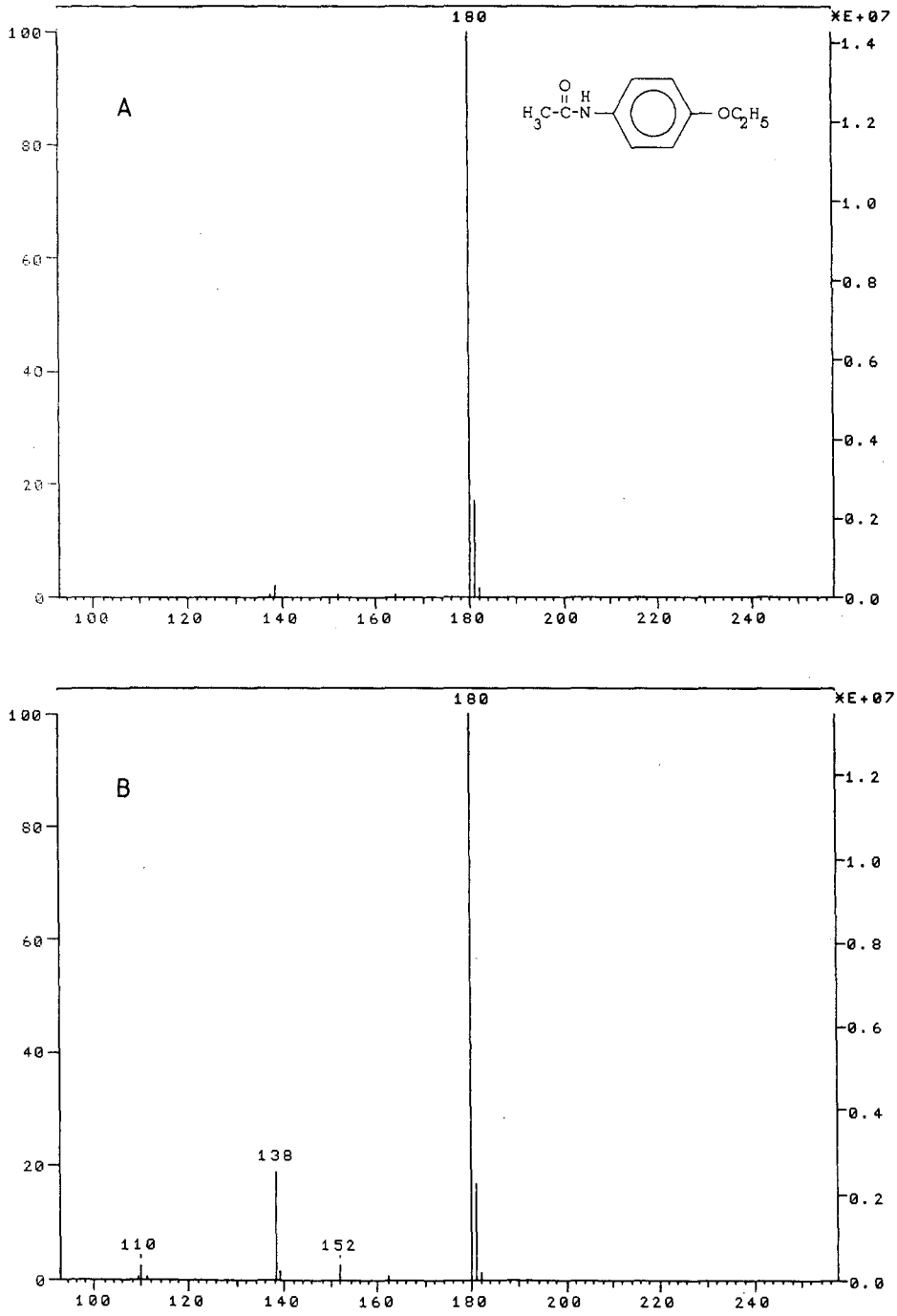

Fig. 6.

(*Continued on p. 336*)

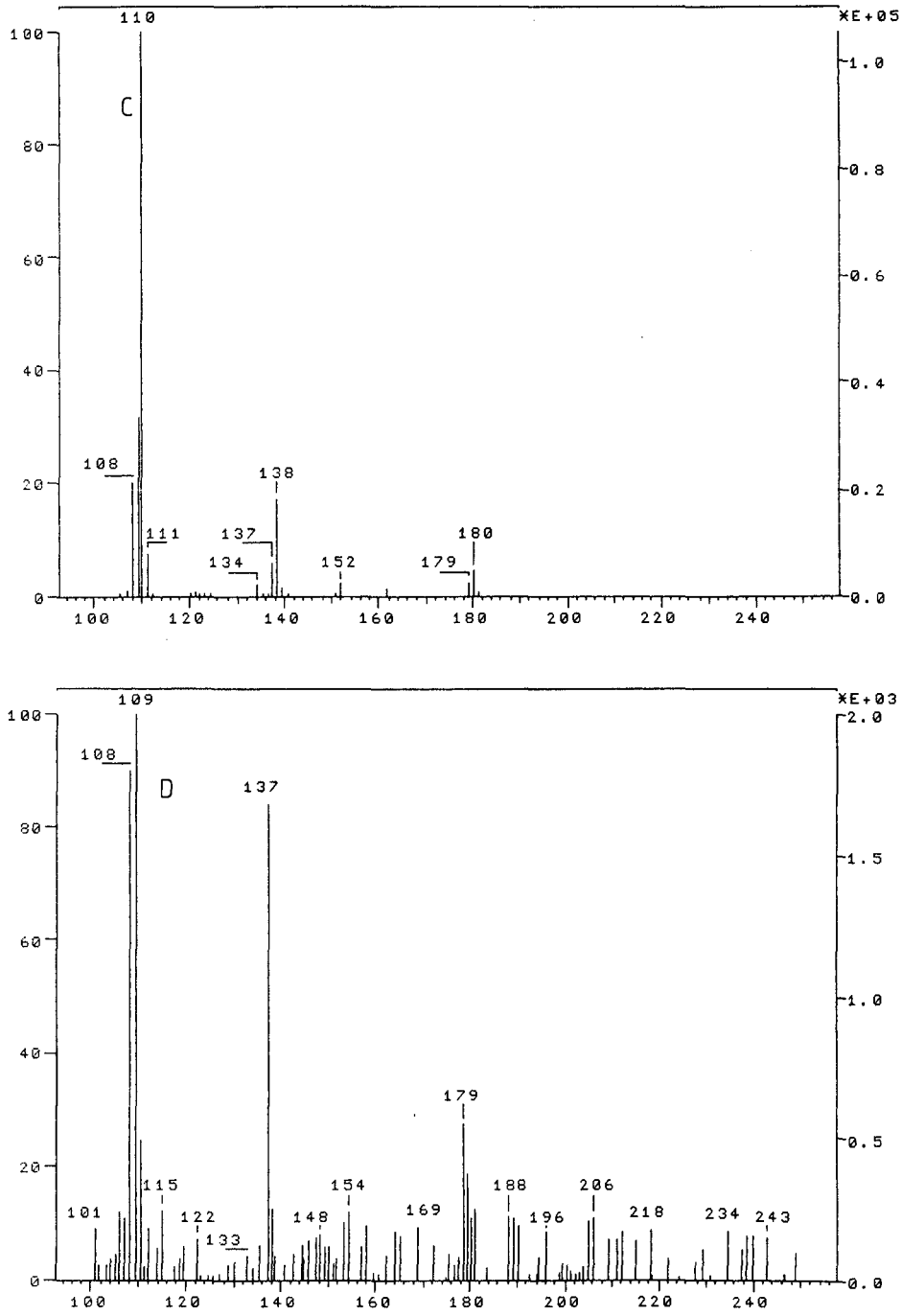

Fig. 6. Mass spectra and structure of phenacetin at repeller potentials of (A) 40, (B) 50, (C) 70 and (D) 150 V. Conditions: SFC–MS with 2% of methanol in carbon dioxide and a C_{18} column. Other conditions: see text.

present under conditions where protonated methanol is the most abundant reagent gas ion. The loss of CH_3–N=C=O from the protonated molecule results in fragment peak at m/z = 138. At still higher repeller potential the fragment peak at m/z = 138 becomes the base peak, while several other fragment peaks are observed, for instance m/z = 110, resulting from the loss of CO from m/z = 138. A weak peak at m/z = 194 is also observed. As in the phenacetin spectrum, the information becomes less clear at higher repeller potential, as a result of the transition from proton-transfer CI to CE phenomena and the drop in sensitivity. The fragments found at intermediate repeller potentials are similar to those found in the MS–MS daughter spectrum of the protonated caffeine.

In LC–MS, caffeine has been studied with 80% methanol in water. Protonated caffeine (m/z = 195) is observed at all repeller potentials studied (0–180 V), while some fragmentation, similar to that described for SFC–MS, is found at repeller potentials above 100 V. While in SFC–MS a considerable loss in RIC is observed at higher potentials, in LC–MS the RIC is not influenced. The intensity of the protonated molecule decreases about twenty-fold when fragmentation is induced.

CONCLUSIONS

Induction of fragmentation at higher repeller potentials is observed as a general trend in the mass spectra of the analytes studied so far with SFC–MS in the discharge-on mode. At intermediate repeller potentials, where protonated methanol and protonated carbon dioxide are the most abundant species in the reagent gas, useful structural information is obtained without much loss in intensity. At high repeller potentials the CE with the carbon dioxide molecular ions results in extensive fragmentation and a significant loss in sensitivity. At high repeller potentials, useful fragmentation is obtained only in some cases. Sometimes the interpretation is also inhibited by the unfavourable signal-to-noise ratio of the spectra. Extensive fragmentation, which can differ from EI fragmentation, is observed; the ionization produces ions with higher internal energy than in the common EI spectra at 70 eV.

Many compounds have been investigated under discharge-on conditions with various mobile phases and at different repeller potentials in LC–MS. In general, it can be stated that useful structural information can be obtained in many cases under these conditions. The loss of sensitivity at high repeller potential is small or absent in LC–MS.

The mechanisms leading to the fragmentation at higher repeller potentials are not clear. The advent of fragmentation coincides with changes in the reagent gas spectrum, and some of the observed effects have also been predicted from those changes in the reagent gas composition. On the other hand, CID of protonated molecules in the high pressure ion source may play an significant role as well. Some changes in the reagent gas spectrum can be explained from CID processes of the reagent gas cluster ions, especially in LC–MS. However, significant differences in high repeller voltage spectra and CID spectra are also observed, especially in SFC–MS, which indicate different mechanisms for different compounds. Further investigations are being performed and will be reported in due course.

REFERENCES

1 R. D. Smith, H. T. Kalinoski and H. R. Udseth, *Mass Spectrom. Rev.*, 6 (1987) 445.
2 L. G. Randall and A. L. Wahrhaftig, *Rev. Sci. Instrum.*, 52 (1981) 1283.
3 H. M. Pang, C. H. Sin, D. M. Lubman and J. Zorn, *Anal. Chem.*, 58 (1986) 1581.
4 R. D. Smith, J. C. Fjeldsted and M. L. Lee, *J. Chromatogr.*, 247 (1982) 231.
5 J. Cousin and P. J. Arpino, *J. Chromatogr.*, 398 (1987) 125.
6 A. J. Berry, D. E. Games, I. C. Mylchreest, J. R. Perkins and S. Pleasance, *Biomed. Environ. Mass Spectrom.*, 15 (1988) 105.
7 J. R. Chapman, *Rapid Commun. Mass Spectrom.*, 2 (1988) 6.
8 A. J. Berry, D. E. Games and J. R. Perkins, *J. Chromatogr.*, 363 (1986) 147.
9 P. Dätwyler, H. J. Walther and P. Hirter, paper presented at the *4th International Symposium on LC–MS and MS–MS, Montreux, October 22–24, 1986.*
10 W. M. A. Niessen, R. A. M. van der Hoeven, M. A. G. de Kraa, C. E. M. Heeremans, U. R. Tjaden and J. van der Greef, *Adv. Mass Spectrom.*, 11 (1989) 860.
11 D. E. Games, S. Y. Hughes and I. C. Mylchreest, *Adv. Mass Spectrom.*, 11 (1989) 1230.
12 D. Zakett, G. J. Kallos and P. J. Savickas, *32nd Annual Conference on Mass Spectrometry and Allied Topics, San Antionio, TX, May 27–June 1, 1984*, p. 3.
13 W. H. McFadden and S. A. Lammert, *J. Chromatogr.*, 385 (1987) 201.
14 W. M. A. Niessen, R. A. M. van der Hoeven, M. A. G. de Kraa, C. E. M. Heeremans, U. R. Tjaden and J. van der Greef, *J. Chromatogr.*, 474 (1989) 113.
15 W. M. A. Niessen, P. J. M. Bergers, U. R. Tjaden and J. van der Greef, *J. Chromatogr.*, 454 (1988) 243.
16 J. Gomez, C. Bruneau, N. Soyer and A. Brault, *J. Agric. Food Chem.*, 30 (1982) 180.
17 A. C. Tas, J. van der Greef, M. C. ten Noever de Brauw, T. A. Plomp, R. A. A. Maes, M. Höhn and U. Rapp, *J. Anal. Toxicol.*, 10 (1986) 46.
18 E. R. Verheij, G. F. LaVos, W. van der Pol, W. M. A. Niessen and J. van der Greef, *J. Anal. Toxicol.*, 13 (1989) 8.

Journal of Chromatography, 478 (1989) 339–347
Elsevier Science Publishers B.V., Amsterdam — Printed in The Netherlands

CHROM. 21 646

RETENTION BEHAVIOUR OF CARDIAC STEROIDS USING CYCLODEXTRIN IN THE MOBILE PHASE IN HIGH-PERFORMANCE LIQUID CHROMATOGRAPHY

KAZUTAKE SHIMADA*, TOMOYUKI OE, YASUKO HIROSE and YOSHIHIRO KOMINE
Faculty of Pharmaceutical Sciences, Kanazawa University, Kanazawa 920 (Japan)
(First received March 28th, 1989; revised manuscript received May 23rd, 1989)

SUMMARY

The retention behaviour of twenty cardiac steroids and four fluorescent derivatives was examined by the addition of cyclodextrin to the mobile phase in reversed-phase high-performance liquid chromatography. The addition of a suitable cyclodextrin improved the separation of isomeric cardiac steroids. The steroid A/B ring junction is the most important factor in the choice of the optimum cyclodextrin to be added; the C/D ring junction is less important. The hydroxyl group at the 3- or 12-position of the steroid enhanced the changes in retention times of these compounds. The effect of an unsaturated lactone ring at the 17β-position on the retention in the presence of cyclodextrin was also determined with cardenolide (five-membered ring) and bufadienolide (six-membered ring) but little difference was observed. Isomeric cardiac steroids, whose separation has not been done by the conventional method, were clearly separated by this method. The fluorescence intensity of 3-(1-anthroyl)-cardiac steroid was enhanced by the addition of cyclodextrin to the mobile phase.

INTRODUCTION

Cyclodextrins (CDs) are toroidal-shaped cyclic oligosaccharides consisting of α-1,4-linked D-glucopyranose units. They exhibit an highly stereoselective ability to form inclusion complexes with a variety of molecules and ions. Some attempts to utilize this phenomenon have been made in gas and liquid chromatography[1]. A CD-bonded column or CD-containing mobile phase in high-performance liquid chromatography (HPLC) is often preferable to conventional ones for the separation of optical, geometrical and structural isomers[2–8].

In previous papers we reported the use of CD in the mobile phase, which is of great advantage in the separation of isomeric steroids (oestrogens[9], bile acids[10]) and their fluorescence detection in reversed-phase HPLC. As a continuation of this work, the present paper deals with the retention behaviour of twenty cardiac steroids and four fluorescent derivatives using CD as a component of the mobile phase in HPLC[a]. The effect of CD on the fluorescence detector response has also been investigated.

[a] Part of this work has been published as a preliminary report[11].

0021-9673/89/$03.50

EXPERIMENTAL

Materials

CDs were kindly supplied by Nihon Shokuhin Kako (Tokyo, Japan). Heptakis(2,6-di-O-methyl-β-CD) (Me-β-CD) was prepared and donated by Kao (Tokyo, Japan). Octakis(2,6-di-O-methyl-γ-CD) (Me-γ-CD) was prepared by the method reported by Casu *et al.*[12]. Cardiac steroids were isolated from the natural source[13] or synthesized from digitoxin and digoxin (Nakarai Tesque, Kyoto, Japan) by known methods[14]. 1-Anthroyl cyanide was obtained from Wako (Tokyo, Japan). Solvents were purified by distillation prior to use.

Apparatus

HPLC was carried out on a Shimadzu LC-6A chromatograph equipped with a Shimadzu SPD-6AV ultraviolet (UV) detector (Shimadzu, Kyoto, Japan) or an Hitachi F-1000 fluorescence (FL) detector (Hitachi, Tokyo, Japan) at a flow-rate of 1 ml/min. A Develosil ODS-5 (5 μm) column (15 cm × 0.4 cm I.D.) (Nomura Chemical, Seto, Japan) was used at ambient temperature unless stated otherwise. The void volume was determined by the use of $NaNO_3$ (UV) or methanol (FL).

Derivatization

Cardiac steroids were derivatized with 1-anthroyl cyanide according to the procedure described by Goto *et al.*[15].

RESULTS AND DISCUSSION

Effect of CD on the retention of cardiac steroids differing in A/B ring junction and/or 3-substituent

In our preliminary work it was suggested that the retention behaviour of cardiac steroids in HPLC is influenced by differences in the steroid A/B ring junction and 3-substituent[11]. On the basis of these findings, the effects of the α-, β- and γ-CD contents in the mobile phase on the capacity factors, k', of compounds **1–10**, which differ in the A/B ring junction and/or 3-substituent, were investigated (Figs. 1 and 2). All the k' values of the compounds examined obtained without CD were kept at greater than 6.81 by changing the concentration of the organic modifier. Since the organic modifier competes with the solute for the hydrophobic CD cavity, a change in the proportion of organic modifier may influence the solute interaction with the CD. However, a change in the proportion was unavoidable to get the appropriate k' value for detection and characterization of the effect of CD.

Among the CDs examined, α-CD had little effect on the k' values of all the compounds examined. On the contrary, the k' values of these compounds decreased with increasing concentration of β- or γ-CD in the mobile phase. This phenomenon can be explained by the cavity size of the CD, that of α-CD being too small to include the cardiac steroid. Regarding the A/B ring junction, γ-CD was remarkably more effective than β-CD in decreasing the k' values of compounds having a A/B *cis* ring junction. A/B *trans* and 5-ene series slightly prefer β-CD to γ-CD, but the reverse effect has been observed with 4-ene series.

Irrespective of the A/B ring junction, the effect of the 3-substituent on the

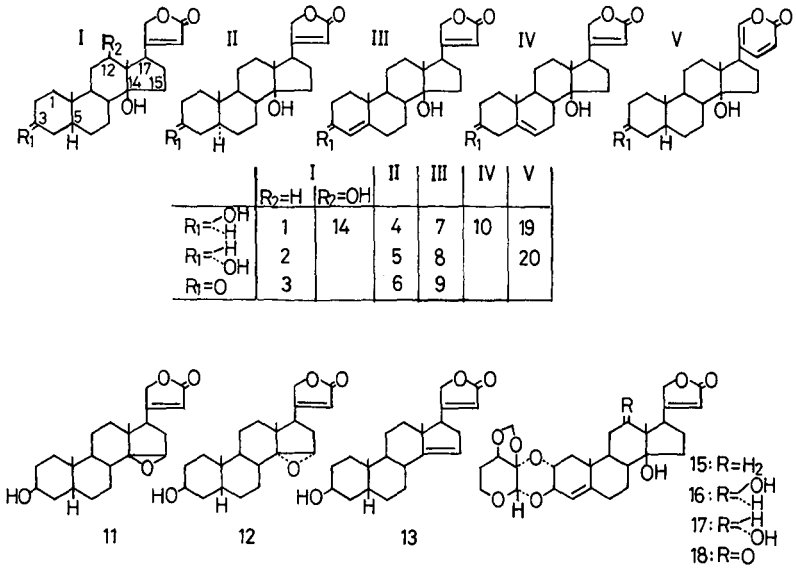

Fig. 1. Structures of cardiac steroids.

relative k' value decreased in the order of 3 β-OH, 3 α-OH and 3-oxo groups with increasing concentration of CDs. The relative k' values of the 3-hydroxyl compounds were influenced more markedly than those of the corresponding 3-oxo compounds in both the A/B *cis* and *trans* series, but only a slight difference was observed in the 4-ene series.

Separation of digitoxigenin (1) and uzarigenin (4)

The above data prompted us to separate digitoxigenin (**1**) and uzarigenin (**4**), whose separation has not been done by the conventional method (Fig. 3a). The effects of β- and γ-CD on the k' values and resolution, R_s, of **1** and **4** are illustrated in Fig. 4. Rapid elution and good separation of geometric isomers were obtained with increasing concentration of β-CD. The addition of 5 mM γ-CD gave rapid elution of the isomers, and although the R_s value decreased it was still 5. Conversely, a lower γ-CD concentration (2mM) affords the best resolution (R_s 9.0) with a corresponding increase in k'. The k' value of compound **1** or **4** was influenced more markedly than that of **4** or **1** with increasing concentration of γ- or β-CD, respectively. A complete separation was attained with shortening of retention time, as shown in Fig. 3b and c. A retention reversal is observed in these chromatograms, and would be helpful in identifying peaks in chromatograms of biological samples.

Effect of CD on the retention of cardiac steroid differing in C/D ring junction, 12- or 17-substituent

Cardiac steroids obtained from natural sources were divided into two categories, cardenolide and bufadienolide having a five- or six-membered lactone ring at the 17β-position, respectively. Many cardiac steroids differing in the C/D ring junction or 12-substituent were synthesized or isolated from natural sources to determine their

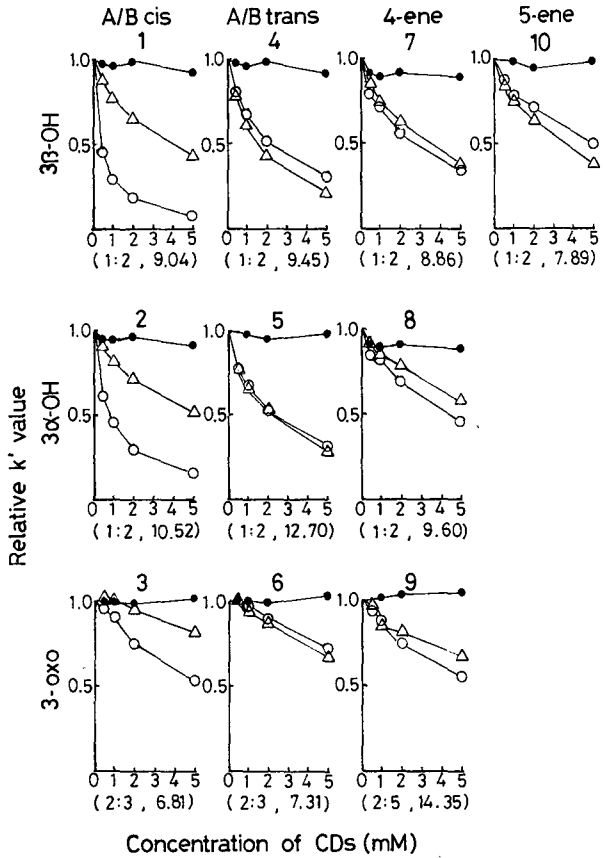

Fig. 2. Effect of CD on the retention of cardiac steroids differing in the A/B ring junction and/or 3-substituent; ●, α-CD; △, β-CD; ○, γ-CD. Conditions: mobile phase, acetonitrile–water containing CD as indicated; detection, UV 240 nm; $t_0 \doteq 1.10$ min. Compound numbers indicated at the top of each figure. The ratio of acetonitrile–water and the k' value obtained without CD, taken as 1.0 for the calculation of the relative k' value, are indicated in parentheses.

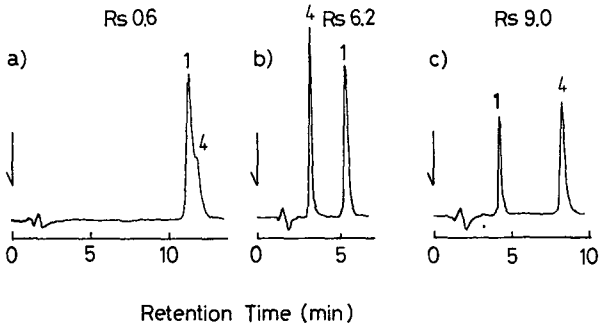

Fig. 3. Separation of digitoxigenin (**1**) and uzarigenin (**4**). Conditions: mobile phase, (a) acetonitrile–water (1:2), (b) and (c) containing β-CD (5.0 m*M*) and γ-CD (1.0 m*M*); detection, UV 240 nm.

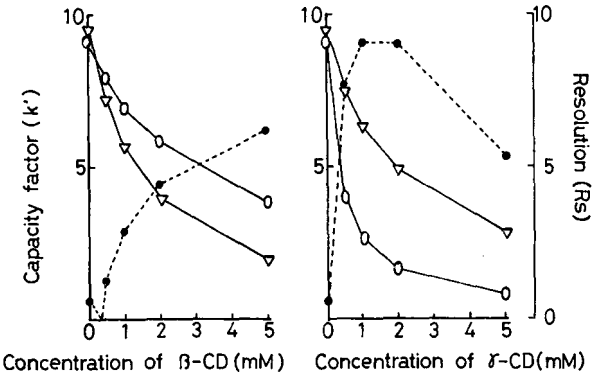

Fig. 4. Effect of CD on the retention and separation of digitoxigenin and uzarigenin; ○, digitoxigenin (**1**); ▽, uzarigenin (**4**); ●, resolution of **1** and **4**. Conditions; mobile phase, acetonitrile–water containing CD as indicated; detection, UV 240 nm.

biological activities. Structure–activity relationships of these compounds showed that these functions are the key structural features for the cardiotonic activity[13]. These data prompted us to examine the retention behaviour of cardiac steroids differing in the C/D ring junction, 12- or 17-substituent (Fig. 5). All the k' values of the compounds examined obtained without CD were kept at >5.50 as described above. The relative k' values of digitoxigenin (**1**) and compounds **11**–**13** differing in the C/D ring junction were affected by the addition of γ-CD to the mobile phase, the contribution of the

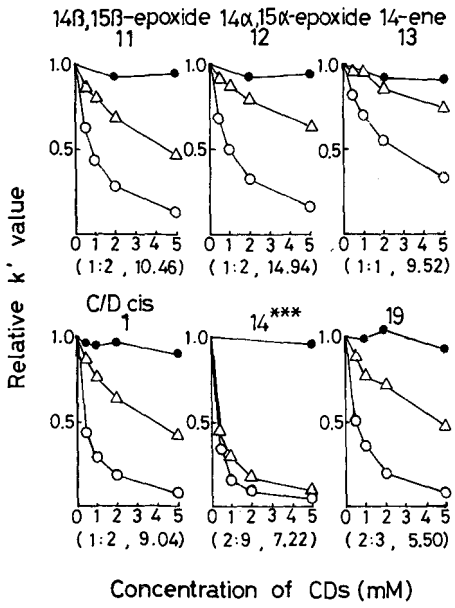

Fig. 5. Effect of CD on the retention of cardiac steroids differing in the C/D ring junction, 12- or 17-substituent: ●, α-CD; △, β-CD; ○, γ-CD. Conditions as in Fig. 2 except for compound **19** which was monitored at 300 nm. ***. From ref. 11.

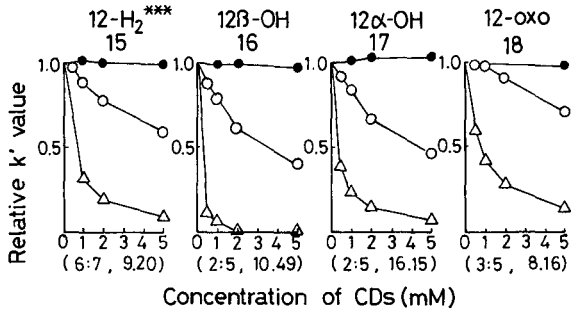

Fig. 6. Effect of CD on the retention of elaeodendroside derivatives differing in the 12-substituent; ●, α-CD; △, β-CD; ○, γ-CD. Conditions as in Fig. 2. *** From ref. 11.

structural feature to the decrease in k' value being in the order of C/D-*cis*> 14β,15β-epoxide> 14α,15α-epoxide> 14-ene. The A/B ring junction of all the compounds examined was *cis*, so γ-CD was a more effective modifier than β-CD for the retention as described above.

Next, the effect of the 12-substituent on the relative k' value was investigated with compound **1** and digoxigenin (**14**) having a 12β-hydroxyl group. The relative k' value of **14** was influenced more than that of **1** by the addition of γ-CD. Although the A/B ring junction of **14** was *cis*, β-CD was as effective as γ-CD in decreasing the k' value. Further investigation on the effect of the 12-substituent on the retention was made by using elaeodendroside derivatives, recently isolated from plant material in these laboratories (Fig. 6)[13]. The relative k' value of compounds having a 12β- or α-hydroxyl group (**16**,**17**) was influenced more than that of the unsubstituted

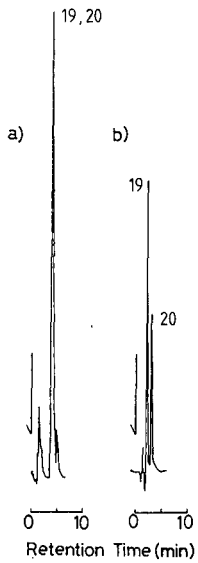

Fig. 7. Separation of bufalin (**19**) and 3-epibufalin (**20**). Conditions: mobile phase, (a) acetonitrile–water (1:1), (b) (5:8) containing 3.9 m*M* γ-CD; detection, UV 300 nm.

compound (**15**) by β- and γ-CDs. On the contrary, the relative k' value of 12-oxoelaeodendroside D (**18**) was affected less than that of **15** by the additives. It is likely that the hydroxyl group on the steroid moiety will be the important factor for the formation of the inclusion complex from the solute and CD. The significant interactions, *e.g.*, hydrogen bonding may occur between solutes bearing OH groups and the 2- and 3-hydroxyl groups of CD.

The effect of the unsaturated lactone ring at the 17β-position on the retention by each CD was also determined with compound **1** and bufalin (**19**). No remarkable difference in the effect on their relative k' values was observed as shown in Fig. 5. This suggested that the above information on cardenolides may be applicable to the separation of bufadienolides by HPLC using CD. The separation of compound **19** and 3-epibufalin (**20**), not achieved by the conventional method, was attempted on this assumption (Fig. 7a). γ-CD was used as an additive in the mobile phase, and gave a satisfactory separation of these compounds as shown in Fig. 7b.

Effect of CD on the retention and FL response of labelled cardenolides

The determination of the serum concentration of cardiac steroids is important in clinical chemistry[16]. Some derivatization methods have been developed for HPLC analysis, but the sensitivity is not so enough to monitor the concentration of this drug in serum. Recently Goto *et al.*[15] synthesized a new fluorescence derivatization agent, 1-anthroyl cyanide, and obtained satisfactory results in the determination of bile acids in biological fluids.

It has also been reported that CD serves to enhance and stabilize the fluorescence intensity of dansyl amino acids on a silica gel layer[17]. Fluorescence enhancement was also observed on inclusion of coumarin derivatives with β-CD[18]. Similar phenomena were observed for oestrogen and labelled bile acids as reported previously[9,10]. On the basis of these findings, the chromatographic behaviours of four cardenolides labelled with 1-anthroyl cyanide and their FL response were investigated (Fig. 8). Owing to the sparing solubility of CDs in the mobile phase containing more than 50% of organic modifier, Me-β- and Me-γ-CDs were used as a substitute for β- and γ-CDs, respectively. The effects of methylated CDs on the k' values of oestriol[9] and digitoxigenin (**1**) were not so different from those of CDs. The chromatographic behaviour is shown in Fig. 9. Only small changes in the retentions were observed with increasing concentration of Me-γ-CD. The addition of Me-β-CD gave some changes in the retention but much less than those of underivatized cardenolides. The bulky

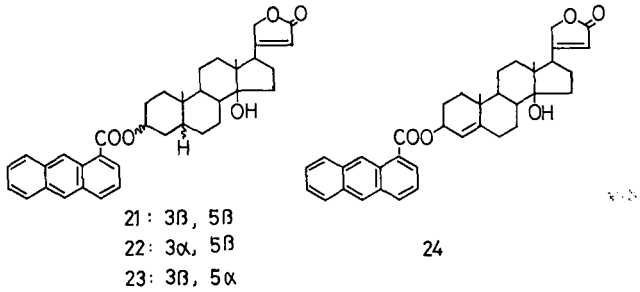

Fig. 8. Structures of 3-(1-anthroyl)cardenolides.

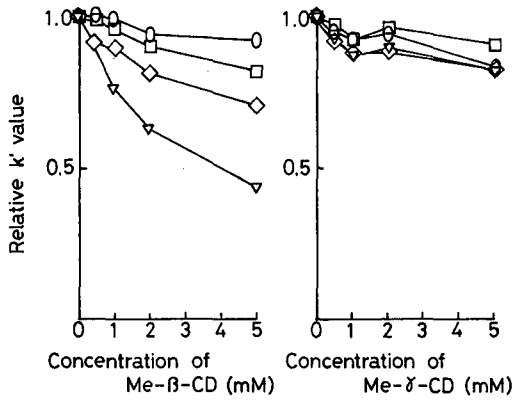

Fig. 9. Effect of CD on the retention of labelled cardenolides: ○, 3-(1-anthroyl)digitoxigenin (**21**); □, 3-epi-(1-anthroyl)digitoxigenin (**22**); ▽, 3-(1-anthroyl)uzarigenin (**23**); ◇, 3-(1-anthroyl)canarigenin (**24**). Conditions: column, YMC-GEL C_8 (5 μm; 15 cm × 0.4 cm I.D.) (Yamamura Chem. Lab., Kyoto, Japan); mobile phase, acetonitrile–water (3:1) containing CD as indicated; detection, FL excitation, 370 nm; emission, 470 nm); t_0 = 1.34 min. The k' value (**21**, 9.41; **22**, 9.61; **23**, 10.91; **24**, 9.45) obtained without CD was taken as 1.0 for the calculation of the relative k' values.

anthracene residue may interfere with the formation of the inclusion complex, but further studies are necessary to clarify this.

The fluorescence intensity of 3-(1-anthroyl)uzarigenin (**22**), whose k' value was most influenced by the additive, was enhanced approximately 1.15 times by the addition of 5 m*M* Me-β-CD to the mobile phase. This datum is compatible with our previous results[9,10].

CONCLUSION

The retention behaviour of twenty cardiac steroids and four fluorescence derivatives was demonstrated by HPLC using CD as the mobile phase additive. The present data show that: differences in the A/B ring junction are more effective than those in the C/D ring junction for changes in the k' values; hydroxyl group at the 3- and 12-positions enhance the decrease in k'. This information is useful for the separation of isomeric cardiac steroids whose separation has not been done by the conventional method. Also such a characteristic chromatographic behaviour reflecting chemical structure would be helpful in identifying the peaks in chromatograms of biological samples. The method is also of advantage in the detection of fluorescent derivatives. Further application of the present method to clarify the metabolic pathways of cardenolide and bufadienolide is being carried out in these laboratories and the details will be reported elsewhere.

ACKNOWLEDGEMENTS

The authors are indebted to Mr. T. Nemoto (Kao Co.) and Nihon Shokuhin Kako Co. for supplying CDs. This work was supported in part by grants from the Takeda Research Foundation and Ministry of Education, Science and Culture of Japan.

REFERENCES

1 W. L. Hinze, *Sep. Purif. Methods*, 10 (1981) 159; and references cited therein.
2 K. Uekama, F. Hirayama, K. Ikeda and K. Inaba, *J. Pharm. Sci.*, 66 (1977) 706.
3 D. W. Armstrong, W. DeMond, A. Alak, W. L. Hinze, T. E. Riehl and K. H. Bui, *Anal. Chem.*, 57 (1985) 234.
4 M. Gazdag, G. Szepesi and L. Huszár, *J. Chromatogr.*, 351 (1986) 128.
5 M. Gazdag, G. Szepesi and L. Huszár, *J. Chromatogr.*, 371 (1986) 227.
6 M. Gazdag, G. Szepesi and L. Huszár, *J. Chromatogr.*, 436 (1988) 31.
7 M. Gazdag, G. Szepesi and K. Mihályfi, *J. Chromatogr.*, 450 (1988) 145.
8 J. Zukowski, D. Sybilska, J. Bojarski and J. Szejtli, *J. Chromatogr.*, 436 (1988) 381.
9 K. Shimada, T. Masue, K. Toyoda, M. Takani and T. Nambara, *J. Liq. Chromatogr.*, 11 (1988) 1475.
10 K. Shimada, Y. Komine and T. Oe, *J. Liq. Chromatogr.*, 12 (1989) 491.
11 K. Shimada, T. Oe, C. Kanno and T. Nambara, *Anal. Sci.*, 4 (1988) 377.
12 B. Casu, M. Reggiani, G. G. Gallo and A. Vigevani, *Tetrahedron*, 24 (1968) 803.
13 K. Shimada, T. Kyuno, T. Nambara and I. Uchida, *Chem. Pharm. Bull.*, 30 (1982) 4075; and references cited therein.
14 D. Satoh and K. Aoyama, *Chem. Pharm. Bull.*, 18 (1970) 94.
15 J. Goto, N. Goto, F. Shamsa, M. Saito, S. Komatsu, K. Suzaki and T. Nambara, *Anal. Chim. Acta*, 147 (1983) 397.
16 K. Shimada, S. Mizusawa, T. Ohkubo and T. Nambara, *Chem. Pharm. Bull.*, 32 (1984) 2301; and references cited therein.
17 T. Kinoshita, F. Iinuma, K. Atsumi, Y. Kamada and A. Tsuji, *Chem. Pharm. Bull.*, 23 (1975) 1166.
18 A. Takadate, H. Fujino, S. Goya, F. Hirayama, M. Otagiri, K. Uekama and H. Yamaguchi, *Yakugaku Zasshi*, 103 (1983) 193.

Journal of Chromatography, 478 (1989) 349–367
Elsevier Science Publishers B.V., Amsterdam — Printed in The Netherlands

CHROM. 21 644

MULTIRESIDUE PROCEDURES FOR THE DETERMINATION OF CHLORINATED DIBENZODIOXINS AND DIBENZOFURANS IN A VARIETY OF FOODS USING CAPILLARY GAS CHROMATOGRAPHY–ELECTRON-CAPTURE DETECTION

JAMES S. JASINSKI

U.S. Department of Health and Human Services, Food and Drug Administration (Detroit District), 1560 E. Jefferson Avenue, Detroit, MI 48207 (U.S.A.)

(First received February 10th, 1989; revised manuscript received May 25th, 1989)

SUMMARY

Multiresidue digestion–extraction procedures for the determination of chlorinated dioxins and furans in a wide variety of products are presented. Procedure selection is dependent upon the residue(s) of interest, and on the fat content of the product. Additional cleanup is accomplished using column chromatography and a Florisil trap. The separation of residues is achieved by fraction collection off of two high-performance liquid chromatographic systems. Capillary gas chromatography employing electron-capture detecton is used for quantitation. The extracts are suitable for gas chromatography–mass spectrometry or gas chromatography with Hall electrolytic conductivity detection. Results of analysis, recovery data, and interlaboratory comparisons are presented. Spike recoveries will typically average 90% ± 10%.

INTRODUCTION

The occurrence of polychlorinated dibenzodioxins (PCDDs) in the environment has presented a formidable challenge to the residue chemists who have had to devise procedures for their analyses at part per trillion[a] (ppt) levels. Most of the procedures have been developed for the highly toxic 2,3,7,8-tetrachlorodibenzo-*p*-dioxin (2378-TCDD)[1–4]. Other procedures have been developed for the higher chlorinated dioxins, and for the polychlorinated dibenzofurans (PCDFs)[5–8]. In general the method of choice for these procedures involve some sample pretreatment followed by determination with gas chromatography–mass spectrometry (GC–MS). Albro *et al.*[9] reported the results of an interlaboratory study involving the determination of PCDDs and PCDFs in human adipose tissue. Eight different laboratories participated in the study, each using their own procedure, and all of which used GC–MS for quantitation of unspiked and spiked sample portions. The results indicated that the procedures were qualitatively reliable. The quantitative correlation of sample and recovery data was

[a] Throughout this article, the American billion (10^9) and trillion (10^{12}) are meant.

0021-9673/89/$03.50

not as obvious. Through an evaluation of the data the authors identified significant problem areas which resulted in the scatter of the data. These included: (1) the application of procedures developed for 2378-TCDD which were inappropriate for the higher PCDDs and PCDFs, (2) the use of procedures which had not been tested on a wide variety of sample matrices such as adipose tissue, and (3) the differences in capabilities of the GC–MS systems used in the determinative step.

Our laboratory does not have a GC–MS unit which can be dedicated to dioxin analysis since it must service a variety of analytical disciplines. As a matter of practice, we prefer to reserve the GC–MS technique for confirmation only. Consequently, we require a completely different technique for primary quantitation, namely GC–electron-capture detection (ECD). In addition, we are involved with a wide variety of sample types, the analysis of which includes both the PCDDs and PCDFs. Obviously, we needed a comprehensive procedure applicable to a wide variety of products which is sensitive, quantitative and isomer specific.

The procedure of Niemann *et al.*[10], developed for 2378-TCDD in fish, has been used extensively in our laboratory along with the use of 1378-TCDD as an internal standard[11]. Several additional steps were developed by this laboratory in order to improve spike recoveries through the procedure, to get cleaner sample extracts prior to injection on the high-performance liquid chromatographic (HPLC) systems, and to include a variety of different sample types. The procedure was expanded to include the higher PCDDs and the PCDFs. Fractionation of sample extracts utilizing the C_8/C_{18} HPLC systems allowed for the isomer specificity needed for all of the PCDDs studied. Additional specificity was supplied by the capillary GC–ECD determinative step.

The inclusion of a Florisil trap resulted in extracts which were two orders of magnitude cleaner, upon direct injection into the C_8 HPLC system, than the fraction obtained from the size-exclusion HPLC (HPSEC) system originally used. This allowed the elimination of the HPSEC step and resulted in considerable savings in analytical time and equipment. Florisil had previously been used for sample cleanup[12], but not spcifically as a trap. The Florisil allows for unlimited washing of the extract with hexane while completely retaining all of the PCDDs and PCDFs. The PCDDs and PCDFs are then eluted off the Florisil with methylene chloride.

A methylene chloride extraction was developed for the transfer of residues between the two HPLC systems to replace the original benzene extraction. The methylene chloride extraction has proven to be more reproducible and complete.

With the addition of specific digestion and extraction procedures based on the desired residues, and on the fat content of the product, a comprehensive procedure is presented for the analysis of PCDDs and PCDFs in a wide variety of products.

EXPERIMENTAL

Safety

All laboratory personnel should be aware of the extreme toxicity of these compounds and take every precaution to prevent exposure of these residues to themselves and to others. Training should be provided in the safe handling of these materials, and in the safe disposal of their wastes. The acid-coated silica used in this procedure should be treated as a concentrated acid and also as a potental inhalation hazard.

Reagents and solvents

Water is prepared by passing previously deionized water through a Millipore or similar water purification system. All solvents used are of UV- or HPLC grade obtained from Burdick and Jackson, or EM Science. Florisil (Fisher F-101 or equivalent) is prepared by washing with twice its volume of hexane and methylene chloride. The Florisil is activated and stored in a 125°C oven. All other chemicals are of ACS reagent grade and used without further purification. All glassware is scrubbed with hot detergent, followed by rinsing sequentially with tap water, deionized water, and acetone.

Digestion solution and chromatographic supports

The digestion solution is a 40% (w/v) KOH in water. The digestions are performed in a 120-ml, glass bottles equipped with PTFE-lined screw-caps. The preparation of 44% sulfuric acid on silica, and 33% 1 *M* KOH on silica has been previously described[13,14].

Standards

2378-TCDD at 67.8 ng/ml in isooctane was obtained from the National Bureau of Standards as a Standard Reference Material. Other dioxin congeners were obtained from Niemann *et al.*[10], who performed the purity testing of these compounds. The remaining dioxins and furans were obtained commercially through Cambridge Isotopes.

For GC–ECD, a 200-pg/μl 1378-TCDD solution is prepared by serial dilution of a 1-ng/μl stock solution in isooctane. The 2378-TCDD solution is prepared at a nominal 10 pg/μl in isooctane. Mixed standards of the higher chlorinated dioxins are also prepared in isooctane ranging from 2 pg/μl for the penta-, to 5 pg/μl for the octaisomers. The PCDFs are also prepared in isooctane at similar concentrations. Mutual overlap of retention times for some of the higher congeners of the dioxins and furans precludes the preparation of mixed dioxin–furan standards for the hepta- and octa-congeners.

For HPLC the standards used to set the collection windows are made to contain 1 to 1.5 ng/μl of the individual component in the same solvent used to dissolve the sample. Detector sensitivities of 0.01 to 0.02 AUFS are normally used to set the collection windows.

The acid–silica column is prepared by packing a 30 × 2 cm glass column sequentially with layers of 1 g silica, 2 g 33% 1 *M* KOH on silica, 1 g silica, and finally 10 g 44% sulfuric acid on silica. The column is packed by gentle tapping after each addition. The Florisil column is prepared by adding 2.0 g of hot Florisil to a 25 × 1 cm glass column, gently tapping the column, and quickly covering the Florisil with hexane.

The prepurified nitrogen used for evaporations must be further purified. The assembly of this apparatus has been previously described[13].

Separate C_8 and C_{18} HPLC systems were set up as previously described[10]. The C_8 system was eluted at 45°C with acetonitrile–water (75:25, v/v) at 2.4 ml/min. A reservoir containing 100% acetonitrile was connected to another port of the solvent selection switch on the pump to allow for washing of the column after window collection. The C_{18} system was eluted at 45°C using acetonitrile at 1.2 ml/min. Solvent

reservoirs were continuously sparged with helium during use. UV detection at 235 nm is recommended for both systems. All injections were made with 100-μl syringes equipped with PTFE-tipped plungers.

All GC–ECD separations were performed on the J & W DB-1, fused-silica columns, 60 m × 0.25 mm, 0.25-μm film. A Varian 6000 GC–ECD system equipped with an on-column injector, and a Varian 3700 GC–ECD system equipped with a splitless injector were used in this study. Both instruments were equipped with constant-current, pulse-modulated, ^{63}Ni electron-capture detectors operated at 350°C. On-column injections were made at 170°C and then ramped at 140°C/min to 310°C and held for 15 min. Splitless injections were made at 310°C using the timed sequence described earlier[10]. Similar column conditions are used in both instruments. Nitrogen is used as the makeup and/or purge gas, and flows are adjusted for optimum response. After injection the column oven temperature is held at 75°C for 2 min, then programmed to 195°C at 25°C/min, then to 310°C at 5°C/min and held for 2 min. This program adequately separates all of the residues studied, and can be modified for other desired residues. The hydrogen carrier gas supplied to the instruments is passed through a series of traps containing activated charcoal, molecular sieve, and an oxygen scrubber in that order. The nitrogen is also passed through a similar trap system except that a furnace type gas purifier is installed in the line between two molecular sieve traps.

Sample preparation

(a) Fish samples are filleted and skinned. The fillets are passed through a meat grinder three times, mixing between each pass through the grinder.

(b) Meat and fatty tissue are deboned, and treated the same as the fish above. Samples of fat are heated on a steam bath until clarified and mixed.

(c) Egg samples are shelled and blended at moderate speed. Milk samples are blended similarly.

(d) Viscous samples are manually mixed.

(e) Dry products are ground in a suitable mill to pass a 1.0-mm screen.

(f) Sediments are dried under moderate heat (60°C) and ground in a motorized mortar and pestle to a powder. The moisture loss is determined for each sample so that results can be calculated back to the wet basis.

All analytical sample portions are weighed immediately after compositing, especially for samples containing both oil and water. Reserve portions are frozen for storage. If additional analysis is required, the frozen samples are thawed and reblended to ensure homogeneity in the analytical portion taken.

Digestion and extraction procedures

According to the procedure of Niemann[11], 20 ng of 1378-TCDD is added to each sample as an internal standard (I.S.). All 2378-TCDD results are corrected for the I.S. recovery. A reagent blank, which also contains the I.S., accompanies each set of samples.

Dioxins in high- and low-fat samples. (a) Weigh a 20.0-g sample into a digestion bottle and add 100 μl 1378-TCDD standard. Add 40 ml of KOH solution and 20 ml ethanol, stopper and mix. Place bottle on a mechanical shaker and shake for 3 h at room temperature. Transfer the digestate to a suitable separator using a 20-ml hexane rinse. Shake vigorously for 1 min and allow the layers to separate.

(b) If only two layers are visible at this point, drain the lower aqueous layer into a second separator, and transfer the hexane layer into the original bottle with the aid of a 2 ml hexane rinse. This procedure is normally applicable to products of intermediate fat content such as liver, eggs, milk and fish. A 125-ml separator is adequate for the extraction. Repeat the extraction with three 20-ml portion of hexane. After the last extraction, discard the aqueous layer and combine all the hexane extracts in the last separator with several 3-ml hexane rinses. Gently rinse the combined extracts with two 25-ml portions of water and discard the water. Add 25 ml concentrated sulfuric acid slowly and carefully to start, allowing time for the reaction to subside and cool. Shake well and allow to set for at least 1 h. Break any emulsions by carefully adding small increments of water. Drain and discard the acid layer. Repeat the acid treatment until the upper hexane layer is clear and colorless, and the lower acid layer is moderately brown. Reserve the hexane extract for the acid–silica column.

(c) If more than two layers are visible after the first hexane extraction, allow the separator to set for several hours to allow the lower aqueous layer to separate as much as possible. This procedure is usually required for high-fat products. A 250-ml separator is required for this purpose. Drain the aqueous layer into a second separator, and transfer the organic layers into the original digestion bottle. Extract the aqueous layer with an additional $3 \times$ 20 ml hexane, combining the hexane extracts with the organic layers. Discard the aqueous layer and combine all the hexane extracts in the last separator. Wash the combined layers with an additional 100 ml of KOH solution and allow to separate several hours. Drain and discard only the clear aqueous layer. Carefully add 25 ml of concentrated sulfuric acid, shake frequently for 1 h, and treat as in (b) above.

Dioxins in non-fatty products. (a) Honey and skimmings: treat 20 g as in (a) and (b) of the section *Dioxin in high- and low-fat samples* above.

(b) Treated wood: extract 5.0 g of shavings with 20 ml ethanol overnight and treat as in (a) of the section *Dioxin in high- and low-fat samples* above. Filter through glass wool and wash filter with 20 ml hexane when transferring to separator. Treat as in (b) of the section *Dioxin in high- and low-fat samples* above.

(c) Rice: extract 20 g ground rice with 50 ml methylene chloride for 3 h and filter through glass wool with rinsing. Evaporate the solvent and dissolve residue in 100 ml hexane.

(d) Gelatin: treat 20.0 g as in (a) and (b) of the section *Dioxin in high- and low-fat samples* above. Warm the digestion bottle slightly if solidification occurs.

(e) Sediments and soils: use the procedure of Albro *et al.*[6]. Sandwich 2–20-g portions of dried and ground sample between 15-g layers of sodium sulfate in a suitable column. Moisten with acetone, and elute with 50 ml ethyl acetate, and then 100 ml methylene chloride. Evaporate the solvent to dryness and dissolve the residue in 10 ml hexane.

(f) Chemical wastes: a suitable quantity of waste is mixed with 50 ml water in a 125-ml separator and extracted with three 25-ml portions of methylene chloride. The solvent is evaporated and the residue dissolved in 100 ml of hexane.

Furans and dioxins in high- and low-fat samples. As will be discussed later, the furans are not stable in the presence of base. This precludes the use of an alkaline digestion. Acid digestions have been used for their determination[15,16]. The following procedure using 80% sulfuric acid, although somewhat tedious, has been used successfully in our laboratory for both furans and dioxins.

The recommended amount of sample to be analyzed depends on the amount of fat present in the sample. For samples containing less than 20% fat, 20 g can normally be analyzed. For samples with 25–70% fat, only 10 g is recommended. For higher fat levels, 5 g is recommended.

Procedure: mix the sample portions with 100 ml hexane in a 250-ml separator. Cautiously add 25 ml 80% sulfuric acid and shake frequently for 1–2 h. Break any emulsions with small amounts of water and drain the acid layer. Repeat the procedure with additional portions of acid until the hexane layer is clear and the acid layer is not appreciably darkened after 1 h. After the bulk of the sample has been reacted, concentrated acid can be used to speed up the digestion. The initial use of concentrated acid leads to excessive charring of the sample. Emulsions are broken with small amounts of water. The hexane extract is then saved for the acid–silica treatment.

Furans and dioxins in non-fat samples. (a) The furans, as well as the dioxins, can be determined in all of the hexane extracts obtained under the section *Dioxins in non-fatty products* that did not involve alkaline digestion.

(b) Honey and other carbohydrates: dissolve 20.0 g sample in 60 ml water in a 125-ml separator and extract with three 25-ml portions of methylene chloride. Evaporate the combined extracts to dryness and dissolve the residue in 100 ml hexane.

(c) Treated wood: extract 5.0 g of shavings with 50 ml methylene chloride for 3 h on a mechanical shaker. Quantitatively filter the extract through glass wool. Evaporate the solvent to dryness, and dissolve the residue in 100 ml hexane.

Column chromatography

An acid–silica column is prepared and prewashed with 40 ml of hexane. After washing, the acid–silica column is mounted directly over a Florisil column so that the effluent from the acid column passes through the Florisil. Pass the sample extracts in hexane completely through both columns, followed by two 20-ml hexane rinses. Remove and discard the acid column, and rinse the Florisil column with an additional four 20-ml portions of hexane. Discard all of the hexane rinses. Elute the dioxins and furans off of the Florisil with 20, 20 and 10-ml portions of methylene chloride, collecting the eluates in a 250-ml Florence flask. The methylene chloride is conveniently evaporated by adding a few carborundum boiling chips and placing the flask on the metal edge of a covered steam bath, and brought carefully to a low boil. Care must be taken not to let the flask get too hot or loss of sample may occur. Alternatively, Kuderna-Danish equipment may be used for this concentration step using a 60°C water bath. When the volume of solvent approaches 1 or 2 ml, remove the flask, allow to cool, and transfer the extract to a 10-ml Mills tube with the aid of three 2-ml methylene chloride rinses. Evaporate the extract to dryness under nitrogen. Then rinse the walls of the tube sequentially with 250, 150, 100 and 50-μl portions of methylene chloride, evaporating each rinse to dryness separately. The purpose of the rinsing is to concentrate the residue in the bottom 100 μl of the tube. Dissolve the residue in 40 μl of acetonitrile–methylene chloride (75:25, v/v). Fill a 100-μl syringe with the extract along with three 20-μl rinses, and inject the sample extract into the C_8 HPLC system.

High-performance liquid chromatography

The C_8 and C_{18} HPLC cleanup systems used have been reported by other investigators[10], and have been expanded to include the other PCDDs and the PCDFs.

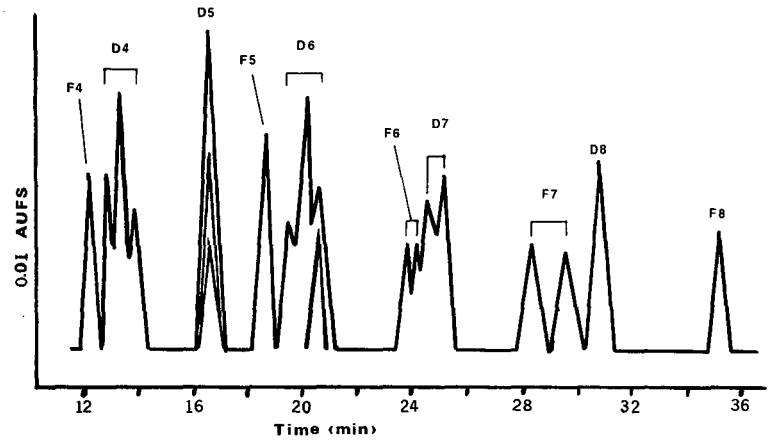

Fig. 1. The HPLC separation of a mixture of dioxin and furan standards on the C_8 system. See text for experimental conditions. The dioxin and furan peaks are identified by D or F respectively, followed by a number indicating the amount of chlorine substitution. The lower, single peaks represent the response of isomers injected individually.

Of the two, the C_8 system offers the greater resolution and variability of window selection as seen in Fig. 1, 2 and 3, which are partially redrawn. Fig. 4 represents actual chromatograms obtained from the injection of a mixed dioxin standard on both HPLC systems. Windows are set by the injection of appropriate, concentrated standards. The time of peak onset and return are measured with a stopwatch and normally 15 s are added to either side of the selected window. The standard solvent should be the same as that used for the samples, and the standard aliquot taken should be diluted to the same injection volume as that for the sample. After the injection of concentrated standards, the injectors should be backflushed. At low screening levels no dioxin peaks are

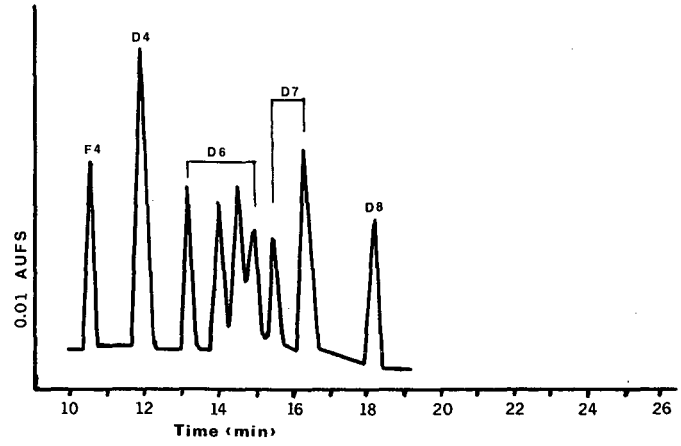

Fig. 2. The retention of dioxin standards on the C_{18} HPLC system. See text for experimental conditions. The standard peaks and amount of chlorine substitution are identified as in Fig. 1.

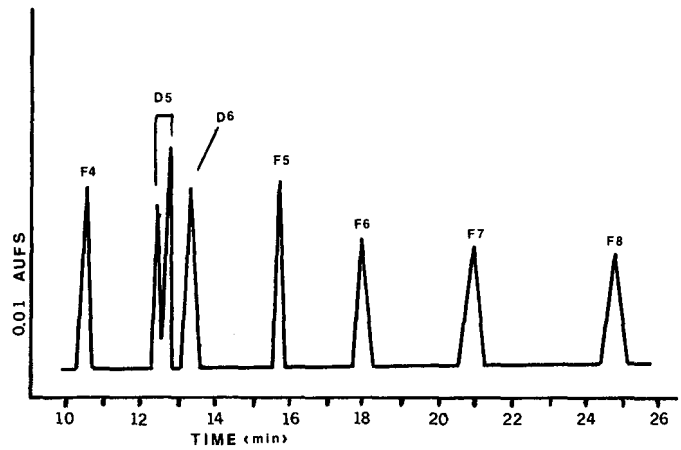

Fig. 3. The retention of a standard mixture containing mostly furan congeners on the C_{18} system. All of the congeners contain 2,3,7,8-chlorine substitution, and are identified as in Fig. 1.

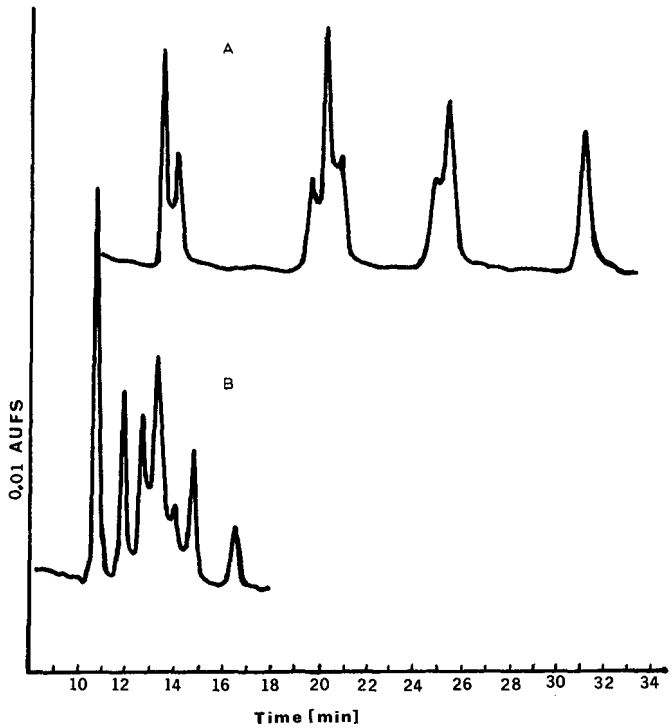

Fig. 4. Actual HPLC chromatograms for a standard mixture containing nine dioxins on (A) the C_8 system and (B) the C_{18} system.

normally observed in the sample chromatogram. Only the internal standard peak can be seen if not obscured by sample background.

Inject the sample extract into the C_8 system and at the proper time, manually switch the column effluent to a separator and collect the window, switching the effluent back to waste at the end of the window. The separator must be large enough to allow for a minimum 1:4 dilution of the collected volume. Some samples will have late eluting peaks which can be washed off of the column by switching the mobile solvent to 100% acetonitrile for about 20 min, and then switching back.

Dilute the collected window at least 1:4 by volume with an aqueous 2% sodium bicarbonate solution saturated with methylene chloride, and extract with three 2-ml portions of methylene chloride saturated with bicarbonate solution. Collect the extracts in a clean Mills tube, and evaporate to dryness under nitrogen. Wash down the sides of the tube with methylene chloride as before, concentrating the residue in the lower portion of the tube.

The sample is ready for injection into the C_{18} system. The procedures for window selection mentioned for the C_8 system are applicable here. Dissolve the residue in 40 μl of acetonitrile and draw into a 100-μl syringe followed by three 20-μl rinses. Inject the sample and collect the desired windows in a suitable Mills tube, the size of which depends on the volume of the window collected. The hepta- and octa- furans must be collected in a separate window since they interfere with the dioxins in the GC–ECD determination. Evaporate the solvent and concentrate the residues as before.

Capillary gas chromatography

Initially dissolve the residue in 15 μl of toluene added from a 100-μl syringe. Add 85 μl of isooctane to give a total volume of 100 μl. Based on a 20-g sample size, a 1-μl injection of this solution represents 0.2 g of sample. Quantitation is accomplished by comparison with a chromatogram of a similarly injected standard mixture containing the appropriate residue(s). In order to minimize any error due to detector non-linearity, all significant residues are quantitated by matching the response of the sample and standard chromatograms as closely as possible. Recoveries and control samples are calculated the same way. Most of the presented data are based on peak height measurements.

RESULTS AND DISCUSSION

KOH digestion

The KOH digestion originally used by Baughman and Meselson[17] generally does an excellent job of saponification. It has been reported that PCDDs are degraded in the presence of hot alkali, however, based on the recoveries obtained in this study, no significant degradation appears to occur with a 3-h room temperature digestion. PCDDs have also been reported to be light sensitive[12]. Therefore all dioxin and furan solutions are protected from light as much as possible, especially in aqueous solution.

Conversely, the PCDFs are degraded by alkali with the amount of degradation increasing with the increasing molecular weight of the congeners. In a fish matrix, the amount of degradation varies from 12% for 2378-TCDF, to 89% for octachloro-dibenzofuran. In the absence of a sample matrix, the degradation is even more

pronounced. As a result, the PCDFs can be determined by using only neutral or acid pretreatments.

For most samples, the KOH digestion is adequate for a 20-g sample size, and after elution from Florisil, there is usually no visible fat residue in the Mills tube. On rare occasions, certain high-fat samples, such as hamburger, can present problems due to the quantity and type of fat present. Using a 20-g sample size, some fat occasionally passes through the Florisil column. Even though the quantity is small (approximately 200-μl), this is too much to inject into the C_8 HPLC system. If this occurs the analysis must be repeated using a smaller portion of sample.

Trap evaluations

Activated alumina has been used to clean samples for 2378-TCDD[17]. Therefore an attempt was made to determine its suitability as a trap for all the dioxins. A mixture of eight dioxin standards in 60 ml of hexane were put on a 1.0-g alumina column and allowed to drain. The column was then eluted with separate 20-ml portions of methylene chloride and analyzed separately. Only 2378-TCDD and octachlorodibenzodioxin (OCDD) were quantitatively retained. Varying amounts of the hexa- and hepta-congeners washed through the column with the hexane with losses ranging from 8 to 69%. Alumina was deemed unsuitable for use as a trap.

Florisil had also been used[12] for the cleaning of samples using mixtures of hexane and methylene chloride or chloroform. The procedures worked for 2378-TCDD, however the break-through volume of the dioxin had to be determined beforehand. This was time-consuming and was based on the assumption that the sample matrix had little effect on the break-through volume. A study was therefore initiated to investigate the use of Florisil strictly as a trap for dioxins using only hexane for washing the extracts. Initially, a mixture of dioxins in 60 ml of hexane were put through an 0.5-g Florisil column. After the hexane had drained, the column was eluted with separate 20-ml portions of methylene chloride. All the dioxins were found to be completely retained on the column with no loss in the hexane prewash. All of the dioxins were quantitatively recovered in the first methylene chloride eluate. The same standard mixture was then put through 1.0 g Florisil in 100 ml of hexane. The column was then eluted with four 5-ml portions of methylene chloride, analyzing each portion separately. As seen in Table I, all of the dioxins studied were quantitatively retained on the column even with a 300-ml hexane wash. 2378-TCDD eluted completely in the first 5-ml portion of methylene chloride, however, the higher chlorinated dioxins required at least two additional portions for complete elution. Additional study with standards and sample extracts showed that wash volumes of hexane exceeding 500 ml had no effect on the retained dioxins, while removing fats, oils and other interferents.

Using the original procedure[10], eluates from the acid–silica columns had residues which were not completely soluble in the HPLC injection solvent for the HPSEC system. Even the dioxin fraction from the HPSEC system had residues that were not soluble in the C_8 injection solvent, and even less soluble in the mobile phase. This caused severe problems with the C_8 HPLC system and resulted in very short column life. The Florisil eluates proved to be at least two orders of magnitude cleaner than that of the HPSEC dioxin eluate. This allowed the elimination of the HPSEC system, and greatly improved the performance of the C_8 system with columns lasting a year or more rather than several months.

TABLE I
ELUTION PATTERN OF A STANDARD DIOXIN MIXTURE OFF OF FLORISIL WITH 5-ml PORTIONS OF METHYLENE CHLORIDE FOLLOWING A 300-ml HEXANE PREWASH

Dioxin	*Recovery per 5-ml cut (%)*			
	1	*2*	*3*	*Total*
2378-TCDD	104	–	–	104
124679-PCDD	67	25	7	99
123679-PCDD	74	23	7	104
123678-PCDD	77	18	4	99
123789-PCDD	67	27	3	97
1234679-PCDD	50	40	–	90
1234678-PCDD	70	41	–	111
OCDD	13	57	30	100

Since polychlorinated biphenyl (PCB) residues are frequently found in fish at high levels, the separating power of Florisil was investigated in regard to PCBs. An amount of Arochlor 1254 equivalent to 1 ppm in a fish sample (20 μg) was placed on a 2-g Florisil column and eluted with 200 ml of hexane. More than 99.9% of the PCB was found to wash through the Florisil with the hexane, indicating an excellent separation from the dioxins, and good agreement with the results of Firestone[12].

The separating power of Florisil was further demonstrated by two hazardous waste samples analyzed for 2378-TCDD. These wastes contained up to 200 components including PCBs, polybrominated biphenyls, all types of chlorinated and phosphated insecticides, herbicides, fungicides, phthalates, wood preservatives and other chemicals. These samples were simply diluted with hexane and put through a Florisil column, followed by several hexane rinses. After HPLC cleanup, the GC–ECD chromatograms of the samples were virtually identical to that of the reagent blank. No interfering peaks were found and the recoveries of 1378-TCDD were excellent. No 2378-TCDD was detected.

Due to the high cost of dioxin standards, no attempt was made to determine the adsorptive capacity of Florisil. However, the analysis of high-level samples indicate that the capacity is quite high, and more than adequate for ppt levels. Two river sediment samples exhibited levels of up to 11 ppb for OCDD which represents a loading of 220 ng on the Florisil (2 g) for only the OCDD. In addition, a treated wood sample containing 38 ppb OCDD represented a loading of 140 ng for OCDD alone.

The linearity of the system was tested by analyzing duplicate portions of an egg sample fortified at four different levels, ranging from 13 to 130 ppt for 124679-PCDD to 41 to 410 ppt for OCDD. All the recoveries were essentially complete, and no significant difference in recovery values were found between the four spike levels. In addition, the sediment samples mentioned above, which contained high levels of the higher chlorinated dioxins, gave the same results for the analysis of a 2-g or 20-g sample.

Florisil has proven to be an excellent trap for the dioxins studied as shown by the cleanliness of the extracts, its separating abilities from other contaminants, its adsorptive capacity, and its linearity. As additional dioxin and furan standards were obtained, they were tested on the Florisil and all were found to behave similarly.

C_8 HPLC

As seen in Fig. 1, this system offers the most selectivity and flexibility in terms of window selection. Any single window, or the window containing all of the dioxins and furans, can be collected. Obviously the smaller the window selected, the cleaner the extract will be. In practice, the TCDD window is usually collected separately if the penta-dioxins are also to be determined, since there is a slight overlap of their respective windows on the C_{18} system. The system is reproducible and standard injections are normally needed only at the beginning and end of the day. Once the elution pattern of all the residues on a particular system has been determined, only individual standards need to be injected to isolate any desired window.

The back-pressure of the pump is a good indicator of system performance. Some extracts may still have some particulate matter present in their solution prior to injection. Multiple injections of these extracts may cause clogging of prefilters or column frits, and these problems are indicated by slight increases in back-pressure. If the back-pressure gets too high, back-flushing of the columns and prefilters with acetonitrile is indicated. As mentioned previously, the columns are routinely cleaned after each sample injection by switching to acetonitrile for about 20 min, and the switching back.

Methylene chloride extraction

Due to the collection of larger volumes of mobile solvent, the original benzene extraction[10] proved to be inconvenient and incomplete. This required the development of another extraction procedure using methylene chloride instead of benzene. Aqueous dilution of the total volume of mobile solvent collected was necessary to minimize the amount of acetonitrile coextracted with the small volumes of methylene chloride used. The total volume of methylene chloride extract was adjusted so as not to exceed the volume of a 10-ml Mills tube. This required a minimum of a 1:4 (v/v) dilution with the bicarbonate solution. For small windows, larger dilutions are recommended to save time in the subsequent evaporation step. Occasionally small crystals of salt are observed on the wall of the tube after evaporation. They do not interfere in the next step.

Initial investigation found that the extraction of 2378-TCDD to be complete in the first 2-ml methylene chloride extract with the remaining extracts serving as rinses. The recovery of 2378-TCDD averaged 99.3% $\pm$ 3.8% for three determinations. The recovery of a mixture of seven higher chlorinated dioxins only through the extraction averaged 100.8%, with a range of 97–111%. A recovery of the same seven dioxins after injection, collection, and extraction averaged 99.4% with a range of 97–104%.

C_{18} HPLC

As seen in Fig. 2 and 3, this system offers lower selectivity in terms of windows for the lower chlorinated dioxins and furans. Its primary advantage is in the complete separation of the hepta- and octa-furans from the other residues. Both OCDD and OCDF have identical GC–ECD retention times, as do at least one hepta-dioxin/furan pair. Therefore, the hepta-/octa-furan window must be excluded from the lower chlorinated window, and collected and determined separately if their analysis is required.

Gas chromatography

The GC–ECD chromatograms of reagent blanks are generally clean in the areas of interest, and the number of extraneous peaks is dependent on the quality of the solvents used. Even with the best of solvents, some peaks were always present, but they seldom interfere with the desired residues. These facts however emphasize the need for taking blanks through the entire procedure. For sample chromatograms, no interference problems were generally encountered for the tetra-, hepta- and octa-congeners. Low-level peaks were occasionally observed for some of the lower congeners; however, their levels were not considered toxicologically significant enough to justify reanalysis for the specific residue. Many of these peaks were eliminated through adjustment of the GC temperature program, or by using the standard coinjection technique.

TCDD validation

Table II is a statistical compilation of data for the recovery of 1378-TCDD from various products. Most of our efforts have concentrated on the analysis of fish and seafood; however, sufficient samples of other products have been analyzed to demonstrate the applicability of this procedure to their analysis. The average recovery of 1378-TCDD from all products studies is adequate, and there is little statistical difference between the various products in terms of recovery and standard deviation. The recovery of 1378-TCDD from reagent blanks has had a tendency to be lower than in samples. Even using other procedures, the presence of a sample matrix has tended to give higher TCDD recoveries presumably due to the presence of residual oils which may act as a "keeper". Since all 2378-TCDD results are corrected for 1378-TCDD recovery, this is not considered a critical point.

TABLE II
RECOVERY OF 1378-TCDD INTERNAL STANDARD FROM VARIOUS PRODUCTS

Product	*Recovery (%)*	
	Average ± S.D.	*n*
Fish	89.5 ± 11.6	126
Milk	90.4 ± 12.4	21
Eggs	92.2 ± 12.0	13
Sediments	93.9 ± 16.2	7
Misc.	94.2 ± 12.1	16
Reagent blanks	86.2 ± 10.7	29

Two fish samples (carp and catfish) containing bio-incurred levels of 2378-TCDD were used as control samples. One portion of a control was routinely analyzed with each batch of samples being analyzed for 2378-TCDD to assure consistent recovery through the procedure. As seen in Table III, the combined results for each species are reproducible and have comparable standard deviations. Also included in Table III are recovery data for various products fortified with 2378-TCDD at a nominal level of 50 ppt. Again, the recoveries are consistent and essentially complete.

TABLE III
2378-TCDD RECOVERIES CORRECTED FOR INTERNAL STANDARD RECOVERY

Sample	*Recovery (%)*	
	Average ± S.D.	*n*
Control samples containing bio-incurred 2378-TCDD		
Carp	84 ± 5.2 ppt	6
Catfish	75 ± 8.7 ppt	8
Spiked samples		
Eggs	94.3 ± 7.6%	12
Fish	94.5 ± 9.3%	6
Milk	97.3 ± 6.3%	4
Gelatin	98.0 ± 14.0%	2
Rice	89.0 ± 11.0%	2
Honey	106.0 ± –%	1
Spiked reagent blanks		
	97.3 ± 8.3%	6

Interlaboratory studies

Table IV is a statistical comparison of analytical data for 1378/2378-TCDD generated in Detroit and Chicago districts. The Chicago laboratory used similar instrumentation and the identical procedure. The close correlation of the results indicate that the procedure is reproducible and rugged between laboratories.

Detroit district also participated in a blind quality assurance study in cooperation with the Michigan Department of Natural Resources (DNR). The DNR took samples of game fish from a Michigan river, composited them, and split the composites between Food and Drug Administration, Detroit and Dow Chemical, Midland, MI for 2378-TCDD analysis. Detroit used the proposed procedure, while Dow used a GC–MS procedure. The results were submitted directly to the DNR for evaluation. Table V is a comparison of the results obtained by both laboratories. The results indicate close agreement between the two procedures.

TABLE IV
INTERLABORATORY COMPARISON OF TCDD RECOVERIES FROM FISH

Lab.	*Recovery (%)*			
	1378-TCDD		*2378-TCDD*	
	Average ± S.D.	*n*	*Average ± S.D.*	*n*
Chicago	92 ± 10	26	102 ± 6	2
Detroit	90 ± 12	126	95 ± 9	6

TABLE V
INTERLABORATORY COMPARISON OF SPLIT-SAMPLE RESULTS FOR 2378-TCDD IN FISH
Blind study prepared by Michigan DNR (see text).

Sample No.	*Species*	*Dow[a] results (ppt)*	*Detroit results (ppt)*
1	Walleye	5.2	2.9
2	Walleye	5.1	3.5[b]
3	Walleye	3.0	3.1
4	Walleye	2.6	1.4
5	N. Pike	15.0	16.5
6	Bass	5.8	8.0
7	Crappie	4.4	5.4
8	W. Bass	15.0	15.9

[a] GC–MS procedure.
[b] 95% Recovery of 2378-TCDD from a separate portion fortified at 50 ppt.

Validation of PCDDs and PCDFs

The validation of these procedures for the higher chlorinated dioxins is based on recovery data of fortified samples. The results for these dioxins are calculated by direct comparison of sample GC–ECD responses to that of a similarly injected standard. The GC retention times these congeners are too far removed from TCDD for internal standard correction. In addition, peak shapes and responses at these long retention times are more dependent on other factors such as matrix effects, and type of injector used.

Initial evaluation of the recovery data for each product indicate that they are statistically similar. In the interest of simplicity, the statistical data for each dioxin includes all of the various products analyzed, and the digestion procedure used. The results are presented in Table VI. As can be seen, the recoveries are consistent and acceptable. Table VII presents the recovery data from spiked reagent blanks taken through the varous extraction digestion procedures. Again good recoveries and precision were indicated, and the results are comparable to the spiked sample data.

TABLE VI
RECOVERY OF DIOXINS AND FURANS FROM ALL SAMPLE TYPES
Most spike levels vary from 10 to 60 ppt in proportion to their GC retention time.

Residue	*Recovery (%)*		*Residue*	*Recovery (%)*	
	Average ± S.D.	*n*		*Average ± S.D.*	*n*
12347-PCDD	100.0 ± 11.6	4	1234678-PCDD	93.9 ± 8.6	34
12378-PCDD	99.7 ± 12.8	6	OCDD	85.0 ± 8.0	29
124679-PCDD	95.0 ± 9.0	30	2378-PCDF	96.2 ± 10.4	5
123679-PCDD	94.3 ± 9.7	34	12378-PCDF	100.0 ± 11.6	5
123478-PCDD	92.1 ± 12.5	7	123478-PCDF	94.4 ± 11.8	5
123678-PCDD	96.3 ± 9.1	32	1234678-PCDF	100.0 ± 10.8	5
123789-PCDD	97.0 ± 9.2	34	OCDF	87.4 ± 15.6	5
1234679-PCDD	92.8 ± 9.6	34			

TABLE VII
RECOVERY OF DIOXINS FROM SPIKED REAGENT BLANKS
Spike levels vary from 10 to 60 ppt in proportion to their increasing GC retention time.

Residue	*Recovery (%)*	
	Average ± S.D.	*n*
124679-PCDD	98.3 ± 5.8	7
123679-PCDD	98.6 ± 4.4	7
123678-PCDD	102.0 ± 7.9	7
123789-PCDD	100.0 ± 8.7	7
1234679-PCDD	96.9 ± 6.5	7
1234678-PCDD	99.9 ± 8.1	7
OCDD	89.0 ± 15.0	7

The validation of these procedures for the furans is also based on spiked sample recovery data. The furan recovery data are presented in Table VI. Although considerably fewer determinations were performed, the furan recovery data closely parallel that of the dioxins.

Results of sample analysis

The bulk of our dioxin work consisted in the analysis of fish for 2378-TCDD, and representative data for these analyses are presented in Table VIII. As can be seen, the highest levels and incidence of TCDD levels occurred in fresh water bottom feeders from lakes and rivers receiving heavy loads of industrial wastes. Fresh water game fish tended to be lower in both incidence and dioxin level. Salt water species exhibited little or no contamination.

Table IX presents the results of market basket survey of commodities analyzed for only the higher chlorinated dioxins. The survey consisted of five commodities sampled from five different geographical areas of the country. The tabulated data includes only the more significant hepta- and octa-dioxin levels since the results for the lower congeners are considered negligible at less than 5 ppt. In general, liver was found

TABLE VIII
INCURRED LEVELS OF 2378-TCDD DETECTED IN FISH AND SEAFOOD
All results confirmed by GC–MS.

Sample type	*No. samples analyzed*	*No. samples positive*	*Average (ppt)*	*Range (ppt)*
Freshwater				
Carp	13	10	31.4	7–90
Catfish	17	16	25.6	5–85
Gamefish	10	4	15.0	13–17
Saltwater				
Fish	55	3	8.0	2–11
Shellfish	18	2	7.0	5–9

TABLE IX
RESULTS OF MARKET BASKET SURVEY
Analyzed for higher chlorinated dioxins only. Results above 20 ppt confirmed by GC–MS, or GC with Hall electrolytic conductivity detection.

Product	*No. samples analyzed*	*1234678-PCDD*			*OCDD*		
		No. samples positive	*Avg. (ppt)*	*Range (ppt)*	*No. positive samples*	*Avg. (ppt)*	*Range (ppt)*
Beef liver	15	12	9.6	3–21	13	47.6	11–182
Pork chops	15	9	6.1	2–20	13	19.8	6–80
Chicken	15	6	8.5	2–32	9	12.4	4–43
Ground beef	15	6	4.0	2–5	4	11.3	6–22
Eggs	15	3	2.7	2–4	3	6.3	5–8

to have the highest levels of dioxins and the highest incidence. Pork, chicken, ground beef and eggs follow in decreasing levels of occurrence. With the limited data, no correlation between dioxin level and geographical area could be made at this time.

All other products or sample types which have shown sigificant levels of dioxins or furans are listed in Tables X and XI. Of interest are the high levels of higher chlorinated dioxins in river sediments located downstream from a paper plant. The sediment samples are also the only samples which contained significant levels of furans. The high levels found in the preservative-treated wood sample, and in the egg sample were the result of specific grower-related problems.

TABLE X
INCURRED LEVELS OF DIOXINS[a] IN OTHER SAMPLE TYPES

Sample type	*No.*	*Dioxin congener (ppt)*					
		124679	*123679*	*123678*	*1234679*	*1234678*	*OCDD*
Eggs		0	0	26	29	127	451
Preserved wood		813	277	269	3800	5600	38 000
Honey skimmings	1	0	0	0	37	63	392
	2	0	0	0	24	37	193
River sediments	1	0	0	0	52	27	172
	2	66	0	0	0	0	65
	3	19	30	42	124	186	270
	4	0	0	0	467	210	1600
	5	61	45	18	870	398	4900
	6	64	41	14	902	393	4600
	7	129	80	26	1600	471	7100
	8	136	55	29	1900	908	10 300
	9	318	379	429	3300	2700	10 600

[a] Only the more significant dioxin levels are included.

TABLE XI
INCURRED LEVEL OF FURANS IN RIVER SEDIMENTS

Sample No.	*Furan congener (ppt)*		
	1234678	*1234689*	*OCDF*
1	15	27	23
5	0	356	348
6	0	395	383

Isomer specificity

Due to the high cost of reliable standards as well as a lack of sources for reliable standards, not all of the isomers for each of the dioxin and furan congeners were included in this study. An attempt was made to include a reasonable cross-section of isomers for each of the congeners, and included as much as possible, those isomers considered to be the most toxic, namely, those having substitution in the 2,3,7,8 positions.

Considering the cross-section of isomers actually studied, it seems reasonable that the remaining isomers would behave similarly, at least quantitatively. Isomer specificity, therefore, is limited to those congeners for which all the isomers were available, namely the 21 isomers of TCDD, the hepta-isomers of the PCDDs and PCDFs, OCDD and OCDF.

Whether or not the chromatographic systems would adequately separate all of the penta- or hexa-isomers does not appear critical. Based on the analytical results, any significant levels of hexa-dioxins were always accompanied by much higher levels of the hepta- and octa-dioxins, thus minimizing the importance of the lower congener. This follows the general trend that, in environmental samples the lower congeners result from the degradation of the higher congeners. In addition, no PCDFs have been detected in any of the foodstuffs analyzed. These statements are made in a general sense, however, and do not preclude the fact that in special cases, isomer specificity could be a problem.

CONCLUSION

Multiresidue procedures have been presented for the screening of PCDDs and PCDFs in a variety of products. Through the incorporation of a Florisil trap, sample extracts are clean enough for determination by capillary GC–ECD, and confirmation by GC–MS. Analytical data from fortified samples, and replicate analysis of samples with incurred residues, indicate that recoveries are reproducible and essentially complete. A comparison of data for 2378-TCDD from two independent laboratories showed good agreement with these results, one laboratory using the same procedure, and the other using a GC–MS procedure.

ACKNOWLEDGEMENT

The author wishes to thank James A. Howell, of Western Michigan University, Kalamazoo, Michigan, for his valuable advice and assistance in the preparation of this paper.

REFERENCES

1 D. G. Patterson, J. S. Holler, C. R. Lapeza, L. R. Alexander, D. F. Groce, R. C. O'Connor, S. J. Smith, J. A. Liddle and L. L. Needham, *Anal. Chem.*, 58 (1986) 705.
2 R. A. Hummel, *J. Agric. Food Chem.*, 25 (1977) 1049.
3 L. A. Shadoff, R. A. Hummel and L. Lamparski, *Bull. Environ. Contam. Toxicol.*, 18 (1977) 478.
4 D. J. Jensen, M. E. Getzendaner, R. A. Hummel and J. Turley, *J. Agric. Food Chem.*, 31 (1983) 118.
5 L. M. Smith, D. L. Stalling and J. L. Johnson, *Anal. Chem.*, 56 (1984) 1830.
6 P. W. Albro, J. S. Schroeder, D. J. Harvan and B. J. Corbett, *J. Chromatogr.*, 312 (1984) 165.
7 L. L. Lamparski, N. H. Mahle and L. A. Shadoff, *J. Agric. Food Chem.*, 26 (1978) 1113.
8 L. L. Lamparski and T. J. Nestrick, *Anal. Chem.*, 52 (1980) 2045.
9 P. W. Albro, W. B. Crummet, A. E. Dupuy, M. L. Gross, M. Hanson, R. L. Harless, F. D. Hileman, D. Hilker, C. Jason, J. L. Johnson, L. L. Lamparski, B. P. Y. Lau, D. D. McDaniel, J. L. Meehan, T. J. Nestrick, M. Nygren, P. O'Keefe, T. L. Peters, C. Rappe, J. J. Ryan, L. M. Smith, D. L. Stalling, N. C. A. Weerashinghe and J. M. Wendling, *Anal. Chem.*, 57 (1985) 2717.
10 R. A. Niemann, W. C. Brumley, D. Firestone and J. A. Sphon, *Anal. Chem.*, 55 (1983) 1497.
11 R. A. Niemann, *J. Assoc. Off. Anal. Chem.*, 69 (1986) 976.
12 D. Firestone, *J. Agric. Food Chem.*, 25 (1977) 1274.
13 L. L. Lamparski, T. J. Nestrick and R. H. Stehl, *Anal. Chem.*, 51 (1979) 1453.
14 M. L. Langhorst and L. A. Shadoff, *Anal. Chem.*, 52 (1980) 2037.
15 J. J. Ryan and J. C. Pilon, *Can. Vet. J.*, 24 (1983) 72.
16 J. J. Ryan, R. Lizotte and W. H. Newsome, *J. Chromatogr.*, 303 (1984) 351.
17 R. Baughman and M. Meselson, *Environ. Health Perspect.*, Exptl. Issue No. 5, (1973) 27.
18 D. Firestone, *J. Assoc. Off. Anal. Chem.*, 60 (1977) 354.

Journal of Chromatography, 478 (1989) 369–377
Elsevier Science Publishers B.V., Amsterdam — Printed in The Netherlands

CHROM. 21 628

ENHANCED ULTRAVIOLET DETECTION IN HIGH-PERFORMANCE LIQUID CHROMATOGRAPHIC ANALYSIS OF DRUGS BY "ON-LINE" PHOTOCHEMICAL REACTION

RAINER W. SCHMID* and CHRISTIAN WOLF
Laboratory of Psychoactive Drug Analysis, Psychiatric University Hospital of Vienna, Währinger Gürtel 18-20, 1090 Vienna (Austria)
(First received February 14th, 1989; revised manuscript received May 17th, 1989)

SUMMARY

The effect of on-line photochemical reaction on UV detection in high-performance liquid chromatography (HPLC) has been studied. For on-line irradiation a photoreactor utilizing a low pressure mercury light source and a crocheted reaction capillary has been used by which the chromatographic performance of the HPLC separation is only slightly influenced. On-line irradiation of the drugs methadone, methoin, nirvanol and several barbiturate analogues results in a significant increase in their UV absorptivity, either due to the appearance of new spectral bands or due to absorption enhancement at longer UV wavelengths. By these photochemical effects, the detectability of drugs at longer UV wavelengths will be increased, in some cases more than 80-fold. Thus routine analysis of these drugs in biological samples may be simplified considerably, allowing more specific detection and less complex sample preparation.

INTRODUCTION

Pre- or postcolumn chemical modification of an analyte is a common approach to increase the sensitivity and specificity in high-performance liquid chromatographic (HPLC) trace analysis of pharmacological substances in biological fluids. At the same time there are a number of drawbacks. While in precolumn derivatizations increased variability occurs due to variable reaction times and rates, in postcolumn derivatization, for on-line addition of reagent(s), an additional pumping system is required introducing pulsation, dilution and peak broadening into the chromatographic system.

Recently, photochemical reaction has been demonstrated to be an efficient postcolumn reaction system[1]. Because light is the only "reagent" which has to be "added" in on-line photochemical reactions, many properties of an ideal on-line reaction system are exhibited.

Although a wide range of different chemical reactions have been described in photochemistry[2], on-line photochemical reactions in HPLC have been described only

0021-9673/89/$03.50

for a small number of substances, nearly all of them leading to an fluorescent or electrochemically active product after irradiation[3]. Extending this principle of postcolumn photochemical reaction to other HPLC detection systems, we have investigated whether by on-line irradiation drugs of various molecular structures are modified in their spectral properties, in the search for a more specific or sensitive HPLC determination of these drugs in biological samples.

EXPERIMENTAL

The photochemical reactor

For on-line, postcolumn irradiation experiments, a photochemical reactor was used which was constructed in the laboratory and has been described in detail before[3]. Up to 40 m of 1/16-in. heavy wall, narrow bore PTFE tubing (1/16 in. O.D., 0.01 in. I.D.; Pierce Europe, Oud-Beijerland, The Netherlands) was crocheted into a rectangular pad of side approximately 6 cm. It was fixed on a stainless-steel mesh and mounted around a tubular 8-W low pressure mercury lamp (GTE, Sylvania G8-T5). This light source emits the known mercury spectrum including the strong line in the UV at 254 nm.

To increase the light yield and the efficiency of the photochemical reaction, the inner side of the reactor housing may be covered by reflecting aluminium foil. Because of the low power rating of the light source, no active cooling in the photoreactor is necessary.

Depending on the length of the crocheted reaction capillary, irradiation times of up to 240 s (at a nominal flow-rate of 0.8 ml/min) are possible in this photoreactor geometry. For certain experiments in which the influence of the irradiation spectrum on the photochemical reaction was studied, the mercury light source was exchanged for an identical lamp with a spectral cut-off at *ca.* 366 nm (Sylvania, F8-T5).

In "off-line" irradiation experiments, samples were irradiated in a quartz cuvette using a low pressure mercury pen-ray lamp (Analamp, BHK, Monrovia, CA, U.S.A.).

Chromatographic system

The HPLC system used consisted of a 302 pump (Gilson, Villiers le Bel, France), a six-port injection valve (Valco, Houston, TX, U.S.A.) and a SPD-6A variable wavelengh detector (Shimadzu Europe, Duisburg, F.R.G.). The photochemical reactor was connected between the analytical column and the UV detector by means of zero dead volume unions (Valco).

Chromatographic separations were generally done on a 11 cm × 4.7 mm Whatman cartridge packed with PartiSphere C_{18}, 5-μm silica material (Whatman, Clifton, NJ, U.S.A.). Mobile phase compositions (methanol or acetonitrile–phosphate buffer mixtures) were chosen depending on the compounds to be separated.

For off-line spectral analysis a Perkin-Elmer Lambda 7 spectral photometer (Bodenseewerk, F.R.G.) was used.

Chemicals

Water and organic solvents used for HPLC were distilled from glass apparatus and of HPLC grade (HiPerSolv; BDH, Poole, U.K.); buffer salts were of the highest purity available (Merck, Darmstadt, F.R.G.). Methadone hydrochloride was ob-

tained from Heilmittelwerke (Linz, Austria). Mephenytoin and nirvanol were gifts from Gerot Pharmaceuticals (Vienna, Austria). Barbiturates were obtained from Merck.

Analysis of blood plasma sample

To 100 μl blood plasma an equal volume of acetonitrile was added. Precipitated proteins were centrifuged at *ca.* 10000 *g* in a Biofuge A (Haraeus, F.R.G.). After dilution of the supernatant in an equal volume of distilled water, 50 μl were injected into the HPLC system.

RESULTS

Influence of the photochemical reactor on chromatographic performance

One basic question, when on-line postcolumn reactions are used in HPLC, is to what extent the postcolumn reactor influences the chromatographic performance of the separation system. When connected to the HPLC system in front of the UV detector, the photochemical reactor described results in only a minor deterioration of the chromatographic resolution. Because of the crocheted geometry of the reaction capillary, by which the turbulent flow within the capillary is induced[4,5], the contribution to extracolumn peak broadening by the photochemical reactor is very low ($<1\%$/m), even when longer capillaries (irradiation times >90 s) were chosen. This was tested by injection of C_6-alkylphenone as a test substance. The apparent plate counts dropped by only 14% when the photoreactor with a 15-m crocheted reaction capillary was installed ($N=6135$ without, 5279 with the photoreactor). In contrast, when using a different (non-crocheted) reaction capillary design, the efficiency of the chromatographic system drops dramatically by more than 60% ($N=2385$, using a loosely coiled reaction capillary).

Influence of irradiation on UV absorbance of drugs

Methadone. This drug (Fig. 1), of great importance in clinical opiate substitution programmes, is generally analyzed in blood by HPLC, with UV detection below 235 nm. At lower wavelengths the purity of the mobile phase systems becomes an important factor, excluding certain buffer systems, for example nitrate buffers (as needed in highly selective separations on unmodified silica[6].

Photochemical irradiation of methadone has a pronounced effect onto its absorbance spectrum (Fig. 2), which results in the appearance of a spectral peak in the region of 250 nm. When using on-line photochemical reaction in HPLC separation of

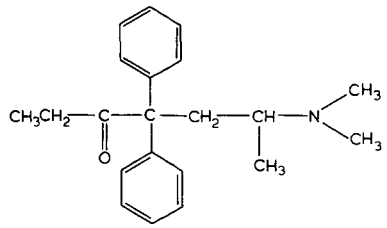

Fig. 1. Chemical structure of methadone.

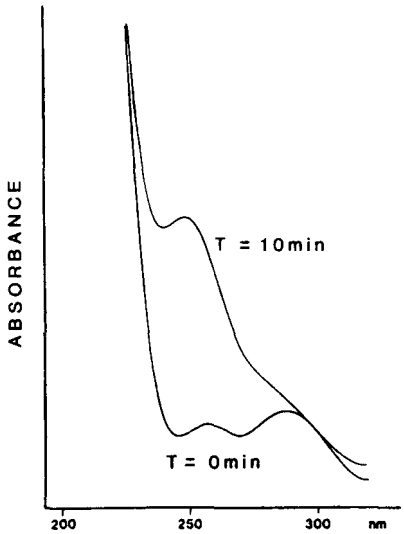

Fig. 2. UV spectrum of methadone before and after off-line irradiation with a low pressure mercury light source.

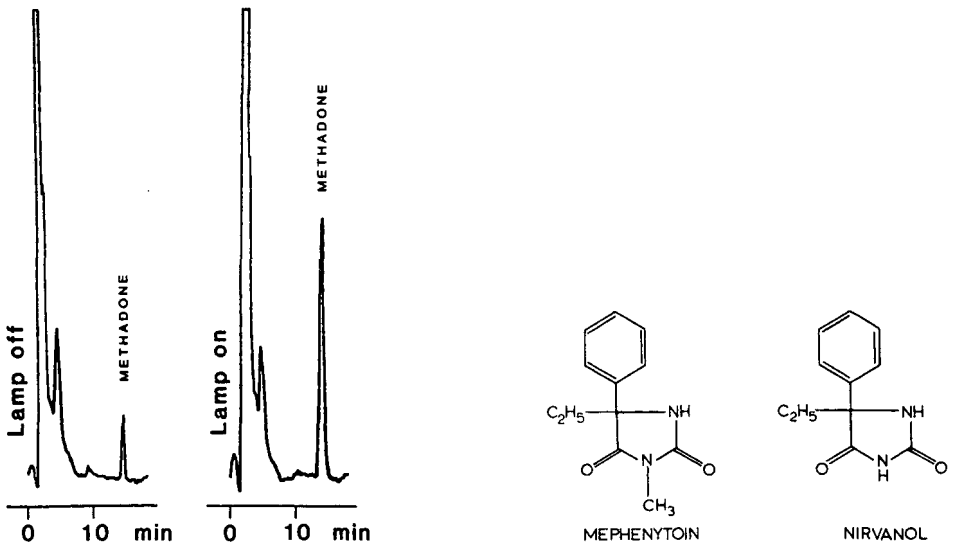

Fig. 3. Chromatogram of a blood plasma sample containing 75 ng/ml methadone. Column: Whatman PartiSphere Si, 110 mm × 4.7 mm. Mobile phase: acetonitrile–methanol–ammonium nitrate buffer, pH 9.5 (55:35:10). Flow-rate: 1.4 ml/min. Detection: 254 nm. Plasma sample extracted by a two-step solid phase extraction. Left chromatogram: without photochemical reaction. Right chromatogram: with photochemical reaction, reaction capillary 15 m (irradiation time 65 s).

Fig. 4. Chemical structures of methoin (mephenytoin) and nirvanol.

methadone a four-fold enhancement in UV detection at 254 nm was observed after only 65 s of irradiation (Fig. 3).

By chosing longer wavelengths for detection in comparison to 235 nm without on-line irradiation, a much higher specificity and less interference from the sample matrix were seen when analyzing biological samples.

Methoin and nirvanol. The hydantoin methoin is clinically used as an anti-convulsant drug and, because of strong side-effects, methoin and its pharmacological active metabolite, 5-ethyl-5-phenylhydantoin (nirvanol) (Fig. 4), should be routinely determined in blood of patients treated with this drug. In drug monitoring with HPLC, methoin is generally detected[7] in the UV at 211 nm.

Although structurally totally different from methadone, after on-line photochemical reaction similar effects on their absorbances are observed for methoin and nirvanol: irradiation of methoin and nirvanol leads to a strong increase in the absorption in the region of 254 nm, which is the result of a bathochromic shift, as revealed by spectral analysis (Fig. 5). In on-line irradiation in HPLC, a net gain of more than 20-fold in the detection of mephenytoin and nirvanol at 254 nm was observed. Because of the increased sensitivity and specificity, when measuring at longer wavelengths, the sample preparation of blood samples can be simplified: in combination with photochemical reaction, only deproteinization is necessary in routine HPLC analysis of plasma samples, allowing the two hydantoins to be determined from less than 50 μl of blood sample by a much more rapid and simplified HPLC procedure (Fig. 6).

Barbiturates. For sensitive HPLC determination of barbiturates (Fig. 7) either

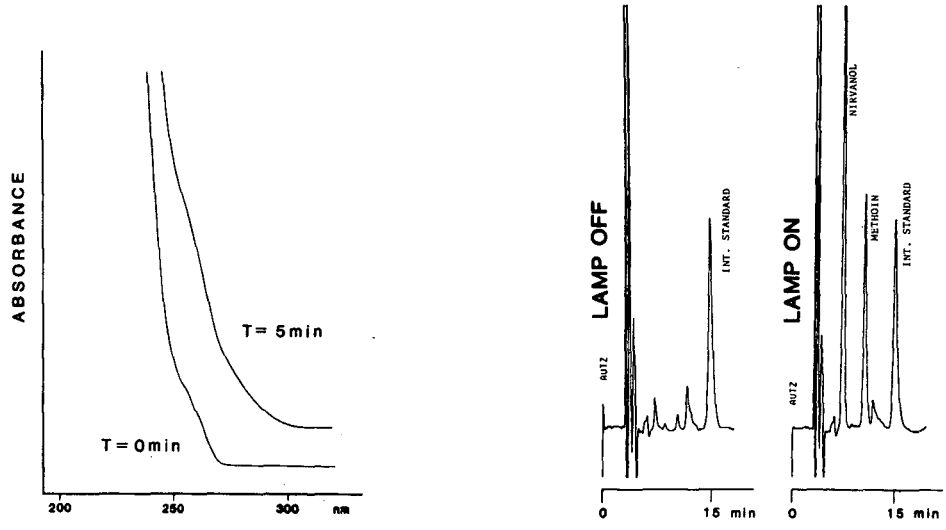

Fig. 5. UV spectrum of methoin before and after off-line irradiation.

Fig. 6. Chromatogram of a plasma sample containing methoin (9 μg/ml), nirvanol (14 μg/ml) and internal standard (mephobarbital, 30 μg/ml). Column: Whatman PartiSphere C_{18}, 110 mm × 4.7 mm. Mobile phase: acetonitrile–20 m*M* phosphate buffer, pH 7 (30:70). Flow-rate: 0.8 ml/min. Detection: 254 nm. Injection of 50 μl of deproteinized and diluted plasma sample. Left chromatogram: without photochemical reaction. Right chromatogram: with photochemical reaction, reaction capillary 10 m (irradiation time 75 s).

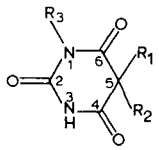

Fig. 7. Structures of barbiturates.

	R_1	R_2	R_3
Aprobarbital	Allyl	Isopropyl	H
Butethal	Ethyl	Butyl	H
Pentobarbital	Ethyl	1-Methylbutyl	H
Secobarbital	Allyl	1-Methylbutyl	H

UV detection at very low wavelengths(< 220 nm)[8] or complex postcolumn procedures have to be used[9].

When considering the structural similarities to the hydantoins, a similar positive spectral effect is expected for barbiturates. Photochemical reaction has been performed with several barbiturates: on-line UV irradiation with the photoreactor described showed a pronounced effect on the UV absorbance. However, except for the hydantoins, a characteristic increase in absorbance at longer wavelengths, in the region of 270 nm was seen. The resulting gain in absorbance at 270 nm is only two-fold for hexobarbital, but in the case of the barbiturate pentobarbital this increase may be as large as 80-fold after only 45 s of on-line UV irradiation (Table I). For different barbiturates the extent of observed spectral changes is different. Their reactivity upon irradiation cannot directly be associated with their molecular structures, preventing prediction as to the photochemical effects to be expected for an individual barbiturate.

Although the absolute detectability for barbiturates at 270 nm will not be increased by on-line photochemical reaction, in comparison to measurements below 220 nm without irradiation, again, detection at longer wavelengths has the effect of simplifying the HPLC analysis of barbiturates: on reducing the sample clean-up to protein precipitation only, in contrast to measuring at 220 nm, a nearly interference-free chromatogram was obtained, after injection of a blood plasma sample, by on-line photochemical reaction and detection at 270 nm (Fig. 8).

TABLE I

GAIN IN UV DETECTION BY POSTCOLUMN PHOTOCHEMICAL REACTION

Substance	*Enhancement factor*	*Wavelength (nm)*	*Irradiation time (s)*
Aprobarbital	35	270	45
Buthetal	44	270	45
Methadone	4	254	50
Methoin	29	254	240
Nirvanol	33	254	240
Pentobarbital	85	270	45
Secobarbial	40	270	45

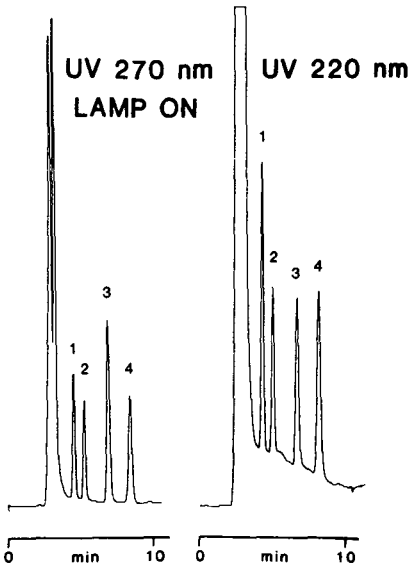

Fig. 8. Chromatogram of a spiked plasma sample containing aprobarbital (1), butethal (2), pentobarbital (3) and secobarbital (4), each 10 μg/ml. Column: Whatman PartiSphere C_{18}, 110 mm × 4.7 mm. Mobile phase: acetonitrile–20 m*M* phosphate buffer, pH 7 (30:70). Flow-rate: 0.8 ml/min. Injection of 50 μl of deproteinized and diluted plasma sample. Right chromatogram: detection at 220 nm without photochemical reaction. Left chromatogram: detection at 270 nm with photochemical reaction, reaction capillary 7.5 m (irradiation time 45 s).

Influence of the reaction time in postcolumn irradiation

Although the spectral changes described are generally seen after very short irradiation times (few tens of seconds), the rate change of absorbance as a function of the irradiation time has been studied in detail for the two hydantoins methoin and nirvanol. Variable irradiation periods were obtained with the standard photoreactor system by installing the longest available reaction capillary (32 m, representing an irradiation time of 240 s at a nominal flow-rate of 0.8 ml/min) and by protecting fractions of the reaction capillary from light, resulting in irradiation of the column effluent between 20 and 240 s (at constant flow-rates). For methoin and nirvanol a steady increase in absorbance at 254 nm was found when the irradiation time was increased. Under our experimental conditions, no maximum in the formation of the photoproduct was reached, even after irradiation for as long as 4 min (Fig. 9).

Photochemical reaction will be observed for methoin and nirvanol only if light of a certain minimum energy level is utilized for irradiation: exchanging the light source in the photoreactor for a mercury lamp of identical geometry but with an UV-emission cut-off at 366 nm, no absorbance increase at 254 nm was seen for the two hydantoins, indicating that mainly the major mercury UV line at 254 nm is responsible for the observed photochemical effect. For the other drugs studied no detailed time dependance has been established, but individual irradiation times were optimized for the maximum absorbance increase at a certain wavelength.

As for the hydantoins, for methadone, saturation of the photochemical effect was not seen even after on-line irradiation for 4 min. A further absorbance increase

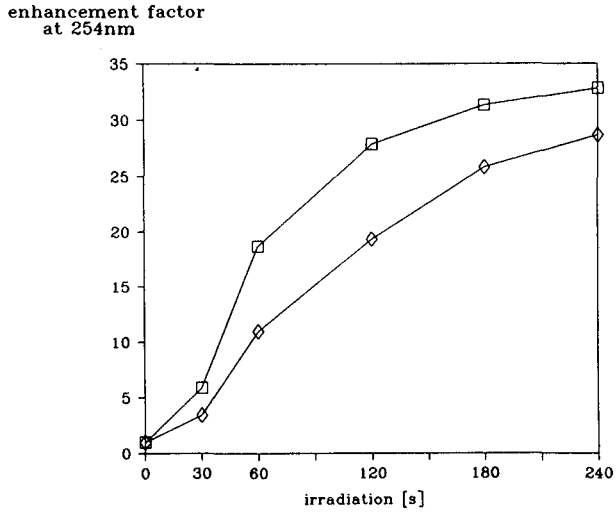

Fig 9. Time dependence of the UV absorbances of (◇) methoin and (□) nirvanol with increasing on-line irradiation of the column eluate.

might be obtained with longer irradiation, but under such conditions the adverse influence of the photoreactor on the chromatographic separation would become dominant.

In the case of the barbiturates, a maximum "photoproduct" formation is reached after much shorter irradiation periods: optimum irradiation times were found after *ca.* 25–45 s, varying for the different members of this drug class.

DISCUSSION

In Table I the drugs studied, the experimental conditions of on-line post-column photochemical reaction and its effect on the absorbance spectra are summarized. It is seen that a significant absorbance increase is observed generally after a relatively short period of irradiation, a precondition to integrate photochemical reactions into HPLC in the on-line mode. On-line irradiation of the column eluate leads in the cases of the drugs studied either to a bathochromic shift or to the appearance of an additional spectral band in the longer wavelength UV region. While all the drugs exhibit a hyperchromic shift, the type of photochemical reaction which takes place or the kind of photochemical product(s) formed during on-line irradiation has still to be clarified. However, from the structural differences between the drugs studied it must be assumed that more than one type of photochemical reaction is responsible for the absorbance changes. In the case of barbiturates and possibly also of methoin, it might be based on a photochemical modification of the molecule by which one tautomeric form of the barbiturate structure is more favoured, as can be observed[10] after a basic shift of the pH.

Nevertheless the generally observed absorbance increase in the longer wavelength range has a significant practical consequence for HPLC analysis of drugs: the use of longer wavelengths for UV detection after photochemical reaction generally

allows more specific but also more sensitive detection of the drugs studied with the positive consequence that lower sample volumes or less complex sample preparation procedures are required in routine HPLC analysis of biological samples.

Although only a small number of drugs have been described in this study, similar photochemical effects are expected for a much larger number of substances. Because of the simplicity in the use of on-line irradiation and because of the fact that it places nearly no constraints on the chromatographic performance a much wider application of post-column photochemical reaction in HPLC is indicated.

REFERENCES

1 I. S. Krull and W. R. LaCourse, in I. S. Krull (Editor), *Reaction Detection in Liquid Chromatography*, Marcel Dekker, New York, 1986, Ch. 7, p. 303.
2 A. Zweig, *Pure Appl. Chem.*, 33 (1973) 389.
3 Ch. Kikuta and R. Schmid, *Pharm. Biomed. Anal.*, 7 (1989) 329.
4 B. Lillig and H. Engelhardt, in I. S. Krull (Editor), *Reaction Detection in Liquid Chromatography*, Marcel Dekker, New York, 1986, Ch. 1, p. 1.
5 K. Hofmann and I. Halász, *J. Chromatogr.*, 173 (1979) 211.
6 R. Schmid and Ch. Wolf, *Chromatographia*, 24 (1987) 713.
7 A. Küpfer, R. James, K. Carr and R. Branch, *J. Chromatogr.*, 232 (1982) 93.
8 P. M. Kabra, H. Y. Koo and L. J. Martin, *Clin. Chem.*, 24 (1978) 657.
9 C. R. Clark and J. L. Chan, *Anal. Chem.*, 50 (1978) 635.
10 L. A. Gifford, W. P. Hayes, L. A. King, J. N. Miller, D. Thorburn Burns and J. W. Bridges, *Anal. Chem.*, 46 (1974) 94.

Journal of Chromatography, 478 (1989) 379–386
Elsevier Science Publishers B.V., Amsterdam — Printed in The Netherlands

CHROM. 21 652

DIASTEREOMERIC RESOLUTION OF CAROTENOIDS

III. β,β-CAROTEN-2-OL, β,β-CAROTENE-2,2′-DIOL AND 2-HYDROXY-ECHINENONE

TAKASHI MAOKA and TAKAO MATSUNO*
Department of Natural Products Research, Kyoto Pharmaceutical University, Yamashina-ku, Kyoto 607 (Japan)
(First received February 28th, 1989; revised manuscript received May 29th, 1989)

SUMMARY

A method is described for the diastereomeric resolution of carotenoids with an 2-hydroxy-β-end group (β,β-caroten-2-ol and β,β-carotene-2,2′-diol) and an 2-hydroxy-4-oxo-β-end group (2-hydroxyechinenone). The separation of each carotenoid into individual optical isomers was achieved by using a chiral resolution column, Sumipax OA-2000, after conversion into the corresponding benzoates.

INTRODUCTION

In the course of our stereochemical studies of naturally occurring carotenoids, we have reported on the diastereomeric resolution of carotenoids with an 3-hydroxy-β-end group (zeaxanthin)[1], an 3-hydroxy-4-oxo-β-end group (astaxanthin and phoenicoxanthin)[2,3], an 3-hydroxy-ε-end group (tunaxanthin)[4] and an 3-oxo-ε-end group (ε,ε-carotene-3,3′-dione)[4] by high-performance liquid chromatography (HPLC) using a chiral resolution column, Sumipax OA-2000.

In this paper we report the separation of optical isomers of carotenoids with an 2-hydroxy-β-end group (β,β-caroten-2-ol and β,β-carotene-2,2′-diol) and an 2-hydroxy-4-oxo-β-end group (2-hydroxyechinenone = 2-hydroxy-β,β-caroten-4-one) from animals.

EXPERIMENTAL

Biological materials

Biological materials used were the stick insect *Neohirosea japonica* and the sea louse *Ligia exotica*. The details of the studies on carotenoids from *N. japonica* and *L. exotica* will be reported elsewhere.

Apparatus

HPLC was carried out on a Waters Model 510 instrument with a Waters Lamb-

0021-9673/89/$03.50

da-Max Model 418 LC spectrophotometer set at 450 nm. The column used was a 300 mm × 8 mm I.D. stainless-steel column packed with Sumipax OA-2000 (particle size 5 μm) (Sumitomo Chemical, Osaka, Japan). Visible (VIS) absorption spectra were recorded in diethyl ether on a Shimadzu UV 240 spectrophotometer. Mass spectra were recorded with an Hitachi M-80 mass spectrometer using an inonization energy of 25 eV. ^{1}H NMR spectra were recorded on a Varian XL-300 spectrometer at 300 MHz in C^2HCl_3. Circulair dichroism (CD) spectra were obtained by a Jasco J-500C spectropolarimeter in diethyl ether–isopentane–ethanol (5:5:2) (EPA) solution at 20°C.

Isolation of β,β-caroten-2-ol, β,β-carotene-2,2'-diol and 2-hydroxyechinenone from biological materials

The isolation of these carotenoids from biological materials was carried out according to our routine procedures[5]. Identification of each carotenoid was based on VIS, MS and ^{1}H NMR spectral data by comparison with those reported by Kjøsen *et al.*[6] and Foss *et al.*[7].

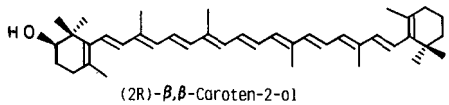

(2R)-β,β-Caroten-2-ol

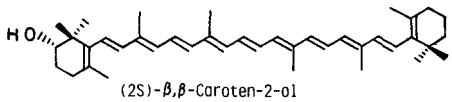

(2S)-β,β-Caroten-2-ol

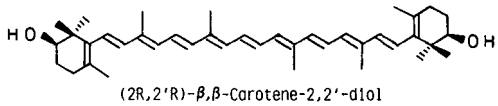

(2R,2'R)-β,β-Carotene-2,2'-diol

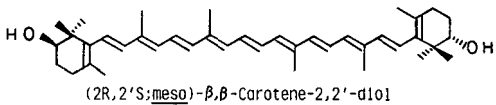

(2R,2'S;meso)-β,β-Carotene-2,2'-diol

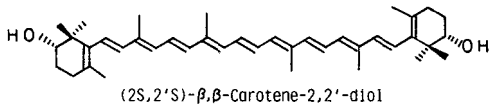

(2S,2'S)-β,β-Carotene-2,2'-diol

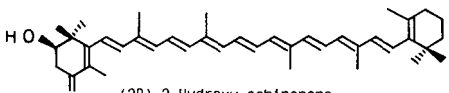

(2R)-2-Hydroxy-echinenone

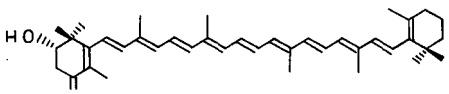

(2S)-2-Hydroxy-echinenone

β,β-Caroten-2-ol from *L. exotica* showed λ_{max} 425 (shoulder), 449 and 476 nm, *m/z* 552 (M^+, compatible with $C_{40}H_{56}O$), 534 $[M-18]^+$, 460 $[M-92]^+$ and 446 $[M-106]^+$ and ^1H NMR δ 1.03 s (6H, CH_3-16',17'), 1.04 s (3H, CH_3-16), 1.08 s (3H, CH_3-17), 1.72 s (6H, CH_3-18,18'), 1.97 s (12H, CH_3-19,20,19',20'), ≈ 2.02 m (2H, H-4'), ≈ 2.15 m (2H, H-4), 3.55 d,d (1H, H-2) and 6.1–6.7 m (14H, olefinic H) and CD at 224 [$\Delta\varepsilon$ (in dm^3 mol^- cm^{-1}) = −0.8], 236 (0), 245 (+1.0), 260 (0), 284 (−1.6), 325 (0) and 350 nm (+0.2).

β,β-Carotene-2,2'-diol from *N. japonica* showed λ_{max} 425 (shoulder), 449 and 476 nm, *m/z* 568 (M^+, compatible with $C_{40}H_{56}O_2$), 550 $[M-18]^+$, 532 $[M-36]^+$, 476 $[M-92]^+$ and 462 $[M-106]^+$, ^1H NMR δ 1.04 s (6H, CH_3-16,16'), 1.08 s (6H, CH_3-17,17'), 1.72 s (6H, CH_3-18,18'), 1.98 s (12H, CH_3-19,20,19',20'), ≈ 2.15 m (2H, H-4.4'), 3.55 d,d (2H, H-2,2') and 6.1–6.7 m (14H, olefinic H) and CD at 224 ($\Delta\varepsilon$ = −1.8), 236 (0), 245 (+2.0), 260 (0), 284 (−3.0), 325 (0) and 350 nm (+0.5).

2-Hydroxyechinenone from *L. exotica* showed λ_{max} 455–460 nm, *m/z* 566 (M^+, compatible with $C_{40}H_{54}O_2$), 548 $[M-18]^+$, 474 $[M-92]^+$ and 460 $[M-106]^+$, ^1H NMR δ 1.03 s (6H, CH_3-16',17'), 1.21 s (3H, CH_3-16), 1.25 s (3H, CH_3-17'), 1.72 s (3H, CH_3-18'), 1.89 s (3H, CH_3-18), 1.98 s (9H, CH_3-20,19',20'), 2.00 s (3H, CH_3-19), 2.62 d,d (1H, H-3_{ax}), 2.80 d,d (1H, H-3_{eq}), 3.90 d,d (1H, H-2) and 6.1–6.7 (14H, olefinic H) and CD at 225 ($\Delta\varepsilon$ = −2), 250 (−0.2) and 285 nm (−0.8).

Preparation of benzoates of β,β-caroten-2-ol, β,β-carotene-2,2'-diol and 2-hydroxyechinenone

The preparation of the benzoates of these carotenoids was carried out by the method described previously[1,4].

Saponification of benzoates of β,β-caroten-2-ol and β,β-carotene-2,2'-diol

Saponification of these benzoates was carried out by a routine procedure[8].

Enzymatic hydrolysis of benzoates of 2-hydroxyechinenone

Foss *et al.*[7] have shown that 2-hydroxyechinenone is readily dehydrated to the 3,4-didehydro product by base. Therefore, hydrolysis of benzoates was carried out by enzymatic hydrolysis with lipase as described by Matsuno *et al.*[9].

Saponification and enzymatic hydrolysis caused a slight *trans/cis* isomerization of the polyene chain. Thus each hydrolysed product was further purified by HPLC on Sumipax OA-2000 with a mobile phase of *n*-hexane–dichloromethane–ethanol (48:16:0.6).

(2*R*)-β,β-Caroten-2-ol (0.08 mg available) showed λ_{max} 425 (shoulder), 449 and 476 nm and no *cis* peak and CD 224 ($\Delta\varepsilon$ = +1.6), 236 (0), 245 (−2.8), 260 (0), 284 (+4.2), 325 (0) and 350 nm (0.8). These data were identical to those of (2*R*)-β,β-caroten-2-ol isolated from *Trentepohlia iolithus*[6].

(2*S*)-β,β-Caroten-2-ol (0.12 mg available) showed λ_{max} 425 (shoulder), 449 and 476 nm and no *cis* peak and CD at 224 ($\Delta\varepsilon$ = −1.6), 236 (0), 245 (+2.8), 260 (0), 284 (−4.2), 325 (0) and 350 nm (−0.8).

(2*R*, 2'*R*)-β,β-Carotene-2,2'-diol (0.04 mg available) showed λ_{max} 425 (shoulder), 449 and 476 nm and no *cis* peak, and CD at 224 ($\Delta\varepsilon$ = +4.6), 236 (0), 245 (−4.2), 260 (0), 284 (+7.2), 325 (0) and 350 nm (+1.2). These data were identical to those of (2*R*,2'*R*)-β,β-carotene-2,2'-diol isolated from *T. iolithus*[6].

(2*R*,2′*S*;*meso*)-β,β-Carotene-2,2′-diol (0.1 mg available) showed λ_{max} 425 (shoulder), 449 and 476 nm and no *cis* peak and no CD activity.

(2*S*,2′*S*)-β,β-Carotene-2,2′-diol (0.06 mg available) showed λ_{max} 425 (shoulder, 449 and 476 nm and CD at 224 ($\Delta\varepsilon$ = −4.6), 236 (0), 245 (+4.2), 260 (0), 284 (−7.2), 325 (0) and 325 nm (−1.2).

(2*R*)-2-Hydroxyechinenone (0.04 mg available) showed λ_{max} 455–460 nm and no *cis* peak and CD at 225 ($\Delta\varepsilon$ = +4.2), 250 (+0.5) and 285 nm (+2.8). These data were identical to those of (2*R*)-2-hydroxyechinenone isolated from *Daphnia magna*[7].

(2*S*)-2-Hydroxyechinenone (0.06 mg available) showed λ_{max} 455–460 nm and no *cis* peak and CD at 225 ($\Delta\varepsilon$ = −4.2), 250 (−0.5) and 285 nm (−2.8).

RESULTS

Separation of β,β-caroten-2-ol into (2R)- and (2S)-β,β-caroten-2-ol

β,β-Caroten-2-ol obtained from *L. exotica* showed an opposite and weaker Cotton effect to that of (2*R*)-β,β-caroten-2-ol isolated from the green alga *Trentepohlia iolithus*[6]. This suggested that β,β-caroten-2-ol obtained from *L. exotica* is a mixture of two enantiomers.

The diastereomeric separation of these two compounds was achieved by HPLC on a chiral resolution column, Sumipax OA-2000, after conversion into the corresponding monobenzoate. Good resolution was accomplished by recycling ten times (Fig. 1). *cis*-Isomers of the polyene chain were also separated from the corresponding all-*trans*-isomers and they were removed before recycling. The *cis*-isomers have not been identified.

Saponification of each monobenzoate separated gave optically pure (2*R*)- and (2*S*)-β,β-caroten-2-ol- The identification of each enantiomer was based on CD spectral data as shown in Fig. 2. Peaks 1 and 2 represent (2*R*)- and (2*S*)-β,β-caroten-2-ol, respectively.

Separation of β,β-carotene-2,2′-diol into (2R,2′R)-, (2R,2′S;meso)- and (2S,2′S)-β,β-carotene-2,2′-diol

β,β-Carotene-2,2′-diol obtained from *N. japonica* showed an opposite and weaker Cotton effect to that of (2*R*,2′*R*)-β,β-carotene-2,2′-diol isolated from *T.*

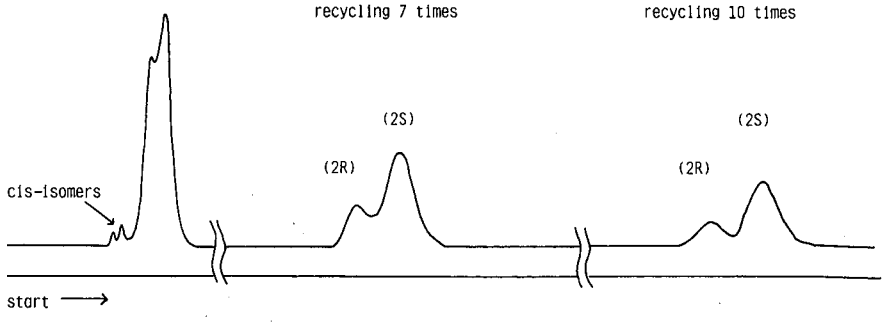

Fig. 1. Separation of (2*R*)- and (2*S*)-β,β-caroten-2-ol monobenzoates (0.2 mg available in one operation). Column: Sumipax OA-2000, 5 μm (300 mm × 8 mm I.D.). Mobile phase: *n*-hexane–dichloromethane–ethanol (48:8:0.01). Flow-rate: 2.0 ml/min. Detection 450 nm.

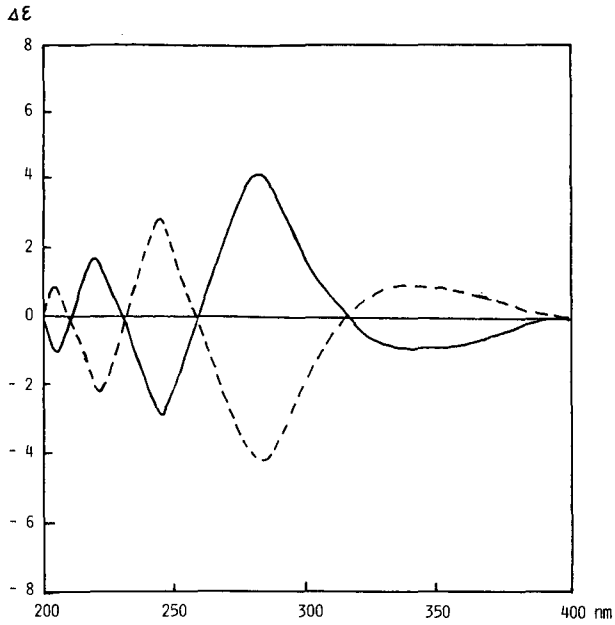

Fig. 2. CD spectra of (2*R*)-β,β-caroten-2-ol (———) and (2*S*)-β,β-caroten-2-ol (– – –) in EPA at 20°C.

iolithus[6]. This fact suggested that the β,β-carotene-2,2′-diol fraction from *N. japonica* was partly racemized.

The diastereomeric separation of three stereoisomers was achieved by the method described above (Fig. 3). Saponification of each dibenzoate separated gave optically pure (2*R*,2′*R*)-, (2*R*,2′*S*;*meso*)- and (2*S*,2′*S*)-β,β-carotene-2,2′-diol. The identification of each stereoisomer was based on CD spectra data as shown in Fig. 4.

cis-Isomers were also separated from the corresponding all-*trans*-isomers and they were removed before recycling. The *cis*-isomers have not been identified.

Separation of 2-hydroxyechinenone into (2R)- and (2S)-2-hydroxyechinenone

2-Hydroxyechinenone obtained from *L. exotica* showed an opposite and weaker Cotton effect to that of (2*R*)-2-hydroxyechinenone from *Daphnia magna*[7]. This

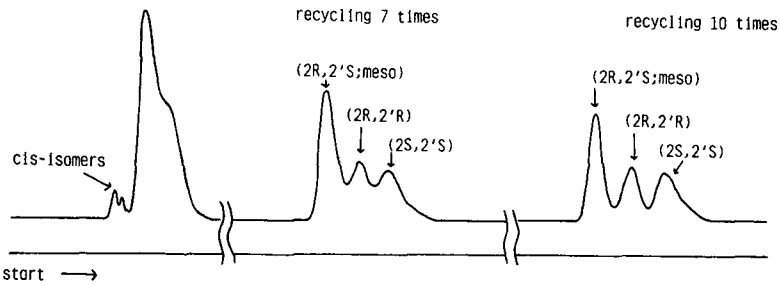

Fig. 3. Separation of (2*R*,2′*R*)-, (2*R*,2′*S*;*meso*)- and (2*S*,2′*S*)-β,β-carotene-2,2′-diol dibenzoates (0.2 mg available in one operation). Conditions as in Fig. 1.

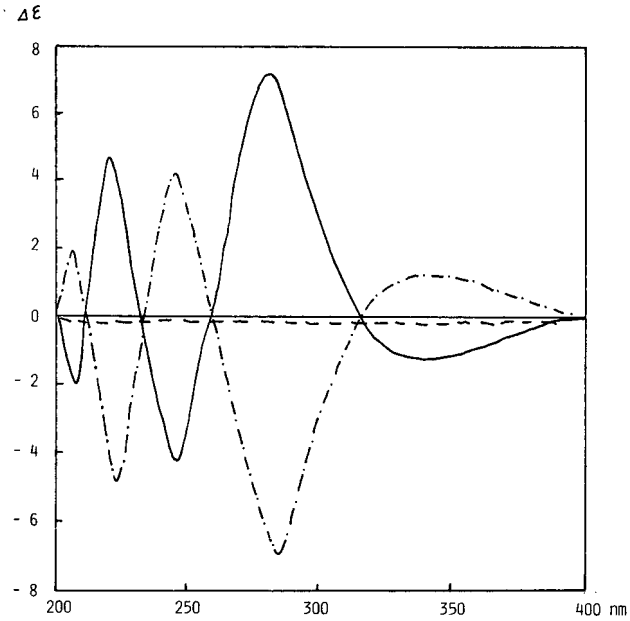

Fig. 4. CD spectra of (2*R*,2′*R*)-β,β-carotene-2,2′-diol (———), (2*R*,2′*S*;*meso*)-β,β-carotene-2,2′-diol (– – –) and (2*S*,2′*S*)-β,β-carotene-2,2′-diol (– · – · –) in EPA at 20°C.

suggested that 2-hydroxyechinenone from *L. exotica* was a mixture of two enantiomers.

The separation into each enantiomer was accomplished by recycling HPLC on Sumipax OA-2000 after conversion into the corresponding monobenzoate (Fig. 5). Enzymatic hydrolysis of each separated monobenzoate with lipase gave optically pure (2*R*)- and (2*S*)-2-hydroxyechinenone. The identification of each enantiomer was based on CD spectral data (Fig. 6). *cis*-Isomers were also separated from the corresponding all-*trans*-isomers and they were removed before recycling. The *cis*-isomers have not been identified.

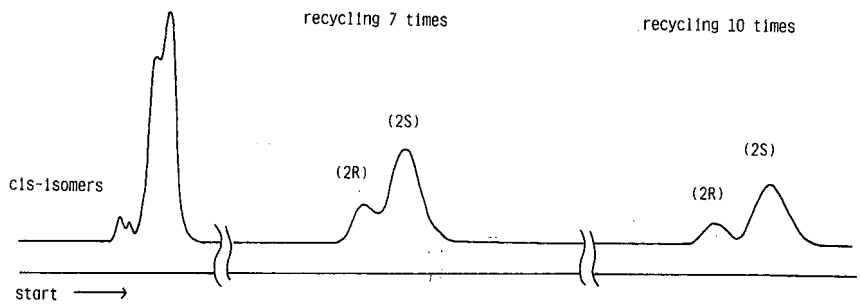

Fig. 5. Separation of (2*R*)- and (2*S*)-2-hydroxyechinenone monobenzoates (0.1 mg available in one operation). Conditions as in Fig. 1.

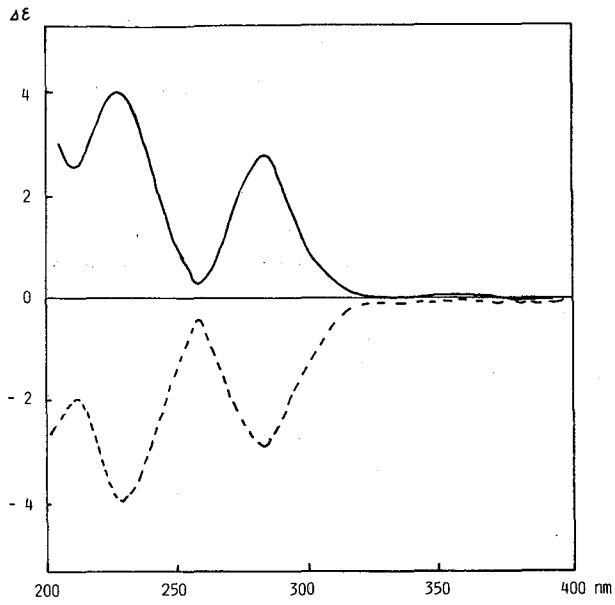

Fig. 6. CD spectra of (2*R*)-2-hydroxyechinenone (———) and (2*S*)-2-hydroxyechinenone (– – – –) in EPA at 20°C.

DISCUSSION

β,β-Caroten-2-ol and β,β-carotene-2,2′-diol were first isolated from the green alga *T. iolithus* by Kjøsen *et al.*[6], and the absolute configurations were determined to be (2*R*) and (2*R*,2′*R*), respectively by Buchecker *et al.*[10,11]. These carotenoids were also obtained from the moth *Cerula vinula*[12] and stick insect *Carausius morosus*[13], but the CD spectra of both compounds from insects showed opposite and weaker Cotton effects to those of β,β-caroten-2-ol and β,β-carotene-2,2′-diol from *T. iolithus*. These facts suggested that β,β-caroten-2-ol and β,β-carotene-2,2′-diol from insects were mixtures of stereoisomers.

However, diastereomeric derivatization with (−)-camphanyl chloride[14] and with (*S*)-(+)-α-(1-naphthyl)ethyl isocyanate[15] did not result in chromatographic separation by HPLC. On the other hand, Aareskjold and Liaaen-Jensen[16] and Kayser *et al.*[17] succeeded in the configurational analysis by using ^{1}H NMR spectroscopy in the presence of a shift reagent, Eu(fod)$_3$ (fod is 1,1,1,2,2,3,3-heptafluoro-7,7′-dimethyl-4,6-octanedionate), after conversion into the corresponding methoxy α-methoxy-α-(trifluoromethyl)phenylacetic acid (MTPA) esters. However, separation of the diastereomeric MTPA esters by HPLC was not achieved.

On the other hand, we have succeeded in the separation of β,β-caroten-2-ol, β,β-carotene-2,2′-diol and 2-hydroxyechinenone into their individual stereoisomers by using a chiral resolution column, Sumipax OA-2000, after conversion into the corresponding benzoates as described above. Saponification or enzymatic hydrolysis with lipase of the benzoates gave optically pure stereoisomers of β,β-caroten-2-ol, β,β-carotene-2,2′-diol and 2-hydroxyechinenone.

In conclusion, this is the first report on the HPLC-separation of enantiomeric or diastereomeric mixtures of (2*R*)- and (2*S*)-β,β-caroten-2-ol, (2*R*,2′*R*)-, (2*R*,2′*S*;*meso*)- and (2*S*,2′*S*)-β,β-carotene-2,2′-diol and (2*R*)- and (2*S*)-2-hydroxyechinenone.

REFERENCES

1 T. Maoka, A. Arai, M. Shimizu and T. Matsuno, *Comp. Biochem. Physiol.* B, 83 (1986) 121.
2 T. Matsuno, T. Makao, M. Katsuyama, M. Ookubo, K. Katagiri and H. Jimura, *Nippon Suisan Gakkaishi*, 50 (1984) 1598.
3 T. Maoka, K. Komori and T. Matsuno, *J. Chromatogr.*, 318 (1985) 122.
4 Y. Ikuno, T. Maoka, M. Shimizu, T. Komori and T. Matsuno, *J. Chromatogr.*, 328 (1985) 387.
5 T. Matsuno and T. Maoka, *Nippon Suisan Gakkaishi*, 47 (1981) 377.
6 H. Kjøsen, N. Arpin and S. Liaaen-Jensen, *Acta Chem. Scand.*, 26 (1972) 3053.
7 P. Foss, V. Partali, Y. Olsen, G. Borch and S. Liaanen-Jensen, *Acta Chem. Scand. Ser. B*, 40 (1986) 157.
8 T. Matsuno, T. Akita and M. Hara, *Nippon Suisan Gakkaishi*, 39 (1973) 51.
9 T. Matsuno, M. Ookubo, T. Nishizawa and I. Shimizu, *Chem. Pharm. Bull.*, 32 (1984) 4309.
10 R. Buchecker, C. H. Eugster and S. Liaaen-Jensen, *Helv. Chim. Acta*, 56 (1973) 299.
11 R. Buchecker, C. H. Eugster, H. Kjøsen and S. Liaaen-Jensen, *Acta Chem. Scand., Ser. B*, 28 (1974) 499.
12 H. Kayser, *Z. Naturforsch., Teil C*, 31 (1976) 122.
13 H. Kayser, *Z. Naturforsch., Teil C*, 31 (1976) 646.
14 R. K. Müller, K. Bernhard, H. Mayer, A. Ruttiman and M. Vecchi, *Helv. Chim. Acta*, 63 (1980) 1654.
15 A. Rüttiman, K. Schiedt and M. Vecchi, *J. High Resolut. Chromatogr. Chromatogr. Commun.*, 6 (1983) 612.
16 K. Aareskjold and S. Liaaen-Jensen, *Acta Chem. Scand., Ser. B*, 36 (1982) 499.
17 H. Kayser, K. Aareskjold, G. Borsch and S. Liaaen-Jensen, *Insect Biochem.*, 14 (1984) 51.

Journal of Chromatography, 478 (1989) 387–397
Elsevier Science Publishers B.V., Amsterdam — Printed in The Netherlands

CHROM. 21 651

ISOLATION OF TURBOT (*SCOPHTHALMUS MAXIMUS*) VITELLOGENIN BY HIGH-PERFORMANCE ANION-EXCHANGE CHROMATOGRAPHY

CHRISTER SILVERSAND* and CARL HAUX
Department of Zoophysiology, University of Göteborg, P.O. Box 25059, S-400 31 Göteborg (Sweden)
(First received March 7th, 1989; revised manuscript received May 26th, 1989)

SUMMARY

The use of high-performance anion-exchange chromatography on a Mono Q column for isolation of a glycolipophosphoprotein, vitellogenin, from turbot plasma has been evaluated. The method is an effective, rapid one-step procedure, which gives a pure preparation of vitellogenin as assessed by electrophoresis, [^{32}P]orthophosphate incorporation and amino acid composition.

INTRODUCTION

In egg laying vertebrates, a large hepatically derived glycolipophosphoprotein serves as the macromolecular precursor to the egg yolk proteins[1–8]. This glycolipophosphoprotein, vitellogenin (VTG), is synthesized by the liver in response to circulating estrogens. Normally, this synthesis occurs in female oviparous animals during the oocyte development, but it can also be induced in female, male and juvenile animals by administration of estradiol-17β[7,8]. VTG is secreted by the liver into the blood and transported to the ovaries, where it is incorporated into the growing oocytes[2–4,7,8]. Inside the oocyte, VTG is cleaved and processed to form the two major yolk proteins: lipovitellin (lipoprotein) and phosvitin (phosphoprotein)[3,4,6,7]. These yolk proteins form the principal nutritive reserve of the egg, and constitute the food supply for the developing embryo before it is capable of feeding.

The VTG molecule is a complex, high-molecular-weight plasma protein, containing variable amounts of lipids, carbohydrates, phosphates and metal ions[1,6,10]. In teleost fish, the total lipid content of VTG is about 20%[6,11,12]. VTG is of wide physiological and biochemical interest because the vitellogenic process is an unique developmental system, which allows the study of many of the facets of cell biology. VTG provides a useful tool for detailed analysis of protein induction and regulation of gene expression[13], and the uptake of VTG into maturing oocytes is an excellent system for studies of the mechanism of receptor mediated endocytosis[8,9]. Further, VTG has a vital role as a nutritional source for the embryo during embryogenesis.

Research centered on vitellogenesis and related processes often requires purified, intact VTG. The molecule has therefore been isolated from several vertebrates and insects, and a multitude of different separation techniques have been used, in-

0021-9673/89/$03.50

cluding DEAE-cellulose chromatography[14], selective precipitation[14], ultracentrifugal separation[2], high-pressure liquid chromatography[15,16] and electrophoresis[14]. These methods are usually tedious and yield adequate isolation results only if two or more methods are combined. Furthermore, the purification of VTG from certain teleosts has demonstrated that VTG is sensitive to degradation during isolation procedures[7,11]. Disintegration may occur despite the use of proteolytic inhibitors, such as phenylmethylsulphonyl fluoride or aprotinin.

In the present study, the isolation of VTG from estradiol-17β-treated turbot (*Scophthalmus maximus*) plasma using a Mono Q anion-exchange column connected to a fast protein liquid chromatography (FPLC) system has been investigated. The purity of the turbot VTG isolated was evaluated by native acrylamide gel electrophoresis. To compare the results obtained in this study with those from earlier purification methods, VTG was also isolated from rainbow trout (*Salmo gairdneri*) plasma, a species from which VTG has been purified previously[5,11,12,16]. In addition, a partial characterization of turbot VTG was performed.

MATERIALS AND METHODS

Apparatus and chemicals

As anion exchanger, Mono Q (Pharmacia, Sweden), based on monodisperse 10-μm spheres was employed. The gel was supplied packed in HR 5/5 columns (50 mm × 5 mm I.D.). Ion-exchange chromatography was performed with an FPLC system consisting of a GP 250 gradient programmer, P-500 pump, V-7 injection valve, solvent mixer, prefilter, sample loop of 1000 μl, UV-1 UV monitor with an HR low-dead-volume flowcell and a Rec-482 recorder, all from Pharmacia (Sweden). Estradiol-17β and bovine serum albumin were obtained from Sigma Chemicals (U.S.A.), [^{32}P]orthophosphate from Amersham (U.K.), acrylamide, Coomassie Brilliant Blue (R-250) and tris(hydroxymethyl)aminomethane (Tris) from Merck (F.R.G.), Trasylol (aprotinin with 10^4 trypsin inhibiting units/ml) from Bayer Leverkusen (F.R.G.), glass microfibre filters (GF/B; diameter 24 mm) from Whatman (U.K.), filters (22 μm) from Millipore (France) and Instagel scintillation cocktail from Packard (The Netherlands). The electrophoresis calibration kits were obtained from Pharmacia (Sweden). All other chemicals were of analytical grade.

Fish, hormone treatment and sampling

A total of 20 juvenile turbot (*Scophthalmus maximus*), with an average weight of 80 g, were obtained from a marine fish hatchery (Øye Havbruk, Øyestranda) in southern Norway. The fish were transported to the laboratory and acclimatized for 2 weeks in 50-l aquaria with aerated sea-water at a temperature of 18°C. The water was renewed every second day, and the photoperiod was 12 h light/12 h dark. No food was given during the experiments. In order to induce VTG synthesis, ten turbot were injected intraperitoneally (i.p.) twice a week with estradiol-17β (E-17β) dispersed in peanut oil. The dose level was 20 mg E-17β kg^{-1} week^{-1} and the volume injected each time was 0.2 ml. Control fish were not injected.

To monitor the presence of VTG in each turbot, both hormone treated and control fish were injected i.p. with 250 μCi of carrier-free [^{32}P]orthophosphate 24 h prior to blood sampling.

Two weeks after the first hormone injection, blood was taken from the caudal vessels, using a cold and heparinized syringe. The blood was centrifuged and the resulting plasma collected. To avoid protease activity, a trypsin inhibitor, aprotinin (0.2 ml Trasylol), was injected i.p. 30 min before blood was taken. All preparative procedures were carried out at 4°C.

In parallel to the turbot, a total of ten juvenile rainbow trout (*Salmo gairdneri*), obtained from a local hatchery (Antens laxodling AB), were kept and treated in the same way as the turbot, except that the rainbow trout were kept in fresh water at 8°C.

Isolation procedure

The plasma preparation obtained was either loaded directly onto the Mono Q column or first processed by selective precipitation of VTG before chromatography. The ion-exchange chromatography was carried out as follows.

All solutions pumped onto the Mono Q column contained Trasylol (1%, v/v) and were degassed and filtered through 0.22-μm filters. Before a sample was loaded, the column was equilibrated with three volumes of 20 m*M* Tris–HCl, pH 8.0 (buffer A). Immediately after the blood was centrifuged, 1.0 ml of plasma was diluted in 10 ml buffer A, and 0.50 ml of this dilution was injected onto the equilibrated column. Unbound substances were eluted with 5.0 ml of buffer A. The bound plasma proteins were separated by a 15-ml linear gradient from 0.00 to 0.50 *M* NaCl or by a 17-ml stepwise gradient of 0.00, 0.32, 0.30, 0.50 *M* NaCl. To ensure that no other proteins remained on the column, it was eluted with three volumes of 1.0 *M* NaCl. The absorbance at 280 nm was measured. The flow-rate through the column was 1.0 ml min^{-1} and fractions of 0.50 ml were collected. The chromatographic procedure was carried out at 4 and 20°C. To optimize the chromatographic conditions, buffers with three different hydrogen ion concentrations (pH 7.5, 8.0 and 8.5) were tested.

To concentrate VTG from plasma prior to chromatography, it was precipitated by mixing 1.0 ml of plasma with 4.0 ml of 20 m*M* EDTA, pH 7.7, and by subsequently adding 0.30 ml of 0.50 *M* $MgCl_2$[14]. After centrifugation at 5000 *g* for 15 min, the precipitate was dissolved in 1.0 ml of 1.0 *M* NaCl. A sample of 0.50 ml of the dissolved precipitate was diluted in 5.0 ml of buffer A and 1.0 ml was then applied on the Mono Q column.

Phosphate and plasma protein determination

Protein labelled with [^{32}P]orthophosphate was measured by a slight modification of the method described by Mans and Novelli[17]. Samples of 200 μl of each of the chromatographic fractions were applied to individual glass micro filters placed at the bottom of scintillation vials. After the discs had been dried, protein was precipitated with 1.0 ml of a cold mixture of 10% (v/w) trichloroacetic acid (TCA) and 1% (v/w) phosphotungstic acid, $H_3[P(W_3O_{10})_4]$. The discs were left for 1 h at 4°C and then washed three times with 4 ml chloroform–methanol (2:1, v/v) and dried overnight. To each vial, 10 ml of scintillation cocktail were added and the samples counted for radioactivity in a β-scintillation counter (LKB 215 Rackbeta). Total plasma protein was determined by the biuret method[18] using bovine serum albumin as a reference.

Gel electrophoresis

To assess the purity of the VTG preparation obtained by FPLC on a Mono Q

ion exchanger, native discontinuous polyacrylamide gel electrophoresis (PAGE) was carried out. Samples of the main fractions chromatographed and plasma from both E-17β-treated and control fish were electrophoresed on the same kind of gel. Native PAGE was performed according to the procedure of Chrambach *et al.*[19], system 2860.O.X, on a gradient slab gel (80 mm × 0.75 mm, LKB 2050 midget electrophoresis unit) with 5–10% (w/v) and 2% bis-acrylamide. To determine the molecular weight (MW) of turbot VTG, PAGE in the presence of sodium dodecyl sulphate (SDS) and mercaptoethanol was performed according to Laemmli[20], on a gradient slab gel (80 mm × 0.75 mm) with 5–15% (w/v) total acrylamide concentration and 2% bisacrylamide. The gels were stained with Coomassie Brilliant Blue R-250 in 40% methanol–10% acetic acid in water and with silver staining[21]. The MW was estimated by comparing the mobility of the unknown proteins with those of marker proteins. The logarithm of MW was plotted against electrophoretic mobility, and linear regression was used to estimate the MW of the samples. [^{32}P]Orthophosphate-labelled proteins in the native polyacrylamide gels were detected autoradiographically using an X-ray film (Agfa Osray). The film was exposed for 2 weeks at 8°C.

Amino acid analysis

The purified VTG was hydrolysed at 110°C in 6 *M* HCl in vacuum-sealed tubes for 24 or 72 h. Samples for cysteine, methionine and proline determination were treated by oxidation. Quantitative amino acid analysis was performed by ion-exchange chromatography at the Central Amino Acid Analysis Laboratory, Institute of Biochemistry, Uppsala, Sweden.

RESULTS

Isolation procedure

After administration of E-17β to juvenile turbot, there was a rapid increase in total plasma protein concentration. The protein levels increased from 3.5 ± 0.2 g per 100 ml (n = 5) in control fish to 10.0 ± 0.2 g per 100 ml (n = 8) in estradiol-treated fish.

Plasma from E-17β-treated turbot chromatographed on a Mono Q column, at 4°C, gave a large and apparently homogeneous absorbance peak, appearing as the last component (Fig. 1B). This peak, which was eluted at a chloride ion concentration of 0.34 *M*, was absent when plasma from control fish was subjected to chromatography (Fig. 1A). When measuring the protein-bound [^{32}P]orthophosphate activity in the different fractions chromatographed, it appeared that all radioactivity was associated with this major absorbance peak. Since VTG is known to be a phosphorus-rich protein and will incorporate [^{32}P]orthophosphate during synthesis[1,7,11,14], we tentatively identified the absorbance peak at 0.34 *M* NaCl as VTG.

The chromatographic procedure was performed at two different temperatures, 4 and 20°C. At room temperature (20°C) the major absorbance peak, present when plasma from estrogenized turbot was chromatographed, became irregular and dissociated (chromatogram not shown). When the FPLC system was moved to a cold-storage room at 4°C, the elution profile changed and the main fraction appeared homogeneous as in Fig. 1B. Thus, during the rest of the study all chromatographic work was carried out at 4°C. To select the best buffer conditions, 20 m*M* Tris–HCl

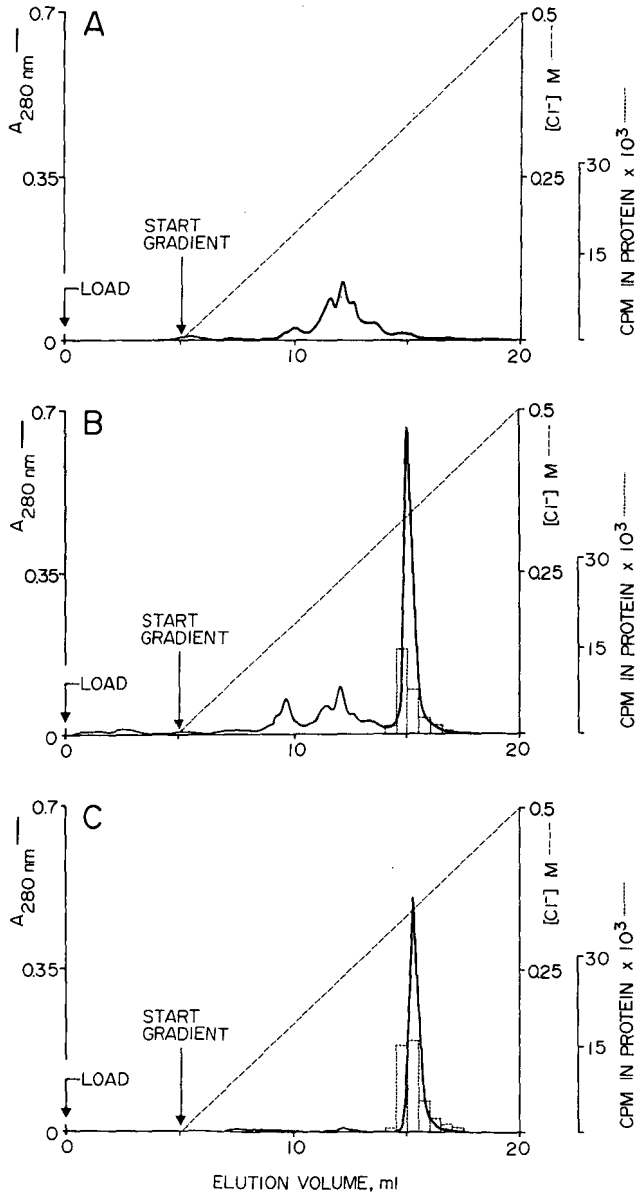

Fig. 1. Elution profiles after Mono Q chromatography of (A) plasma from control turbot, (B) plasma from estradiol-17β-treated turbot and (C) protein precipitated with Mg^{2+}–EDTA from plasma of estradiol-17β-treated turbot. The fish were injected intraperitoneally with 250 μCi of [^{32}P]orthophosphate 24 h prior to blood sampling. Elution buffer: 20 m*M* Tris–HCl, pH 8.0; gradient, 0.00–0.50 *M* NaCl. Absorbance at 280 nm (——) land cpm in protein (- - - -) were measured.

buffer at three different pH values, 7.5, 8.0 and 8.5, was examined. No significant change in resolution was observed, and only small alterations of the elution positions of the various plasma proteins. We selected pH 8.0 in subsequent studies, in order to stay inside the buffering pH range not too far from the pK_a value for the Tris buffer.

In order to increase the resolution and reach baseline separation between VTG and other plasma components, a complex stepwise gradient was used (Fig. 2). The gradient was stopped at a chloride ion concentration of 0.32 *M*, and a negative gradient step of 2.0 ml from 0.32 to 0.30 *M* was introduced before the gradient continued to 0.50 M. Alternatively, baseline separation was achieved by using a selective precipitation step with $MgCl_2$ in the presence of EDTA prior to chromatography. Other proteins in the plasma were reduced relative to VTG (Fig. 1C).

The elution positions of VTG and the other plasma proteins were dependent upon the sample concentration loaded onto the Mono Q. At lower protein concentrations, between 0.10 and 1.00 mg, VTG were eluted reproducibly at 0.34 *M* Cl^-. With progressively higher loads, the VTG peak were eluted earlier. Sample loads of up to 10 mg total plasma protein were used, and the elution ion strength of VTG showed a displacement of 0.02 *M* Cl^- to 0.32 *M*, compared to the chromatogram shown in Fig. 1B.

Electrophoresis and autoradiography

Fig. 3 shows the native electrophoretic patterns of plasma from control and estrogenized turbot and of the various VTG fractions prepared chromatographically. When plasma was electrophoresed and stained with Coomassie Brilliant Blue, two new bands, I and II, appeared during estradiol treatment (Fig. 3, lanes a and b). These two bands were absent in control fish plasma (Fig. 3, lanes c and d). The apparent MW of bands I and II was estimated as 530 000 and 275 000 respectively. When the chromatographed VTG fractions were electrophoresed on native gel two protein bands were visible at the same position and with the same relative mobility, R_m, as those of bands I and II in plasma from E-17β-treated fish. All plasma protein bands, except I and II and a thin band situated just beneath band I, disappeared after the isolation procedures (Fig. 3, lane e). When plasma was selectively precipitated with $MgCl_2$ prior to chromatography and when the stepwise gradient was used, the thin

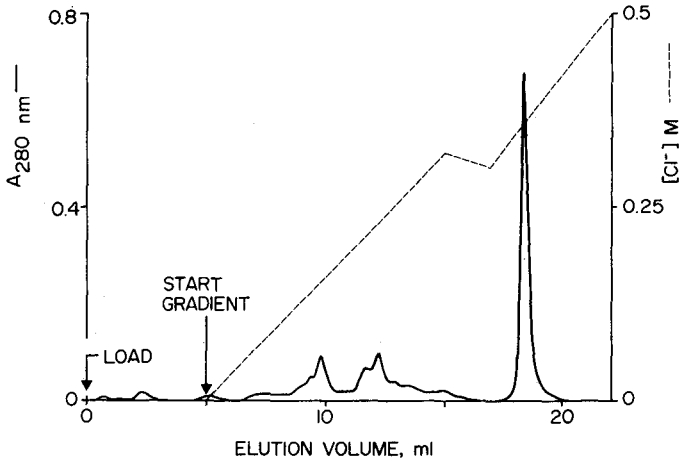

Fig. 2. Elution profiles after Mono Q chromatography of plasma from estradiol-17β-treated turbot using a stepwise gradient. Elution buffer: 20 m*M* Tris–HCl, pH 8.0; gradient 0.00, 0.32, 0.30, 0.50 *M* NaCl. Absorbance at 280 nm (——) was measured.

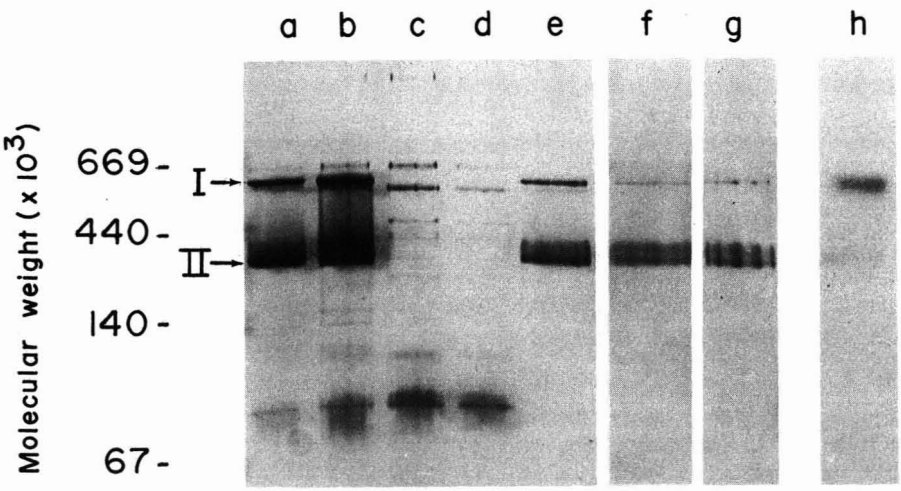

Fig. 3. Native polyacrylamide gel electrophoresis patterns of plasma proteins from turbot on a 5–10% (w/v) total acrylamide concentration gradient slab gel with 2% bis-acrylamide. Lanes: a, plasma (0.05 μl) from estradiol-17β-treated fish; b, plasma (0.10 μl) from estradiol-17β-treated fish; c, plasma (0.10 μl) from control fish; d, plasma (0.05 μl) from control fish; e, vitellogenin (VTG) obtained by Mono Q chromatography using a linear salt gradient; f, VTG obtained by Mono Q chromatography using a non-linear gradient; g, VTG precipitated with Mg^{2+}–EDTA and chromatographed on Mono Q column; h, autoradiography of the gel for samples a, b, e–g. VTG dimer and monomer are designated I and II, respectively. Numbers to the left refer to the molecular weights of the standard proteins.

band close to band I disappeared (Fig. 3, lanes f and g). The native gels were also stained with silver to see if other proteins were present in the purified fractions that were not stained by Coomassie Brilliant Blue; none was discernible. To ensure that bands I and II on the native gel were VTG, and that no other [^{32}P]orthophosphate-binding proteins were present that had not been stained by the methods used in this study, the gel was autoradiographed on an X-ray film (Fig. 3, lane h). After incubation, two labelled bands were visible on the autoradiogram. These two bands were equivalent to bands I and II on the gel. Both bands consisted of VTG. The MW of turbot VTG was estimated by SDS-PAGE by comparing the mobility of the unknown plasma proteins with those of marker proteins (Fig. 4). VTG from turbot has a MW close to 185 000.

Amino acid analysis

The results of the amino acid analyses of purified turbot VTG and the amino acid composition of VTG from two other teleost species are shown in Table I. The amino acid composition of turbot VTG is similar to that of VTG from goldfish[7] and rainbow trout[22].

To evaluate whether the isolation procedure developed in the present study can be used as a general method for purifying VTG from other fish species, plasma from vitellogenic rainbow trout was applied to a Mono Q column (Fig. 5). Rainbow trout plasma provided elution profiles very similar to those achieved with turbot plasma, the peak eluting at a chloride ion concentration of 0.35 *M*.

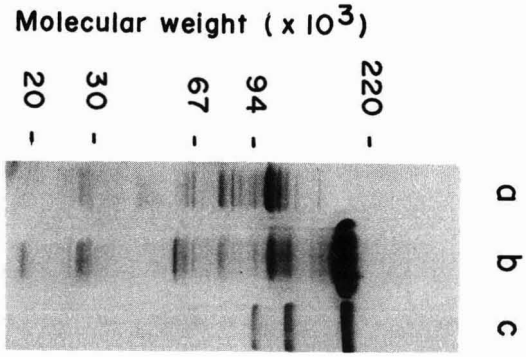

Fig. 4. SDS–PAGE patterns of turbot plasma proteins on a 5–15% (w/v) total acrylamide concentration gradient slab gel with 2% bisacrylamide. Lanes: a, plasma from control fish (0.20 μl); b, plasma from estradiol-17β-treated fish (0.20 μl) and c, vitellogenin obtained by Mono Q chromatography. Numbers to the left refer to the molecular weights of the standard proteins.

DISCUSSION

The present study demonstrates the advantage of using a Mono Q anion-exchange column connected to an FPLC system for isolation of turbot VTG. The

TABLE I

AMINO ACID COMPOSITION OF VITELLOGENIN FROM TURBOT, RAINBOW TROUT AND GOLDFISH

ND = Not determined.

Amino acid	*Mol % of total amino acid*		
	Turbot	*Rainbow trout*[a]	*Gold fish*[b]
Asp	7.8	8.5	6.5
Thr	5.2	5.0	5.5
Ser	7.5	7.6	6.9
Glu	10.1	11.6	11.9
Pro	4.5	5.3	5.5
Gly	4.6	4.3	4.6
Ala	12.0	11.8	12.8
Cys/2	1.7	ND	ND
Val	7.6	7.2	6.9
Met	2.8	2.6	2.0
Ile	6.3	5.5	6.6
Leu	10.2	9.6	10.8
Tyr	2.9	3.0	2.6
Phe	3.0	4.1	2.9
His	2.2	2.1	2.3
Lys	7.1	7.2	7.0
Arg	4.4	4.6	4.9

[a] Data from ref. 22.
[b] Data from ref. 7.

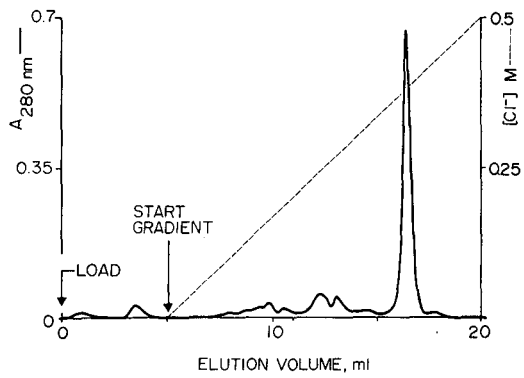

Fig. 5. Elution profile obtained after plasma from estradiol-17β-treated rainbow trout was subjected to Mono Q column chromatography. Elution buffer: 20 m*M* Tris–HCl, pH 8.0; gradient 0.00–0.50 *M* NaCl. Absorbance at 280 nm (——) was measured.

method is an effective one-step procedure, which gives a pure preparation of VTG in a short processing time. This is also exemplified by the isolation of VTG from rainbow trout, and presumably VTG from other species would be similarly purified.

The phosphorylation of VTG in combination with the very low level of other phosphorylated proteins in plasma makes the determination of [^{32}P]orthophosphate a widely used method for detecting and quantifying VTG during purification[1,3,7,14]. Since all [^{32}P]orthophosphate was associated with one absorbance peak in the chromatogram, present only in E-17β-treated fish, this peak was identified as VTG. By measuring [^{32}P]orthophosphate in all chromatographed fractions, it was possible to verify that there were no other proteins rich in phosphorus that eluted in other fractions. This verification is critical, as earlier investigations have shown that phosphorylated fragments, or the highly phosphorylated subunit of VTG, phosvitin, can dissociate from the VTG molecule during the isolation procedure[7,11]. Furthermore, phosvitin is difficult to detect spectrophotometrically because of its low absorbance at 280 nm, due to a general lack of aromatic amino acids[6,7,11].

When 10 μl plasma from E-17β-treated turbot were chromatographed, VTG eluted from the column as the last protein at a chloride concentration of 0.34 *M*. Chromatography of identical plasma samples verified the excellent reproducibility of the method. However, the elution position of VTG, as for the other plasma proteins, was dependent upon the sample load, and the proteins were eluted earlier when the sample load was increased. In this study, sample loads of up to 10 mg total plasma protein, which is 40% of the total recommended capacity for the column, were used without any reduction of the separation capacity.

The elution patterns, and thus the separation results, can be changed by using different gradient slopes. The linear salt gradient used initially provided reliable and reproducible chromatographic profiles and was used to test the effect of pH, salt and temperature. When the chemistry of the chromatography was fully optimized, a more complex gradient was introduced to improve the separation. With this stepwise gradient, the absorbance curve reached zero before VTG was eluted. Thus, the FPLC system gives the opportunity to program complex gradients in order to isolate certain peaks.

Temperature had a significant influence on the elution profile. When chromatography was carried out at room temperature (20°C), the absorbance peak for turbot VTG became irregular. These results were consistent, even when the trypsin inhibitor aprotinin was present. When chromatography was instead performed at a lower temperature, 4°C, VTG did not disintegrate and the peak was homogeneous. According to earlier investigations, VTG from some teleosts proved to be sensitive to proteolysis during isolation[7,11]; thus, precautions to prevent proteolytic activity are essential. In the present study, all preparative and chromatographic procedures were therefore carried out at low temperature and in the presence of the trypsin inhibitor aprotinin. In addition, each fish was treated with an injection of aprotinin half an hour before sampling.

When plasma from E-17β-treated turbot was electrophoresed on native gel, two new protein bands, I and II, became visible. Both bands contained [^{32}P]phosphorylated proteins, indicating that they consisted of VTG. The MW of band I was about twice that of band II, suggesting that bands I and II consist of VTG in dimeric and monomeric forms. Further evidence in support of this suggestion is that bands I and II exhibited the same patterns upon electrophoresis in the presence of SDS. The finding that turbot VTG exists in dimeric form in plasma and appears as both dimeric and monomeric forms on native electrophoresis is in accord with earlier work on other fish species[7,23].

To assess the purity of the VTG preparations obtained by chromatography, the different VTG peak fractions were applied to native PAGE. When the VTG preparation obtained by chromatography with a linear salt gradient (Fig. 1A) was applied to native electrophoresis, two bands appeared with the same R_m as those of bands I and II from plasma of estrogenized turbot. All other plasma components disappeared except for the thin band adjacent to band I. This band was present in both E-17β-treated and control turbot, indicating that this protein is not induced by E-17β. Use of the more complex stepwise gradient to elute the proteins from the Mono Q column, or inclusion of the selective precipitation step prior to chromatography, resulted in the disappearance of this faint protein band.

The MW of turbot VTG was estimated by SDS-PAGE to be 185 000. This value is very similar to that of VTG from other fish species, *e.g.*, MW 170 000[12,24] for rainbow trout. The difference observed between the MW on SDS and on native PAGE may be due partly to the relatively high lipid content of VTG. The lipid fraction is non-covalently bound to VTG and is therefore removed during treatment with SDS. This is in line with the finding made when purified turbot VTG was analyzed for its amino acid composition. Thus, when VTG was analyzed, only 68% (w/w) of the preparation consisted of amino acids; the rest was probably predominantly lipids. Even if the MW, provided by native electrophoresis, may be subject to considerable error, the calculation of the MW of SDS-treated turbot VTG by subtracting 32% (non-peptide content) from the value obtained by native PAGE results in a value of 187 000. This is very close to the MW estimated by SDS-PAGE.

ACKNOWLEDGEMENTS

This study was financially supported by the Swedish Council for Forestry and Agricultural Research. We thank Dr. Joachim Stoss, Øye Havbruk A/S, Norway for

supplying the experimental fish, and Dr. Per-Erik Olsson for initial support during chromatographic procedures.

REFERENCES

1 R. A. Wallace and D. W. Jared, *Can. J. Biochem.*, 46 (1968) 953.
2 M. R. Redshaw and B. K. Follet, *Biochem. J.*, 124 (1971) 759.
3 E. W. Bergink and R. A. Wallace, *J. Biol. Chem.*, 249 (1974) 2897.
4 R. A. Wallace and E. W. Bergink, *Am. Zool.*, 14 (1974) 1159.
5 C. M. Campbell and D. R. Idler, *Biol. Reprod.*, 22 (1980) 605.
6 R. A. Wallace, in R. E. Jones (Editor), *The Vertebrate Ovary*, Plenum, New York, 1978, p. 469.
7 V. L. de Vlaming, H. S. Wiley, G. Delahunty and R. A. Wallace, *Comp. Biochem. Physiol. B*, 67 (1980) 613.
8 R. A. Wallace and J. N. Dumont, *J. Cell. Physiol.*, 72 (1968) 73.
9 L. K. Opresko and H. S. Wiley, *J. Biol. Chem.*, 262 (1987) 4109.
10 B. Th. Björnsson and C. Haux, *J. Comp. Physiol. B.*, 155 (1985) 347.
11 B. Norberg and C. Haux, *Comp. Biochem. Physiol. B.*, 81 (1985) 869.
12 L. Fremont and A. Riazi, *Réprod. Nutr. Develop.*, 28 (1988) 939.
13 J. R. Tata, *J. Steroid Biochem.*, 11 (1979) 361.
14 H. S. Wiley, L. Opresko and R. A. Wallace, *Anal. Biochem.*, 97 (1979) 145.
15 G. Della-Cioppa and F. Engelmann, *Insect Biochem.*, 17 (1987) 401.
16 R. Waagboe and K. Sandnes, *J. Chromatogr.*, 427 (1988) 138.
17 R. J. Mans and G. D. Novelli, *Arch. Biochem. Biophys.* , 94 (1961) 48.
18 R. J. Henry, C. Sobel and S. Berkman, *Anal. Chem.*, 29 (1957) 1491.
19 A. Chrambach, T. M. Jovin, P. J. Svendsen and D. Rodbard, *Methods Protein Sep.*, 2 (1976) 27.
20 U. K. Laemmli, *Nature (London)*, 227 (1970) 680.
21 W. Wray, T. Boulikas, V. P. Wray and R. Hancock, *Anal. Biochem.*, 118 (1981) 197.
22 A. Hara and H. Hirai, *Comp. Biochem. Physiol. B*, 59 (1978) 339.
23 S. H. Hori, T. Kodama and K. Tamahashi, *Gen. Comp. Endocrinol.*, 37 (1979) 306.
24 T. T. Chen, *Can. J. Biochem. Cell Biol.*, 61 (1983) 802.

Journal of Chromatography, 478 (1989) 399–407
Elsevier Science Publishers B.V., Amsterdam — Printed in The Netherlands

CHROM. 21 647

IDENTIFICATION OF NITROPHENOLS IN RAIN-WATER BY HIGH-PERFORMANCE LIQUID CHROMATOGRAPHY WITH PHOTODIODE ARRAY DETECTION

H. B. BÖHM, J. FELTES, D. VOLMER and K. LEVSEN*
Fraunhofer Institut für Toxikologie und Aerosolforschung, Nikolai-Fuchs-Str. 1, D-3000 Hannover 61 (F.R.G.)
(First received March 14th, 1989; revised manuscript received May 26th, 1989)

SUMMARY

Nitrophenols were extracted from rain-water with dichloromethane in two steps. Isocratic separation by high-performance liquid chromatography was achieved with methanol–phosphate buffer (40:60) at pH 3.25. A photodiode array detector was employed to detect the individual nitrophenols at their optimum wavelengths and to identify these compounds by comparison of their UV spectra with those of reference compounds. Depending on the individual compound and the extraction method, the recoveries ranged from 26 to 100% while the detection limit was 0.1–0.5 μg/l. 4-Nitrophenol, 2,4-dinitrophenol, 2,6-dimethyl-4-nitrophenol, 4,6-dinitro-2-methylphenol and most likely 3-methyl-4-nitrophenol were identified in rain-water.

INTRODUCTION

Nitrophenols and in particular dinitrophenols are toxic compounds[1]. They uncouple the oxidative phosphorylation and are used in part as pesticides. 4-Nitrophenol, 2-nitrophenol, 2,4-dinitrophenol (DNP) and 4,6-dinitro-2-methylphenol (DNOC) are listed as priority pollutants by the US Environmental Protection Agency[2]. Although nitrophenols have been rarely identified in surface water[3], they were found recently in relatively high concentrations in rain-water[4–7]. It is most likely that nitrophenols in the atmosphere are formed by photochemical reaction of aromatic hydrocarbons such as benzene and toluene with NO_x and OH radicals as demonstrated by smog chamber studies[8,9].

So far, nitrophenols in rain-water have been determined by gas chromatography–mass spectrometry (GC–MS) without prior derivatization. However, although adequate GC behaviour of phenols is observed if new fused-silica colums with immobilized stationary phases are used[10,11], considerable tailing in particular of nitrophenols is observed after repeated use of the column due to adsorption of these polar compounds at the active centres of the column. Thus, phenols are usually derivatized prior to their determination by GC[12].

Alternatively, phenols in water can be analyzed by high-performance liquid

0021-9673/89/$03.50

chromatography (HPLC)[13–23]. While phenols have been determined as their 4-aminoantipyrine derivatives[13–15], most often the underivatized compounds are used and an UV detector is employed. In these studies only a very limited number of nitrophenols and only spiked samples were analyzed. We report here the analysis of sixteen nitrophenols by HPLC with photodiode array detection. The method was applied to the analysis of rain-water. It is demonstrated that the use of a photodiode array detector is particularly valuable for an unambiguous identification of these compounds in real environmental samples.

EXPERIMENTAL

Instruments

The analysis was performed with a Varian Model 5000 liquid chromatograph and a Waters Model 990 photodiode array detector using a Merck LiChrosorb RP-18 column (250 × 4 mm, 5-μm particles). Methanol–phosphate buffer (40:60) was used as the mobile phase. The phosphate buffer was prepared from a 0.05 *M* potassium dihydrogenphosphate solution adjusted to pH 3.25 with orthophosphoric acid. Flow-rates: 0–20; min, 1 ml/min; 20–21.5 min, linear gradient to 1.2 ml/min; > 20 min, 1.2 ml/min.

Sampling

Rain-water was collected on the roof of the institute using a stainless-steel sampler with a sampling area of 1 m^2. The sampler can be closed with a lid to prevent dry deposition. Mercury dichloride was added to the sample to avoid biological degradation. The sample was stored at 4°C until analyzed.

Extraction

Two extraction methods were used.

A 1-l volume of rain-water was extracted three times with 50 ml dichloromethane (shaking for 1 min). The pooled organic phases were shaken with 10 ml 1 *M* potassium hydroxide. The organic phase was analyzed for neutral and basic compounds. The aqueous phase was diluted in 40 ml water, adicified with 1.4 ml 6 *M* hydrochloric acid to pH < 2 and extracted three times with 20 ml dichloromethane (shaking for 1 min). (When fatty acids were to be determined, the pooled organic phase was treated further with boron trifluoride–methanol). The pooled organic phases were dried over sodium sulphate and reduced in volume with a rotary evaporator. After exchange of the solvent (methanol instead of dichloromethane), the volume was adjusted to exactly 250 μl

The second method was similar but here the water sample was first adjusted to pH > 12 with 20 ml 1 *M* potassium hydroxide prior to extraction with dichloromethane. After acidification to pH < 2, the aqueous phase was again extracted with dichloromethane as described above.

Chemicals

Nitrophenols were obtained from Fluka and Aldrich. Orthophosphoric acid, potassium dihydrogenphosphate, acetic acid, citrate buffer and heptanesulphonic acid were obtained from Merck, methanol and dichloromethane (HPLC grade) from

Rathburn. Twice distilled water, potassium hydroxide and hydrochloric acid were extracted with dichloromethane prior to use.

RESULTS AND DISCUSSION

HPLC separation

Binary mixtures of methanol–water or acetonitrile–water are not useful as mobile phases for the separation of phenols, as partial dissociation of the phenols leads to peak tailing. Thus seventeen different isocratic mixtures of methanol–water acidified with acetic acid, a citrate buffer (pH 2), heptanesulphonic acid or a phosphate buffer were tested. Methanol–0.05 *M* K_2HPO_4 (H_3PO_4) (40:60) proved to be best. Fig. 1 shows the separation of sixteen nitrophenols (and three non-nitrated phenols). 2-Nitrophenol/3-methyl-4-nitrophenol as well as 5-methyl-2-nitrophenol/4-methyl-2-nitrophenol are not resolved. The use of a gradient, *i.e.*, from 20 to 40 min, to shorten the analysis time was not attempted as the reproducibility of isocratic mixtures is better. Retention times and capacity factors, k', are summarized in Table I.

The selective detection of nitrophenols from a complex matrix (containing, *e.g.*, also other non-nitrated phenols) is facilitated by the fact that nitrophenols usually show absorption maxima also at > 300 nm. Fig. 1 shows the suppression of non-nitrated phenols at 317 nm.

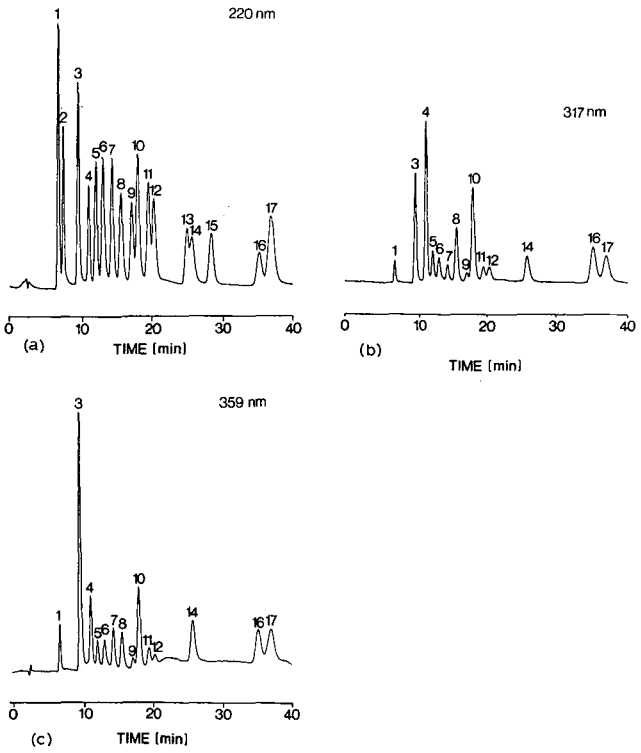

Fig. 1. HPLC chromatogram of nineteen phenols (sixteen nitrophenols) (see Table I for peak assignment).

TABLE I

RETENTION TIMES AND CAPACITY FACTORS

Compound		*Retention time (min)*	*Capacity factor, k'*
1	2,6-Dinitrophenol	6.62	1.57
2	Phenol	7.31	1.83
3	2,4-Dinitrophenol	9.43	2.66
4	4-Nitrophenol	10.96	3.25
5	3-Nitrophenol	11.97	3.64
6	2,3-Dinitrophenol	12.91	4.00
7	2,5-Dinitrophenol	14.20	4.50
8	3,4-Dinitrophenol	15.46	4.99
9	3-Methyl-2-nitrophenol	17.03	5.60
10	2-Nitrophenol/3-methyl-4-nitrophenol	17.91	5.94
11	4-Methyl-3-nitrophenol	19.43	6.53
12	2-Methyl-3-nitrophenol	20.27	6.86
13	2,5-Dimethylphenol	25.02	8.70
14	4,6-Dinitro-2-methylphenol	25.71	8.97
15	2,6-Dichlorophenol	28.32	9.98
16	2,6-Dimethyl-4-nitrophenol	35.12	12.61
17	5-Methyl-2-nitrophenol/4-methyl-2-nitrophenol	36.85	13.28

The use of a photodiode array detector is particularly valuable as it allows the recording of chromatograms at the optimum wavelength for each nitrophenol. Furthermore, comparison of the UV spectra with those of reference compounds in gener-

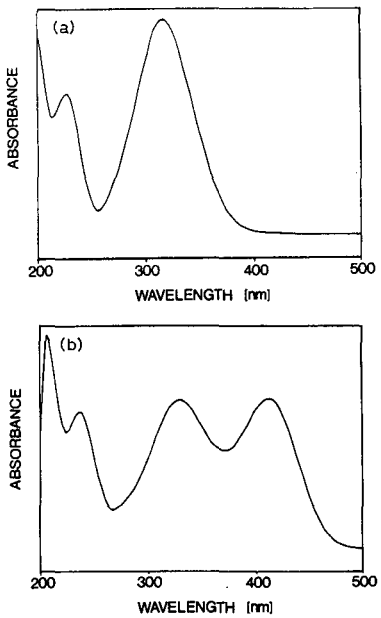

Fig. 2. UV spectra of 4-nitrophenol at (a) pH 3.25 and (b) 7.

TABLE II

ABSOLUTE DETECTION LIMITS OF THE PHOTODIODE ARRAY DETECTOR (S/N = 3)

Compound	*Wavelength (nm)*	*Detection limit (ng)*
2,6-Dinitrophenol	220	0.4
	435	0.9
2,4-Dinitrophenol	220	0.4
	435	1.1
4-Nitrophenol	220	0.6
	317	0.9
2,5-Dinitrophenol	220	0.8
3-Methyl-2-nitrophenol	220	1.0
2-Methyl-3-nitrophenol	220	0.9

al allows unambiguous identification of nitrophenols. In particular, most nitrophenols show unique UV spectra with several pronounced absorption maxima between 200 and 500 nm. It should, however, be kept in mind that the UV spectra strongly depend on the pH value as shown in Fig. 2 for 4-nitrophenol. Thus reference spectra must be recorded at the pH at which the actual analysis is carried out (UV spectra of the various nitrophenols are available upon request from the authors).

The linearity of the detector was tested for the concentration range of 4 to 2000 ng with five nitrophenols. Good linearity was observed in each case. The reproducibility was tested by four injections of a mixture of five standard compounds at 4–2000 ng (injected volume = 20 μl). The coefficient of variation is < 1% at 2000 ng. 1–6% at 8 ng and 1–14% at 4 ng. The detection limit is shown in Table II for six nitrophenols (signal-to-noise ratio, S/N = 3).

Extraction

The extraction scheme was designed to allow not only the determination of nitrophenols but also of other compound classes which are present in rain. In view of the complexity of a rain sample in which usually a large variety of organic compounds are present at in part high concentrations[4,5], a separation of the acidic compounds (mainly phenols and fatty acids) and the neutral/basic compounds is desirable. Two extraction methods have been employed as described in the Experimental section. Recoveries are reported in Table III. It is apparent that the recoveries strongly depend on the individual compounds. Recoveries by the first method (three successive extractions at pH 7, > 12 and < 2) are particularly poor for 4-nitrophenol, 2,4-dinitrophenol and 2,6-dinitrophenol. When in the first step extraction occurred at pH < 2, identical recoveries were determined except for 2,6-dinitrophenol where a substantial improvement (103%) was observed. The second method is more straightforward. With this method the recovery was improved for the dinitrophenols, but became poorer for 4-nitrophenol (see Table II). The latter result is difficult to explain. Poor recoveries for 4-nitrophenol have also been reported by other authors[21,24,25]. Moreover, solid phase extraction with XAD-2, C_{18} or phenyl phases did not improve the recovery.

After extraction and solvent exchange, the extract is reduced to 250 μl using a

TABLE III

RECOVERIES OF NITROPHENOLS BY EXTRACTION WITH DICHLOROMETHANE FROM WATER

Triplicate determinations, 10 μg/l, 220 nm. First method: extraction at pH 7; extraction at pH > 12; extraction at pH < 2. Second method: extraction at pH > 12; extraction at pH < 2. n.d. = Not determined.

Compound	*Recovery (%)*	
	First method	*Second method*
2-Nitrophenol	73 ± 3	75 ± 7
3-Nitrophenol	48 ± 2	24 ± 1
4-Nitrophenol	33 ± 2	19 ± 3
2,4-Dinitrophenol	45 ± 2	99 ± 8
2,5-Dinitrophenol	84 ± 4	94 ± 4
2,6-Dinitrophenol	26 ± 5	84 ± 3
3-Methyl-2-nitrophenol	69 ± 8	n.d.
2-Methyl-3-nitrophenol	64 ± 2	69 ± 9
4-Methyl-3-nitrophenol	85 ± 3	n.d.

rotary evaporator at 40°C. This may lead to evaporation losses. To explore this effect a mixture of five nitrophenols was evaporated to dryness at 40°C. The recoveries are shown in Table IV. It is apparent that substantial evaporation losses are observed for 3-methyl-2-nitrophenol only.

The detection limit of the method was not determined systematically. Rather a mixture of five nitrophenols at 0.5 μg/l was extracted according to the first method and reduced in volume to 1 ml. The nitrophenols were adequately quantified, with recoveries shown in Table V. If reduced to 0.25 ml, 4-nitrophenol can still be quantified at a level of 100 ng/l as shown in Fig. 3 (recovery 29%, coefficient of variation 9%).

Rain samples

Rain samples were collected on the roof of our institute from May 1987 until December 1988 as described in the Experimental section and extracted as described above.

Fig. 4 shows the chromatogram of a rain sample from June 4th, 1987, recorded

TABLE IV

RECOVERIES OF NITROPHENOLS AFTER EVAPORATION TO DRYNESS

Compound	*Recovery (%)*
2,5-Dinitrophenol	81
2,6-Dinitrophenol	101
4-Nitrophenol	92
3-Methyl-2-nitrophenol	5
2-Methyl-3-nitrophenol	70

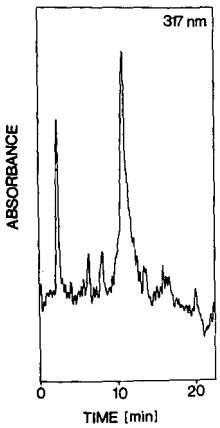

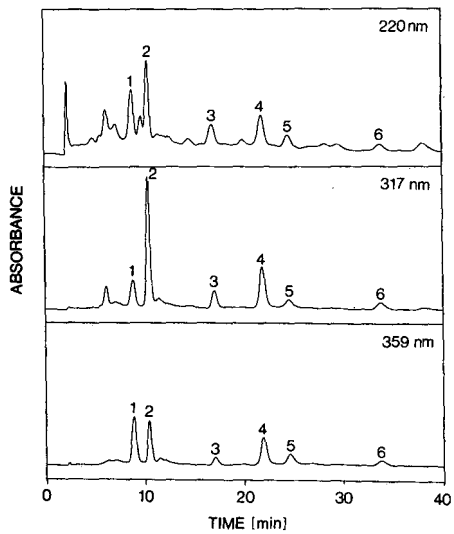

Fig. 3. Chromatogram of a water sample spiked with 100 ng/l of 4-nitrophenol; monitored at 317 nm.

Fig. 4. HPLC chromatogram of a rain-water sample at pH 3.25. Peaks: 1 = 2,4-dinitrophenol; 2 = 4-nitrophenol; 3= 3-methyl-4-nitrophenol(?) + coeluting unknown component; 4 = unknown; 5 = 4,6-dinitro-2-methylphenol; 6 = 2,6-dimethyl-4-nitrophenol.

at 220, 317 and 359 nm; the wavelength 317 nm corresponds to an absorption maximum of 4-nitrophenol, 359 nm to one of 2,4-dinitrophenol. 4-Nitrophenol and 2,4-dinitrophenol can readily be identified by their retention times and UV spectra. Fig. 5 shows the UV spectrum of peak 2 (4-nitrophenol, compare with Fig. 2). Even minor peaks can be assigned. Thus Fig. 6 compares the UV spectrum of peak 5 with that of 4,6-dinitro-2-methylphenol (DNOC), Fig. 7 the UV spectrum of peak 6 with that of 2,6-dimethyl-4-nitrophenol. Similarly, peak 3 was assigned as 3-methyl-4-nitrophenol. The contour plot of this peak revealed, however, a second, minor coeluting component. Similarly, peak 4 must result from two coeluting components. A definite

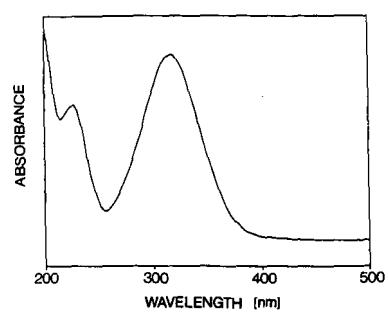

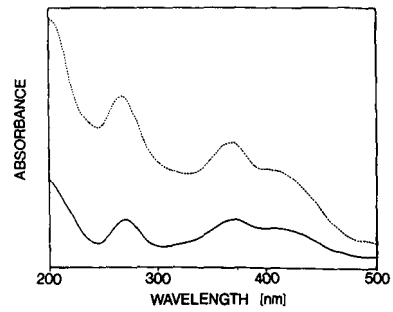

Fig. 5. UV spectrum of peak 2 in Fig. 4 (4-nitrophenol).

Fig. 6. Comparison of the UV spectrum of peak 5 in Fig. 4 (dashed line) with that of 4,6-dinitro-2-methylphenol (solid line).

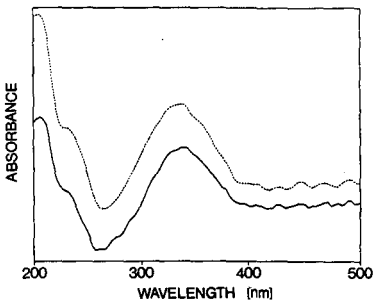

Fig. 7. Comparison of the UV spectrum of peak 6 in Fig. 4 (dashed line) with that of 2,6-dimethyl-4-nitrophenol (solid line).

TABLE V

RECOVERIES OF FIVE NITROPHENOLS FROM WATER AT A CONCENTRATION OF 500 ng/l

Triplicate determinations, 220 nm.

Compound	*Recovery (%)*	*Coefficient of variation (%)*
2,5-Dinitrophenol	79	15
2,6-Dinitrophenol	35	12
4-Nitrophenol	30	8
3-Methyl-2-nitrophenol	57	11
2-Methyl-3-nitrophenol	63	6

assignment was, however, not possible. The fact that this compound absorbs at long wavelengths (see 359 nm in Fig. 4) indicates the presence of a further nitrophenol. Unfortunately, not all isomers of methylnitrophenol and dimethylnitrophenol were commercially available to aid assignment of peak 4. The above assignments are corroborated by comparison of the retention times.

More details including the identification and quantitation of additional nitrophenols by other methods are reported elsewhere[26].

ACKNOWLEDGEMENTS

Financial support by the Bundesministerium für Forschung und Technologie is kindly acknowledged. We are grateful to Mrs. Behnert for technical assistance.

REFERENCES

1 D. W McLeese, V. Zitko and M. R. Peterson, *Chemosphere*, 9 (1979) 53.
2 L. H. Keith and W. A. Teilliard, *Environ. Sci. Technol.*, 13 (1979) 416.
3 *Concerted Action. Analysis of Organic Micropollutants in Water* (COST 64 b bis), Commission of the European Communities, 4th ed., 1984; Addendum, 1987.
4 C. Leuenberger, M. P. Ligocki and J. F. Pankow, *Environ. Sci. Technol.*, 19 (1985) 1053.
5 K. Kawamura and I. R. Kaplan, *Atmos. Environ.*, 20 (1986) 115.
6 G. Rippen, E. Zietz, R. Frank, T. Knacker and W. Klöpffer, *Environ. Technol. Lett.*, 8 (1987) 475.

7 C. Leuenberger, J. Czuczwa, J. Tremp and W. Giger, *Chemosphere*, 17 (1988) 511.
8 K. Nojima, K. Fukaya, S. Fukui and S. Kanno, *Chemosphere*, 4 (1975) 77.
9 K. Nojima, K. Fukaya, S. Fukui, S. Kanno, S. Nishiyama and Y. Wada, *Chemosphere*, 5 (1976) 25.
10 J. Nolte, H. Mayer and B. Paschold, *Fresenius' Z. Anal. Chem.*, 325 (1986) 20.
11 O. H. Masi and W. M. Gulick, *J. High Resolut. Chromatogr. Chromatogr. Commun.*, 10 (1987) 647.
12 E. Tesarova and V. Pacakova, *Chromatographia*, 17 (1983) 269.
13 G. Blo, F. Dondi and C. Bighi, *J. Chromatogr.*, 295 (1984) 231.
14 G. Blo, F. Dondi, A. Betti and C. Bighi, *J. Chromatogr.*, 257 (1983) 69.
15 F. P. Bigley and R. L. Grob, *J. Chromatogr.*, 350 (1985) 407.
16 J. J. Scanlon, P. A. Flaquer, G. W. Robinson, G. E. O'Brien and P. E. Sturrock, *Anal. Chim. Acta*, 158 (1984) 169.
17 H. K Lee, S. F. Y. Li and Y. H. Tay, *J. Chromatogr.*, 438 (1988) 429.
18 N. G. Buckman, J. O. Hill, R. J. Magee and M. J. McCormick, *J. Chromatogr.*, 284 (1984) 441.
19 G. K. J. Chao and J. C. Suatoni, *J. Chromatogr. Sci.*, 20 (1982) 436.
20 P. A. Realini, *J. Chromatogr. Sci.*, 19 (1981) 124.
21 B. Schultz, *J. Chromatogr.*, 269 (1983) 208.
22 A. F. Haeberer and T. A. Scott, *Adv. Identif. Anal. Org. Pollut. Water*, 1 (1981) 359.
23 J. C. Hoffsommer, D. J. Glover and C. Y. Hazzard, *J. Chromatogr.*, 195 (1980) 435.
24 G. Bengtsson, *J. Chromatogr. Sci.*, 23 (1985) 397.
25 J. W. Eichelberger, E. H. Kerns, P. Olynyk and W. L. Budde, *Anal. Chem.*, 55 (1983) 1471.
26 M. Alber, H. B. Böhm, J. Brodesser, J. Feltes, K. Levsen and H. F. Schöler, *Fresenius' Z. Anal. Chem.*, in press.

Journal of Chromatography, 478 (1989) 408–414
Elsevier Science Publishers B.V., Amsterdam — Printed in The Netherlands

CHROM. 21 653

Note

Reversed-phase high-performance liquid chromatography of aluminium(III) and indium(III) with 1-phenyl-3-methyl-4-benzoyl-5-pyrazolone

A. TONG and Y. AKAMA*

Department of Chemistry, Faculty of Science and Engineering, Meisei University, Hodokubo, Hino, Tokyo 191 (Japan)

and

S. TANAKA

Department of Fundamental Science, Faculty of Science and Engineering, Iwaki Meisei University, Iwaki, Fukushima 970 (Japan)

(First received November 29th, 1988; revised manuscript received May 26th, 1989)

Reversed-phase high-performance liquid chromatography (RP-HPLC) is a well known method for the separation and determination of organic compounds. In recent years, great interest has been shown in the potential of this method for metal ions and many research papers have been published. Metal ions are commonly separated and determined by RP-HPLC as their chelates. So far, many chelating agents, such as acetylacetone[1], benzoylacetone, quinolin-8-ol[2], dithiocarbamic acids[3] and 2-(5-bromopyridylazo)-5-diethylaminophenol[4], have been employed.

We now introduce 1-phenyl-3-methyl-4-benzoyl-5-pyrazolone (PMBP) as a chelating agent for studies of the chromatographic behaviour of aluminium(III) and indium(III). PMBP has frequently been used as an extraction agent for various metals[5,6] and is known to have the ability to form stable chelates with most metals non-selectively at around pH 7. This suggests that it is possible to use PMBP for RP-HPLC studies of metals.

The purpose of this work is to search for the optimum conditions for the separation and determination of aluminium(III) and indium(III) in the form of PMBP chelates by RP-HPLC with spectrophotometric detection.

EXPERIMENTAL

Materials

PMBP was prepared and recrystallized as reported previously[5].

The PMBP chelates of aluminium(III) and indium(III) were synthesized as follows. About 1 g each of potassium aluminium sulphate and indium chloride were dissolved in water. The solutions were adjusted to about pH 7 with ammonium citrate and ammonia. Then the PMBP–methanol solution was added in a molar ratio of 1:3 (metals to PMBP). The mixture was allowed to react thoroughly in a water-bath at

0021-9673/89/$03.50

temperature of 70–80°C with agitation. The precipitates were washed with deionized water after filtration. The products were then dissolved and agitated in methanol by heating to remove the unreacted PMBP. After separation of the two phases, the refining process was repeated twice. The precipitates were then dried under vacuum and used as our testing chelates. The identities of the two PMBP chelates synthesized were confirmed by elemental analysis, as shown in Table I.

All other reagents and solvents were of analytical reagent grade, obtained from commercial sources. The solvents were degassed before use as the mobile phase.

Preparation of synthetic mixture

Sample solution containing 0.284 mg of aluminium and 5.23 mg of indium was taken in a 100-ml beaker, 10 ml of 0.1 *M* ammonium citrate solution and 10 ml of water were added and the mixture was adjusted to pH 5 with 1 *M* ammonia solution. Then 30 ml of 0.01 *M* PMBP solution in methanol were added with stirring and the beaker was placed in a water-bath at 70°C for at least 1 h to ensure complete precipitation of metal–PMBP complexes. The product (containing free PMBP) was separated by filtration and washed with water, then dissolved in 15 ml of dioxane. The solvent (containing a small amount of water) was then evaporated and the precipitate was dried completely at 70–75°C under vacuum, then dissolved in 50 ml of dioxane. A 5 μl aliquot of this dioxane solution was injected into the chromatograph. Acetonitrile was used as the mobile phase. The flow-rate was 1.0 ml/min. The amount of each metal was determined by measuring the peak heights.

Instrumentation

The high-performance liquid chromatograph consisted of a Japan Spectroscopic Model 880-PU pump, a Rheodyne injector and a Japan Spectroscopic Model 875-UV detector, together with a Rikadenki Multi Pen recorder. A Shim-Pack CLC-ODS(M) column 25 (250 mm × 4.6 mm I.D.) was used. The detector was operated at 290 nm, the mobile phase flow-rate was 1.0 ml/min and the recorder chart speed was 1.0 cm/min.

The PMBP chelates of aluminium(III) and indium(III) synthesized were dissolved in dioxane and were mixed to give suitable concentrations. An aliquot of the sample solution was injected into the chromatograph.

TABLE I

ELEMENTAL ANALYSIS OF THE CHELATES SYNTHESIZED

Complex	*Element*	*Calculated (%)*	*Found (%)*
$Al(PMBP)_3$	C	71.35	71.38
	H	4.54	4.37
	N	9.79	9.76
$In(PMBP)_3$	C	64.70	64.46
	H	4.16	4.01
	N	8.88	8.66

RESULTS AND DISCUSSION

The ultraviolet absorption spectra for PMBP chelates of aluminium(III) and indium(III) in dioxane at a concentration of $1.28 \cdot 10^{-6}$ *M* are shown in Fig. 1. Two maxima appear at 240 and 290 nm for each chelate. However, as at 240 nm the noise level was high due to absorption by the solvent (dioxane), 290 nm was chosen. The molar absorptivities for aluminium(III) and indium(III) chelates in dioxane at 290 nm calculated from the above spectra were found to be $6 \cdot 10^4$ and $5.5 \cdot 10^4$ $dm^3\ mol^{-1}\ cm^{-1}$, respectively, indicating that an highly sensitive determination of aluminium(III) and indium(III) at 290 nm is feasible.

The combination with acetonitrile of several solvents, such as water, methanol and dioxane, as the dissolving solvent for PMBP chelates, was investigated as the mobile phase for chromatography of the two PMBP chelates of interest. The results of using acetonitrile–water system as the mobile phase for the separation of PMBP chelates of aluminium(III) and indium(III) are shown in Fig. 2. The retention time of the aluminium chelate increased with increasing content of water in acetonitrile, while the peak related to the indium chelate was at first very low and then disappeared abruptly. However, as the peak of indium chelate disappeared, a new broad peak was seen near the peak of dioxane, indicating that dissociation of indium chelate may occur during the chromatographic process. Noda *et al.*[7] think this may be due to the hydrolysis of indium chelate.

A similar result for the indium chelate was obtained by adding methanol to acetonitrile, which was used as the main component of the mobile phase. When increasing the methanol content, the peak of indium chelate became lower and gradu-

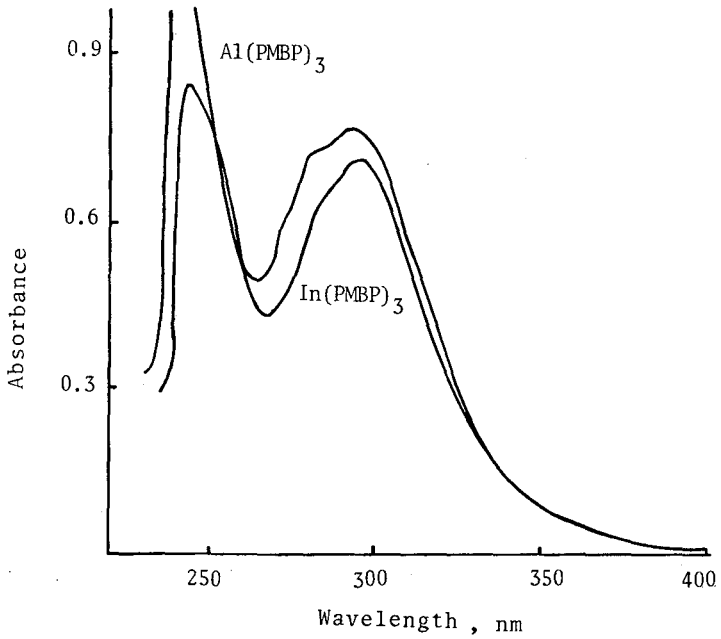

Fig. 1. Absorption spectra of $Al(PMBP)_3$ and $In(PMBP)_3$ ($1.28 \cdot 10^{-6}$ *M*) in dioxane.

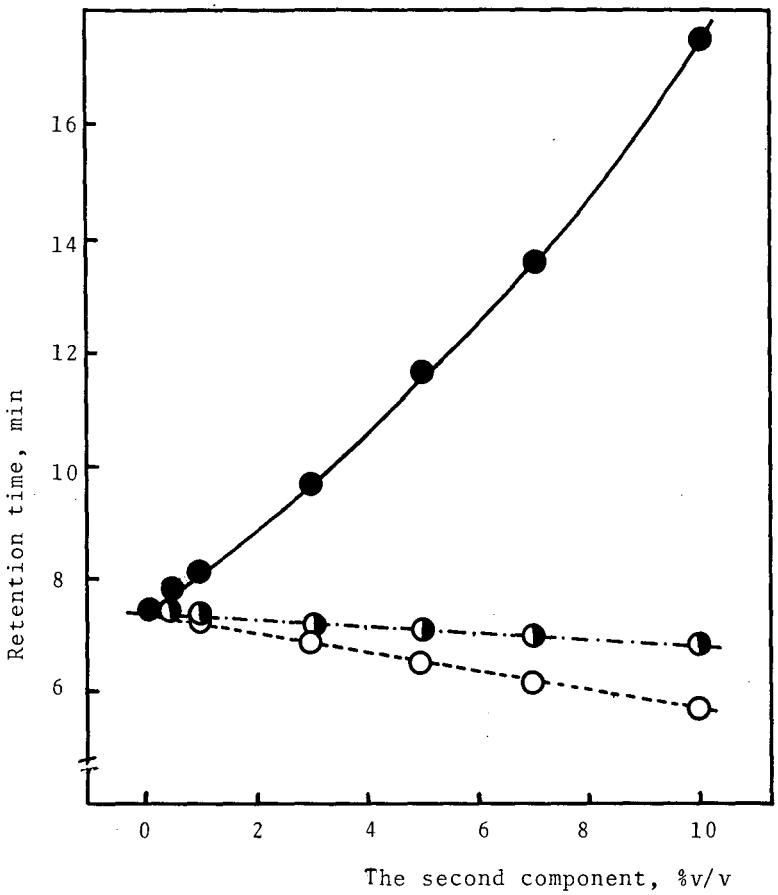

Fig. 2. Effect of the second component in acetonitrile on the retention time of $Al(PMBP)_3$ ($8.0 \cdot 10^{-6}$ *M*). ○, Acetonitrile–dioxane; ●, acetonitrile–water; ◑, acetonitrile–methanol.

ally disapppeared. On the other hand, when methanol was added to the mobile phase, the retention time of the aluminium chelate decreased slightly on increasing the methanol content and the elution peaks were sharp and symmetric, indicating that the PMBP chelate of aluminium was stable enough for the RP-HPLC determination.

Both aluminium(III) and indium(III) chelates can be dissolved in dioxane more easily than in acetonitrile or in methanol; thus the disappearance of the indium chelate peak may be suppressed by adding dioxane to acetronitrile. The effects of the dioxane content in the mobile phase on the retention of aluminium and indium chelates are shown in Fig. 2. The retention time of the two metal chelates decreased on increasing the dioxane content and the phenomenon of the disappearance of the indium chelate peak was no longer observed. However, the retention times of the two chelates became closer and their separation became worse when the content of dioxane increased. The optimum separation condition was obtained when the mobile phase was dioxane–acetonitrile (0.1:100).

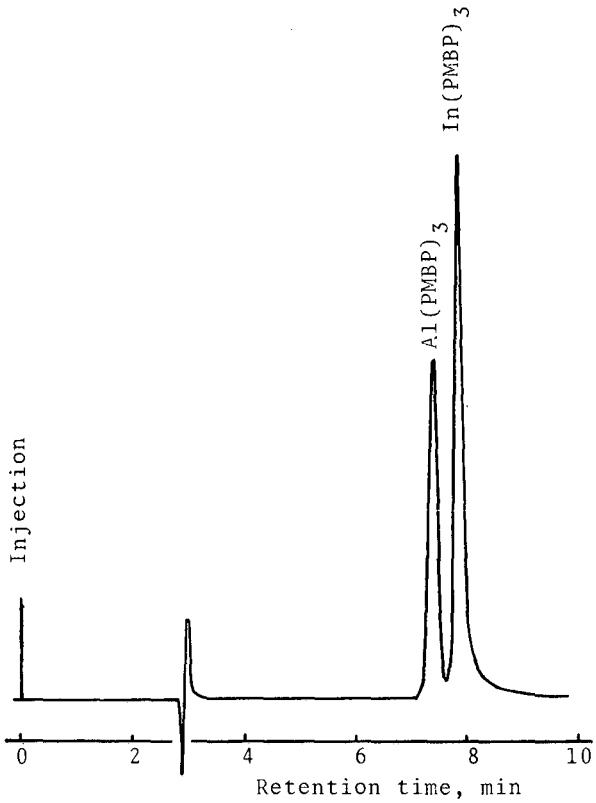

Fig. 3. Separation of $Al(PMBP)_3$ ($2.0 \cdot 10^{-4}$ *M*) and $In(PMBP)_3$ ($6 \cdot 10^{-4}$ *M*) with acetonitrile as the mobile phase. Volume injected: 5 μl.

TABLE II

ANALYTICAL RESULTS FOR ALUMINIUM AND INDIUM IN A SYNTHESIZED SAMPLE

Standard values: Al, 0.284 mg; In, 5.23 mg.

Expt. No.	*Al (mg)*	*In (mg)*
1	0.27	5.28
2	0.28	5.22
3	0.27	5.22
4	0.28	5.31
$\bar{x}$	0.28	5.26
σ	$5.8 \cdot 10^{-3}$	0.045
Recovery (%)	98.6	100.6

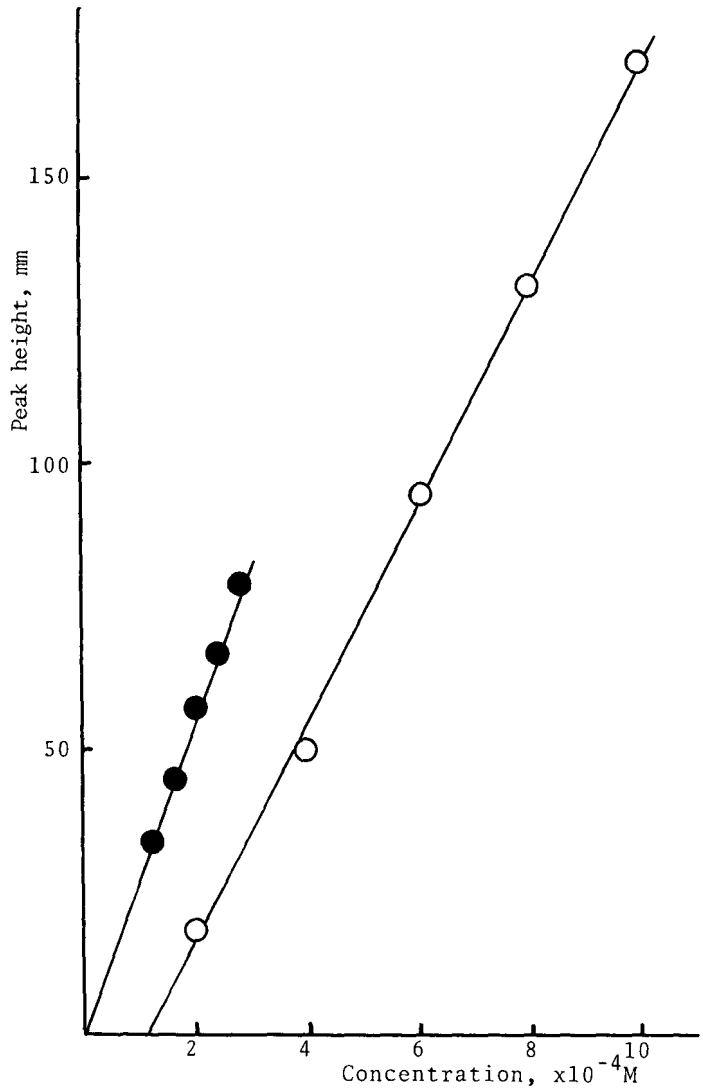

Fig. 4. Calibration graphs for $Al(PMBP)_3$ (●) and $In(PMBP)_3$ (○). Mobile phase: acetonitrile. Flow-rate: 1.0 ml/min. Volume injected: 5 μl.

An attempt was also made to separate the chelates simply by using acetonitrile as the mobile phase. A typical chromatogram is shown in Fig. 3 and it is clear that a similar result has been achieved.

The calibration graphs of peak height *versus* metal concentration injected were linear in concentration ranges 0–$2.8 \cdot 10^{-4}$ *M* for aluminium(III) and $2 \cdot 10^{-4}$–$10 \cdot 10^{-4}$ *M* for indium(III), as shown in Fig. 4. In the case of the indium chelate, the line does not pass through the origin, which may be due to the interference from trace amounts of water contained in acetonitrile, or from the silanol groups remaining in the stationary phase.

Finally, the method developed was applied to the separation and determination of aluminium and indium in synthetic mixtures. The results showed good agreement with the certified values (Table II).

CONCLUSION

The separation of aluminium(III) and indium(III) PMBP chelates has been achieved simply by using acetonitrile or by adding a smalll amount of dioxane to acetonitrile as the mobile phase. However, because of the lability of the indium(III) PMBP chelate, its peak can easily be destroyed by adding only a small amount of water to the mobile phase. It is therefore possible to determine aluminium(III) in samples containing indium(III) selectively by the proposed method.

REFERENCES

1 R.C. Gurira and P.W. Carr, *J. Chromatogr. Sci.*, 20(1982) 461.
2 A. M. Bond and Y. Nagaosa, *Anal. Chim. Acta*, 178 (1985) 197.
3 S. Ichinoki and M. Yamazaki, *Bunseki Kagaku*, 31 (1985) 319.
4 C. S. Lin and X. S. Zhang, *Analyst (London)*, 112 (1987) 1659.
5 Y. Akama, K. Sato, M. Ukaji, T. Kawata and M. Kajitani, *Polyhedron*, 4 (1985) 59.
6 A. Tong, Y. Akama and S. Tanaka, *Bull. Soc. Sea Water Sci. (Jpn.)*, 42 (1988) 59.
7 H. Noda, K. Saitoh and N. Suzuki, *J. Chromatogr.*, 435 (1988) 368.

Journal of Chromatography, 478 (1989) 415–421
Elsevier Science Publishers B.V., Amsterdam — Printed in The Netherlands

CHROM. 21 715

Note

Capillary column gas chromatography of methyl and trimethylsilyl derivatives of some naturally occurring flavonoid aglycones and other phenolics

COLIN S. CREASER*, MOHAMMED R. KOUPAI-ABYAZANI and G. RICHARD STEPHENSON
School of Chemical Sciences, University of East Anglia, Norwich NR4 7TJ (U.K.)
(First received March 14th, 1989; revised manuscript received June 13th, 1989)

Flavonoids and related phenolic compounds are widespread components in all parts of higher plants, and are important as flower pigments, growth regulators, phytoalexins and animal toxins[1,2]. They are active in the control of legume root nodulation and are implicated in the induction of *Rhizobium* nod gene expression[3–5]. In the course of investigations aimed at the identification of these plant intermediary metabolites, we have examined the application of capillary gas chromatography (GC) for the separation and identification of some flavones (I), flavanones (II), flavonols (III) and isoflavones (IV). The sensitivity and resolving power of capillary GC make this technique particularly suitable for application to natural product mixtures.

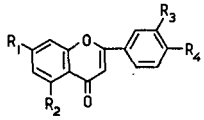

I

I_a : R_1, R_2 = OH; R_3, R_4 = H
I_b : R_1, R_2, R_4 = OH; R_3 = H
I_c : R_1, R_3, R_4 = OH; R_2 = H
I_d : R_1, R_2, R_3, R_4 = OH

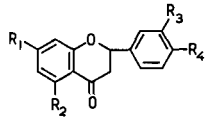

II

II_a : R_1, R_2, R_4 = OH; R_3 = H
II_b : R_1, R_2, R_3 = OH; R_4 = OMe
II_c : R_1, R_2, R_3, R_4 = OH

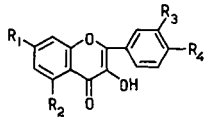

III

III_a : R_1 = OMe; R_2, R_3, R_4 = OH
III_b : R_1, R_2, R_4 = OH; R_3 = H

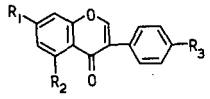

IV

IV_a : R_1, R_3 = OH; R_2 = H
IV_b : R_1, R_2, R_3 = OH

0021-9673/89/$03.50

Paper chromatography[7–9], column chromatography[7,10–12], thin-layer chromatography (TLC)[7,13,14] and spectrophotometric methods[6,7], have all previously been applied to the separation and identification of flavonoid and phenolic compounds, but these methods are time consuming or limited in separation power[15]. The methyl[16,17] and trimethylsilyl (TMS)[18–20] derivatives of these compounds have been prepared for GC analysis on non-polar packed columns. The GC of methyl and TMS derivatives of hydroxyflavones on mixed (OV-1 + OV-17) liquid phases has also been reported[21]. Hemingway and Hillis[22] applied packed column GC of TMS derivatives to the determination of dihydroquercetin, a flavanone aglycone, in wood. Nine flavonoid aglycone TMS derivatives have been separated on a GC column, packed with OV-17, by Vanhaelen and Vanhaelen-Fastré[23] who concluded that the conditions required to elute flavonoids are incompatible with the use of capillary columns.

We report for the first time the successful use of capillary column GC for the separation of methyl and TMS derivatives of flavonoid aglycones and other phenolic compounds.

EXPERIMENTAL

Flavonoid and phenolic compounds were gifts from the AFRC Institute of Plant Science Research and John Innes Institute, Norwich, U.K. These compounds were used without further purification. MethElute, 0.2 *M* trimethylanilinium hydroxide (TMAH) in anhydrous methanol, was purchased from Pierce. Pyridine, 99% (anhydrous), 1,1,1,3,3,3-hexamethyldisilazane, 98% (HMDS) and trimethylchlorosilane (TMCS) were obtained from Aldrich.

Methylation

MethElute (0.1 ml) was added to approximately 1 mg of each flavonoid or phenolic compound in a screw-cap vial. The mixture was shaken vigorously for 1 min and then maintained at 50°C for 45 min using a heating block. A 0.5–2-μl volume of the solution was used for injection into the gas chromatograph.

Trimethylsilylation

A 1–2-mg amount of each flavonoid or phenolic compound was dissolved in 0.1 ml of anhydrous pyridine in a screw-cap vial. A 0.1-ml volume of HMDS and 0.05 ml of TMCS were added. The mixture was shaken vigorously for 1 min and allowed to stand at room temperature for 30 min for phenols or heated at 60°C overnight for the flavonoids. After centrifugation 0.5 to 2 μl of supernatant solution was used for injection into the gas chromatograph.

Gas chromatography

GC analysis was carried out on a Pye Unicam series 104 gas chromatograph equipped with flame ionisation detection (FID) and a modified capillary inlet injector [SGE (UK)]. The FID output was recorded using a Phillips Analytical Chromate PC data system. Two non-polar bonded-phase fused-silica capillary columns were used, a 25 m × 0.22 mm I.D. × 0.25 μm film thickness BP-5 column [SGE (UK)] for methyl derivatives of phenolic compounds and a 50 m × 0.25 mm I.D. × 0.2 μm film thickness RSL 200 BP column (Alltech U.K.) for methyl and TMS derivatives of

flavonoids and phenolics. The linear velocity of oxygen-free nitrogen carrier gas was 17.5 cm s^{-1} for both columns and the split flow-rate was 30 ml min^{-1}. The following oven temperature programmes were used: 180°C isothermal (phenolics), 280°C isothermal and 235°C (for 2 min) to 290°C at 1°C min^{-1} (flavonoids).

RESULTS AND DISCUSSION

Volatile derivatives were readily prepared for the phenolic compounds and the di- and trihydroxyflavones (I), flavanones (II) and isoflavones (IV), by reaction with MethElute under mild conditions (45 min at 50°C). However, attempts to methylate the tetrahydroxyflavanone, eriodictyol (II_c) and the tetrahydroxyflavonols rhamnetin (III_a) and kaempferol (III_b) were unsuccessful even after heating overnight at 60°C. The only tetrahydroxyflavonoid which gave a permethylated product was the flavone, luteolin (I_d). The poor reactivity of the flavonols has been previously reported and is attributed to the presence of the 3-hydroxyl group[21]. In contrast to the unsuccessful methylation of some flavonoids, all the flavonoids investigated were successfully converted into TMS ethers by HMDS and TMCS.

The chromatograms obtained for the methyl derivatives of the trihydroxyflavanones (II_a and II_b) and the TMS ethers of the tri- and tetrahydroxyflavanones (II_a, II_b and II_c) showed a minor peak followed by a major peak after derivatisation under mild conditions (30 min at room temperature). A few small additional peaks were also observed for the methyl derivatives of the flavanones. The methylation reaction of hesperetin (II_b), a flavanone, resulted in a single chromatographic peak after heating overnight at 60°C while the two peaks observed for naringenin (II_a) remained unchanged. TMS derivatives of the di- and trihydroxyflavones (I_a, I_b, I_c), isoflavones (IV_a, IV_b) and the tetrahydroxyflavonol (III_a) prepared under mild condition (30 min at room temperature) gave a single chromatographic peak, while a seconday peak was observed for TMS derivatives of the tetrahydroxyflavone, luteolin (I_d) and the flavonol, kaempferol (III_b) under these conditions. Luteolin gave a single peak after heating overnight at 60°C while the secondary peak for kaempferol remained even after reaction overnight. Heating the TMS ethers of the flavanones (II_a, II_b and II_c) caused the growth of the minor peak in the chromatogram at the expense of the major peak. After overnight heating, the TMS ethers of the flavanones, hesperetin (II_b) and eriodictyol (II_c) showed a single peak at the retention time of the original minor peak, but, naringenin (II_a) still exhibited two peaks.

The presence of two peaks for the methyl and TMS derivatives of the flavanones (II) has been reported before in packed-column GC and was discussed in terms of an interconversion between flavanones and the corresponding chalcones[16,18]. On further investigation of the TMS derivatives of the flavanones (II) we have found that temperature, derivatisation time and capillary column injection technique all have an influence on the relative heights of the chromatographic peaks[24]. The relative intensities of the multiple peaks being particularly susceptible to small variations in capillary column injection technique. The sensitivity of some of the chromatographic results to the experimental conditions employed indicates that the derivitisation chemistry is not always straightforward. However, under the conditions reported here for the formation of TMS derivatives (60°C, overnight) characteristic and reproducible major peaks were obtained for each of the flavonoid compounds investigated.

The retention times for some typical di-, tri- and tetrahydroxyflavonoid and other phenolic derivatives with a variety of subsitution patterns are given in Tables I and II. These results demonstrate the potential of high-resolution capillary GC as an alternative to the packed-column methods for such separations reported by other workers[15–23]. The phenol derivatives were easily prepared and chromatographed as expected on the non-polar BP-5 and RSL 200 BP capillary colums. Although attempts to improve the separation of methyl and TMS derivatives of the flavonoid compounds by temperature-programmed packed-column chromatography met with little success[21], this work presents a successful separation of several flavonoid derivatives by capillary GC. Fig. 1 shows the capillary gas chromatograms obtained for mixtures of TMS or methyl derivatives of several dihydroxy-, trihydroxy- and tetrahydroxyflavonoids. Both isothermal and temperature-programming conditions were investigated to obtain the optimum separation. As expected, the retention times of the compounds in a particular group of flavonoids (flavones, flavanones and isoflavones) increase with the number of methyl or TMS ether groups. For example, the elution order for the flavones is: chrysin (5,7-dihydroxyflavone, I_a) < apigenin (4′,5,7-trihydroxyflavone, I_b), 3′,4′,7-trihydroxyflavone (I_c) < luteolin (3′,4′,5,7-tetrahydroxyflavone, I_d). When the substitution pattern of the flavonoid skeleton remains constant, the observed elution order is: flavanone, isoflavone and flavone in all the cases examined. Thus, for 4′, 5, 7-substituted flavonoids, the elution order is naringenin (flavanone), genistein (isoflavone) and apigenin (flavone). A comparison of the retention times of the flavones, chrysin (two hydroxyl groups) and apigenin (three hydroxyl groups), with those of the isoflavones, daidzein (two hydroxyl groups) and genistein (three hydroxyl groups), suggests that the increase in retention times with increasing number of hydroxyl groups is more marked with the flavones than the isoflavones for both the methyl and more particularly the TMS derivatives.

TABLE I

ADJUSTED RETENTION TIMES OF METHYL AND TRIMETHYLSILYL DERIVATIVES OF SOME NATURALLY OCCURRING PHENOLIC COMPOUNDS

GC conditions: capillary columns, 25 m × 0.22 mm I.D. BP-5 for methyl and a 50 m × 0.25 mm I.D. RSL 200 BP for TMS derivatives; column temperature, 180°C isothermal, linear velocity of nitrogen carrier gas 17.5 cm s^{-1} for both columns. s = Minor peak; m = main peak.

Compound	*Adjusted retention time (min)*	
	Methyl	*TMS*
Carboxylic acids		
Syringic acid	8.1	21.2
Sinapic acid	17(s), 26.7(m)	41.3
Aldehyde		
Syringaldehyde	5.1	9.9
Acetophenones		
Acetovanillone	4.3	7.1
Acetosyringone	7.1	13.0
4-Hydroxyacetophenone	1.9	4.1

TABLE II

ADJUSTED RETENTION TIMES OF METHYL AND TRIMETHYLSILYL DERIVATIVES OF SOME NATURALLY OCCURRING FLAVONOID AGLYCONES

GC conditions: 50 m × 0.25 mm I.D. RSL 200 BP capillary column for both methyl and TMS derivatives, temperature programme, A: 235°C (for 2 min) to 290°C at 1°C min^{-1}; B: 280°C isothermal. Other conditions as for Table I. s = Minor peak; m = main peak.

Compound	*Number of OH Groups*	*Adjusted retention time (min)*			
		Methyl		*TMS*	
		A	*B*	*A*	*B*
Flavones					
I_a Chrysin	2	21.21	6.38	18.58	5.31
I_b Apigenin	3	36.32	12.82	36.84	12.49
I_c 3',4',7-Trihydroxyflavone	3	34.53	11.32	39.40	13.63
I_d Luteolin	4	46.15	18.79	44.70	16.98
Flavanones					
II_a Naringenin	3	25.12(s), 26.00(m)	7.32(s), 7.62(m)	23.60(m), 24.06(s)	6.35(m), 6.58(s)
II_b Hesperetin	3	33.40	10.53(s), 11.07(m)	27.64	8.18
II_c Eriodictyol	4	–	–	29.16	8.28
Flavonols					
III_a Rhamnetin	4	–	–	40.89	14.32
III_b Kaempferol	4	–	–	33.37(s), 34.14(m)	10.42(s), 10.69(m)
Isoflavones					
IV_a Daidzein	2	19.56	5.27	26.23	7.71
IV_b Genistein	3	29.43	9.40	27.81	8.28

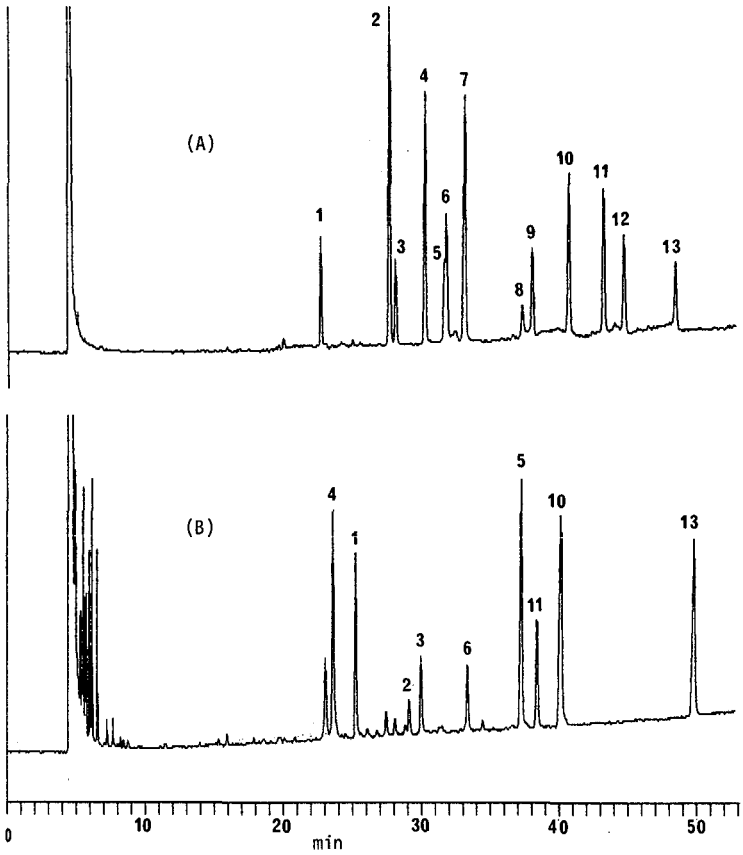

Fig. 1. Capillary gas chromatograms of trimethylsilyl (A) and methyl (B) derivatives of some naturally occurring flavonoid aglycones. GC conditions: column, bonded-phase fused-silica capillary RSL 200 BP (50 m × 0.25 mm I.D. × 0.2 μm film thickness); column temperature programme, 235°C (for 2 min) to 290°C at 1°C min^{-1}; linear velocity for nitrogen carrier gas, 17.5 cm s^{-1}. Peaks: 1 = chrysin; 2, 3 = naringenin; 4 = daidzein; 5 = hesperetin; 6 = genistein; 7 = eriodictyol; 8, 9 = kaempferol; 10 = apigenin; 11 = 3′,4′,7-trihydroxyflavone; 12 = rhamnetin; 13 = luteolin.

Capillary GC offers an attractive method for the separation and identification of flavonoid aglycones in complex mixtures. In general, TMS derivatives of the flavonoid aglycones have been found to be more suitable for GC than methyl derivatives, because of the superior derivitisation reaction with the tetrahydroxy flavonoids. The conditions for TMS derivatives reported here overcome the complexity arising from the occurrence, in certain cases, of multiple GC peaks, and provide a basis for the high-resolution separation of flavonoid aglycones.

ACKNOWLEDGEMENTS

We would like to thank Dr. A. W. B. Johnston and Dr. J. L. Firmin, from the AFRC Institute of Plant Science Research and John Innes Institute, for the gift of flavonoid and phenolic samples.

REFERENCES

1 E. E. Conn, *The Biochemistry of Plants*, Vol. 7, Academic Press, New York, 1981, p. 425.
2 J. W. McClure, in J. B. Harborne, T. J. Mabry and H. Mabry (Editors), *The Flavonoids*, Chapman & Hall, London, 1975, Ch. 18, p. 970.
3 J. L. Firmin, K. E. Wilson, L. Rossen and A. W. B. Johnston, *Nature (London)*, 324 (1986) 90.
4 G. F. Hong, J. Burn and A. W. B. Johnston, *Nucleic Acids Res.*, 15 (1987) 9677.
5 N. K. Peters, J. W. Frost and S. R. Long, *Science (Washington, D.C.)*, 233 (1986) 977.
6 L. Jurd, in T.A. Geissman (Editor), *The Chemistry of Flavonoid Compounds*, Pergamon, New York, 1962, Ch. 5, p. 107.
7 T. J. Mabry, K. R. Markham and M. B. Thomas, *The Systematic Identification of Flavonoids*, Springer, Berlin, 1970.
8 C. F. Van Sumere, H. Teuchy and F. Parmentier, *J. Chromatogr.*, 6 (1961) 481.
9 C. F. Van Sumere, F. Parmentier and H. Teuchy, *J. Chromatogr.*, 6 (1961) 484.
10 K. R. Markham and T. J. Mabry, *Photochemistry*, 7 (1968) 1197.
11 M. K. Seikel, in T. A. Geissman (Editor), *The Chemistry of Flavonoid Compounds*, Pergamon, New York, 1962, Ch. 3, p. 34.
12 K. R. Markham, in J. B. Harborne, T. J. Mabry and H. Mabry (Editors), *The Flavonoids*, Chapman & Hall, London, 1975, Ch. 1, p. 1.
13 N. A. M. Saleh, *J. Chromatogr.*, 124 (1976) 174.
14 H. Schmidtlein and K. Herrmann, *J. Chromatogr.*, 123 (1976) 385.
15 K. Vande Casteele, H. De Pooter and C. F. Van Sumere, *J. Chromatogr.*, 121 (1976) 49.
16 N. Narasimhachari and E. Von Rudloff, *Can. J. Chem.*, 40 (1962) 1123.
17 E. Von Rudloff, *J. Gas Chromatogr.*, 2 (1964) 89.
18 T. Furuya, *J. Chromatogr.*, 19 (1965) 607.
19 E. S. Keith and J. J. Powers, *J. Food Sci.*, 31 (1966) 971.
20 T. Katagi, A. Horii, Y. Oomura, H. Miyakawa, T. Kyu, Y. Ikeda and K. Isoi, *J. Chromatogr.*, 79 (1973) 45.
21 C. G. Nordström and T. Kroneld, *Acta Chem. Scand.*, 26 (1972) 2237.
22 R. W. Hemingway and W. E. Hillis, *J. Chromatogr.*, 43 (1969) 250.
23 M. Vanhaelen and R. Vanhaelen-Fastré, *J. Chromatogr.*, 187 (1980) 255.
24 C. S. Creaser, M. R. Koupai-Abyazani and G. R. Stephenson, in preparation.

Journal of Chromatography, 478 (1989) 422–428
Elsevier Science Publishers B.V., Amsterdam — Printed in The Netherlands

CHROM. 21 720

Note

Narrow-bore high-performance liquid chromatography separations of 22 sulfonamides

R. F. CROSS[a]
Varian Associates, 2700 Mitchell Drive, Walnut Creek, CA 94598 (U.S.A.)
(First received October 31st, 1988; revised manuscript received June 20th, 1989)

Sulfonamides (sulfa drugs) have been analysed successfully by thin-layer chromatography (TLC) for several decades[1], and, with the more recent development of high-speed automated TLC scanners, quantitation has been greatly aided.

However, sulfonamides have a strong absorption band (molar absorptivity *ca.* 10^4 l mol^{-1} cm^{-1}) with a maximum between 250 and 280 nm, frequently at about 270 nm. Consequently, it is not surprising that high-performance liquid chromatography (HPLC) with ultraviolet absorption detection has been investigated extensively for the analysis of these drugs. Several studies have been concerned with monitoring levels of a sulfonamide with metabolite(s) and/or a dihydrofolate reductase inhibitor (DHFR) in biological samples[2–13]. Pharmaceutical assays have also been published[14,15]. In addition, there have been some selectivity studies[14–22]. The stationary phases used include ion-exchange[17], amino[2], cyano[14,15], silica[3,5,8,9,19], octadecylsilane[4,6–8,10–13,15,17,18,20] and porous copolymers[21,22]. A complete and detailed overview can be obtained from three recent reviews[23–25].

Good separations of a wide range of sulfonamides have not been obtained.

To achieve greater resolution in HPLC it is necessary to attack the limiting feature of the technique, namely, the limited number of plates available. In this study a 3-μm reversed phase was the most efficient phase available. To maximise the sensitivity and facilitate greater column lengths, capillary columns were chosen.

As sulfonamides are frequently used in conjunction with a DHFR, those available were included in the study. DHRFs have a weak absorbance band (20–30% of the sulfonamides) in the vicinity of 270 nm. A list of sulfonamides and DHFRs was compiled from the Centre for Veterinary Medicine, U.S. Food and Drug Administration priority list of 40 drugs for analytical methods development[26] (including 9 sulfonamides), the Index of Veterinary Specialities[27] and the various investigations mentioned above.

[a] Present address: Department of Applied Chemistry, Swinburne Institute of Technology, John St., Hawthorn, Victoria 3122, Australia.

0021-9673/89/$03.50

EXPERIMENTAL

Instrumentation

A Varian (Palo Alto, CA, U.S.A.) Model 5560 high-performance liquid chromatograph and a Varian Model 9050 ultraviolet detector modified with a Varian 0.5-μl (0.5 mm pathlength) flow cell were used along with a Valco submicroliter injector (0.5 μl insert) and a Varian Model 402 Vista data system. To achieve suitably low flow-rates with the capillary column, a split-column configuration was adopted. An air oven was used (Spark Holland Model SpH99) and the micro flow meter was by Phase Sep.

Chromatography

The 30 and 60 cm long capillary analytical columns were 0.014 in. (0.35 mm) I.D. $\times$ 0.019 in. O.D. (syringe needle) stainless steel packed with MicroPak SP C_{18}-3 Phase Sep (Spherisorb) 200 m^2 g^{-1} 3-μm silica C_{18} bonded and capped with trimethylsilane (TMS) to yield 12–13% carbon. Mobile phase conditions were standardized to a flow-rate of 5.5 μl min^{-1} and reservoirs A, water; B, acetonitrile; C, acetic acid–acetonitrile–water (1:12.5:86.5) (pH 2.75). Isocratic analyses used mobile phase C.

Sigma (St. Louis, MO, U.S.A.) supplied all of the sulfonamides and DHFRs.

The 30 cm $\times$ 1 mm microbore column used contained the Micropack MCH-10 C_{18} packing: The Separations Group Vydac (IDI TP) 80 m^2 g^{-1} 10-μm silica C_{18} bonded and capped with TMS to yield 6–7% carbon. A flow-rate of 0.2 ml min^{-1} was adopted for the microbore column and the isocratic mobile phase was from reservoir C as detailed above.

A standard mixture was prepared by weighing 1-mg amounts of each of the 22 sulfonamides and 3 DHFRs, combining these, dissolving in acetonitrile–water (5:95) and filtering. A 25-ng amount of each compound was injected unless otherwise stated. All absorbances were measured at 270 nm.

RESULTS AND DISCUSSION

Preliminary runs were carried out on the 1-mm microbore column. Fig. 1 is the chromatogram of 1 ng of each of the sulfonamides (with the exception of sulfanilic acid) and the DHFRs. A comparison with the best separation previously obtained is as

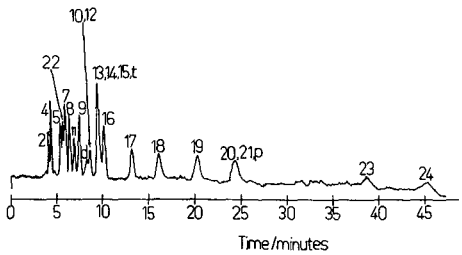

Fig. 1. Isocratic analysis of the standard mixture of 1 ng of each of 21 sulfonamides and 3 DHFRs on the 1 mm microbore column. Identifications for the sulfonamides as in Fig. 2. For the DHFRs: d = diaveridine; t = trimethoprim; p = pyrimethamine.

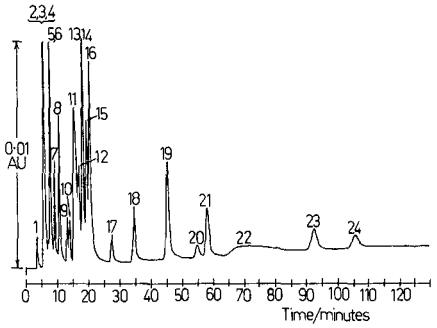

Fig. 2. Isocratic analysis of the standard mixture of 25 ng of each of the 22 sulfonamides and 3 DHFRs on the 30-cm capillary column. The order of elution was: 1 = sulfanilic acid; 2 = sulfaguanidine; 3 = sulfamoxole hydrolysis product 1; 4 = sulfanilamide; 5 = sulfacetamide; 6 = sulfamoxole hydrolysis product 2; 7 = sulfadiazine; 8 = sulfathiazole; 9 = sulfamerazine; 10 = succinyl sulfathiazole; 11 = sulfapyridine; 12 = sulfamoxole; 13 = sulfameter; 14 = sulfamethizole; 15 = sulfamethazine; 16 = sulfamethoxypyridazine; 17 = sulfachloropyridazine; 18 = sulfamethoxazole; 19 = sulfisoxazole; 20 = phthalyl sulfathiazole; 21 = sulfabenzamide; 22 = sulfisomindine; 23 = sulfadimethoxine; 24 = sulfaquinoxaline.

follows: Roos[15] (μBondapak C_{18}, 10 μm, 300 × 3.9 mm), 13 peaks separated in 50 min, peak widths 0.8 at 10 min, 1.6 at 20 min and 2.9 at 40 min. This study (Micropak MCH-10 C_{18}, 10 μm, 300 × 1.0 mm), for the analytes in common, 16 peaks separated in 50 min, peak widths 0.57 at 10 min, 1.2 at 20 min and 2.0 at 40 min. The same mobile phase was used in each case and the elution order was similar.

Fig. 2 is the chromatogram obtained for the isocratic analysis of the mixture of 22 sulfonamides and 3 DHFR standards on the 30-cm 3-μm phase. Twenty peaks were obtained in 107 min. The sulfapyridine (11) peak is broadened as was expected from its $pK_{a,1}$ and the work of Rotsch *et al.*[21]. The isomindine peak (22) is similarly broadened, badly of course due to its late elution. Sulfamoxole (12) hydrolyses in aqueous solutions to form the hydrolysis products 1 (3) and 2 (6). Phthalyl sulfathiazole (20) also slowly hydrolyses to sulfathiazole (8).

Fig. 3 is the best reproducible gradient separation obtained on the 30-cm 3-μm phase. Table I gives the details of the gradient. For the 22 sulfonamides 22 peaks were observed in 65 min but the third peak is one of the sulfamoxole hydrolysis products (3) and the second peak can be seen to be a fused pair [sulfaguanidine (2) and sulfanilamide (4)]. A considerable number of variations on the stated gradient were

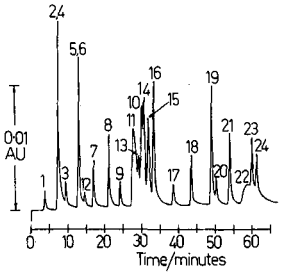

Fig. 3. Gradient analysis of the standard mixture of 25 ng of each of the 22 sulfonamides and 3 DHFRs on the 30-cm capillary column. Gradient conditions are given in Table I. Identifications as in Fig. 2.

TABLE I

GRADIENT CONDITIONS

	Time (min)				
	0	*20*	*25*	*55*	*90*
%A (water)	60	–	–	–	–
%B (acetonitrile)	–	–	–	15	60
%C (acetic acid–acetonitrile–water, 1:12.5:86.5)	40	100	100	85	40
Total acetonitrile (%)	5	12.5	12.5	25.6	65

tried, initially to improve the resolution of the 6 peaks eluted between 27 and 33 min. Weaker or stronger initial gradients and/or initial solvent strengths invariably lead to loss of resolution in this region, frequently lead to fusion of the pair eluted around 50 min [sulfisoxazole (19) and phthalyl sulfathiazole (20)] and often resulted in poorer peak shape and/or worse positioning of the highly mobile sulfisomindine peak.

The introduction of methanol at various times was universally unhelpful. In view of these experiences, very weak gradient and isocratic steps were inserted at the start in an attempt to separate sulfaguanidine and sulfanilamide without disturbing the rest of the separation. These compounds were only resolved under extremely weak conditions and then at great cost of increased analysis time and serious loss of resolution in those vulnerable areas of the chromatogram already mentioned.

Diaveridine, trimethoprim and pyrimethamine are absent from both Fig. 2 (isocratic) and Fig. 3 (gradient) in spite of being present in the standard mixture. Spiking the mixture with several times the initial 25 ng or running concentrated samples of the individual DHFRs failed to yield identifiable peaks even when run in mobile phases containing only highest purity bottled water and chromatographed under strong eluting conditions (80% acetonitrile) for extended periods. There is no change in the absorption band of trimethoprim near 270 nm between 5 and 60% acetonitrile. Irreversible adsorption on the column is indicated.

To investigate the possibility of chelation of the DHFRs with metal impurities in the silica, EDTA was added to the mobile phase. With EDTA added to reservoir C at $5 \cdot 10^{-5}$ mol l^{-1} (mobile phase as for time 0, Table I; 5% acetonitrile overall), a peak emerged at the solvent front for each of the DHFRs. In attempt to achieve retention, the EDTA concentration was decreased. When no peak was observed, a systematic study of the effect of EDTA concentration yielded the following results for trimethoprim. At sufficiently low concentrations of EDTA, there was no effect observed. At sufficiently high concentrations of EDTA, trimethoprim was eluted at the solvent front. At intermediate concentrations of EDTA, fractions of the trimethoprim were eluted, but again at the solvent front.

A further indication of the complicity of the metal impurities in the Phase Sep silica is given by the elution of the DHFRs from the alternate stationary phase prepared from the metal-free Vydac silica.

EDTA appears to play a complex role in the elution of the DHFRs from the MicroPak SP C_{18} phase. The dependence upon EDTA concentration is consistent

with a competitive chelating function, however, the amount of DHFR kept in solution by EDTA blocking some or all of the metal-binding sites seems to be prevented from interacting with the C_{18} hydrocarbon part of the stationary phase. This implies the formation of a polar, lipophobic complex. At pH 2.75, EDTA is present in aqueous solution in about equal parts of the doubly (H_2Y^{2-}) and singly charged (H_3Y^{1-}) forms with 5% of the uncharged form (H_4Y) (ref. 28). No pK_a data could be located for the DHFRs, but a consideration[29] of the tabulated effects of amino and alkyl substituents on the pK_a values of pyridine and pyridazine[30] leads to an estimate of 7.5 for the $pK_{a,2}$ of the ring nitrogens, indicating that the DHFRs have a single positive charge at pH 2.75. The formation of a DHFR–EDTA (1:1) hydrophilic complex with a single net negative charge therefore seems possible.

Fig. 4 is the chromatogram obtained for the isocratic analysis of the 22 sulfonamides on the 60-cm capillary column using the same stationary phase, mobile phase, flow-rate and sample as on the 30-cm column (Fig. 2). Twenty-one peaks were obtained for the 22 sulfonamides in 260 min. There is only one co-elution of sulfas [sulfameter (13) and sulfamethizole (14) at 44 min]. Sulfaguanidine (2) and sulfanilamide (4) at 12–13 min are now largely resolved and the crowded group of peaks centered on 17 min in Fig. 2 and 30 min in Fig. 3 (31–49 min in Fig. 4) are also further separated: sulfapyridine (11) and sulfamoxole (12) are better resolved than previously and are separated from the following three peaks to which they were previously fused.

As there was a factor of 2 difference in length, the increased resolving power of the longer column was expected to be 1.41. Table II gives the resolution (R_s) of all pairs of peaks that are at least partially separated, up to the times after which baseline separation is achieved for all compounds on both columns. Retention times were taken directly from the printout from the data station for Figs. 2 and 4, as were the peak widths at half-height for Fig. 2 (30-cm column). In the case of the 60-cm column, peak widths at the half-height were taken from chromatograms of more concentrated samples where the assignments were unambiguous. The ratios of $R_s(60)/R_s(30)$ are distributed about 1.41 as predicted and the mean of all 11 values is 1.42. Whilst this result would be self-evident for an homologous series, and perhaps for other series in which the molecular structure varied systematically, inspection of the structures[19,25,31] of the sulfonamides reveals that the R and R′ substituents vary in all of shape, size and polarity so that the 22 make up a set not dissimilar to the phenylthiohydatoin amino acids. It is impossible to predict much of the detail of the elution order simply on the basis of structure. Also, it was observed in the gradient work on the 30-cm column that either stronger or weaker conditions of elution lead to rapid deterioration of the separation in the most congested region of the chromato-

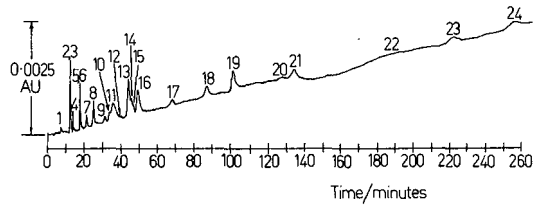

Fig. 4. Isocratic analysis of the standard mixture of 25 ng of each of the 22 sulfonamides and 3 DHFRs on the 60-cm capillary column. Identifications as in Fig. 2.

TABLE II

COMPARISON OF RESOLUTION BETWEEN 30- AND 60-cm CAPILLARY COLUMNS

t_R = Retention time (min); R_s = resolution; (30) and (60) = 30- and 60-cm columns, respectively; HP = hydrolysis product.

No.	*Drug*	$t_R(30)$	$R_s(30)$	$t_R(60)$	$R_s(60)$	$R_s(60)/R_s(30)$
1	Sulfanilic acid	3.672	2.660	7.783	5.249	1.974
2	Sulfaguanidine	5.667		12.945		
3	Sulfamoxole, HP1	5.720		12.945		
4	Sulfanilamide	5.774	2.275	13.763	3.691	1.622
5	Sulfacetamide	7.500		17.838		
6	Sulfamoxole, HP2	7.500	1.995	17.838	2.600	1.303
7	Sulfadiazine	9.202	1.571	21.287	2.345	1.493
8	Sulfathiazole	10.662	2.733	25.000	3.212	1.175
9	Sulfamerazine	13.229	0.823	31.114	1.285	1.561
10	Succinyl sulfathiazole	14.001	0.694	33.950	0.729	1.050
11	Sulfapyridine	15.424	0.650	35.722	1.442	2.218
12	Sulfamoxole	16.916	0.905	39.649	1.458	1.611
13	Sulfameter	18.100		44.249		
14	Sulfamethizole	18.140	0.916	45.860	0.260	0.284
15	Sulfamethazine	19.390	0.643	46.710	0.837	1.302
16	Sulfamethoxypyridazine	20.349		49.367		

gram, clearly indicating unsystematic behaviour for that group of analytes. A further indication of the unpredictable nature of chromatographic relationships between the sulfonamides is given by the wide range of values of the $R_s(60)/R_s(30)$ ratio: from 0.284 to 2.218. These factors highlight the advantage of longer columns and higher total available plates in difficult liquid chromatographic separations of complex mixtures. Gradient work on the 60 cm column would reduce the analysis time by at least a factor of 2 and would have good potential for the separation of all pairs of sulfonamides.

However, the attenuation in Fig. 4 is only half of that in Fig. 2. As the sample is the same but the retention is approximately doubled, we would therefore have expected peak heights and areas to have been the same. Inspection of the two chromatograms shows a huge deficiency in Fig. 4. Peak areas losses are between 80 and 96%. Doubling the exposure times of the sulfonamides —and to a fresh stationary phase— has drastically exacerbated any losses that must have occurred on the shorter column. Hence a retrospective estimate was made of losses on the 30-cm capillary column. Because the microbore and capillary work were done at the same linear flow-rate (within experimental error of the micro flow meter), the peak volumes will be proportional of the square of the column internal diameters. Hence the peak areas obtained on the 1 mm, C_{18}-10 metal-free stationary phase have been scaled-up to compare with those actually obtained on the same length, 0.35 mm, C_{18}-3 Phase Sep column. Losses are thus estimated between 46 and 73% with a mean of (59 $\pm$ 9)%.

In spite of the observed losses of sulfonamides when small amounts are chromtographed, I believe the above results will be of interest in showing the potential for better separations by the use of narrow bore columns. However, I have neither had the need nor the opportunity to investigate the above problems further.

A stationary phase of similar particle size, surface area and carbon loading but

free from metal contamination may provide a good basis for trace analysis of the sulfonamides and DHFRs.

ACKNOWLEDGEMENTS

I wish to acknowledge the generosity of Swinburne Institute of Technology for providing leave and Varian Instruments for making this short sabbatical possible at Walnut Creek. In particular, I wish to thank Terry Sheehan for making the arrangements and for some very useful discussions, Rich Simpson for providing the split-flow capillary equipment for use and for invaluable guidance, Manuel Madruga for packing the columns and to Gerry Mayer for general support.

REFERENCES

1 E. Stahl (Editor), *Thin-Layer Chromatography*, Springer, Berlin, Heidelberg, 2nd ed., 1969.
2 J. P. Sharma, E. G. Perkins and R. F. Bevill, *J. Pharm. Sci.*, 65 (1976) 1606–1608.
3 C. R. Jones and S. M. Ovenell, *J. Chromatogr.*, 163 (1979) 179–185.
4 R. Gochin, I. Kanfer and J. M. Haigh, *J. Chromatogr.*, 223 (1981) 139–145.
5 V. Ascalone, *J. Chromatogr.*, 224 (1981) 59–66.
6 S. L. Ali and H. Moller, *Fresenius' Z. Anal. Chem.*, 311 (1982) 514–516.
7 O. Spreux-Varoquaux, J. P. Chapalain, P. Cordonnier and C. Advenier, *J. Chromatogr.*, 274 (1983) 187–199.
8 M. Patthy, *J. Chromatogr.*, 275 (1983) 115–125.
9 A. Weber and K. E. Opheim, *J. Chromatogr.*, 278 (1983) 337–345.
10 J. G. Eppel and J. J. Theissen, *J. Pharm. Sci.*, 73 (1984) 1635–1638.
11 M. Edstein, *J. Chromatogr.*, 305 (1984) 502–507.
12 M. Edstein, *J. Chromatogr.*, 307 (1984) 426–431.
13 C. Midskov, *J. Chromatogr.*, 308 (1984) 217–227.
14 H. Umagat, P. F. McGarry and R. J. Tscherne, *J. Pharm. Sci.*, 68 (1979) 922–924.
15 R. W. Roos, *J. Assoc. Off. Anal. Chem.*, 64 (1981) 851–854.
16 B. L. Karger, S. C. Su, S. Marchese and B. Persson, *J. Chromatogr. Sci.*, 12 (1974) 678–683.
17 T. C. Kram, *J. Pharm. Sci.*, 61 (1975) 254–256.
18 N. H. C. Cooke, R. L. Viavattene, R. Eksteen, W. S. Wong, G. Davis and B. L. Karger, *J. Chromatogr.*, 149 (1978) 391–415.
19 P. H. Cobb and G. T. Hill, *J. Chromatogr.*, 123 (1976) 444–447.
20 D. Henry, J. H. Block, J. L. Anderson and G. R. Carlson, *J. Med. Chem.*, 19 (1976) 619–626.
21 T. D. Rotsch, R. J. Sydor and D. J. Pietrzyk, *J. Chromatogr. Sci.*, 17 (1979) 339–344.
22 D. P. Lee, *J. Chromatogr. Sci.*, 20 (1982) 203–208.
23 J. J. Kirschbaum and A. Aszalos, in A. Aszalos (Editor), *Modern Analysis of Antibiotics*, Marcel Dekker, New York, 1987, Ch. 7.
24 R. J. Heitzman, in A. G. Rico (Editor), *Drug Residues in Animals*, Academic Press, Orlando, FA, 1986, Ch. 8.
25 W. F. Rehm, K. Teelmann and E. Weidekamm, in A. G. Rico (Editor), *Drug Residues in Animals*, Academic Press, Orlando, FL, 1986, Ch. 4.
26 G. Guest, *47th Annual Meeting of the Animal Health Institute, Tuscon, AR, May 1987.*
27 *Index of Veterinary Specialities*, IMS, Crows Nest, Australia, February 1987.
28 R. A. Day and A. L. Underwood, *Quantitative Analysis*, Prentice-Hall, Englewood Cliffs, NJ, 1974.
29 P. J. Havlicek, personal communication.
30 D. D. Perrin, Dissociation Constants of Organic Bases in Aqueous Solution, Butterworths, London, 1965.
31 M. Windholz (Editor), *Merck Index*, Merck, Rahway, NJ, 10th ed., 1983.

Journal of Chromatography, 478 (1989) 429–432
Elsevier Science Publishers B.V., Amsterdam — Printed in The Netherlands

CHROM. 21 685

Note

Preparative high-performance liquid chromatography using detection by thermospray mass spectrometry

FONG-FU HSU, SUCHITRA GHOSH and WILLIAM R. SHERMAN*
Department of Psychiatry, Washington University School of Medicine, 4940 Audubon Avenue, St. Louis, MO 63110 (U.S.A.)
(First received March 16th, 1989; revised manuscript received June 13th, 1989)

There are many situations wherein preparative chromatographic procedures are made more difficult because of the lack of an on-line detector to monitor the separation process. Examples are where the substrate to be separated lacks a chromophore, in the use of UV-opaque solvents, and in situations wherein detector baseline distortions are encountered when gradient elution is used with refractive index detection. Thermospray mass spectrometry (MS)[1], in total ion current mode, is a sensitive general liquid chromatographic (LC) detector; however, it is a destructive method. With thermospray MS, the use of a chromatographic effluent splitter, made with a simple tee and a flow restrictor on one leg, and the mass spectrometer on the other leg, has limitations because the back-pressure of the thermospray vaporizer is variable with temperature, and by occlusion with use, thus causing the split ratio to vary. We describe a device that can be adjusted to changing conditions and that allows 75% to 93% of a chromatographic eluent to be collected, with the balance sent to the mass spectrometer. We illustrate its use in the separation of one of the three isomers of di-O-cyclohexylidene-1,2,3,4,5,6-[$^2H_6$]*myo*-inositol from a crude reaction mixture.

EXPERIMENTAL

The thermospray system used was a Vestec (Houston, TX, U.S.A.) Model 210 liquid chromatograph–mass spectrometer operated with a Teknivent (St. Louis, MO, U.S.A.) Vector 1 data system. Two Shimadzu (Tokyo, Japan) Model LC-6A pumps controlled by a Shimadzu Model SCL-6A gradient mixing unit were used to supply the chromatographic elution buffer. Chromatographic characterization of the system was carried out on a 25 × 0.46 cm, 5 μm particle diameter Supelcosil (Supelco, Bellefonte, PA, U.S.A.) ODS analytical column at a flow-rate of 0.8 ml/min. The separations for collection were carried out on a Beckman (Berkeley, CA, U.S.A.) Ultrasphere 5 μm, 25 × 1 cm ODS preparative-scale column operating at a flow-rate of 3 ml/min.

The construction of the effluent splitter used with the Vestec thermospray LC–MS system is shown schematically in Fig. 1. The effluent from the column is first divided with a low-dead-volume stainless-steel tee, the splitter tee in Fig. 1 (part

0021-9673/89/$03.50

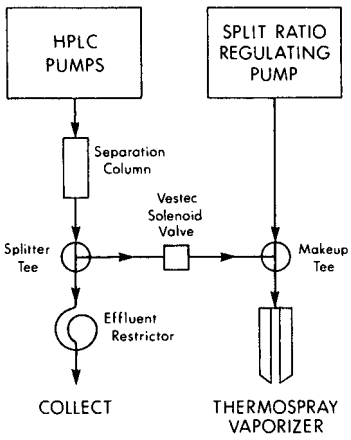

Fig. 1. Splitter flow system.

U-428, Upchurch Scientific, Oak Harbor, WA, U.S.A.), the sample-collecting leg of which was connected to an effluent restrictor made of 45 cm of 100 μm I.D. × 1/16 in O.D. stainless-steel tubing. The other leg of the tee was connected to the thermospray inlet solenoid valve. The LC–MS side of the solenoid valve was connected to a second low-dead-volume tee, the makeup tee, by 5 cm of 100 μm I.D. tubing. One leg of the second tee was supplied with water, at flow-rates that determined the split ratio, by a Waters (Milford, MA, U.S.A.) Model 9000 pump (the split ratio regulating pump in Fig. 1). The remaining leg of the makeup tee carries the minor portion of the split to the vaporizer of the thermospray mass spectrometer.

The need for a continuously monitored HPLC effluent splitter arose in the separation of the products of the acid-catalyzed reaction of deuterium-labeled *myo*-inositol with 1-ethoxycyclohexene in which three di-O-cyclohexylidene ketals are formed, the 1,2:4,5-, 1,2:3,4- and 1,2:5,6-isomers. The reaction was carried out according to Garegg *et al.*[2] except for the use of 100 mg of [$^2H_6$]*myo*-inositol (MSD Isotopes, St. Louis, MO, U.S.A.). After washing the reaction mixture to remove *p*-toluenesulfonic acid, it was taken to dryness and dissolved in methanol. The methanolic solution was chromatographed, 3 mg per run, on the large ODS column eluted with a linear gradient of 25 min duration and a flow-rate of 3 ml/min, starting with methanol–water (1:1) and ending with methanol–water (8:2).

RESULTS AND DISCUSSION

The ratio of sample diverted to collection *versus* that sent to the mass spectrometer was monitored with the column effluent pumped at 3 ml/min and the split ratio regulating pump operating at various rates. The split ratio was measured by comparing the elution of adenosine at the collection leg of the splitter with that at the mass spectrometer. The amount of adenosine diverted to the collection leg was measured at 254 nm using an LKB (Cambridge, U.K.) Ultrospec K UV–VIS spectrometer, while that entering the mass spectrometer was measured at *m/z* 268 (MH^+). At a split ratio regulating pump flow-rate of 0.1 ml/min at the makeup tee, the collected

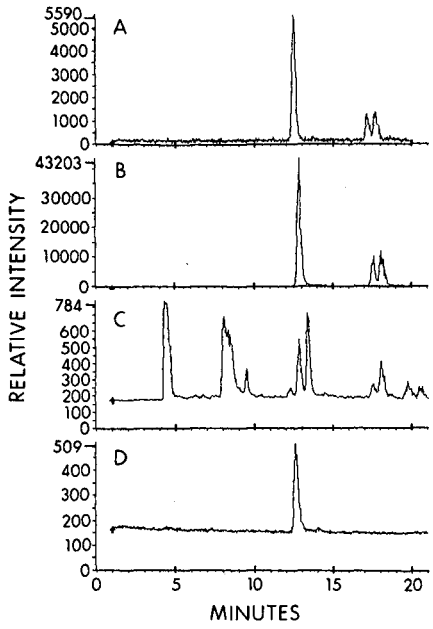

Fig. 2. HPLC separation of bis(cyclohexylidene) isomers of [$^2H_6$]*myo*-inositol from a preparative reaction with detection by MS. (A) Reconstructed mass chromatogram of *m/z* 347 (MH^+) obtained by LC–MS of the mixture on an analytical HPLC column connected directly to the LC–MS system. The peak at 12.5 min is 1,2:4,5-di-O-cyclohexylidene-[$^2H_6$]*myo*-inositol. (B) As A but with the mixture separated on the preparative-scale column and with the use of the splitter assembly. The later retention times relative to A result from the use of the large column. (C) Reconstructed total ion current mass chromatogram of the reaction mixture separated on the preparatory-scale column with the splitter. The 1,2:4,5-di-O-cyclohexylidene isomer elutes at 12.8 min barely separated from two unknowns. (D) Total ion current chromatogram of the collected and purified 1,2:4,5-di-O-cyclohexylidene-[$^2H_6$]*myo*-inositol, rechromatographed on the analytical column.

amount was 93%, which is the recovery of adenosine from the column without the splitter assembly in place (*i.e.*, 100% for pratical purposes). Intermediate flow-rates gave split ratios that bore a linear relationship to those values.

In Fig. 2A is shown the reconstructed mass chromatogram of *m/z* 347 (MH^+) from the washed reaction mixture containing the mixed isomers of the di-O-cyclohexylidene derivatives of deuterated *myo*-inositol. The peaks at *m/z* 347 are, in order of elution, the 1,2:4,5-isomer at 12.5 min, with the 1,2:3,4- and 1,2:5,6-isomers only partially resolved at 17–18 min. Fig. 2A was made using the ODS analytical column without a splitter and with a flow-rate of 0.8 ml/min. Fig. 2B is the *m/z* 347 reconstructed mass chromatogram of the same material separated on the preparative-scale ODS column with the splitter operating. As can be seen, no degradation of the separation results from the use of the preparative column or the splitter. The slightly different retention times of the analytical and preparative columns are due to differences in the chromatographic conditions. Fig. 2C is the total ion chromatogram (*i.e.*, non-selective detection) of the reaction mixture separated by the preparative-scale column showing the complexity of the mixture and the presence of an unknown eluting at 13.5 min, close to the desired 1,2:4,5-isomer. Fig. 2D is the reconstructed

total ion chromatogram of the collected 1,2:4,5-isomer, run on the analytical-size column, which is free of the unknown at 13.5 min as well as the other substances in the mixture.

In conclusion, we have described an effluent splitter suitable for use with a thermospray LC–MS system which enables the collection of non-chromophore-bearing substrates as well as gradient separations to be carried out by LC–MS. The collection of deuterium-labeled 1,2:4,5-di-O-cyclohexylidene-*myo*-inositol from a complex reaction mixture with > 90% efficiency illustrates the close match between detector and collection for the collection of closely eluting samples.

ACKNOWLEDGEMENTS

This research was supported by the following grants from the National Institutes of Health: NS-05159, AM-20579 and RR-00954.

REFERENCES

1 C. R. Blakley, J. C. Carmody and M. R. Vestal, *J. Am. Chem. Soc.*, 102 (1980) 5931.
2 P. J. Garegg, T. Iverson, R. Johanson and R. Lindberg, *Carbohydr. Res.*, 130 (1984) 322.

Journal of Chromatography, 478 (1989) 433–437
Elsevier Science Publishers B.V., Amsterdam — Printed in The Netherlands

CHROM. 21 617

Note

Separation of non-polar compounds by droplet counter-current chromatography

HOLGER MIETHING* and VOLKMAR SEGER

Free University of Berlin, Institute of Pharmacognosy and Phytochemistry, Königin-Luise-Str. 2+4, D-1000 Berlin 33 (F.R.G.)

(First received February 20th, 1989; revised manuscript received April 25th, 1989)

Droplet counter-current chromatography (DCCC) is a widely used technique for the separation or enrichment of natural compounds[1]. Because of the requirement to form droplets, especially water-containing solvent systems have been developed, although some studies with non-aqueous solvent systems have been made[2–4]. During our investigations on non-polar compounds from anise fruits we found that a non-aqueous solvent system of *n*-hexane and methanol can be used in DCCC. This binary solvent system is easy to handle and can be used even in the descending and the ascending modes. Its capability is shown by the separation of an extract from anise fruits and additionally by the separations of some synthetic mixtures containing non-polar compounds with very similar R_F values in thin-layer chromatography (TLC).

EXPERIMENTAL

Apparatus

For DCCC a DCCC-A instrument (Rikakikai, Eyela Tokyo, Japan), 300 columns (2 mm I.D.), an LKB 2138 Uvicord S detector, operating at 254 nm (range 0.2), an LKB 7000 Ultrorac fraction collector, and a two-channel recorder LKB 2210 (speed 0.2 mm/min, 100 mV) were used. For gas chromatography (GC) a Perkin-Elmer F 22 chromatograph, a fused-silica-OV-1-CB column (50 m × 0.25 mm I.D., 0.35 μm) (Chrompack, Frankfurt, F.R.G.) and a carrier gas (nitrogen) flow-rate of 1 ml/min, 1.5 bar at 60°C were employed. The temperature of the injection port was 300°C, that of the oven was 60°C raised at 6°C/min to 220°C. Flame ionization detection (FID): air flow-rate 350 ml/min, 3 bar; hydrogen flow-rate 35 ml/min, 2 bar; attenuation 8, range 1; split 1:35; recorder PE-56, 2.5 mV, 10 mm/min.

Reagents

Anethole (Merck, Darmstadt, F.R.G.), safrole (Roth, Karlsruhe, F.R.G.), anisaldehyde (Merck), myristicine (isolated from the essential oil of nutmeg), foeniculine (isolated from the essential oil of star anise fruits) and pseudoisoeugenyl-(2-methylbutyrate) (isolated from the essential oil of anise fruits) were used. The solvents *n*-hexane and methanol (Merck, pure grade) were distilled once.

0021-9673/89/$03.50

Preparation of solvent system

n-Hexane and methanol were mixed in a separating funnel and shaken intensively. After 1 h the two phases were separated and used for the DCCC experiments.

Preparation of the anise extract

Spanish anise fruits were extracted by percolation with light petroleum (b.p. 50–70°C). After evaporation of the solvent the crude extract was treated by steam distillation under atmospheric pressure. The distillate obtained was investigated by GC. A 1-μl volume of a solution of the distilled oil (1% in *n*-hexane) was injected. Retention times (min) and contents (%) were: sesquiterpenes (10.88, 1.5); anethole (11.15, 87); anisaldehyde (13.80, 0.5); pseudoisoeugenyl-(2-methylbutyrate) (23.23, 3).

Preparation of sample solutions for DCCC

A 102-mg amount of the anise extract was diluted in 18 ml of a mixture of the upper and lower phases (ratio 1:1) of the solvent system. A 50-mg amount of each pair of the synthetic mixtures (ratio 1:1) was prepared in the same manner: I, pseudoisoeugenyl 2-methylbutyrate/anisaldehyde; II, myristicine/safrole; III, foeniculine/anethole; IV, foeniculine/safrole.

DCCC separation procedures

The upper phase of the solvent system was used as the stationary phase. An 18-ml volume of sample solution was injected into the sample reservoir. The lower phase of the solvent system was used as the mobile phase.

Separation of the anise extract. The flow-rate of the mobile phase was 20 ml/h; fractions of 7 ml were collected.

Separation of the synthetic mixtures. The flow-rate was 16 ml/h; fractions of 5 ml were collected.

TLC analysis procedure

The conditions were as follows: silica gel 60 (aluminium foils, Merck); toluene; anisaldehyde–sulphuric acid reagent (0.5 ml anisaldehyde, 10 ml CH_3COOH, 85 ml methanol, 5 ml H_2SO_4), 100°C.

RESULTS

First we investigated an extract from the fruits of anise. The fractionation of this extract was carried out using the solvent system *n*-hexane–methanol and the descending mode. Fig. 1 shows the result. The extract contained mainly anisaldehyde, pseudoisoeugenyl-(2-methylbutyrate), anethole and some sesquiterpenes. By using the present solvent system the separation of all these compounds was possible. Additionally, we obtained some fractions containing a not yet identified compound (D-1). The thin-layer chromatogram (Fig. 1) of this extract yielded R_F values from 0.20 to 0.95 for the diverse compounds.

We were interested in the capability of the solvent system for the separation of compounds with more similar R_F values. For the synthetic mixtures, four pairs (I–IV)

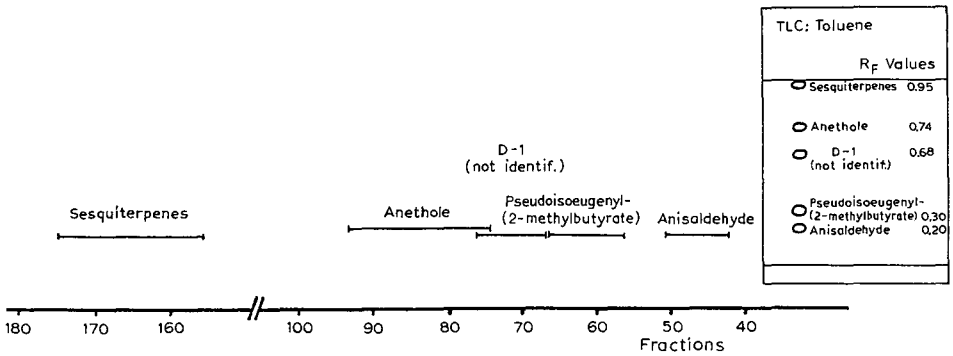

Fig. 1. DCCC elution chromatogram of an extract from the fruits of anise (102 mg) monitored at 254 nm, and TLC of this extract (silica gel, toluene).

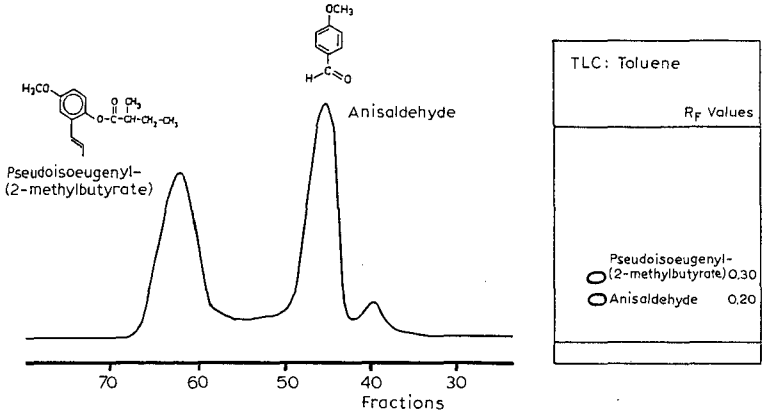

Fig. 2. DCCC elution chromatogram of a mixture of pseudoisoeugenol-(2-methylbutyrate) and anisaldehyde (50 mg, 1:1) monitored at 254 nm, and TLC of this mixture (silica gel, toluene).

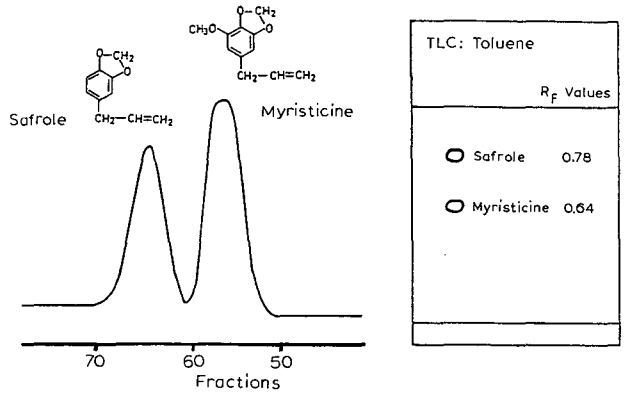

Fig. 3. DCCC elution chromatogram of a mixture of myristicine and safrole (50 mg, 1:1) monitored at 254 nm, and TLC of this mixture (silica gel, toluene).

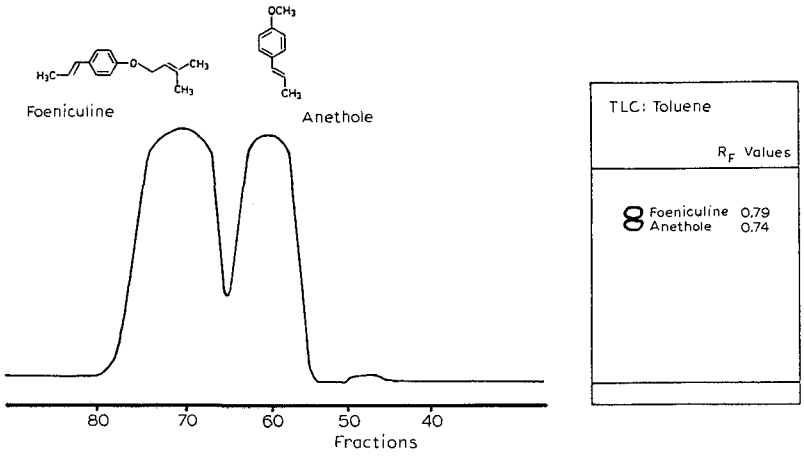

Fig. 4. DCCC elution chromatogram of a mixture of foeniculine and anethole (50 mg, 1:1) monitored at 254 nm, and TLC of this mixture (silica gel, toluene).

of non-polar substances were used, some of them (*) occurring naturally in the fruits of anise: I, pseudoisoeugenyl-(2-methylbutyrate)(*)/anisaldehyde(*); II, myristicine/safrole; III, foeniculine/anethole(*) and IV, foeniculine/safrole. From each pair, 50 mg were taken for the DCCC separations. The ratio of the compounds in each pair was 1:1. The separations of these samples were also carried out by using the solvent system *n*-hexane–methanol in the descending mode. Fig. 2 shows the result for the first pair. The differences in their R_F values in TLC with toluene as the solvent is 0.1. In the DCCC experiment a very good baseline separation was obtained. The second pair (Fig. 3) shows a greater difference in its R_F values of about 0.24. The DCCC separation was not as good as that of the first pair, but a baseline separation was achieved. The components of the third pair show very little differences in their R_F

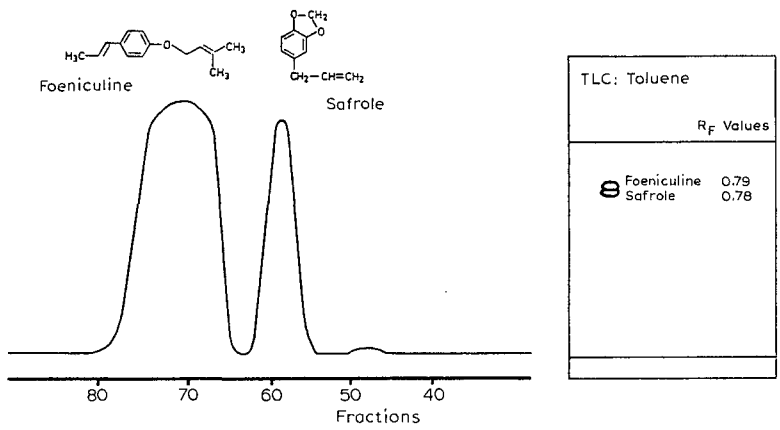

Fig. 5. DCCC elution chromatogram of a mixture of foeniculine and safrole (50 mg, 1:1) monitored at 254 nm, and TLC of this mixture (silica gel, toluene).

values. In toluene the difference is only about 0.05. However, even this pair was separated sufficiently with DCCC and the present solvent system (Fig. 4). The compounds of the fourth pair show the most similar R_F values in TLC, the difference being only about 0.01. The capability of the present solvent system was demonstrated by a sufficient separation of the components of this pair (Fig. 5).

CONCLUSIONS

A solvent system suitable in DCCC in the non-aqueous mode for the separation of non-polar compounds is presented. This binary solvent system containing *n*-hexane and methanol forms droplets sufficiently. Its capability is shown by the separation of several compounds from an extract from the fruits of anise. Some synthetic mixtures of compounds with very similar R_F values (TLC, toluene) can be separated quantitatively.

REFERENCES

1 K. Hostettmann, M. Hostettmann and A. Marston, *Nat. Prod. Rep.*, 1 (1984) 471–481.
2 H. Becker, J. Reichling and W. Ch. Hsieh, *J. Chromatogr.*, 237 (1982) 307–310.
3 B. Domon, M. Hostettmann and K. Hostettman, *J. Chromatogr.*, 246 (1982) 133–135.
4 H. Becker, *Fresenius' Z. Anal. Chem.*, 318 (1984) 225–227.

Journal of Chromatography, 478 (1989) 438–445
Elsevier Science Publishers B.V., Amsterdam — Printed in The Netherlands

CHROM. 21 686

Note

Quantitative determination of sulfanilamide in sodium sulfacetamide raw material and ophthalmic solutions by high-performance liquid chromatography

LON HALL* and VICTORIA CHADWICK

Pharmaceutical Development, Analytical Chemistry Section, Allergan Pharmaceuticals, 2525 DuPont Drive, Irvine, CA 92715 (U.S.A)

(First received April 24th, 1989; revised manuscript received June 13th, 1989)

Sodium sulfacetamide (SUL) is a sulfonamide anti-infective used in ophthalmic solutions for the treatment of conjunctivitis, corneal ulcer and other superficial ocular infections[1]. Both the British Pharmacopoeia[2] and the Deutsches Arzneibuch[3] require the determination of sulfanilamide (SFN) in SUL raw material. (The structures of SFN and SUL are shown in Fig. 1.) The current compendial method shared by both is a semi-quantitative thin-layer chromatographic (TLC) analysis. A method that is more accurate and reproducible and which can be automated is desirable.

There are a number of procedures for the analysis of sufonamides in the literature, including colorimetric[4–5], TLC[6–7], gas chromatography (GC)[9–10], electroanalytical[11], and high-performance liquid chromatography (HPLC)[10,12–22]. Only a few references addressed analysis of SFN and SUL[12,18,20]. The methods described by Penner[12] and by Elrod *et al.*[20] separate SFN from SUL but do not permit quantitation of SFN due to its very low capacity factor (k'). Jandera *et al.*[18] carried out extensive optimization studies on mobile phase composition which led to our decision to use methanol–water (1:9, v/v). However, the columns they used are not readily available. The HPLC method reported herein permits quantitative determination of SFN and SUL.

EXPERIMENTAL

Apparatus

The HPLC system consisted of the following: a 6000A pump (Waters Assoc., Milford, MA, U.S.A.); a Model 440 UV detector (Waters Assoc.); a μBondapak C_{18}

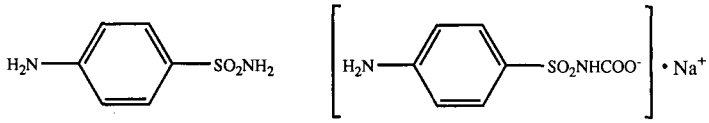

SFN SUL

Fig. 1. Chemical structures of sulfanilamide (SFN) and sodium sulfacetamide (SUL).

0021-9673/89/$03.50

column (10 μm particle size), 30 cm × 3.9 mm I.D. with USP Packing Type L1 (Waters Assoc.); a 710B WISP autoinjector (Waters Assoc.); a 3357 data collection system integrator (Hewlett-Packard, Fullerton, CA, U.S.A.); and an OmniScribe recorder (Houston Instruments, Austin, TX, U.S.A.). UV spectra analysis was performed on a HP1040M photodiode array detector (Hewlett-Packard).

Materials and reagents

Methanol (HPLC grade) was obtained from Baxter (McGraw Park, IL, U.S.A.). Acetic acid, glacial (ACS reagent grade) was obtained from Mallinckrodt (Paris, KY, U.S.A.). Water was distilled twice from an all glass apparatus then deionized and filtered through activated carbon through a Milli-Q system (Millipore, Waters Assoc.).

Standards and samples

The stock standard solution was prepared by weighing 100 ± 10 mg SFN (Aldrich, Milwaukee, WI, U.S.A.) into a 50-ml volumetric flask which was brought to volume with methanol–water (20:80, v/v) and mixed well. Then 5.0 ml of this solution was pipetted into a 100-ml volumetric flask and brought to volume with methanol–water (20:80, v/v). The working standard was prepared by pipetting 3.0 ml of 0.1 mg/ml SFN stock standard solution into a 100-ml volumetric flask and bringing to volume with methanol-water (20:80, v/v).

SUL raw material samples were prepared by weighing 250 ± 10 mg into a 25-ml volumetric flask and bringing to volume with methanol–water (20:80, v/v). Ophthalmic solutions containing 10% (w/v) SUL were prepared by pipetting 1.0 ml into a 100-ml volumetric flask. In either case, 3.0 ml of the resulting solution was pipetted into a 100-ml volumetric flask and brought to volume with methanol–water (20:80, v/v).

Reversed-phase HPLC analysis

A mobile phase of methanol-glacial acetic acid–water (10:1:89) was used. The system had the following parameters: flow-rate of 1.5 ml/min; injection volume, 90 μl; detection at 254 nm, 0.2 a.u.f.s.; analysis time, 7 min; chart speed, 0.25 cm/min. HPLC was performed at room temperature. Calculations for the samples were based on peak area measurements.

RESULTS AND DISCUSSION

Typical chromatograms of SFN standard and of SUL raw material sample are shown in Fig. 2. Samples of an ophthalmic solution placebo containing polyvinyl alcohol, benzalkonium chloride, sodium edetate and excipients but without SUL showed no interferences at the locations of either the SFN or SUL peaks (Fig. 3).

Linearity was checked from 0.000149 to 0.00596 mg/ml (equivalent to 0.05% to 2.0% degradation of the sodium sulfacetamide raw material after dilution for analysis). The correlation coefficient was 0.999 for both peak area and peak height data. For both peak area and peak height data, there were no significant differences ($\alpha = 0.05$) between the y-intercept and the origin (Figs. 4 and 5). Therefore, a single point standard was used.

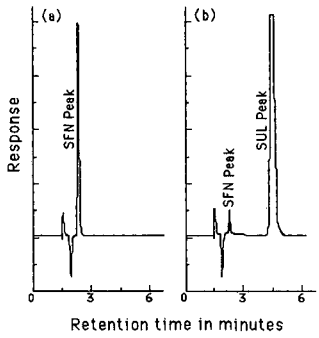

Fig. 2. Chromatograms of SFN standard (a) and SUL raw material (b).

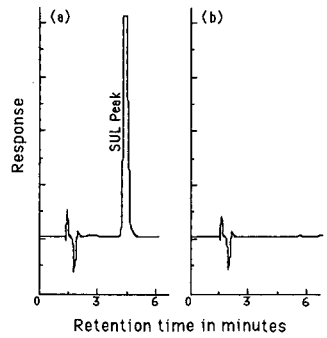

Fig. 3. Chromatograms of ophthalmic solution containing 10% SUL (a) and containing no SUL (b).

Recovery studies to show method accuracy were completed at levels equivalent to 1.014% and 0.334% degradation of SUL. Results are summarized in Table I.

The limit of SFN detection is less than $1.8 \cdot 10^{-6}$ mg/ml. An average of three peak height measurements at this concentration gave a signal-to-noise ratio greater than 10:1 with a relative standard deviation (R.S.D.) of $\pm 3.1\%$. This demonstrates

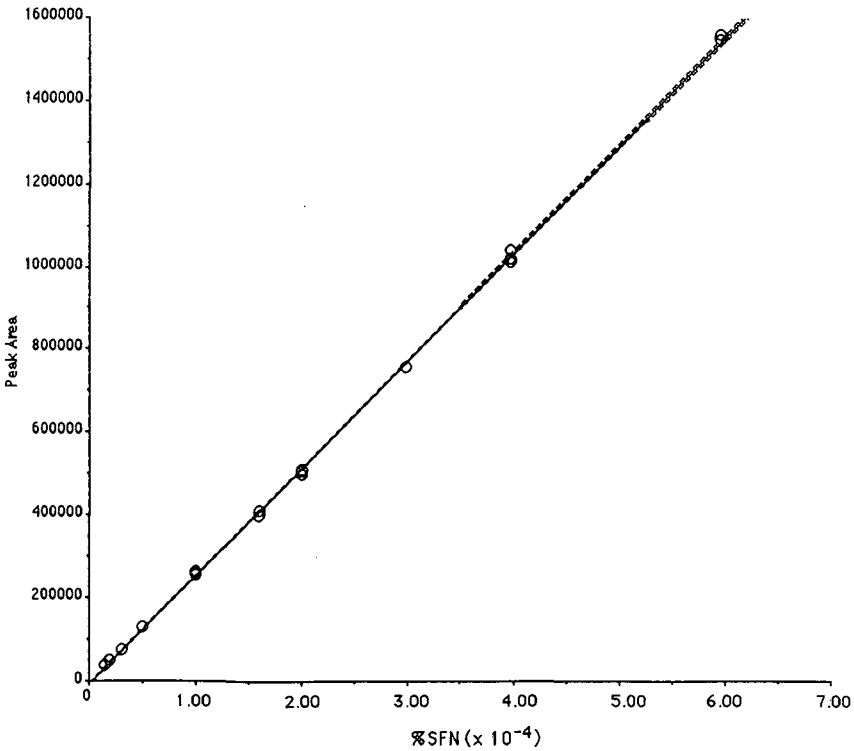

Fig. 4. Peak area linearity. —— = Calibration curve: $y = 2.59 \cdot 10^9 x - 3597$. - - - = Two-tailed 95% confidence intervals.

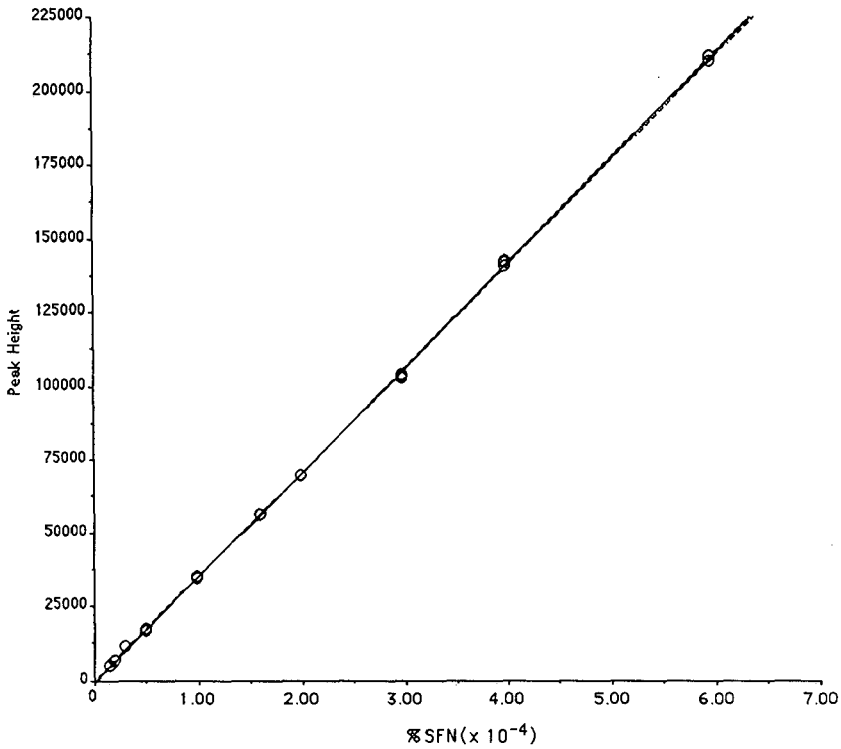

Fig. 5. Peak height linearity. —— = Calibration curve: $y = 3.53 \cdot 10^8 x - 68.4$. - - - = Two-tailed 95% confidence intervals.

excellent detectability at a level representing only 0.006% degradation of SUL raw material.

Six replicates of the 1.0% (w/v) spike used in the accuracy studies were obtained to determine single-day precision. The percent (w/w) SFN was calculated. On a second day, six replicates of the same sample were obtained to provide information concerning day-to-day precision values. Person-to-person precision experiments were run on the same sample to provide information about precision values between different analysts as well as providing feedback with respect to clarity of method write-up. Peak area data are summarized in Table II.

TABLE I

RECOVERY OF SFN FROM SPIKED SAMPLES

	1.014% (w/w)		*0.334% (w/w)*	
	Peak area	*Peak height*	*Peak area*	*Peak height*
Mean	98.7	100.4	101.7	103.4
S.D.	0.4	0.8	0.6	0.4
R.S.D. (%)	0.4	0.7	0.6	0.4
n	6	6	3	3

TABLE II

SUMMARY OF DAY-TO-DAY AND OPERATOR-TO-OPERATOR PRECISION

	Operator A		*Operator B*
	Day 1	*Day 2*	
Mean	1.001	1.013	1.019
S.D.	0.004	0.009	0.022
R.S.D. (%)	0.4	0.9	2.2
n	6	6	6

The following parameters for system suitability are suggested, based on measurements made of "suitable" and "unsuitable" chromatograms obtained in our lab (Fig. 6): no less than 4400 plates/m for SFN; k' values of 0.2 to 1.0 for SFN and $\geqslant 2$ for SUL; tailing factor $\leqslant 1.5$ for SFN; and a resolution of $\geqslant 2$ between SFN and SUL peaks[23]. It is necessary to examine chromatograms to assure a suitable system for quantitative analysis. There is a large negative signal that elutes just before the SFN peak. There must be some observable baseline between this negative signal and the forward edge of the SFN peak to assure accurate and reproducible quantitation (Fig. 6). The "suitable" separation was run on a relatively new column; the "unsuitable" separation on a very old column that had been used for other analyses for several months. All other analytical conditions were identical for both separations.

Samples of a 10% SUL ophthalmic solution were adjusted to pH 2 with 1 *M* hydrochloric acid or left untreated. All samples, treated and untreated, were stored at a temperature of 45°C for nineteen days. All samples showed loss of SUL and increase of SFN, indicating degradation of SUL to SFN via hydrolysis. The absence of other detectable peaks, and the fact that the mass balance of SUL and SFN accounted for 99.9% of the SUL originally present in undegraded samples, indicates that no significant hydrolysis of SFN to sulfanilic acid occurs. See Fig. 7 for chromatograms of these samples.

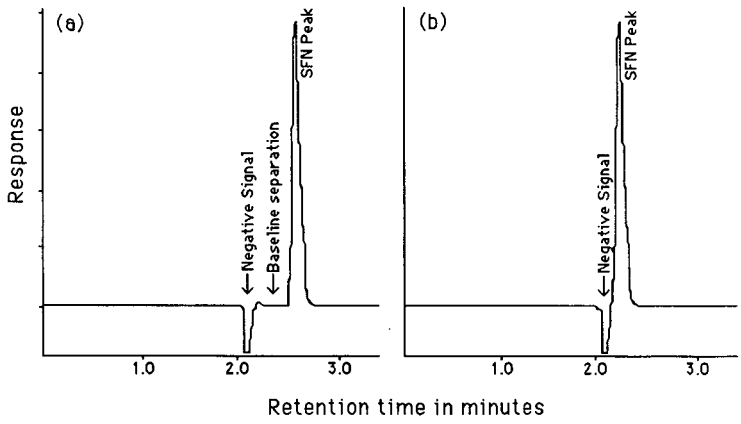

Fig. 6. Suitable (a) and unsuitable (b) retention of SFN.

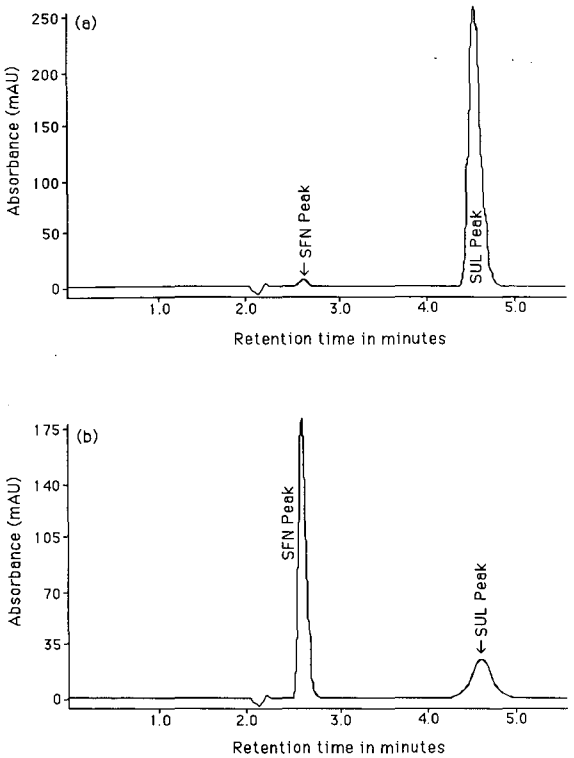

Fig. 7. Chromatograms of thermally stressed samples: untreated (a) and pH 2 (b).

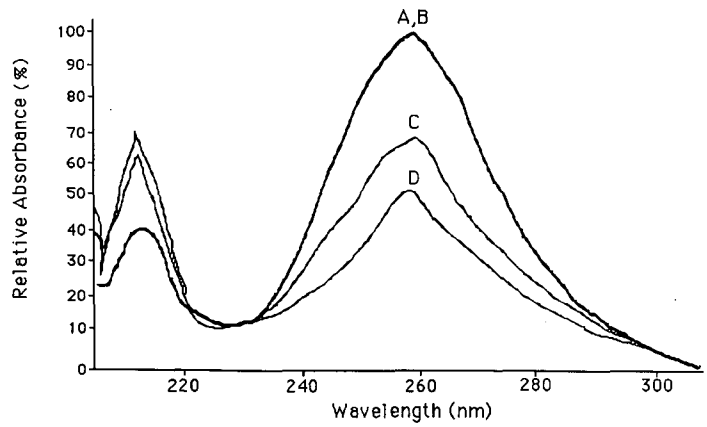

Fig. 8. UV spectra of the SFN peak in a thermally stressed, pH 2 sample. (A) Standard UV scan; (B) peak apex UV scan; (C) peak front UV scan; (D) peak tail UV scan.

TABLE III

SUMMARY OF SFN DATA FROM SIX RAW MATERIALS

Raw material	*Date of manufacturing*	*Mean SFN concentration, % (w/w) of SUL*	*R.S.D. (%)*
13690	May 1985	0.0882	6.7
15233	Aug 1985	0.0459	7.8
15562	Dec 1987	0.0881	3.1
15714	Jun 1988	0.0532	3.0
16215	Jan 1989	0.0637	3.3
IPL No. 15588-208	Feb 1988	0.0838	0.7

Each stressed sample was analyzed by the proposed analysis procedure, using a diode array detector to obtain UV spectra of all eluting peaks. Overlays of UV spectra from the front, apex and back of the eluting SFN peak in each sample demonstrated the homogeneity of this peak throughout its elution. Fig. 8 shows UV spectra from the SFN peak in the pH 2-adjusted sample compared with a SFN standard. These data demonstrate that the method is specific and stability indicating for the determination of SFN in the presence of SUL.

Six SUL raw materials supplied by Napp Chemicals were analyzed for SFN. Mean SFN concentrations for all raw materials were $\leqslant 0.09\%$ (w/w). The results are summarized in Table III as the mean of three replicates.

CONCLUSION

A simple, accurate, sensitive and precise HPLC method was developed to determine SFN in SUL raw materials and ophthalmic solutions. With this method, the SFN resulting from the degradation of SUL can be monitored accurately at concentrations representing 0.05 to 2.0% degradation of SUL.

ACKNOWLEDGEMENTS

We wish to thank Julia Petrauskas for editorial assistance.

REFERENCES

1 J. B. Walsh and A. Gold (Editors), *Physician's Desk Reference for Ophthalmology*, Medical Economics Company, Oradell, NJ, 17th ed., 1989.
2 *British Pharmacopoeia 1988*, Her Majesty's Stationery Office, London, 1988.
3 *Deutsches Arzneibuch 9*, Deutscher Apotheker Verlag, Stuttgart, 1986.
4 C. Bratton, E.K. Marshall, D. Babbutt and A.R. Hendrickson, *J. Biol. Chem.*, 128 (1939) 537.
5 D.W. Fink, R.P. Martin and J. Blodinger, *J. Pharm. Sci.*, 67 (1978) 1415.
6 P. Heizmann and P. Haefelfinger, *Fresenius' Z. Anal. Chem.*, 302 (1980) 410.
7 M. Kreisner, *Zentralbl. Veterinarmed., Reihe A*, 29 (1982) 767.
8 O. Gyllenhaal and H. Ehrsson, *J. Chromatogr.*, 107 (1975) 327.
9 N. Nose, S. Kabayashi, A. Hirose and A. Watanabe, *J. Chromatogr.*, 123 (1976) 167.
10 C. L. Holder, H. C. Thompson and M. C. Bowman, *J. Chromatogr. Sci.*, 19 (1981) 625.
11 E. Bishop and W. Hussein, *Analyst (London)*, 109 (1984) 913.
12 M. H. Penner, *J. Pharm. Sci.*, 64 (1975) 1017.

13 T. J. Goehl, L. K. Mathur, J. D. Strum, J. M. Jaffe, W. H. Pitlick, V. P. Shah, R. I. Poust and J. L. Colaizzi, *J. Pharm. Sci.*, 67 (1978) 404.
14 D. Jung and S. Øie, *Clin. Chem.*, 26 (1980) 51.
15 T. C. Kram, *J. Pharm. Sci.*, 61 (1972) 254.
16 A. Sioufi, J. Godbillon and F. Caudal, *J. Chromatogr.*, 221 (1980) 419.
17 R. Cochin, I. Kanfer and T. M. Haigh, *J. Chromatogr.*, 223 (1981) 139.
18 P. Jandera, J. Churácek and D. Szabó, *Chromatographia*, 14 (1981) 7.
19 R. Whelpton, G. Watkins and S. H. Curry, *Clin. Chem.*, 27 (1981) 1911.
20 L. Elrod, R. D. Cox and A. C. Plasz, *J. Pharm. Sci.*, 71 (1982) 161.
21 M. Patthy, *J. Chromatogr.*, 275 (1983) 115.
22 O. Spreux-Varoquaux, J. P. Chapalain, P. Cordonnier and C. Advenier, *J. Chromatogr.*, 274 (1983) 187.
23 *The United States Pharmacopeia, 21st revision (USP XXI)*, Mack Publishing Co., Easton, PA, 1985.

Journal of Chromatography, 478 (1989) 446–448
Elsevier Science Publishers B.V., Amsterdam — Printed in The Netherlands

CHROM. 21 648

Letter to the Editors

Chromatographic separation of the heavier lanthanoids on the spherical cation exchanger OSTION with α-hydroxy-α-methylbutyrate

Sir,

The common eluting agents for the chromatographic separation of lanthanoids and transplutonium elements on cation exchangers are α-hydroxycarboxylic acids, with α-hydroxyisobutyric acid (HIB) being mostly used. The first use of α-hydroxy-α-methylbutyrate (HMB) for chromatographic separation of lanthanoids was described by Nishi and Fujiwara[1] and Karol[2]. This ligand was also used for the paper chromatographic separation of lanthanoids (fission products of uranium)[3]. The separation efficiency for Am, Cm and Cf on the selected cation exchanger Ostion LG KS 0800 using HIB and HMB was measured and high values of the separation factors were found for α-hydroxy-α-methylbutyrate[4].

The purpose of this work was to determine the separation factors for heavier lanthanoids on Ostion cation exchanger under the same experimental conditions.

EXPERIMENTAL

Glass columns (15 mm × 1.4 mm I.D. and 40 mm × 2.0 mm I.D.) were packed with a spherical strongly acidic cation exchanger Ostion LG KS 0800 (NH_4^+), particle size 7–11 μm, capacity 5 mequiv. per g, 8% divinylbenzene, supplied by Chemapol, Department of Pure and Special Chemicals, Prague, Czechoslovakia.

The elution rate was 2 drops per minute and the drop volume was 25 and/or 30 μl. The elution rate was controlled by a peristaltic eluent delivery pump S-31 (Domet, Pruszków, Poland), maximum pressure 2 bar.

The eluting agent was a solution of α-hydroxy-α-methylbutyric acid, adjusted to pH 4.0 with ammonia. The acid was prepared by hydrolysis of α-hydroxy-α-methylbutyronitrile with hydrochloric acid and isolated as described earlier for α-hydroxyisobutyric acid[5]; m.p. of pure α-hydroxy-α-methylbutyric acid 72.5°C.

Radioactive indicators of high specific radioactivity, ^{177}Lu, ^{169}Yb, ^{153}Gd and ^{152}Eu, were prepared by irradiation in a nuclear reactor. The carrier-free radionuclide ^{88}Y was used together with the spallogenic carrier-free radionuclides obtained by bombardment of tantalum with protons of energy 680 MeV: ^{170}Lu, ^{171}Lu, ^{166}Yb, ^{165}Tm, ^{168}Tm, ^{160}Er, ^{160}Ho.

The γ radiation from the fractions eluted was measured by a microprocessor controlled system Gamma 8500 (Beckman). The radionuclides were identified by a gamma spectrometer equipped with an HPGe detector full width at half maximum [(FWHM) 1.8 keV, efficiecy 20%].

0021-9673/89/$03.50

RESULTS AND DISCUSSION

The values of the separation factors, α, for most of the heavier lanthanoids on OSTION LG KS 0800 at room temperature with ammonium α-hydroxy-α-methylbutyrate as eluent are given in Table I. For comparison, also shown are published values for HMB at 87°C on Dowex 50-X8[1]. The separation factors of the heavier lanthanoids are not consistent with the values published by Nishi and Fujiwara[1], while the value $\alpha = 1.50$ for the pair Yb–Tm obtained by Karol[2] corresponds to the value determined in this work. The elution peaks obtained by Nishi and Fujiwara[1] are not symmetric; in many cases the resolution of the elements achieved was not complete and the determination of α was performed with different column mass loadings. These seem to be the main reasons for the inconsistencies between the values of α, which is also accompanied by the violation of the relation between the respective α values of individual pairs of the lanthanoid elements. The chemical purity of the eluent must be considered (the published[1] m.p. of α-hydroxy-α-methylbutyric acid is 68°C). Because of the extremely high value of the α reported for the pair Lu–Yb[1], I have used for its determination, besides the radioactive indicators ^{177}Lu and ^{169}Yb of high specific activity, also spallogenic radionuclides in a carrier-free form. In both cases α was 1.3.

From the values of α determined for the heavier lanthanoids given in Table I and from published data for lighter lanthanoids[2], it is evident that for the ligand HMB the values of α are higher the lower is the atomic number.

TABLE I
SEPARATION FACTORS, α, OF HEAVIER LANTHANOIDS

Elements	*This work*[a]	*Nishi and Fujiwara*[b]
Lu–Yb	1.3	2.41
Yb–Tm	1.5	1.35
Tm–Er	1.5	1.70
Er–Ho	1.6	1.30
Y–Tb	1.6	1.95
Tb–Gd	2.3	1.89
Gd–Eu	1.5	1.38

[a] Ostion LG KS 0800, HMB pH 4.0, room temperature.
[b] Dowex 50-X8, 100–200 mesh, HMB pH 4.0, 87°C; ref. 1.

According to a comparison of the separation factors of the individual pairs of lanthanoids (see Table I, refs. 2 and 6), for the separation of heavier lanthanoids HIB is more suitable, while HMB is useful for lighter lanthanoids. This assessment has been made using data obtained under corresponding experimental conditions (quality of cation exchanger).

ACKNOWLEDGEMENTS

The author wishes to acknowledge Dr. N. A. Lebedev of the Joint Institute for

Nuclear Research, Dubna, U.S.S.R., for providing to spallogenic radionuclides. Mr. Ch. Chromec is also thanked for technical assistance.

Czechoslovak Academy of Sciences,
Institute of Nuclear Biology
and Radiochemistry, Prague
(Czechoslovakia)

M. VOBECKÝ[a]

REFERENCES

1 T. Nishi and I. Fujiwara, *J. At. Energy Soc. Jpn.*, 6 (1964) 15.
2 P. J. Karol, *J. Chromatogr.*, 79 (1973) 287.
3 C. Dubuquoy, S. Gusmini, D. Poupard and M. Verry, *J. Chromatogr.*, 57 (1971) 455.
4 M. Vobecký, *J. Radioanal. Nucl. Chem. Lett.*, 135 (1989) 165.
5 M. Vobecký and A. Maštalka, *Collect. Czech. Chem. Commun.*, 28 (1963) 709.
6 M. Vobecký, *J. Radioanal. Nucl. Chem. Lett.*, 105 (1986) 335.

(First received April 5th, 1989; revised manuscript received May 18th, 1989)

[a] Present address: Joint Institute for Nuclear Research, Laboratory of Nuclear Problems, Dubna, U.S.S.R.

Author Index

Instructions to Authors

JOURNAL OF CHROMATOGRAPHY

JOURNAL OF CHROMATOGRAPHY, BIOMEDICAL APPLICATIONS

JOURNAL OF CHROMATOGRAPHY, SYMPOSIUM VOLUMES

Elsevier Science Publishers
Desk-Editorial Office Journal of Chromatography:
Sara Burgerhartstraat 25, 1055 KV Amsterdam, The Netherlands
P.O. Box 330, 1000 AH Amsterdam, The Netherlands
Tel. 31-20-5862790
FAX 31-20-5862845
Telex 10704 espom

ELSEVIER
AMSTERDAM – OXFORD – NEW YORK – TOKYO

General

The JOURNAL OF CHROMATOGRAPHY publishes papers on all aspects of chromatography, electrophoresis and related methods. Contributions consist mainly of research papers dealing with chromatographic theory, instrumental development and their applications.

BIOMEDICAL APPLICATIONS. This section, which is under separate editorship, deals with the following aspects: developments in and applications of chromatographic and electrophoretic techniques related to clinical diagnosis or alterations during medical treatment; screening and profiling of body fluids or tissues with special reference to metabolic disorders; results from basic medical research with direct consequences in clinical practice; drug level monitoring and pharmacokinetic studies; clinical toxicology; analytical studies in occupational medicine.

SYMPOSIUM VOLUMES. This publication, which is under separate editorship, publishes proceedings of symposia on chromatography, electrophoresis and related methods.

Types of contributions

The following types of papers are published in the JOURNAL OF CHROMATOGRAPHY and the section on BIOMEDICAL APPLICATIONS: Regular research papers (full-length papers), Notes, Review articles and Letters to the Editor. Notes are usually descriptions of short investigations and reflect the same quality of research as full-length papers, but should preferably not exceed six printed pages. Letters to the Editor can comment on (parts of) previously published articles, or they can report minor technical improvements of previously published procedures; they should preferably not exceed two printed pages. Review articles are invited or proposed in writing to the Editors. An outline of the proposed review should first be forwarded to the Editors for preliminary discussion prior to preparation.

Submission of an article is understood to imply that the article is original and unpublished and is not being considered for publication elsewhere.

Upon acceptance of an article by the journal, the author(s) will be asked to transfer the copyright of the article to the publisher. This transfer will ensure the widest possible dissemination of information.

Submission of papers

Papers in English, French and German may be submitted.

Manuscripts (*four* copies are required) should be submitted to:

for the JOURNAL OF CHROMATOGRAPHY:

Editorial office
JOURNAL OF CHROMATOGRAPHY
P.O. Box 681
1000 AR Amsterdam, The Netherlands

for the BIOMEDICAL APPLICATIONS section:

Dr. K. Macek
The Editor of
JOURNAL OF CHROMATOGRAPHY,
BIOMEDICAL APPLICATIONS
P.O. Box 681
1000 AR Amsterdam, The Netherlands

Manuscripts for the SYMPOSIUM VOLUMES section (*three* copies are required) should be sent by *regular airmail (NOT by registered, special delivery or private mail services)* to:

Dr. E. Heftmann
The Editor of
JOURNAL OF CHROMATOGRAPHY,
SYMPOSIUM VOLUMES
P.O. Box 928
ORINDA, CA 94563-0818, U.S.A.

Every paper must be accompanied by a letter from the senior author, stating that he/she is submitting the paper for publication in the *Journal of Chromatography.*

Manuscripts

Manuscripts should be typed in ***double spacing*** on consecutively numbered paper of uniform size. The manuscript should be preceded by a sheet of manuscript paper carrying the title of the paper and the name and full postal address of the person to whom the proofs are to be sent. Authors of papers in French or German are requested to supply an English translation of the title of the paper. As a rule, papers should be divided into sections, headed by a caption (*e.g.* Summary, Introduction, Experimental, Results, Discussion). All illustrations, photographs, tables, etc. should be on separate sheets. **Four** copies of the complete manuscript should be submitted.

Title

The title of the paper should be concise and informative. Since titles are widely used in information retrieval systems, care should be taken to include the key words. The title should be followed by the authors' full names, academic or professional affiliations, and the address of the laboratory where the work was carried out. If the present address of an author is different from that mentioned, it should be given in a footnote. Acknowledgements of financial support are not to be made in a footnote to the title or name of the author, but should be included in the Acknowledgements at the end of the paper.

Introduction

Every paper must have a concise introduction mentioning what has been done before on the topic described, and stating clearly what is new in the paper now submitted.

Summary

Full-length papers and Review articles should have a summary of 50–100 words which clearly and briefly indicates what is new, different and significant. In the case of French or German articles an additional summary in English, headed by an English translation of the title, should also be provided. (Notes and Letters to the Editor are published without a summary.)

Illustrations

The figures should be submitted in a form suitable for reproduction, drawn in Indian ink on drawing or tracing paper. Axes of a graph should be clearly labelled. Please note that any lettering should also be in a form suitable for reproduction.Lettering (which should be kept to a minimum) and spacing on axes of graphs should be such that numbers, etc., remain legible after reduction. One original and three photocopies are required. The figures should preferably be of such a size that the same degree of reduction can be applied to all of them. Standard symbols should be used in line drawings, the following are available to the printers and can also be used in the legends:

○ ● □ ■ △ ▲ ◇ ◆

Photographs should have good contrast and intensity. Sharp, glossy photographs are required to obtain good halftones. References to the illustrations should be included in appropriate places in the text using Arabic numerals and the approximate position of the illustration should be indicated in the margin of the manuscript. Each illustration should have a legend, all the *legends* being typed (with double spacing) together on a *separate sheet.*

If structures are given in the text, the original drawings should be provided.

Coloured illustrations are reproduced at the author's expense, the cost being determined by the number of pages and by the number of colours needed.

The written permission of the author and publisher must be obtained for the use of any figure already published. Its source must be indicated in the legend.

Tables

The tables should be typed (in double spacing) on separate pages, and numbered in Roman numerals according to their sequence in the text. A brief descriptive heading should be given above each table. Below the heading the experimental conditions should be described. The layout of the tables should be given serious thought, so that the reader can grasp quickly the significance of the results.

Nomenclature, symbols and abbreviations

Widely accepted symbols, abbreviations and units (SI) should be used. If there is any doubt about a particular symbol or abbreviation, the full expression followed by the abbreviation should be given the first time it appears in the text. Abbreviations used in tables and figures should be explained in the legends. In general, the recommendations of the International Union of Pure and Applied Chemistry (I.U.P.A.C.) should be followed.

References

References should be numbered in the order in which they are cited in the text, and listed in numerical sequence on a separate sheet at the end of the article. The numbers should appear in the text at the appropriate places in square brackets. In the reference list, periodicals [1], books [2], multi-author books [3], and proceedings [4] should be cited in accordance with the following examples:

1 A.T. James and A.J.P. Martin, *Biochem. J.*, 50 (1952) 679.
2 L.R. Snyder, *Principles of Adsorption Chromatography*, Marcel Dekker, New York, 1968, p. 201.
3 R.D. Marshall and A. Neuberger, in A. Gottschalk (Editor), *Glycoproteins*, Part A, Elsevier, Amsterdam, 2nd ed., 1972, Ch. 3, p. 251.
4 R.H. Doremus, B.W. Roberts and D. Turnbull (Editors), *Growth and Preparation of Crystals, Proc. Int. Conf. Crystal Growth, Coopertown, NY, August 27–29, 1958*, Wiley, New York, 1958.

Abbreviations for the titles of journals should follow the system used by *Chemical Abstracts*. Articles not yet published should be given as "in press" (journal should be specified), "submitted for publication" (journal should be specified), "in preparation" or "personal communication". The JOURNAL OF CHROMATOGRAPHY; JOURNAL OF CHROMATOGRAPHY, BIOMEDICAL APPLICATIONS and JOURNAL OF CHROMATOGRAPHY, SYMPOSIUM VOLUMES should be cited as *J. Chromatogr.*

Dispatch

Before dispatch of the manuscript please check that the envelope contains four copies of the paper complete with references, legends and figures. One of the sets of figures must be the originals suitable for direct reproduction. Please also ensure that permission to publish has been obtained from your institute.

Proofs

One set of proofs will be sent to the author to be carefully checked for printer's errors. Corrections must be restricted to instances in which the proof is at variance with the manuscript. We shall be obliged to make a charge for all "extra corrections" at a rate in accordance with their cost to us.

To ensure fastest possible publication, proofs are sent to authors by *airmail* and must be returned to the publisher also by *airmail*. If this is not done, the article will be passed for publication with house correction only. Proofs may also be returned by FAX; the FAX number of *Journal of Chromatography* is: 31 (The Netherlands) -20 (Amsterdam) -5862845.

Reprints

Fifty reprints of Full-length papers, Notes and Letters to the Editor will be supplied free of charge. Additional reprints can be ordered by the authors. The order form containing price quotations will be sent to the authors together with the proofs of their article.

Subscription orders

Subscription orders should be sent to Elsevier Science Publishers B.V., P.O. Box 211, 1000 AE Amsterdam, The Netherlands. The JOURNAL OF CHROMATOGRAPHY and the BIOMEDICAL APPLICATIONS section can be subscribed to separately. Cumulative Author and Subject Indexes can also be ordered separately. Write to the Marketing Manager, Chemistry, at the above address for more details.

Vol. 478, No. 2

journal of chromatography news section

PRELIMINARY PROGRAM

9th International Symposium on HPLC of Protein, Peptides and Polynucleotides
Wyndham Franklin Plaza Hotel in Philadelphia, Pennsylvania USA
November 5-8, 1989

SUNDAY, NOVEMBER 5, 1989

12:00 pm **Registration**
6:00 pm **Welcome Reception**

MONDAY, NOVEMBER 6, 1989

8:00 am **Registration**
9:00 am **Welcome**

SESSION 1: COLUMN TECHNOLOGY AND SUPPORT MATERIALS

9:10 am Study of the Retention Behavior of Proteins in Ion Exchange Chromatography. Influence of the Polymeric Stationary Phase Coating—B. Sebille, C. Vidal-Madjar, R. Lemque, V. Housse-Ferrari, B. Chaufer, Univ. Paris-Val-de-Marne, Thiais, FRANCE

9:30 am Perfusion Chromatography: A New Approach to Real-Time Protein Purification—N. Afeyan, S. Fulton, N. Gordon, I. Mazsaroff, L. Varady, F. Regnier, PerSeptive Biosystems, Cambridge, MA USA

9:50 am An Evaluation of HPLC Columns for Separation of High Molecular Weight, Biologically Active Substances—M. Prange, G. Kamperman, G.P. Rozing, Hewlett-Packard, Waldbronn, W GERMANY

10:10 am Hydrophilic Interaction Chromatography: A New Mode for Peptides, Oligonucleotides, & Other Polar Solutes—A.J. Alpert, PolyLC, Columbia, MD USA

10:30 am Adsorption of Bovine Serum Albumin onto Porous and Non-Porous Poly-(Ethyleneimine) & Tentacle-Type Anion Exchangers—R. Janzen*, K.K. Unger**, W. Mueller***, *Univ. Louisville, KY USA, **Joh. Gutenberg Univ., Mainz, FRG, ***E. Merck, Darmstadt, FRG

10:50 am Break

SESSION 2: CHROMATOGRAPHIC BEHAVIOUR

11:10 am Physico-Chemical Aspects of Protein Separation by Chromatography—Cs. Horvath, Yale Univ., New Haven, CT USA

11:40 am Investigations into the Relationships Between Structure, Retention Behaviour & Biological Activity of Proteins & Their Proteolytic Cleavage Peptides on Reversed Phase High Performance Liquid Chromatography—A.W. Purcell, M. Wilce, M.I. Aguilar, M.T.W. Hearn, Monash Univ., Victoria, AUSTRALIA

12:00 pm Microenvironmental Contributions to Chromatographic Behavior of Proteins—R. Chicz, F.E. Regnier, Purdue Univ., W. Lafayette, IN USA

12:20 pm Relation of Protein Electrostatics Computations to Electrophoretic & Ion Exchange Behaviour—L. Haggerty, B.J. Yoon, A.M. Lenhoff, Univ. Delaware, Newark, DE USA

12:40 pm Break

SESSION 3: ANALYTICAL AND MICROPREPARATIVE APPLICATIONS I

2:00 pm Preparative Reversed-Phase Chromatography of Peptides: Optimization & Comparison of Sample Displacement Mode and Gradient Elution Mode—R.S. Hodges, C.T. Mant, T.W. Lorne Burke, Univ. Alberta, CANADA

2:30 pm HPLC Separation & Characterization of the a and B Chains of Alaskan Sockeye Salmon Hemoglobin—L.K. Duffy, R.A. Reynolds, J.P. Harrington, Univ. Alaska, Fairbanks, AK USA

2:50 pm Chromatographic Separation of Chymosins & Their Zymogens, Prochymosins, In Calf Rennet & R-DNA Derived Bacteria—T.-P. I, L.W. Blocker, Pfizer, Groton, CT USA

3:10 pm IMAC, A Relevant Tool for Purification of Fel.dI, a Cat Major Allergen, From a House Dust Extract—J.-P. Dandeu, J. Rabillon, M.-J. Beltrand, M. Lux, B. David, Inst. Pasteur, Paris, FRANCE

3:30 pm Isolation of Isoproteins from Monoclonal Antibodies Using Chromatofocusing—A. Jungbauer, C. Tauer, M. Purtscher, F. Steindl, A. Buchacher, H. Katinger, Univ. Agriculture/Forestry, Vienna, AUSTRIA

4:00 pm **Poster Sessions I, II, III**

6:00 pm **Reception at Art Museum**

TUESDAY, NOVEMBER 7, 1989

SESSION 4: PREPARATIVE/PROCESS CHROMATOGRAPHY

8:30 am Preparative Separation of Protein Samples by Heavily-Overloaded Reversed-Phase Gradient Elution—L.R. Snyder, J.W. Dolan, LC Resources, Lafayette, CA USA

8:50 am Preparative Chromatography of Proteins: A Design Calculation Procedure for Gradient- and Stepwise-Elution—S. Yamamoto, M. Nomura, Y. Sano, Yamaguchi Univ., Ube, JAPAN

9:10 am Membrane Separations—E.N. Lightfoot, Univ. Wisconsin, Madison, WI USA

9:40 am Break

10:00 am The Challenge of Production Scale Purification of Peptide & Protein Products—E.P. Kroeff, Eli Lilly, Indianapolis, IN USA

10:30 am New Products for Large Scale Chromatography of Proteins: Emerging Regulatory Issues & Process Considerations for Production of Biopharmaceuticals —V.K. Garg, B.A. Czuba, M.A.C. Costello, Bio-Response, Hayward, CA USA

10:50 am Purification of Recombinant Biological Products From Research to Manufacturing—D.E. Wampler, E.D. Lehman, R.D. Sitrin, Merck Sharp & Dohme Research Labs, West Point, PA USA

11:10 am Break

SESSION 5: ANALYTICAL AND MICROPREPARATIVE APPLICATIONS II

11:40 am Effect of Purification on Monoclonal Antibody Properties—T. van Sommeren, F. van Dinther, R. van den Bogaart, T. Gribnau, Organon International, Oss, THE NETHERLANDS

12:00 pm An In-Process HPLC Assay for Very Crude Samples of Recombinant Proteins Using Polymeric Supports—P.A. DePhillips, S. Yamazaki, F.S. Leu, B.C. Buckland, K. Gbewonyo, R.D. Sitrin, Merck Sharp & and Dohme Research Labs, West Point, PA USA

12:20 pm Alternative Mobile Phases in RP-HPLC—B.S. Welinder, H.H. Sorensen, Hagedorn Research Lab., Gentofte, DENMARK

12:40 pm Analysis of Native Collagen Monomers & Oligomers by Size Exclusion HPLC—R.A. Condell, V.P. Hanko, Collagen Corp., Palo Alto, CA USA

1:00 pm Break

2:30 pm **Poster Sessions IV, V, VI**

SESSION 6: STRUCTURAL STUDIES

3:30 pm Characterization of Recombinant Soluble CD4—J.J. L'Italien, Smith Kline & French Labs., King of Prussia, PA USA

3:50 pm Automated PTC Amino Acid Analysis of Carboxypeptidase/Amino-peptidase Digests & Acid Hydrolysates with a Varian 9090 Autosampler—R.S. Thoma, D.L. Crimmins, Washington Univ. School of Medicine, St. Louis, MO USA

4:10 pm Purification & Characterization of Recombinant Bovine Somatotropin (BST) Containing an Isoaspartyl Residue—M.R. Schlittler, P.C. Toren, N.R. Siegel, B.N. Violand, Monsanto, St. Louis, MO USA

4:30 pm Analysis of Tryptic Digests on Polybutadiene Coated Silica—C.A. Zezza, P. Puma, J. Hogan, Millipore Corp., Bedford, MA USA

4:50 pm New Electrophoretic Technique for Purifying Cyanogen Bromide Fragments—T.D. Schlabach, J.C. Nolan, D.G. Sheer, Applied Biosystems, Foster City, CA USA

6:00 pm **Discussion Session / Social Events**

- Column Technology and Retention Mechanisms
- Electrokinetic Techniques
- Preparative Chromatography
- Separation Strategy

WEDNESDAY, NOVEMBER 8, 1989

8:00 am **Discussion Session**
Summary of Tuesday Night's Discussion

SESSION 7: SPECIAL TOPICS

9:00 am High Performance Capillary Electrophoresis of Oligonucleotides & Proteins —B.L. Karger, A.S. Cohen, A. Guttman, R.S. Rush, D.N. Heiger, Barnett Inst., Northeastern Univ., Boston, MA USA

9:30 am HPLC & Capillary Electrophoresis: Complementary Techniques for the Analysis of Biomolecules—E.K. Hild, P.B. Harrsch, G. McIntire, B. Vanorman, J. Tomassini, Sterling Research Group, Malvern, PA USA

9:50 am Modern HPLC Approaches Coupled to Low Angle Laser Light Scattering Detection for Biopolymer Molecular Weight Determination—H.H. Stuting, I.S. Krull, S.-L. Wu, W.S. Hancock*, Barnett Inst., Northeastern Univ., Boston, MA USA, *Genentech, S. San Francisco, CA USA

10:10 am HPLC-Mass Spectrometry of Peptides, Proteins and Polynucleotides—I. Jardine, H.J. Schweingruber, M.E. Hail, C. Whitehouse*, Finnigan MAT, San Jose, CA USA, *Analytica of Branford, CT USA

10:30 am Break

SESSION 8: QUALITY CONTROL OF PROTEINS

11:00 am Method Optimization & Reproducibility for Tryptic Mapping of hGH by Capillary Zone Electrophoresis—D.S. LeFeber, R.G. Nielsen, E.C. Rickard, R.M. Riggin, Eli Lilly, Indianapolis, IN USA

11:20 am Rapid HPLC Quantitation of Purified Proteins Containing Interferring Substances—W. Schroder, M.L. Dumas, U. Klein, Miles, Berkeley, CA USA

11:40 am Simultaneous Determination of Pertussis Toxin & Filamentous Hemagglutinin Concentration by Hydroxylapatite HPLC—P.C.S. Chong, R.J. Robinson, G.E.D. Jackson, W.M. Cwyk, M.H. Klein, Connaught Centre for Biotechnology Research, Ontario, CANADA

12:00 pm Peptide Mapping of HIV Derived Polypeptides—S. Renlund, I.-M. Klintrot, Pharmacia LKB Biotechnology, Bromma, SWEDEN

12:20 pm Validation of the Determination of Somatotropin Monomer & Oligomer by Gel Permeation Chromatography (GPC)—O.F. Fox, L.M. Yunger, Pitman-Moore, Terre Haute, IN USA

12:40 pm Break

2:00 pm **Poster Sessions VII, VIII, IX**

SESSION 9: POLYNUCLEOTIDES AND CARBOHYDRATES

3:30 pm Separation Purification of a Polynucleotide Based Therapeutic—J.J. Kirkland, E.I. duPont, Wilmington, DE USA

4:00 pm Separation of Mutated Biopolymers by Temperature-Gradient Gel Electrophoresis (TGGE)—D. Riesner, G. Steger, R. Zimmat, S. Vollbach*, K. Henco, Heinrich-Heine Univ., Dusseldorf, FRG, *Diagen Inst. Molekularbiol. Diagnostik, Dusseldorf, FRG

4:20 pm Use of Liquid Chromatography for Identification & Quantitation of Products of Polymerase Chain Reaction—E.D. Katz, L.A. Haff, R. Eksteen*, Perkin-Elmer, Norwalk, CT USA, *TosoHaas, Woburn, MA USA

4:40 pm Fluorescent Labeling of Nucleotides for the Determination of DNA Adducts —D. Cecchini, A.N. El Deen, R. Giese, Northeastern Univ., Boston, MA USA

5:00 pm **Closing Remarks**

POSTER SESSION - MONDAY, NOVEMBER 6, 1989

I. COLUMN TECHNOLOGY AND SUPPORT MATERIALS

- Size Exclusion Chromatography of Biopolymers on PVP-Coated Silica—J.M. DiBussolo, N.T. Miller, PQ Corporation, Conshohocken, PA USA
- Porous Polymeric Packings for Production Purification of Proteins & Peptides, Effect of Pore & Particle Size on Performance—P.G. Cartier, K.C. Deissler, J.J. Maikner, Rohm & Haas Research Lab., Spring House, PA USA
- Effects of Sample Mass on Ion Exchange & Hydrophobic-Interaction Chromatographic Parameters for Non-Silica Based Packings—R.W. Stout, R.C. Wright, A.T. Rousak, E.I. du Pont, Wilmington, DE USA
- Mass Transfer Resistances in Ion Exchange & Dye Affinity Chromatography of Proteins—M.T.W. Hearn, A. Johnston, Monash Univ., Victoria, AUSTRALIA
- Adsorption Kinetics of Proteins onto Porous Weak Anion Exchangers—R. Janzen*, K.K. Unger**, W. Muller***, *Univ. Louisville, KY USA, **Joh. Gutenberg-Univ., Mainz, FRG, ***E. Merck, Darmstadt, FRG
- Analytical and Preparative Purifications of Proteins on a New Class of Transportable Ion-Exchange Chemistries—P. Puma, T. Evers, J. Kremsky, J. Hogan, Millipore Corp., Bedford, MA USA
- Preparative Separations Using a Unique High Speed Macroporous Resin—L.L. Lloyd, F.P. Warner, Polymer Labs., Shropshire, UNITED KINGDOM
- Effects of Chromatographic Pore Size, Particle Size & Surface Area On The Binding of IgM to BAKERBOND ABx* Under Various Operating Conditions—D.R. Nau, J.T. Baker, Phillipsburg, NJ USA
- RPLC Separation of Peptides at High pH, Using Dial-In Hydrophobicity Columns—K. Benedek, Millipore Corp., Bedford, MA USA
- Separation of High Molecular Weight Biopolymers with Novel Macroporous Ion Exchangers Prepared from Glucomannan—H. Morita, T. Tomoda, M. Yamaguchi, I. Joko, Y. Motozato*, C. Hirayama**, Kurita Water Industries, Kanagawa, JAPAN, *Kumamoto Institute of Technology, JAPAN, **Kumamoto Univ., JAPAN
- Azlactone Copolymer Beads: Supports for a Wide Variety of Chromatographic Separations of Proteins—P.L. Coleman, M.M. Walker, D.S. Milbrath, S.M. Heilmann, J.K. Rasmussen, L.R. Krepski, 3M Company, St. Paul, MN USA
- High Capacity HPLC Packing Materials for High Speed Protein Separations—N. Kitagawa, Interaction Chemicals, Mountain View, CA USA
- HPLC Composite Sorbents for Peptide & Protein Separation—E. Boschetti, P. Girot, L. Guerrier, IBF Biotechnics, Savage, MD USA
- High Performance Liquid Chromatography of Proteins with Silica-Bound Ethylenediamine-N,N-Diacetic Acid—Z. El Rassi, M.D. Bacolod, Oklahoma State Univ., Stillwater, OK USA
- Silicone Polymer-Coated Silicas for Reversed Phase Liquid Chromatography—J.T. Kowalewski, M.R. Derolf, N.T. Miller, PQ Corp., Conshohocken, PA USA
- Producing & Characterizing a New Type of Packing in Which Mixed Interactions are Tailored for HIC or RP Separations of Proteins—H. Kolesinski, V. Berry*, Globalinx, Waltham, MA, *SepCon Separations Consultants, Boston, & Salem State College, MA USA
- Purification of a Rat IgG_{2a} on a New High Performance Hydrophobic Interaction Media—D.R. Fourby, S. Scott, K.A. Schooley*, R.E. Baunio*, Bio-Rad Laboratories, Richmond, CA USA, *Immunex, Seattle, WA USA
- High Performance Affinity Chromatography for Scalable Purification of Biomolecules—R.A. Mastico, M. Cava, W.H. Madeville, D.J. Phillips, G. Vella, A. Weston, Waters, Div. of Millipore, Milford, MA USA
- Preparative Affinity Chromatography Using Group Specific Ligands—T.S. Reid, D.J. Gisch, A.M. Stancavage, Supelco, Bellefonte, PA USA
- Application of High-Performance Immunoaffinity Chromatography—K. Nakamura, K. Toyoda, Y. Kato, K. Shimura*, K.-I. Kasai*, Tosoh Corp., Yamaguchi, JAPAN, *Teikyo Univ., Kanagawa, JAPAN

- Column Performance in Immunoaffinity Chromatography with Immobilised Monoclonal Antibodies—J.D. Davies, M.T.W. Hearn, Monash Univ., Victoria, AUSTRALIA
- Affinity Chromatography Using a Novel Activated Hydrophilic Support, Azlactone-Acrylamide Copolymers—P.L. Coleman, M.M. Walker, D.S. Milbrath, S.M. Heilmann, J.K. Rasmussen, L.R. Krepski, 3M Company, St. Paul, MN USA
- Effect of Residual Silanols on Protein Recovery from Silica-Based Bonded Phases —J.M. DiBussolo, C. Xanthopolous, N.T. Miller, PQ Corp., Conshohocken, PA USA
- Utilization of Unmodified Silica Gel in the Purification of Monoclonal Antibodies —J.M. DiBussolo, K. Shields*, J. Adamovics*, PQ Corp., Conshohocken, PA USA, *Cytogen Corp., Princeton, NJ USA
- Novel Acrylate-Based Porous Polymer Packings—H. Kiniwa, M. Annaka, Y. Baba T. Ishida, H. Katoh, Mitsubishi Kasei Corp., Yokohama, JAPAN
- Investigation & Design of Stationary Phases Based on a Thermodynamic Theory— N.B. Afeyan, S.P. Fulton, I. Mazsaroff, L. Varady, F.E. Regnier*, PerSeptive Biosystems, Cambridge, MA USA, *Purdue Univ., W. Lafayette, IN USA
- Protein/Peptide Separations Alumina-Based Reversed Phase Column: UNISPHERE(R)-PBD —C. Conroy, T. Sawyer*, VIP, Blacksburg, VA USA, *Biotage, Cambridge, MA USA
- Application of Polymeric Reverse Phase Media to HPLC & Perfusion Chromatography of Proteins & Peptides—N.B. Afeyan, S.P. Fulton, I. Mazsaroff, L. Varady, G. Thevenon*, Y.B. Yang*, F.E. Regnier*, PerSeptive Biosystems, Cambridge, MA USA, Purdue Univ., W. Lafayette, IN USA

II. CHROMATOGRAPHIC BEHAVIOUR

- Comparison of Peptide Retention by a Hydrophobic Mechanism Using Several HPLC Modes of Chromatography—M.N. Schmuck, M.P. Nowlan, K.M. Gooding, Synchrom, Lafayette, IN USA
- Adsorption Behavior of Human Growth Hormone & Its N-Methionine Variant in Reversed Phase Chromatography: Red-Edge Excitation Fluorescence Spectroscopy— P. Oroszlan, G. Teshima*, S.-L. Wu*, W.S. Hancock*, B.L. Karger, Barnett Inst., Northeastern Univ., Boston, MA USA, *Genentech, S. San Francisco, CA USA
- Chromatographic Retention Behaviour, Computer Graphics Analysis & Synthetic Design of Peptide Analogues—M.T.W. Hearn, M. Wilce, A.N. Purcell, A.N. Hodder, M.I. Aguilar, Monash Univ., Victoria, AUSTRALIA
- Kinetics of Protein Adsorption on Chromatographic Surfaces—C. Tjhen, A.M. Lenhoff, Univ. Delaware, Newark, DE USA
- Effect of Temperature on the High-Performance Ion-Exchange Retention of Selected Proteins Using Non-Denaturing Elution Conditions—E.S. Parente, J.J. Buckley, D.B. Wetlaufer, Univ. Delaware, Newark, DE USA
- The Significance of Chaotropic & Kosmotropic Ions as Displacers in the High Performance Ion Exchange Chromatography of Proteins—M.T.W. Hearn, A.N. Hodder, M.I. Aguilar, Monash Univ., Victoria, AUSTRALIA
- Ion Exchange Chromatography of Recombinant Human Growth Hormone Charge Variants in Porous & Non Porous Modes—G. Teshima, S.-L. Wu, W. Henzel, W.S. Hancock, Genentech, S. San Francisco, CA USA
- Chromatographic Studies on the Refolding & Reassembly of Polypeptide Fragments Related to Growth Hormone—M. Fridman, M.I. Aguilar, M.T.W. Hearn, Monash Univ., Victoria, AUSTRALIA
- Comparative Study of Two Stationary Phases for the HPLC of Peptides & Proteins— C. Bory*, C. Gonnet**, G. Gonot+, *Hopital Debrousse, Lyon FRANCE, **Univ. Lyon, Villeurbanne, FRANCE, +Lab Fournier, Dijon, FRANCE
- Effect of Conformation on Peptide Retention Behaviour in Reversed-Phase Chromatography: a-Helical Peptides with Preferred Binding Domains are Predictable —N.N. Zhou, C.T. Mant, R.S. Hodges, Univ. Alberta, CANADA

III. ANALYTICAL AND MICROPREPARATIVE APPLICATIONS I

- Hyper Expression of High-Mobility-Group 17 (hmg17) in Rat Glucagonoma: Single Step Isolation & Sequencing—E. Nielsen, B.S. Welinder, O.D. Madsen, Hagedorn Research Lab., Gentofte, DENMARK
- An HPLC Approach to the Separation of Antiviral & Immunostimulant Fractions in Neuramide(R)—N. Miraglia, B. Rindone, G. Folchitto*, P. Amicucci**, G. Antonelli**, A. Lanfranchi+, M. Massa+, Univ. Milano, ITALY, *DIBE-Consorzio Ricerca, Roma, ITALY, **Univ. Roma, ITALY, +Univ. Pavia, ITALY
- Purification of Photosystem I-and II-Core Complexes of Synechocystis PCC 6803 by HPLC-Techniques—M. Rogner, B.A. Diner, E.I. du Pont, Wilmington, DE USA
- Immunoaffinity Chromatography of Monoclonal IgG Antibodies from Mouse Ascites—M.W. Trucksess, K.M. Williams, D.L. Shook, R.B. Raybourne, US Food & Drug Administration, Washington, DC USA
- High Performance Affinity Chromatography of Antibodies to Mammalian Immunoglobulins—T.S. McIntosh, A.R. Nazareth, Carter-Wallace, Cranbury, NJ USA
- Purification of Ferret Albumin—S.L. Nelson, J.K. Carter, B.A. Hynd, Procter & Gamble, Cincinnati, OH USA
- High-Resolution of Multiple Forms of Hexokinase from Rabbit Reticulocytes Using a TSK-GEL DEAE Toyopearl 650 S Column—V. Stocchi, L. Masat, B. Biagiarelli, G. Piccoli, L. Cucchiarini, M. Magnani, Univ. degli Studi, Urbino, ITALY
- Affinity Chromatography of Bacillus Neutral Proteases—B. van den Burg, V.G.H. Eijsink, B.K. Stulp, G. Venema, Centre of Biological Sciences, Haren, THE NETHERLANDS
- Chromatography & Generation of Specific Antisera to Synthetic Peptides from a Protective Boophilus Microplus Antigen—P.J. Sharp, B.V. McInerney, D.R. Smith, R.L. Tellam*, K.N. Rand, Biotechnology Australia, NSW, AUSTRALIA, *CSIRO, QLD, AUSTRALIA
- A Simple Purification of a Two-Functional Enzyme, Amylase-Pullulanase from the Culture Broth of B.circulans F-2 by the Successful High-Performance Size-Exclusion & Hydrophobic Interaction Column—C.-H. Kim, H. Taniguchi*, Y. Maruyama, Univ. Tokyo, JAPAN, *National Food Research Institute, JAPAN
- Measurement of Triphosphate: Nucleoside Diphosphate Phosphotransferase Activity by Anionic HPLC—G. Pulido-Cejudo, J.-M. LeClerc, Hopital Ste-Justine, Montreal, CANADA
- Purification & Characterization of Sulfur-Bound Dimetridazole & Ronidazole Derivatives by High Performance Liquid Chromatography Using Photodiode Array Detection—M. Girard, N. Mousseau, G. Carignan, S. Sved, B.A. Dawson, Health & Welfare Canada, Ottawa, CANADA
- Clean-up of Hemolysates: An Efficient Chromatographic Step for Removing Hemoglobin to Purify Red Blood Cell Enzymes at Preparative Level—V. Stocchi, L. Masat, B. Biagiarelli, G. Piccoli, L. Cucchiarini, M. Magnani, Univ. degli Studi, Urbino, ITALY

POSTER SESSION - TUESDAY, NOVEMBER 7

IV. PREPARATIVE/PROCESS CHROMATOGRAPHY

- Predicting the Performance of Gel Filtration Chromatography of Proteins—S. Yamamoto, M. Nomura*, Y. Sano, Yamaguchi Univ., Ube, JAPAN, *Tosoh Corp., Shinnanyo, JAPAN
- Scale-up Considerations for the Chromatographic Processing of Proteins & Peptides —W. Kopaciewicz, Amicon, Danvers, MA USA
- Application of Mathematical Models & Parameter Estimation Techniques to Rapid Scale-Up of Chromatographic Separations—E. Firouztale, M.R. Ladisch*, R.L. Hendrickson*, M.B. Wall**, Rohm & Haas, Spring House, PA USA, *Purdue Univ., W. Lafayette, IN USA, **Univ. Wisconsin, Madison, WI USA
- Preparative Gradient Separations of Proteins: Equal-Cut-Point Comparisons of Packing Utilities as a Function of Particle Size—J.A. Perry, T.J. Szczerba, Regis Chemical, Morton Grove, IL USA
- The Influence of Gradient Elution Parameters Upon Elution Displacement Effects in the Reversed Phase Preparative Chromatography of Proteins—G.B. Cox, B.J. Permar, L.R. Snyder, E.I. du Pont, Newark, DE USA
- An Automated System for Optimization of High Performance Process Chromatography —P.A. DePhillips, R.D. Sitrin, Merck Sharp & Dohme Res. Labs, West Point, PA USA
- Development of a Downstream Process for the Production of Anti-T Cell IgM from Hybridoma Cell Culture Supernatant—A.I. Daniels, T.N. Pettersson, A. Danielsson, K.A. Holmgren, A. Domicelj, C. Mason, Pharmacia LKB Biotechnol., Uppsala, SWEDEN
- Purification of Human Recombinant Insulin-like Growth Factors (IGF's) Using Kromasil Reverse Phase Columns—H. Wadensten, A. Ekebacke, G. Forsberg, B. Baastrup, D. Sanchez*, M. Hartmanis, KabiGen, Stockholm, SWEDEN, *Eka Nobel, Surte, SWEDEN
- Preparative Ion-exchange HPLC Purification of Major Antigens of Parietaria Judaica & Phleum Pratense Pollen Extracts & Immunochemical Evaluation of the Fractions—E. Bolzacchini, P. Di Gennaro, G. Di Gregorio, V. Madonini, B. Rindone, P. Falagiani*, I. Sondergaard**, Univ. Milano, ITALY, *Lofarma Allergeni, Milano, ITALY, **Royal Vet. & Agric. Univ., Frederiksberg, DENMARK
- High Resolution Preparative Chromatography of Proteins on Anion & Cation Exchange Resins in Scaleable Glass Columns—D.J. Phillips, D.M. Dion, H.L. Hodgdon, C. Johnson, G. Vella, W. Warren, Waters Chromatography Div., Milford, MA USA
- Techniques for the Batch Extraction of Immunoglobulins—D.R. Nau, J.T. Baker, Phillipsburg, NJ USA
- Isolation & Purification of Proteins Using the Accell Plus Preparative Ion Exchange Media in Inert Columns—D.J. Phillips, D.M. Dion, Waters Chromatography Div., Milford, MA USA
- Methods to Evaluate the Suitability of HPLC Supports for Preparative Protein Purification—K.M. Gooding, D.L. Gooding, M.P. Nowlan, M.N. Schmuck, Synchrom, Lafayette, IN USA
- Preparative Purification of Monoclonal Antibody from Ascites Fluid by Ion-Exchange HPLC—A. Nazareth, T. McIntosh, J. DiMatteo, Carter-Wallace, Cranbury, NJ USA
- Separation of Monoclonal Antibody from Ascites Fluid by High Performance Hydroxy-apatite & Hydrophobic Interaction Chromatography—Y. Yamasaki, Y. Kato, Tosoh Corp., Yamaguchi, JAPAN
- Isolation of Anti-Idiotypic Antibodies by Immobilized Immunoaffinity Chromatography Using Affinichrom Beads—T.M. Phillips, J.V. Babashak, George Washington Univ. Med. Ctr, Washington, DC USA & Kontes Sci. Glassware, Vineland, NJ USA
- Perfusion Chromatography: Application to the Purification of Antibodies—N.B. Afeyan, S.P. Fulton, N.F. Gordon, I. Mazsaroff, L. Varady, F.E. Regnier*, PerSeptive Biosystems, Cambridge, MA USA, *Purdue Univ., W. Lafayette, IN USA
- Isolation & Biochemical Characterization of a Novel Recombinant Alpha 1-Antitrypsin (AAT) Variant with Pronounced Inhibitory Activity Against Plasma-Kallikrein—R. Bischoff, L. Delatre, C. Roitsch, Transgene, Strasbourg, FRANCE

- Engineering & Economic Implications of High Speed Preparative Chromatography—N.B. Afeyan, S.P. Fulton, N.F. Gordon, I. Mazsaroff, PerSeptive Biosystems, Cambridge, MA USA
- A Synthetic Antibody Fragment as Ligand in Immunoaffinity Chromatography—G.W. Welling, T. Geurts, J.W. Drijfhout, R.A. Damhof, S. Welling-Wester, Rijksuniversiteit Groningen, THE NETHERLANDS

V. ANALYTICAL AND MICROPREPARATIVE APPLICATIONS II

- Subminute Liquid Chromatography (SMLC), An Alternative for Routine Analysis—K. Benedek, Millipore Corp., Bedford, MA USA
- Evaluation of Micro-LC Components & Their Use in Biopolymer Applications—D. Demorest, B. Black, H. Lauer, Applied Biosystems, San Jose, CA USA
- Advances in Fast Reversed-Phase Chromatography of Proteins— M.W. Dong*, J.R. Gant, B.R. Larsen, Perkin-Elmer, Norwalk, CT USA, *Genentech, S. San Francisco, CA USA
- Reverse-Phase Separation of Synthetic Phosphopeptide Isomers—L. Otvos Jr., I.A. Tangoren*, K. Wroblewski, V.M.-Y. Lee*, Wistar Institute, Philadelphia, PA USA, *Univ. Pennsylvania, Philadelphia, PA USA
- Purification by RP HPLC of Peptide Fragments from Human Milk Having Beta-casomorphin 1-8 Immunoreactivity—S. Renlund, I.-M. Klintrot, F. Nyberg, Pharmacia LKB Biotechnology, Bromma, SWEDEN
- RP-HPLC of Rat & Mouse Islet Polypeptides: A Potential Risk of Oxidation of Methionine Residues During Sample Preparation—S. Linde, J.H. Nielsen, B. Hansen, B.S. Welinder, Hagedorn Research Laboratory, Gentofte, DENMARK
- Simultaneous Quantification of Urine Levels of Orotate, Creatinine & N-benzoyl-glycine by Reverse Phase HPLC—G. Pulido-Cejudo, P. Clermont, D. Leblanc, I.A. Qureshi, Hopital Sainte-Justine, Montreal, CANADA
- Further Studies with Weak-Strong Cation Exchange Supports for Protein Purification—D.R. Nau, J.T. Baker, Phillipsburg, NJ USA
- Systematic Optimization of Protein Separations on High Performance Ion Exchange Chromatographic Media—W. Warren, N. Astephen, T. Wheat, Waters Division of Millipore, Milford, MA USA
- Further Studies on Pseudochromatofocusing with a Simple Buffer on "Complex" Ion Exchange Matrices—D.R. Nau, J.T. Baker, Phillipsburg, NJ USA
- Cytidine Deaminase Assay Using Reversed Phase HPLC—P.K. Dutta, M.S. Shanley, G.A. O'Donovan, Univ. North Texas, Denton, TX USA
- Identification of Temperature Sensitive CTP Synthetase Mutation in Bacteria by HPLC—A.J. Bailey, P.K. Dutta, R.A. Kelln, G.A. O'Donovan, Univ. North Texas, Denton, TX USA
- Characterization of the Vinca Moiety of KS1/4-DAVLB Hydrazide Conjugate—A.M. Maloney, E.C. Rickard, M.J. Pikal, M.L. Roy, Eli Lilly, Indianapolis, IN USA
- Proglucagon Processing—E. Nielsen, J.J. Holst, B.S. Welinder, O.D. Madsen—Hagedorn Research Laboratory, Gentofte, DENMARK
- Quantitation of Protein Biopharmaceuticals: Determination of Absorptivity Coefficient for Immunoglobulins & Their Derivatives—C.E. Coonley, P.-H. Lai, Centocor, Malvern, PA USA
- Affinity Constants of Monoclonal Antibodies: Determination & Interpretation, Based on Primarily Non-labeled Reagents & HPSEC—R.V. Erp, T.V. Sommeren, T. Gribnau, Organon International, Oss, THE NETHERLANDS
- Purification of Mouse Monoclonal Antibodies Using Protein G Affinity Chromatography—K.J. Reis, M.W. Hanley, Genex Corp., Gaithersburg, MD USA
- Further Studies on the Chromatographic Analysis & Characterization of Antibodies & Antibody Preparations—D.R. Nau, J.T. Baker, Phillipsburg, NJ USA
- A Novel Method of Simultaneous Identification of Estrogen & Progesterone Receptors by HPLC Using a Double Isotope Assay—P. Folk, J. Dong, J.L. Wittliff, Univ. Louisville, KY USA
- Analysis of N-2-Hydroxyethylpiperazine-N'-2-ethanesulfonic Acid in Protein Preparations by Anion Exchange HPLC—N.C.LeDonne, P.-H. Lai, Centocor, Malvern, PA USA
- Investigations on Cleavage Kinetics of Side Chain Protected Arginine Derivatives Using a Sophisticated Post Column Reaction Detector—G. Grubler, F. Gutjahr, W. Voelter, H. Bauer, Univ. Tubingen, FRG

VI. STRUCTURAL STUDIES

- High-Resolution Analysis of Protein Hydrolysates & Hydrolysis By-Products by the Use of HPLC & Automated Pre-Column Derivatization—H. Godel, P. Seitz, R. Schuster, Hewlett-Packard, Waldbronn, WEST GERMANY
- Automated FMOC Precolumn Derivatization of Physiological Amino Acids: Development of Alternative Elution Conditions, Using Column Switching Techniques & Application—A.G. Mayer, T.L. Sheehan, C.P. Mulvihill, Varian Instrument Group, Walnut Creek, CA USA
- Plasma Amino Acid Profile in Patients Undergoing Liver Transplantation: An HPLC Study Based on Pre-Column Derivatization of OPA with Amino Acid—A.R. Qureshi, G.A. Qureshi, B.G. Ericzon, J. Berstrom, C.G. Groth, Huddinge Univ. Hospital, Stockholm, SWEDEN
- Resolution of Amino Acid Enantiomers by HPLC Using Automated Pre-Column-Derivatization with Chiral Reagents—H. Goetz, Hewlett-Packard, Waldbronn, FRG
- Automated Pre-Column Derivatization with PITC & Analysis of Free Amino Acids from Hydrolyzed Proteins & Peptides & Physiologic Samples—M. Meys, T. Wheat, S.A. Cohen, Waters Chromatography Division, Milford, MA USA
- Amino Acid Analysis of Tryptic Fragments Using DABS Derivatization—D.N. Kelner, J.W. Mayhew, Beckman Instruments, San Ramon, CA USA
- Nitrophenylisothiocyanate: A New Reagent for Amino Acid Analysis—S.A. Cohen, Waters Chromatography Division, Milford, MA USA
- Determination of Tryptophan, Catecholamines & Their Metabolites in Cerebrospinal Fluid in Patients with Neurological Diseases by Ion-Pair HPLC with EC Detection —G.A. Qureshi, S. Baig, Huddinge Univ. Hospital, Stockholm, SWEDEN
- Reverse-Phase & Ion-Exchange HPLC in Separating Small Hydrophilic Fragments from Human Serum Albumin & Its Charged Variants—P. Iadarola, L. Minchiotti, M. Galliano, M.L. Meloni, M. Stoppini, M.C. Zapponi, G. Ferri, Univ. Pavia, ITALY
- Structural Characterization of Apolipoproteins from Chicken Plasma—E.M. Brown, H.J. Dower, H. Le, US Department of Agriculture, Philadelphia, PA USA
- Glycation-Induced Heterogeneity of Human Serum Albumin Analysed by RP-HPLC in Formic Acid Containing Solvent—P. Vidal, E. Nielsen, B.S. Welinder, Hagedorn Research Laboratory, Gentofte, DENMARK
- Racemization Analyses of Synthetic Peptides by Chromatography with Pre-Column Derivatization—G. Szokan, G. Mezo, Z. Majer, I. Schon, O. Nyeki, Eotvos Univ., Budapest, HUNGARY
- Direct Detection of Aromatic, Cysteine, Iodinated Tyrosyl & Iodothyronine-Containing Peptides—J. Escribano, M. Asuncion, M. Arjonilla, J. Miguel, L. Lamas, E. Mendez, Inst. Investigaciones Biomedicas, Madrid, SPAIN
- Optimization of Peptide HPLC Separations with Alternative Mobile & Stationary Phases—P.M. Young, T.E. Wheat, Waters Division of Millipore, Milford, MA USA
- Factors Influencing the Performance of Peptide Mapping by Reversed-Phase Liquid Chromatography—M.W. Dong, A.D. Tran*, Perkin-Elmer, Norwalk, CT USA, *Ortho Pharmaceutical, Raritan, NJ USA
- Fraction Capacity, Mobile-Stationary Phase Transfer Effects, & Selectivity in Fingerprint Peptide Mapping on Polymeric Styrene-Divinyl Benzene (PLRP-S)— J.K. Swadesh, Polymer Laboratories, Amherst, MA USA
- Characterization of Glycoproteins by HPLC: Peptide Mapping & Analysis of Site Specific Glycosylation—G. Vella, C. Phoebe, N. Astephen, P. Young, Millipore Corp., Milford, MA USA
- Chemical Characterization of Recombinant Human Insulin-like Growth Factor I (IGF-1)—V.T. Ling, M. Eng, E. Canova-Davis, Genentech, S. San Francisco, CA USA
- Detection of N-terminal Processing of Recombinant Proteins by Electroblotting or High-Performance Liquid Chromatography Followed by Sequence Analysis— P.R. Fausset, H.S. Lu, Amgen, Thousand Oaks, CA USA
- An Evaluation of Microwave Technology for the Hydrolysis of Proteins— C. Woodward, L. Gilman*, Hewlett-Packard and *CEM Corp., Avondale, PA USA

POSTER SESSION - WEDNESDAY, NOVEMBER 8

VII. SPECIAL TOPICS

- An Assessment of Separation Methods for High Molecular Weight Biological Substances—G.P. Rozing, Hewlett-Packard, Waldbronn, WEST GERMANY
- Analysis of High M.W. Biopolymers at Intermediate pH's Using Capillary Electrophoresis—J.E. Wiktorowicz, J.C. Colburn, H.H. Lauer, Applied Biosystems, San Jose, CA USA
- Construction & Evaluation of Disposable Microbore Columns Made from Glass Capillary Tubes—C.D. Southan, Smith Kline & French Res., Herts, UNITED KINGDOM
- On-line Molecular Weight Detection for Protein Chromatography—P. Claes, P. Griew, P. Vardy, S. Fowell, A. Kenney, Oros Instruments, Berks, UNITED KINGDOM
- Binding of Sodium Dodecyl Sulfate (SDS) to Proteins by High Performance Gel Filtration, Monitored by Continuous Flow Scintillation Counting—M. Wallsten, Q. Yang, P. Lundahl, Univ. Uppsala, SWEDEN
- Rapid Protein Matrix Reduction by Hydrophobic Interaction-Based Solid Phase Extraction Method—D.J. Gisch, L.A. Nolan, R.C. Parry, Supelco, Bellefonte, PA USA
- Effect of Ligand Density in Vesicle-Surface Chromatography & Attempts at the Use of Small-bead Gels—Q. Yang, M. Wallsten, P. Lundahl, Univ. Uppsala, SWEDEN

VIII. QUALITY CONTROL OF PROTEINS

- Biopolymer Separation by Hydrophobic Interaction Chromatography & On-line Monitoring with UV Photodiode Array Spectroscopy—S.-L. Wu, J. Cacia, W.S. Hancock, Genentech, S. San Francisco, CA USA
- Estimation of Residual Yeast Protein in Recombinant Hepatitis B Vaccine—R. Mancinelli, W. Miller, A. Wolfe, W. Hurni, J. McCauley, Merck Sharp & Dohme Research Labs, West Point, PA USA
- HPRB: A New Approach in Determining Biological Activity of Recombinant Proteins —R.H. Carlson, B.R. Larsen, R.D. Hershberg, R.L. Garnick, C.P. du Mee, Genentech, S. San Francisco, CA USA
- Monoiodinated Human Interleukin-1B Preparation Retaining Full Biological Activity —K.R. Hejnaes, P. Nilsson, B. Hansen*, B.S. Welinder*, Novo-Nordisk, Gentofte, DENMARK, *Hagedorn Research Laboratory, Gentofte, DENMARK
- Optimization & Validation of a Peptide Map for Recombinant Human Interferon-gamma —C.J. Democko, J.A. Houk, C.P. du Mee, Genentech, S. San Francisco, CA USA
- The Rapid Detection & Quantitation of Argatroban, A Specific Thrombin Inhibitor, by HPLC—D. Eastman, A. Lucchesi, B. Larsen, M. Mulkerrin, M. Jain, V. Anicetti, Genentech, S. San Francisco, CA USA
- Highly Sensitive Determination of Protein Purity Based on Fast Automated Comparison of Tryptic Digests from Recombinant-DNA-Derived Proteins— H.-J.P. Sievert, S.-L. Wu*, R. Chloupek*, W.S. Hancock*, Hewlett-Packard, Avondale, PA USA, *Genentech, S. San Francisco, CA USA
- RP-HPLC Characterization of Recombinant Human Interleukin-1B: A Comparative Study —B.S. Welinder, H.H. Sorensen*, B. Hansen, K.R. Hejnaes*, Hagedorn Research Laboratory, Gentofte, DENMARK, *Novo-Nordisk, Gentofte, DENMARK
- Analysis of Recombinant aFGF by HPSEC in the Presence of SDS—S. Yamazaki, F. Leu, R. Mancinelli, J. Goldstein, M. Brooks, R. Sitrin, Merck Sharp & Dohme Research Labs, West Point, PA USA
- Reversed Phase HPLC of a Soluble T4 Receptor—L.T. Olszewski, V. Manam, Smith Kline & French Laboratories, King of Prussia, PA USA
- Alternative Methods for the Study of Glycosylated & Deglycosylated Transferrins & Their Peptide Fragments—P. Puma, J. Kremsky, Millipore Corp., Bedford, MA USA
- Characterization of Site-Directed Mutants of Pertussis Toxin—S. Cockle, S. Loosmore, G. Zealey, R. Fahim, M. Klein, Connaught Centre for Biotechnology Research, Ontario, CANADA
- High Performance Displacement Chromatography: Mass Spectrometry of Tryptic Fragments of Biosynthetic Proteins—J. Frenz, J. Bourell, W.S. Hancock, Genentech, S. San Francisco, CA USA
- Evaluation of Oligomarization of Recombinant Polypeptides by Size Exclusion High Performance Liquid Chromatography—S. Burman, J.J. L'Italien, Smith Kline & French Laboratories, King of Prussia, PA USA

IX. POLYNUCLEOTIDES AND CARBOHYDRATES

- Optimization of DNA Separation Using Pulsed Field Gel Electrophoresis—K. Izzo, D. Whitney, Pharmacia LKB Biotechnology, Piscataway, NJ USA
- Convenient Purification of Tritylated & Detritylated Oligonucleotides Up to 100-mer Through Practical Optimization of Ligand Chain Length, Pore Size, & Gradient Shape—T.L. Hill, J.W. Mayhew, J.S. Hobbs, Beckman Instr., San Ramon, CA USA
- Synthesis & Purification of p10, the Single-Stranded Nucleic Acid Binding Protein from Murine Leukemia Virus—W.J. Roberts, J.I. Elliott, K.R. Williams, Yale Univ., New Haven, CT USA
- HPLC Analysis of Phosphorothioate, Methylphosphonate & Phosphoramidate Analogues of Oligodeoxynucleotides—S. Agrawal, P.C. Zamecnik, Worcester Foundation of Exper. Biology, Shrewsbury, MA USA
- Separation of Large DNA Restriction Fragments by High Performance Ion-Exchange Chromatography on a Non-porous Ion-Exchange Resin—A.M. Stancavage, T.S. Reid, Supelco, Bellefonte, PA USA
- New Methods for the HPLC Purification of Synthetic Oligonucleotides—J. Kremsky, P. Puma, Millipore Corp., Bedford, MA USA
- Separation of DNA Restriction Fragments with New Anion-Exchange HPLC Column—N.F. Nelson, Interaction Chemicals, Mountain View, CA USA
- Use of HPLC to Define Salvate Pathways—P.K. Dutta, A.J. Bailey, D.E. Beck, G.A. O'Donovan, Univ. North Texas, Denton, TX USA
- Oligosaccharide Mapping of Therapeutic Glycoproteins by High pH Anion-Exchange HPLC—R. Kumarasamy, Schering-Plough, Kenilworth, NJ USA
- Purification of Chemically Modified Oligonucleotides Using Reversed Phase HPLC—M. Bengtstrom, Orion Pharmaceutica, Helsinki, FINLAND

PUBLICATION SCHEDULE FOR 1989

Journal of Chromatography and Journal of Chromatography, Biomedical Applications

MONTH	J	F	M	A	M	J	J	A	S	
Journal of Chromatography	461 462 463/1	463/2 464/1	464/2 465/1 465/2	466 467/1 467/2	468 469 470/1 470/2	471 472/1 472/2 473/1	473/2 474/1 474/2 475	476 477/1 477/2	478/1 478/2 479/1	The publication schedule for further issues will be published later
Bibliography Section		486/1		486/2		486/3		486/4		
Biomedical Applications	487/1	487/2	488/1 488/2	489/1 489/2	490/1 490/2	491/1	491/2	492 493/1	493/2 494	495

INFORMATION FOR AUTHORS

(Detailed *Instructions to Authors* were published in Vol. 478, pp. 453–456. A free reprint can be obtained by application to the publisher, Elsevier Science Publishers B.V., P.O. Box 330, 1000 AH Amsterdam, The Netherlands.)

Types of Contributions. The following types of papers are published in the *Journal of Chromatography* and the section on *Biomedical Applications:* Regular research papers (Full-length papers), Notes, Review articles and Letters to the Editor. Notes are usually descriptions of short investigations and reflect the same quality of research as Full-length papers, but should preferably not exceed six printed pages. Letters to the Editor can comment on (parts of) previously published articles, or they can report minor technical improvements of previously published procedures; they should preferably not exceed two printed pages. For review articles, see inside front cover under Submission of Papers.

Submission. Every paper must be accompanied by a letter from the senior author, stating that he is submitting the paper for publication in the *Journal of Chromatography*. Please do not send a letter signed by the director of the institute or the professor unless he is one of the authors.

Manuscripts. Manuscripts should be typed in double spacing on consecutively numbered pages of uniform size. The manuscript should be preceded by a sheet of manuscript paper carrying the title of the paper and the name and full postal address of the person to whom the proofs are to be sent. Authors of papers in French or German are requested to supply an English translation of the title of the paper. As a rule, papers should be divided into sections, headed by a caption (*e.g.*, Summary, Introduction, Experimental, Results, Discussion, etc.). All illustrations, photographs, tables, etc., should be on separate sheets.

Introduction. Every paper must have a concise introduction mentioning what has been done before on the topic described, and stating clearly what is new in the paper now submitted.

Summary. Full-length papers and Review articles should have a summary of 50–100 words which clearly and briefly indicates what is new, different and significant. In the case of French or German articles an additional summary in English, headed by an English translation of the title, should also be provided. (Notes and Letters to the Editor are published without a summary.)

Illustrations. The figures should be submitted in a form suitable for reproduction, drawn in Indian ink on drawing or tracing paper. Each illustration should have a legend, all the *legends* being typed (with double spacing) together on a *separate sheet.* If structures are given in the text, the original drawings should be supplied. Coloured illustrations are reproduced at the author's expense, the cost being determined by the number of pages and by the number of colours needed. The written permission of the author and publisher must be obtained for the use of any figure already published. Its source must be indicated in the legend.

References. References should be numbered in the order in which they are cited in the text, and listed in numerical sequence on a separate sheet at the end of the article. Please check a recent issue for the layout of the reference list. Abbreviations for the titles of journals should follow the system used by *Chemical Abstracts.* Articles not yet published should be given as "in press" (journal should be specified), "submitted for publication" (journal should be specified), "in preparation" or "personal communication".

Dispatch. Before sending the manuscript to the Editor please check that the envelope contains three copies of the paper complete with references, legends and figures. One of the sets of figures must be the originals suitable for direct reproduction. Please also ensure that permission to publish has been obtained from your institute.

Proofs. One set of proofs will be sent to the author to be carefully checked for printer's errors. Corrections must be restricted to instances in which the proof is at variance with the manuscript. "Extra corrections" will be inserted at the author's expense.

Reprints. Fifty reprints of Full-length papers, Notes and Letters to the Editor will be supplied free of charge. Additional reprints can be ordered by the authors. An order form containing price quotations will be sent to the authors together with the proofs of their article.

Advertisements. Advertisement rates are available from the publisher on request. The Editors of the journal accept no responsibility for the contents of the advertisements.